JOURNAL
OF
PHYSICS OF THE EARTH

Volume IV May 1956 Number 1

CONTENTS

PUBLISHED BY
THE SEISMOLOGICAL SOCIETY OF JAPAN

JOURNAL OF PHYSICS OF THE EARTH

The object of the publication of JOURNAL OF PHYSICS OF THE EARTH is to provide an international medium for the publication of original contributions in the field of geophysical science, more particularly concerning with physical properties and conditions of and phenomena occurring in the solid part of the earth.

The JOURNAL is open to any one who wishes to contribute his (or her) article. But the authors are, in principle, requested to pay page charges necessary for publishing their respective articles. The authors receive 100 copies of reprints free of charge.

In order to serve the purposes for which this JOURNAL is published, all contributions should be written in widely understandable languages, such as English, French and German, etc. Contributions should be sent to the Editor or to one of the Associate Editors.

For the time being, this JOURNAL will be issued at variable prices and at irregular intervals. The price of this issue is 200 yen inside Japan and $1.00 for foreign countries, the latter including postage.

Chemical Phase Equilibrium and Physical Structure Within the Earth's Mantle.

By

Yasuo SHIMAZU

Institute of Earth Sciences, Nagoya University, Nagoya.

Abstract

Phase equilibrium of Fe-Si-O system within the earth is discussed. Due to the action of gravitational differentiation, there is chemical squeezing of the lighter material out of the earth. Then the silicate or oxide phase is decomposed below certain depths even if the temperature is low. It is concluded that Fe_2SiO_4 layer is decomposed at 1,000 km from the earth's surface. This result suggests the origin and the physical properties of Jeffrey's 20° discontinuity.

§ 1. Introduction

In my previous paper (Y. SHIMAZU [1955]), we studied the chemical equilibrium condition within the earth. Our discussions were based upon an assumption that a mixed crystal can be chemically stable with any mixing ratio of its components. For instance, FeO and SiO_2 were assumed to be able to combine with any mol ratio. There is, however, a very narrow area in the combination, so that the mol ratio cannot diverge from some definite ratios. FeO and SiO_2 can exist either in the form of $2FeO \cdot SiO_2$ (fayalite)or in the form of $FeO \cdot SiO_2$ (ferrosilite). In a system of components which can combine into different compounds, gravity will obviously tend to develop a mechanically stable arrangement of different layers of different chemical phases and of different densities. If the

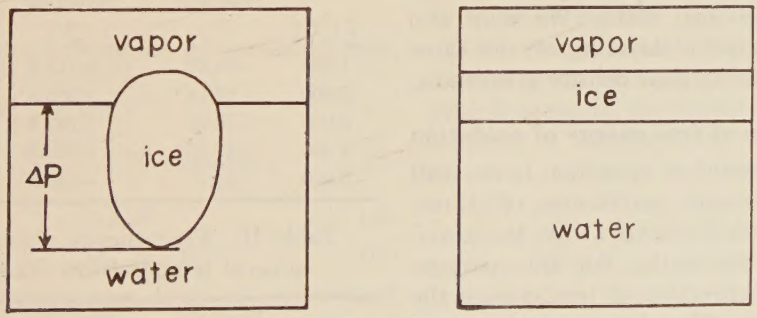

Fig. 1. Phase equilibrium of H_2O-system in the gravitational field.

gravitational differentiation proceeds far enough, as was discussed in my previous paper (Yasuo SHIMAZU [1955]), then the system becomes saturated at the lower end with one compound phase, and further transport of material will form another compound. We then have two phases of different compound concentration ratios. There will be a concentration discontinuity at the point where the chemical potentials of the two phases are equal.

It is interesting to note that ordinary GIBBS phase rule cannot be applied to the phase equilibrium in the gravitational field as W. SWIETOSLAWSKY [1947] pointed out. He discussed one-component system (H_2O) under the action of gravitational force. According to the ordinary GIBBS phase rule, the maximum number of co-existing phases for H_2O-system is three. In fact, at the so-called triple point

in the phase diagram we have solid ice, liquid water, and water vapor.

Let us assume that large amounts of water, ice, and water vapor are put in a closed container. In Figure 1, the initial state (a) and final state (b) are schematically shown. First, the block of ice is partly in the vapor and partly immersed into the liquid. The immersed part is subjected to the action of hydrostatic pressure, which changes from the top vapor pressure p_0 (=0.006 atm. in this system) to $p_0+\Delta p$ and thus the equilibrium temperature between the solid and liquid phases changes from $T°$ (triple point=0.0078°C) to $T°-\Delta T$ as seen in the phase diagram. In Figure 1 (a), there is only one line along which $T°$ can actually be found. As is easily understood, the ice below the surface of the water undergoes melting. On the other hand, the ice surrounded by vaporous space is covered by ice formed. Thus the movement of ice toward the surface takes place. The balance of heat requires that the heat used in melting the ice must be compensated by that in the formation of the corresponding amount of ice. As we see in Figure 1 (b), three phases have no mutual contact with each other in the final state. We may also note that the order of layering of the three phases is governed by their density differences.

§ 2. Calculation of free energy of oxidation

Along the general line in section 1, we shall discuss the chemical equilibrium of three-component system (Fe-Si-O) within the gravitational field of the earth. For this purpose we must get as a function of temperature the heat of formation ΔH and GIBBS free energy change ΔG during the chemical reaction. We can obtain ΔH from the change of specific heat ΔC_p

$$\frac{\partial(\Delta H)}{\partial T}=\Delta C_p\,. \qquad (1)$$

Since the specific heat C_p of each component is known experimentally as a function of temperature, ΔC_p can be obtained from the difference between the C_p of each side of reaction equation. The procedure of calculation is due to W. EITEL [1951]. Experimental values are obtained from the works of F. BIRCH et. al. [1942]. We calculated ΔG^0 ($=\Delta G$ at ordinary pressure) from the integration of

$$\frac{\partial}{\partial T}\left(\frac{\Delta G^0}{T}\right)=-\frac{\Delta H}{T^2}\,. \qquad (2)$$

Results of calculations are as follows

$Fe+\frac{1}{2}O_2\rightleftarrows FeO$

$$\Delta H=-65.6\times10^3+0.631\,T+0.550\times10^{-3}\,T^2 \quad \text{(cal/mol)}.$$

$$\Delta G^0=-65.6\times10^3+23.2\,T-0.631\,T\ln T-0.550\times10^{-3}\,T^2 \quad \text{(cal/mol)}. \qquad (3)$$

$Si+O_2\rightleftarrows SiO_2$

$$\Delta H=-221.9\times10^3+8.79\,T-0.26\times10^{-3}\,T^2,$$

$$\Delta G^0=-221.9\times10^3+116\text{-}5\,T-8.79\,T\ln T+0.26\times10^{-3}\,T^2. \qquad (4)$$

$2FeO+SiO_2\rightleftarrows Fe_2SiO_4$

$$\Delta H=-343.0\times10^3-2.45\,T+1.76\times10^{-3}\,T^2,$$

$$\Delta G^0=-343.0\times10^3+64.9\,T+2.45\,T\ln T-1.76\times10^{-3}\,T^2. \qquad (5)$$

Table I. Heat of formation ΔH at several temperatures (kcal/mol)

T (°K)	Reaction (3)	Reaction (4)	Reaction (5)
1,000	−64.42	−213.4	−343.7
2,000	−62.14	−205.4	−340.9
3,000	−58.76	−197.9	−334.5
4,000	−54.28	−190.9	−324.6
5,000	−48.70	−184.5	−311.3

Table II. Free energy change ΔG^0 at several temperatures (kcal/mol)

T (°K)	Reaction (3)	Reaction (4)	Reaction (5)
1,000	−47.3	−165.9	−262.9
2,000	−31.0	−121.5	−183.0
3,000	−16.2	− 82.6	−105.8
4,000	− 2.53	− 43.4	− 30.3
5,000	+ 9.78	− 7.2	+ 41.8

Since no experimental value is available, another reaction

$$FeO+SiO_2\rightleftarrows FeSiO_3 \qquad (6)$$

is not discussed here. Tables 1 and 2 give

ΔH and ΔG^0 at several temperatures. The quantity ΔG^0 is nothing but the chemical potential at the standard pressure. We have also the following general relation between chemical potential ΔG and the vapor pressure

$$\Delta G = \Delta G^0 + RT \ln P . \qquad (7)$$

The equilibrium condition is given by $\Delta G = 0$. We get the temperatures $T^0 = 4{,}200°K$, $5{,}200°K$ and $4{,}400°K$ at which the equilibrium condition are realized at room for the reactions (3), (4) and (5), respectively. At these temperatures the corresponding oxides or silicates are decomposed. At higher temperatures, oxides or silicates are unstable.

Pressure dependence of the decomposing temperature T^0 is given by the CLAPEYRON equation

$$\frac{dT^0}{dP} = \frac{T_0 \Delta V}{\Delta H} , \qquad (8)$$

where ΔV is the volume change between the left-hand and right-hand sides of the reaction equation. In (3) and (4), ΔV are equal to the volume changes in gaseous oxygen phases, or $-\frac{1}{2} \times 22.4 \times 10^3$cc/mol and -22.4×10^3cc/mol, respectively. In (5), ΔV is the difference in molar volume between both sides of the equation, viz.

$$\underset{23.96}{2FeO} + \underset{27.27}{SiO_2} \rightleftarrows \underset{47.61}{Fe_2SiO_4}, \quad \Delta V = -3.62 \text{ cc/mol.}$$

In conclusion, we get

$$\text{for (3)} \quad \frac{dT^0}{dP} = 1.76 \text{ deg/atm.} \qquad (9)$$

$$\text{for (4)} \quad = 1.36 \qquad (10)$$

$$\text{for (5)} \quad = 1.19 \times 10^{-3}. \qquad (11)$$

These equations show that an exceedingly high temperature is necessary to decompose oxides within the earth's interior. Then we may infer that oxides and silicates are stable within the earth's mantle if the abundance of elements concerned is appropriate.

§ 3. Phase equilibrium within the gravitational field.

As we see in § 1, the phase equilibrium within the gravitational field has a particular character, that is, the ordinary GIBBS phase rule cannot be applied. In one-component system, as stated in § 1, the movement or migration of solid ice occurs. The melting of ice at the bottom has a compensated formation at the top. In a multi-component system, on the other hand, there must be the migration of any one phase through others. This is nothing but the diffusion phenomena. Even in crystalline solid system, there will always be some diffusion effect. Thus, the chemical potential gradient will always cause a diffusion through the system if sufficient time is allowed. We do not concern ourselves with the mechanism of diffusion. The final equilibrium state is assumed *apriori*.

Migration is controlled by gravitational differentiation in which the lighter material moves upward and the relatively heavier material moves downward. If the lighter material is in the fluid form, diffusion through the solid phase will effectively realized. Equilibrium of hydrous minerals, such as mica, has already been discussed by several authors based on this concept of migration (cf. J. B. THOMPSON [1955]). Of these studies the most famous is that on calcite ($CaCO_3$)→wollastonite ($CaSiO_3$) reaction. (cf. "Theoretical Petrology" by T. F. W. BARTH [1948] (p. 286)). As this reaction proceeds to the right, gas phase CO_2 is produced and the equilibrium temperature will therefore increase with increasing pressure. This is given by equation (8). At one atmospheric pressure, the formation of wollastonite requires a temperature of about 450°C. However, the rock is usually semipermeable to CO_2 gas which thus escaping from the locale of the reaction will percolate to the surface. If the gas escapes as soon as it is produced, the molecular volume of the gas can be neglected and the change in the temperature of the reaction with pressure can be calculated from (8), taking into consideration only the molar volumes of the solid phases. The molar volumes in c.c. are as follows:

$$CaCO_3 + SiO_2 \rightleftarrows CaSiO_3 + CO_2 ,$$
$$\Delta V = -18 \text{ c.c./mol} , \qquad (12)$$

$$\frac{dT^0}{dP} = -\frac{18 \times 720}{106} = -0.013 \; deg/atm, \qquad (13)$$

the latter showing that the differential pressure squeezes CO_2 gas out of calcite at a lower

temperature than is otherwise possible. The formation of wollastonite is facilitated with increasing pressure. In this case gas escapes through the fissure rather than by diffusion. As is shown later, however, the above discussion is not rigorous since the chemical potential gradient of CO_2 is neglected.

The idea of chemical squeezing of some light materials out of deeper parts of the earth has also been presented by several authors. Decrease in the degree of oxidation or decrease in the ratio of oxygen to metallic ions at different levels in the earth's crust shows the squeezing of oxygen. H. BROWN and C. PATTERSON [1948] conclude that the main variable elements in meteorites are iron and oxygen, with the decrease in oxygen almost exactly matching the increase in iron. It proves that oxygen is squeezed out of the deeper parts of the protoplanet of meteorites. T. F. W. BARTH [1948] calculates the phase equilibrium of Fe-O system in the crust and concludes that magnetite (Fe_3O_4) is unstable in the deeper parts and underlain by a layer of wüstite (FeO). At still greater depths, Fe becomes stable.

As our first step, we shall study the general theory of equilibrium of reaction

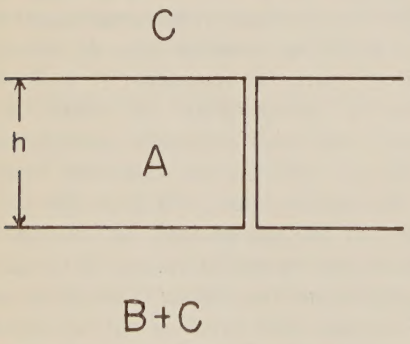

Fig. 2. Phase equilibrium of the reaction $A \rightleftarrows B+C$ in the gravitational field ($\rho_B > \rho_A > \rho_C$).

$$A \rightleftarrows B+C\uparrow , \tag{14}$$

where A, B, C, for example, correspond to FeO, Fe, O_2 in (3). We assume that C can migrate through the system. At low pressure, the reaction (14) proceeds to the right if the temperature is higher than $T°$. If $\rho_B > \rho_A > \rho_C$, the thick layer of A is unstable in the gravitational field even if the temperature is below T^0 in (8). A more stable state exists if the reaction proceeds to the right below a certain depth h, so that the dense phase B is formed, while the liberated phase C is displaced to the top of layer A. The top of layer A is the zero level surface. This state is shown schematically in Figure 2. The migration of C phase is shown by a pipe line (fissure) which passes through A layer.

GIBBS free energy G per mol is a function of pressure P, temperature T, and the depth from the surface h. Thermodynamical identities give

$$\left(\frac{\partial G_i}{\partial T}\right)_{P,h} = -S_i , \tag{15}$$

$$\left(\frac{\partial G_i}{\partial P}\right)_{T,h} = V_i , \tag{16}$$

$$\left(\frac{\partial G_i}{\partial h}\right)_{P,T} = -M_i g , \tag{17}$$

where S_i, V_i, M_i are the entropy, volume, molecular weight per mol, respectively, and suffix i denotes A or B or C. The assumption of hydrostatic equilibrium gives

$$\frac{dP}{dh} = \rho_A g = \frac{M_A}{V_A} g \tag{18}$$

in A layer. Incompressibility is assumed which is allowed in our chemical problem. As we see in the theory of chemical equilibrium, A phase, for instance, does not mean that there is no B or C phase at all. It means only that the partial pressure of A is predominant. Though B phase at the depth h is under the pressures $P = \rho_A g h$, this is not so in C phase at depth h. The pressure P' of C is given by

$$\frac{dP'}{dh} = \rho_C g = \frac{M_C}{V_C} g . \tag{19}$$

Schematically P' is the pressure in the fissure in Figure 2. Thus the phase equilibrium at depth h is attained even if $P \neq P'$. This circumstance is similar to osmotic equilibrium. The wall of the fissure corresponds to a semipermeable membrane. Then from (15)–(17) we get

$$dG_{A,h} = -S_A dT + V_A dP = -S_A dT + V_A \rho_A g dh ,$$

$$dG_{B,h} = -S_B dT + V_B dP = -S_B dT + V_B \rho_A g dh ,$$

$$dG_{c,h}=-S_c dT+V_c dP'=-S_c dT+M_c g dh \quad (20)$$

Chemical equilibrium gives

$$dG_{A,h}=dG_{B,h}+dG_{c,h} \quad (21)$$

Substituting (21) into (20), we have

$$\frac{dT}{dh}=\frac{g(-V_A\rho_A+V_B\rho_A+M_c)}{S_B+S_c-S_A} \quad (22)$$

in which $S_B+S_C-S_A$ equals $(\Delta H/T)$ by definition. Since $M_A=M_B+M_c$ we get finally

$$\frac{dT}{dh}=\frac{TM_B g\left(\frac{\rho_A}{\rho_B}-1\right)}{\Delta H} \quad (23)$$

We see that the thickness of A layer is determined by (ρ_A/ρ_B). At temperature T^0, h

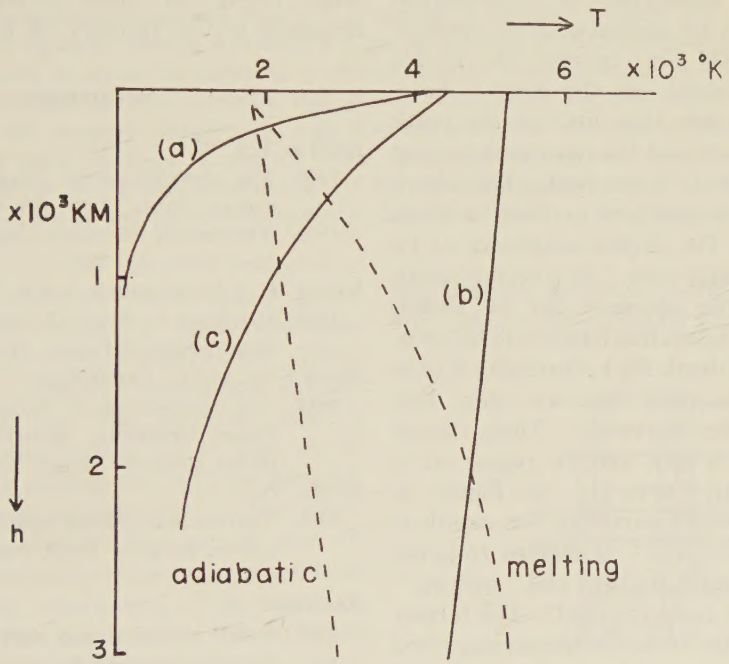

Fig. 3. Temperature-depth curves of chemical stability.
(a) $FeO \rightarrow Fe+\frac{1}{2}O_2$
(b) $SiO_2 \rightarrow Si+O_2$
(c) $Fe_2SiO_4 \rightarrow 2FeO+SiO_2$
adiabatic: temperature derived from adiabatic gradient
melting: temperature derived from melting point gradient

is obviously zero. Even if the temperature is below T_0 for the whole system, A phase is decomposed into B and C at depth h. The lower the temperature, the greater the thickness h. We shall now make the calculation for Fe-O system in (3). As $\rho_A=6.00$, $\rho_B=7.87$, $M_B=55.8$ and $g=10^3$ in the mantle of the earth, we get Curve (a) in Figure 3. Similar calculations for Si-O_2 and FeO-SiO_2 systems are also given in Curves (b) and (c) in Figure 3, respectively. We see that SiO_2 is very stable and will not be decomposed within the earth.

If the condition $\rho_B>\rho_A>\rho_C$ is not fulfilled, the state given in this section does not occur. The equation (23) can easily be modified

$$\frac{dT}{dP}=\frac{T\left(\Delta V_s+\frac{\rho_c}{\rho_A}\Delta V_G\right)}{\Delta H}, \quad (24)$$

where ΔV_s is the volume change of the solid phase $(=V_B-V_A)$ and ΔV_G is of the gaseous phase (V_c). BARTH's discussion in (13) corresponds to the approximation in which the effective volume change in the movable phase $(\rho_c/\rho_A)\Delta V_G$ is neglected. The equation (24) is

a generalized CLAPEYRON's equation corresponding to (8).

Though the discussion in this paper does not give the sufficient condition for the equilibrium, it does give necessary condition. If the abundance ratio of each component is not suitable, the thick layer A cannot be formed and thus our conclusion fails. From cosmic, meteoritic or petrological abundances given by several authors, we may safely assume O: Fe: Si=49: 34: 17 for the simplified model of the earth. Since SiO_2 is much stable than FeO in the earth SiO_2 is first formed and the remaining oxygen combines with Fe to form FeO. The above abundance ratio is sufficient to form a thick SiO_2-FeO layer. The excess abundance of Fe will make the metal core. At a certain depth Si and O_2 will be squeezed out of $FeSiO_3$ lattice and Fe_2SiO_4(fayalite) lattice will be formed. The critical depth for FeO-stablity (Curve (a) in Figure 3) is much shallower than that for Fe_2SiO_4-stability (Curve (c)). Then, silicate mantle (Fe_2SiO_4) is split into Fe region at a depth greater than Curve (c). In Figure 3, the temperature-depth curve for the mantle is also given. "Adiabatic" is derived from the adiabatic temperature gradient and "melting" from the melting point gradient. The former gives the minimum plausible temperature and the latter the maximum within the earth. (cf. Y. SHIMAZU [1954]). FeO, SiO_2 and Fe_2SiO_4 are, thus, stable at the region shallower than the points at which the temperature-depth curves intercept curves (a), (b), (c) respectively. The instability of FeO layer at some depth has already been shown in my previous paper (Y. SHIMAZU [1955]) from a different point of view.

If the earth is formed by accretion process, the oxidized or silicate compound will be stable in the earth's initial stage. As the accretion process proceeds, the silicate phase sphere grows and the temperature is raised at the same time. Then the critical depth as shown in Figure 3 is reached at some stage and a discontinuity in composition will be formed. Possible existence of Fe region due to chemical squeezing at depths greater than 1,000 km suggests the jump in electrical conductivity there and the existence of JEFFREY's 20° discontinuity.

This work was carried out by the writer under receipt of Grant in Aid for Scientific Research of the Ministry of Education.

References

BARTH, T. F. W.:
1948 The distribution of oxygen in the lithosphere. Journ. Geol., **56**, 41–49.
1952 Theoretical Petrology, John Wiley & Sons, New York, pp. 387.

BIRCH, F., J. F. SCHAIRER and H. C. SPICER:
1942 Handbook of Physical Constants, Geol. Soc. Amer., Special Papers NO. 36.

BROWN, H. and C. PATTERSON:
1948 The composition of meteoritic matter, III. Phase equilibria, genetic relations and planet structure. Journ. Geol., **56**, 85–111.

EITEL, W.:
1951 Thermochemical methods in silicate investigation. Rutgers Univ. Press. New Jersey, pp. 132.

RAMBERG, H.:
1948 Radial diffusion and chemical stability in the gravitational field, Journ, Geol., **56**, 448–458.

SHIMAZU, Y.:
1954 Equation of state of materials composing the earth's interior. Journ, Earth Sci., Nagoya Univ., **2**, 15–172.
1955 Chemical structure and physical property of the earth's mantle inferred from chemical equilibrium condition. Journ. Earth Sci., Nagoya Univ., **3**, 85–90.

SWIETOSLAWSKI, W.:
1947 The phase rule and the action of gravity. Journ. Chem. Education, **24**, 606–608.

THOMPSOL, J. B.:
1955 The thermodynamic basis for the mineral facies concept. Amer. Journ. Sci., **253**, 65–103.

On the Variation in Bulk Modulus/Density in the Mantle.

By

Michiyasu SHIMA

Geophysical Institute, Kyoto University.

Abstract

On the assumption that the mantle is composed of the ionic crystals, the distribution of the ratio of bulk modulus k to density ρ and of pressure P is investigated by means of atomic theory to reveal the character of change occuring between the layers B (33–413 km) and D (1000–2898 km). It is found that, if this change were the polymorphic transition from the low pressure phase to the high pressure phase, the decrease of the gradient of k/ρ would occur between B and D. This is against the observed result. Then, the change may be of chemical composition. If so, the dissociation energy E and the reduced density ρ_0 increase and the inverse power n of potential between the atoms hardly changes there.

§ 1. k_s/ρ derived from the seismic P and S wave velocities within the earth increases steadily in the so-called B- and D-layer. Then, in studying the density distribution BULLEN (1947) assumed that the materials are of homogeneous constitutions in B and D. In this paper, this assumption will be adopted. But k_s/ρ increases abnormally in the intermediate layer (C-layer) between B and D, and such an abnormality has been supposed to be due to changes of constitution of the materials in this layer. For example, 1) BERNAL (1936) suggested that such changes could be attributed to a rearrangement in the crystal state of olivine to the high pressure phase and 2) BIRCH (1952) proposed that it could be attibuted to changes of chemical compositions. Here by means of the theory of matter, we shall firstly study the possibility of the polymorphic transition.

§ 2. Since the materials which constitute the earth interior are composed of many kinds of minerals of complex crystal structures, it is difficult to treat the materials as such. Then we are obliged to reduce them to the simple ionic crystals representing their characteristic properties. In the following study, NaCl and CsCl types of crystals will be taken as example. NaCl type crystal changes polymorphically to CsCl type at more than several thousands atm.. For example, the polymorphic transitions occur in AgI at 4500 atm. and in NaI at 50000 atm. (JACOBS, 1938).

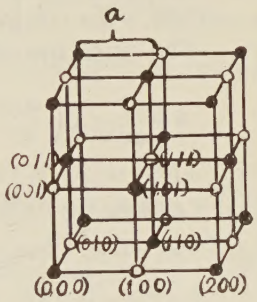

NaCl type

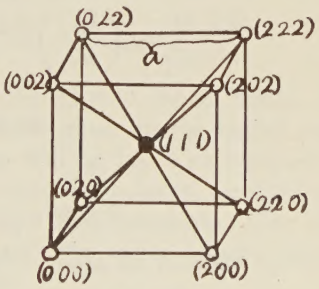

CsCl type

Fig. 1. Crystal lattice

As the modulus of elasticity obtained theoretically as a function of pressure and temperature are isothermal, the adiabatic k_s/ρ derived from the seismic waves velocities

must be converted to compare the calculated elastic modulus with the observed one. The ratio is

$$k_S/k_T=1+T\alpha\gamma_G\ , \qquad (1)$$

where k_S is the adiabatic bulk modulus, k_T the isothermal one, T the temperature, α the coefficient of thermal expansion, γ_G GRÜNEISEN constant. With depth h, T increases and α and γ_G decreases slowly, whereas $T\alpha\gamma_G$ seems to be constant. Assuming $T=1000°\mathrm{K}$, $\alpha=2.0\cdot 10^{-6}$, $\gamma_G=1.5$, we have k_T which is smaller about 3 per cent than k_S.

k_T/ρ and p are expressed as follows (SHIMA, 1954);

$$k_T/\rho=[c_{11}+2(c_{12}+p)]/3\rho\ , \qquad (2)$$

$$p=-(\partial F/\partial e_1)_{e=0}\ ,$$

$$c_{ij}=(\partial^2 F/\partial e_i\partial e_j)_{e=0}\ ,$$

$$F=\Phi+\frac{kT}{vN}\sum_{p=1}^{3N}\log\left(\frac{\hbar\omega_p}{kT}\right)\ , \qquad (3)$$

where N is the numbers of atoms per mole, k BOLTZMANN constant, v the volume per atom, ω_p frequency. The attractive electrostatic force and the repulsive force due to the overlapping of the closed shells are assumed between the different kinds of ions, and the repulsive electrostatic force of the above kind between the same kinds of ions. Then we heve

$$\phi_{AB}=\frac{\alpha_{AB}}{r_{AB}}+b_{AB}\frac{B_0(R_A+R_B)^{n-1}}{r_{AB}{}^n}\ ,$$

$$b_{AB}=\left(\frac{Z_A}{N_A}+\frac{Z_B}{N_B}+1\right). \qquad (4)$$

where N_A, N_B the numbers of outer shell electrons, R_A, R_B their ionic radii, Z_A, Z_B the ionic charges, B_0 a constant. With regard to the second repulsive term derived by PAULING (1940), he reduced the ion to the hydrogenlike one and simplified the expression of potential derived by the HEITLER-LONDON method, assuming that the ions have the certain radii R_A and R_B, and the repulsive potential increases, when the distance between the ions becomes less than the sum of these radii. Then it is

$$\Phi=\frac{1}{2vN}\sum_l\left(\frac{\alpha_{AB}}{r_l}+b_{AB}\frac{B_0(R_A+R_B)^{n-1}}{r_l{}^n}\right)=\frac{1}{2}\left(\frac{\alpha}{a}S_1{}^0+\frac{\beta}{a^n}T_n{}^0\right),$$

$$r_l=a(l_1{}^2+l_2{}^2+l_3{}^2)+a^2\{2(l_1{}^2e_1+l_2{}^2e_2+l_3{}^2e_3+l_2l_3e_4+l_3l_1e_5+l_1l_2e_6)+l_1{}^2(e_1{}^2+e_5{}^2/4+e_6{}^2/4)$$
$$+l_2{}^2(e_2{}^2+e_6{}^2/4+e_4{}^2/4)+l_3{}^2(e_3{}^2+c_5{}^2/4+e_4{}^2/4)+(l_2l_3/4)(e_5e_6+2e_2e_4+2e_4e_3)$$
$$+(l_3l_1/4)(e_4e_6+2e_1e_5+2e_3e_5)+(l_1l_2/4)(e_4e_5+2e_1e_6+2e_1e_6)\}$$

$$\beta T_n{}^0=(\beta_{++}+\beta_{--})\overset{++}{S}_n+2\beta_{+-}\overset{+-}{S}_n=\beta(\overset{++}{S}_n+\delta\overset{+-}{S}_n)=\beta T_n\ , \qquad (5)$$

where l_1, l_2, l_3 are the coordinates of the lattice points taking a in Fig. 1 as unit. Using the potential, we have the vibrational energy terms as follows (BRADBURN, 1943, GOW, 1944);

$$\frac{kT}{vN}\sum_{p=1}^{3N}\log\left(\frac{\hbar\omega_p}{kT}\right)=\frac{kT}{v}\left(\frac{1}{6}\log\det[ij]-\frac{1}{2}\log\mu+\log\frac{\hbar}{kT}\right),$$

$$\det[ij]=\begin{vmatrix}\phi_{11}{}^l & \phi_{12}{}^l & \phi_{13}{}^l\\ \phi_{21}{}^l & \phi_{22}{}^l & \phi_{23}{}^l\\ \phi_{31}{}^l & \phi_{32}{}^l & \phi_{33}{}^l\end{vmatrix},$$

$$\phi_{ij}{}^l=\delta_{ij}\frac{1}{r_l}\frac{\partial\phi^l}{\partial r_l}+r_{li}r_{lj}\frac{1}{r_l}\frac{\partial}{\partial r_l}\left(\frac{\partial}{\partial r_l}\frac{\partial\phi^l}{\partial r_l}\right), \qquad (6)$$

where μ is the mass of an atom. Then from (3), (4), (5), (6), p and c_{ij} are

$$p=-\frac{R\theta}{A}\rho\left[\frac{c}{2}\left(S_3{}^{(1)}-\gamma\left(\frac{\rho}{\rho_0}\right)^{(n-1)/3}\cdot T_{n+2}^{(1)}\right)+\frac{(R_3{}^2+2R_3{}^{11}+5R_2{}^1)T}{2(R_1{}^0+R_2{}^1)\theta}\right], \qquad (7)$$

$$c_{11}=\frac{R\theta}{A}\rho\left[\frac{c}{2}\left\{S_5{}^{(2)}-S_3{}^{(1)}+\gamma\left(\frac{\rho}{\rho_0}\right)^{(n-1)/3}(T_{n+4}^{(2)}-T_{n+2}^{(1)})\right\}\right.$$
$$\left.+\frac{\{(R_1{}^0+R_2{}^1)(R_3{}^2+2R_3{}^{11}+5R_2{}^1)/2+(R^{10}+R_2{}^1)(R_4{}^3+2R_4{}^{21}+3R_3{}^2)/8}{+R_2{}^1(R_3{}^2+2R_3{}^{11})+(7(R_2{}^1)^2+2R_3{}^2R_3{}^{11}+(R_3{}^{11})^2+2R_2{}^1R_3{}^2)/4\}T}{2(R_1{}^0+R_2{}^1)^2\theta}\right], \qquad (8)$$

$$c_{12}=\frac{R\theta}{A}\rho\Bigg[\frac{c}{2}\left(S_5^{(11)}+\gamma\left(\frac{\rho}{\rho_0}\right)^{(n-1)/3}\cdot T_{n+4}^{(11)}\right)$$
$$+\{(R_1^0+R_2^1)(2R_1^{21}+R_1^{111}+3R_3^{111})/2+((R_3^2)+3(R_3^{11})^2+2R_3^2R_3^{11}/4$$
$$+2R_2^1(R_3^2+2R_3^{11})+R_1^0R_3^{11}+9(R_2^1)^2/2\}T\Bigg], \tag{9}$$

$$c=\frac{2(R_1^0+R_2^1)^2\theta}{k\theta}\frac{k\theta}{n-1}\left(\frac{\rho}{\rho_0}\right)\gamma^{1/(n-1)}, \qquad \gamma=-\frac{S_1^{(0)}}{T_n^{(0)}},$$

$$S_n^{(p,q,r)}=\sum_i l_1^{2p}l_2^{2q}l_3^{2r}/(l_1^2+l_2^2+l_3^2)^{n/2}, \tag{10}$$
$$(0,0,0)\to(0)$$
$$(1,0,0)\ (0,1,0)\ (0,0,1)\to(1)$$
$$(2,0,0)\ (0,2,0)\ (0,0,2)\to(2)$$
$$(1,1,0)\ (1,0,1)\ (0,1,1)\to(1,1),$$

$$R_s^{pqr}=[(-1)^{s+1}\cdot 1\cdot(1+2)\cdots\{1+2(s-1)\}S_{1+2s}^{pqr}+\gamma\left(\frac{\rho}{\rho_0}\right)^{(n-1)/3}\cdot$$
$$(-1)^s\cdot 1\cdot(n+2)\cdots\{n+2(s-1)\}T_{n+2s}^{pqr}]\frac{R\theta}{n-1}\left(\frac{\rho}{\rho_0}\right)\frac{1}{a_0^2}\gamma^{1/(n-1)},$$

$$S_n^{(0)}=3S_{n+2}^{(1)}, \qquad 3S_{n+1}^{2)}+6S_{n+4}^{11)}=S_n^{(0)}, \qquad S_{n+6}^{(3)}+2S_{n+6}^{(21)}=S_{n+4}^{(2)} \qquad 2S_{n+6}^{(21)}S+S_{n+6}^{(111)}=S_{n+4}^{(11)}, \tag{11}$$

where ρ_0 is ρ at absolute zero temperature and zero atm., $k\theta=E$ the dissociation energy, R the gas constant, A the mean atomic weight. $S_n^{(pqr)}$ is represented by integral as follows

$$S_n^{(pqr)}=\frac{1}{\Gamma(n/2)}\int_0^\infty u^{n/2-1}(\sum l_1^{2p}l_2^{2q}l_3^{2r}e^{-l^2u})du=\frac{1}{\Gamma(n/2)}\int_0^\infty u^{n/2-1}\sigma^{(pqr)}(u)du. \tag{12}$$

The fundamental functions $\sigma^{(0)}$ and $\sigma^{(2)}$ are represented by θ functions as follows

$$\left.\begin{aligned}
&\sigma_{\mathrm{NaCl}++}^{(0)}(4u)=\theta_3^3(0,e^{-4u})+3\theta_3(0,e^{-4u})\theta_2^2(0,e^{-4u})-1,\\
&\sigma_{\mathrm{NaCl}+-}^{(0)}(4u)=\theta_2^3(0,e^{-4u})+3\theta_3^2(0,e^{-4u})\theta_2(0,e^{-4u}),\\
&\sigma_{\mathrm{NaCl}++}^{(2)}(4u)=\theta_3^2(0,e^{-4u})\frac{\partial^2\theta_3(0,e^{-4u})}{\partial u^2}+\theta_2^2(0,e^{-4u})\frac{\partial^2\theta_3(0,e^{-4u})}{\partial u^2}+2\theta_2(0,e^{-4u})\theta_3(0,e^{-4u})\frac{\partial^2\theta_2(0,e^{-4u})}{\partial u^2},\\
&\sigma_{\mathrm{NaCl}+-}^{(2)}(4u)=\theta_2^2(0,e^{-4u})\frac{\partial^2\theta_2(0,e^{-4u})}{\partial u^2}+\theta_3^2(0,e^{-4u})\frac{\partial^2\theta_2(0,e^{-4u})}{\partial u^2}+2\theta_2(0,e^{-4u})\theta_3(0,e^{-4u})\frac{\partial^2\theta_3(0,e^{-4u})}{\partial u^2},\\
&\sigma_{\mathrm{CsCl}++}^{(0)}=\theta_3^3(0,e^{-4u})-1, \qquad \sigma_{\mathrm{CsCl}+-}^{(0)}(4u)=\theta_2^3(0,e^{-4u}),\\
&\sigma_{\mathrm{CsCl}++}^{(2)}=\theta_3^2(0,e^{-4u})\frac{\partial^2\theta_3(0,e^{-4u})}{\partial u^2}, \qquad \sigma_{\mathrm{CsCl}+-}^{(2)}=\theta_2^2(0,e^{-4u})\frac{\partial^2\theta_2(0,e^{-4u})}{\partial u^2},
\end{aligned}\right\} \tag{13}$$

where we use the Born's method (1940) in the calculation of $S_n^{(pqr)}$. Since, firstly, the possibility of the polymorphic transition from the lower pressure phase to the higher one is investigated, NaCl type crystals of the lower pressure phase will be taken as the materials in the B-layer. Then, adopting the Bullen's density distribution in this layer, we can determine the constants in the expression of k_T/ρ and p corresponding to these materials. The adiabatic temperature distribution derived by Verhoogen (1952) and the mean atomic weight of magnesium olivine ($A=21$) is assumed in this layer. Then

$$\delta=1, \qquad n=6, \qquad \theta=225000, \qquad \rho_0=3.45.$$

In this transition, the atomic configuration changes, but the constants n, θ, δ, ρ_0 do not. The density incresaes from ρ to ρ' by about 4 per cent at the polymorphic transition, and we have

$$\frac{k_T}{\rho}=2.969\cdot 10^{11}\Bigg[\left\{-1.0213\left(\frac{\rho}{\rho_0}\right)^{1/3}+2.298\left(\frac{\rho}{\rho_0}\right)^2+5.333\cdot 10^{-5}T\right\}\frac{800-h}{387}$$
$$+\left\{-0.9440\left(\frac{\rho'}{\rho_0}\right)^{1/3}+1.989\left(\frac{\rho'}{\rho_0}\right)+5.333\cdot 10^{-5}T\right\}\frac{h-413}{387}\Bigg]. \tag{14}$$

If the transition occurs at the same time between 413 and 800 km, k_T/ρ varies as shown by the dotted line in Fig. 2. We see in Fig. 2.

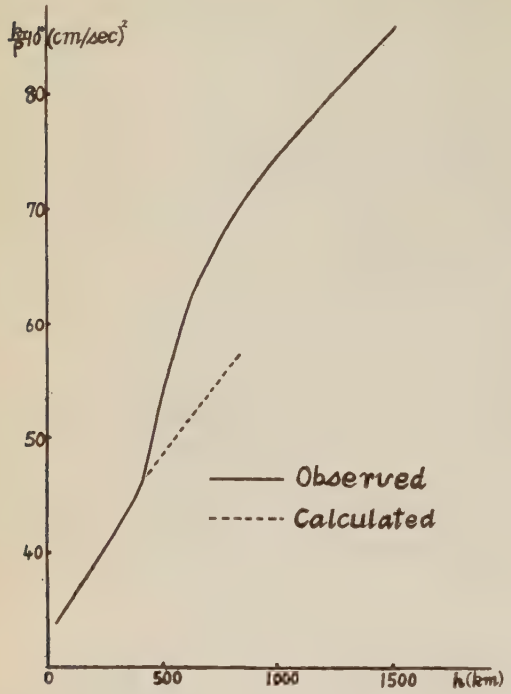

Fig. 2. k_T/ρ in the mantle

that the calculated and observed distribution k_T/ρ have an opposite tendency, and thus k_T/ρ derived from the observed value denies the possibility of the polymorphic transition which was suggested by BERNAL (1936). Next, the possibility of chemical changes will be studied. Only the changes in the constitutive atoms of NaCl type ionic crystals, for instance $CaO \rightarrow MgO$, will be investigated here. Since k_T/ρ is smooth in the boundary between C- and D-layer, the materials in the lower part of C-layer seem to be the same as in D-layer, and the value of the constants may be continuous. Considering these conditions we carry out the above process again and get

$\delta=1$, $\theta=225000$, $\rho_0=3.45$, $n=6$, $A=21$.

$\delta=1$, $\theta=430000$, $\rho_0=4.20$, $n=5$, $A=21$.

Namely, the dissociation energy E and the reduced density ρ_0 remarkably increase between 413 and 1000 km, whereas n hardly changes there. The density distribution is determined so as to agree with the observed total mass and the total moment of inertia of the earth and the error of the estimated density at 1000 km is less than 0.1. With regard to the effect of the density distribution between 413 and 1000 km on the pressure at 1000 km, its deviation from BULLENN's pressure is less than 2 per cent, assuming a linear density distribution instead of BULLEN's. Then his density may be adopted to determine the crystal constants. If the temperature gradient is steeper than the adiabatic one, the density gradient is smaller than that of BULLEN. But as the term dependent on the temperature cancels the term independent of it, this influence is negligible.

Reference

BERNAL, J. L.:
1936 Observatory. **59**, 268.
BIRCH, F.:
1952 Journ. Geophy. Res. **57**, 227.
BORN, M. and Misra, R. D.:
1940 Proc. Camb. Phil. Soc. **36**, 466.
BRADBURN, M.:
1943 Proc. Camb. Phil. Soc. **39**, 113.
BULLEN, K. E.:
1947 Introduction to the theory of seismogy.
GOW, M, M,:
1944 Proc. Camb. Phil. Soc. **40**, 151.
JACOBS, R. B.:
1938 Phys. Rev. **54**, 468.
PAULING, L.:
1940 Nature of the chemical bond. 335.
SHIMA, M.:
1954 Zishin. **7**, 170. (in Japanese).
VERHOOGEN, A. E.:
1952 Trans. Amer. Geophy Union. **32**, 41.

The Dynamo Theory of the Earth's Main Magnetic Field.

By

Hitoshi TAKEUCHI

Geophysical Institute, Faculty of Science, Tokyo University, Tokyo.

Abstract

The possibility of the dynamo action in the earth core is considered in the case when the toroidal fluid velocity is larger than the poloidal velocity. Infinite numbers of stationary dynamos, each corresponding to a different eigen-value $y=4\pi\kappa a V_{2\cdot 2c}$, are shown to be possible there. The dynamo including the dipole field is that for the smallest y. The geophysical significance of this result is considered in section 4. A mechanism of reversion of the earth's main magnetic field is proposed in section 4.

§ 1. It is now suspected that the earth's main magnetic field is maintained by the dynamo action in the earth core. The essence of this dynamo theory of the earth's main magnetic field is as follows. There may exist in the earth's core chains of relations in which a field H_1 interacts with a motion V_1 to produce a field H_2, which, in turn, interacts with another motion V_2 to reproduce H_1. If it is possible to show the existence of self-sustaining dynamo in the earth's core, the main field may be explained. All that is necessary is a weak initial field to start, and the field will then grow automatically until the energy dissipated becomes equal to that supplied. Thus, the central problem here is to examine whether MAXWELL's equations of electrodynamics possess solutions representing such a self-sustaining dynamo.

A method has recently been developed (ELSASSER 1946, 1947; TAKEUCHI and SHIMAZU 1952, 1953; BULLARD and GELLMAN 1954) for deciding whether any specified motion in a fluid sphere will act as a dynamo. In this method, solutions are obtained by expanding the velocity and the fields in spherical harmonics to give a set of simultaneous linear differential equations among the radial functions corresponding to the respective fields. As the plausible fluid motions in the core, two types of motions are selected. One is of rotational type and the other is of convective type. They are usually called the T_1^0 and S_2^{2c} motions, respectively, and are schematically shown in Fig. 1. Mathematical expressions for them will be obtained by putting $n=1$, $m=0$, $T_1^0(r)=V_1^0(r)$ and $n=2$, $m=2$, $S_2^{2c}(r)=V_2^{2c}(r)$ respectively in the following expressions for

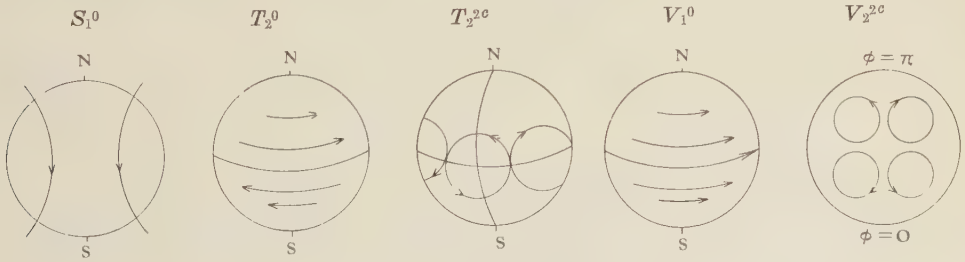

Figure 1.

the (r, θ, ϕ) components of poloidal and toroidal type velocity or fields.

S type (poloidal type) motion or field

r component

$$=-n(n+1)S_n^m(r)r^{n-1}Y_n^m ,$$

θ component

$$=-\left[r\frac{dS_n^m}{dr}+(n+1)S_n^m \right] r^{n-1}\frac{\partial Y_n^m}{\partial\theta} ,$$

ϕ component

$$=-\left[r\frac{dS_n^m}{dr}+(n+1)S_n^m\right]r^{n-1}\frac{\partial Y_n^m}{\sin\theta\,\partial\phi}\,, \quad (1.1)$$

T type (toroidal type) motion or field

r component$=0$,

θ component$=-T_n^m(r)r^n\dfrac{\partial Y_n^m}{\sin\theta\,\partial\phi}$,

ϕ component$=T_n^m(r)r^n\dfrac{\partial Y_n^m}{\partial\theta}$, (1.2)

where

$$Y_n^m=P_n^m(\cos\theta)\begin{matrix}\cos\\ \sin\end{matrix} m\phi\,. \quad (1.3)$$

The upper suffix 2c in S_2^{2c} means $\cos 2\phi$ in Y_2^2.

In order to study the maintenance of magnetic fields by electro-magnetic induction, we must solve the following equations

$$divH=0\,, \quad (1.4)$$

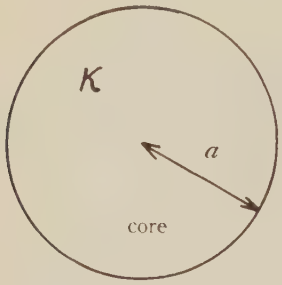

Mantle

Figure 2.

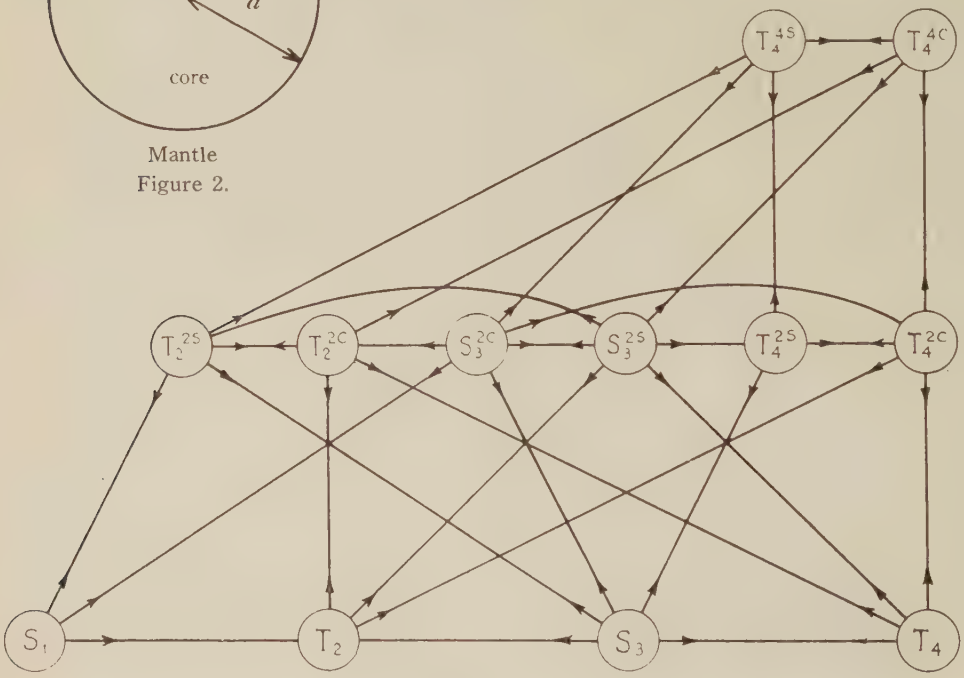

Figure 3.

$$4\pi\kappa\frac{\partial H}{\partial t}=\nabla^2H+4\pi\kappa\,\mathrm{curl}\,(V\times H)=0, \quad (1.5)$$

where H and V are magnetic field and fluid velocity. The system for which the solution is required is shown in Fig. 2. The coordinate system is fixed to the uniformly rotating mantle which is assumed to be an insulator. Thus V in (1.5) denotes the fluid velocity relative to the rotating mantle. By the assumption of "viscous" fluid, V_r, V_θ and V_ϕ must be zero at the core boundary $r=a$.

Taking (1.1) and (1.2) into consideration, we can satisfy these boundary conditions by putting

$$V_1^0(r)=V_2^{2c}(r)=\frac{dV_2^{2c}(r)}{dr}=0\,, \quad (1.6)$$

at $r=a$. In the numerical calculation to follow, we shall take rather tentatively

$$V_1^0(r)=\frac{1}{a}V_{1.0}V_1^0(\xi),\quad V_2^{2c}(r)=\frac{1}{a}V_{2.2c}V_2^{2c}(\xi)\,,$$
$$V_1^0(\xi)=1-\xi,\quad V_2^{2c}(\xi)=(1-\xi)^2,\quad \xi=(r/a), \quad (1.7)$$

which satisfy (1.6). In (1.7), $V_{1.0}$ and $V_{2.2c}$

are some undetermined constants.

On assuming the existence of the above fluid motions in the earth core, we have there a group of magnetic fields which are mutually coupled by the inductive action of the fluid and among which the dipole type field S_1^0 is included. The way of coupling of the fields with n, $m \leq 4$ is shown in Fig. 3. In this figure, the coupling between rows is by the S_2^{2c} motion, that along rows by the T_1^0 motion.

It is needless to say that the chain is continued infinitely with infinite numbers of magnetic fields. In Fig. 3, S_1^0 and T_2^0, for example, mean the magnetic fields by putting $n=1$, $m=0$ in (1.1) and $n=2$, $m=0$ in (1.2), respectively. The first four fields in the chain are shown schematically in Fig. 1.

§ 2. It can be shown (Takeuchi and Shimazu, and Bullard and Gellman, loc. cit.) that the whole problem is reduced to solve the simultaneous differential equations of the following types among the radial functions correspondig to the respective fields

$$
\begin{aligned}
&\xi \frac{d^2 S_1^0}{d\xi^2} + 4 \frac{dS_1^0}{d\xi} = \frac{9\times 24}{5} y \xi^3 V_2^{2c} T_2^{2s} ,\\
&\xi \frac{d^2 T_2^0}{d\xi^2} + 6 \frac{dT_2^0}{d\xi} = -\frac{2}{3} x \frac{dV_1^0}{d\xi} S_1^0 + \frac{72}{7} \frac{y}{\xi^2}\left[\frac{d}{d\xi}(\xi^4 V_2^{2c} T_2^{2c}) + \frac{d}{d\xi}(\xi^3 V_2^{2c}) \xi T_2^{2c}\right],\\
&\xi \frac{d^2 T_2^{2c}}{d\xi^2} + 6 \frac{dT_2^{2c}}{d\xi} = \frac{6}{7} \frac{y}{\xi^2}\left[\frac{d}{d\xi}(\xi^4 V_2^{2c} T_2^0) + \frac{d}{d\xi}(\xi^3 V_2^{2c}) \xi T_2^0\right] - 2x V_1^0 \xi T_2^{2s} ,\\
&\xi \frac{d^2 T_2^{2s}}{d\xi^2} + 6 \frac{dT_2^{2s}}{d\xi} = 2x V_1^0 \xi T_2^{2c} + \frac{2}{3} \frac{y}{\xi^2}\left[3\xi^3 V_2^{2c} \frac{d}{d\xi}\left\{\frac{dS_1^0}{d\xi} + \frac{2}{\xi} S_1^0\right\} + \frac{d}{d\xi}\left\{\frac{d}{d\xi}(\xi^3 V_2^{2c}) S_1^0\right\}\right]
\end{aligned}
\tag{2.1}
$$

under the boundary conditions

$$
\begin{aligned}
&T_2^0(\xi) = T_2^{2c}(\xi) = T_2^{2s}(\xi) = 0,\\
&S_1^0(\xi) + \frac{\xi}{3} \frac{dS_1^0}{d\xi} = 0
\end{aligned}
\tag{2.2}
$$

at $\xi=1$. In (2.1), $S_n^m(\xi)$, $T_n^m(\xi)$, x and y are

$$
\begin{aligned}
&S_n^m(\xi) = a^{n-1} S_n^m(r), \quad T_n^m(\xi) = a^n T_n^m(r),\\
&x = 4\pi\kappa a V_{1\cdot 0}, \qquad y = 4\pi\kappa a V_{2\cdot 2c},
\end{aligned}
\tag{2.3}
$$

respectively. In (2.1), only the magnetic fields with $n \leq 2$ are taken into account. This seems to be a kind of theoretical cut off. Some reasons, however, will be given in section 4 for that this is not a theoretical cut-off and by solving (2.1) we are studying the group of functions corresponding to the first eigen-value. From the above equations, we see at once that our problem is an eigen-value problem for x and y. The physical reason why we get the eigen-value problem here is as follows. From (1.5), we can easily get

$$
\frac{1}{\kappa}\int I^2 dU = \int V \cdot (H \times V) dU , \tag{2.4}
$$

where dU is an element of volume and the integral extends over the whole volume concerned. The left and right hand sides of (2.4) denote the Joule heat and work done on the field by the fluid, respectively. Thus, in order to sustain the fields against the Joule dissipation, we must have a certain amount of work done by the fluid, and this certain amount is determined by solving the eigen-value problem for x and y.

The eigen-value problem (2.1) with (1.7) and (2.2) has been solved numerically by Takeuchi and Shimazu, and Bullard and Gellman (loc. cit.). The noted results obtained are as follows;

(a) We get real eigen-value y in the whole real range of the ratio

$$
\frac{x}{y} = \alpha, \quad \text{say} . \tag{2.5}
$$

Thus, the self-sustaining dynamo is possible, at any rate up to the point where spherical harmonics of the first and second degree are included in the argument.

(b) Except for small α, the eigen-value y and the corresponding eigen-functions vary very slowly with α.

(c) When x or $\alpha \to \infty$, putting

$$T_2^0(\xi)=x\overline{T}_2^0(\xi)\,, \tag{2.6}$$

we have

$$T_2^{2c}(\xi)\sim\frac{1}{x}=0\,,\qquad \frac{d^2\overline{T}_2^0}{d\xi^2}+\frac{6}{\xi}\frac{d\overline{T}_2^0}{d\xi}=\frac{2}{3\xi}\frac{dV_1^0}{d\xi}S_1^0\,,$$

$$\frac{d^2S_1^0}{d\xi^2}+\frac{4}{\xi}\frac{dS_1^0}{d\xi}=\frac{27\times24}{35}y^2\xi^2\frac{V_2^{2c}}{V_1^0}\left[\xi V_2^{2c}\frac{d\overline{T}_2^0}{d\xi}+\left(2\xi\frac{dV_2^{2c}}{d\xi}+7V_2^{2c}\right)\overline{T}_2^0\right]. \tag{2.7}$$

Putting (1.7) into (2.7), we get

$$\frac{d^4\overline{T}_2^0}{d\xi^4}+\frac{12}{\xi}\frac{d^3\overline{T}_2^0}{d\xi^3}+\frac{28}{\xi^2}\frac{d^2\overline{T}_2^0}{d\xi^2}$$

$$+\frac{36\times12}{35}y^2(1-\xi)^2\xi\left[\xi(1-\xi)\frac{d\overline{T}_2^0}{d\xi}+(7-11\xi)\overline{T}_2^0\right]=0\,. \tag{2.8}$$

The corresponding boundary conditions are

$$\overline{T}_2^0(\xi)=0\,,\qquad \frac{dS_1^0}{d\xi}+\frac{3}{\xi}S_1^0\sim\frac{d^3\overline{T}_2^0}{d\xi^3}+10\frac{d^2\overline{T}_2^0}{d\xi^2}+18\frac{d\overline{T}_2^0}{d\xi}=0 \tag{2.9}$$

at $\xi=1$. The eigen-value y in this case is about $42=y_2$, say. The eigen functions corresponding to this eigen value are shown in Table 1.

Table I.

ξ	S_1^0	T_2^0	T_2^{2s}
0	0.2019	—	—
0.1	0.2153	0.01524	1.8432
0.2	0.3442	0.01254	1.1541
0.3	0.6316	0.0^28203	0.3900
0.4	0.8477	0.0^21227	−0.3454
0.5	0.6290	-0.0^27368	−0.6733
0.6	−0.03436	−0.01427	−0.3616
0.7	−0.6540	−0.01626	0.2767
0.8	−0.8300	−0.01301	0.6672
0.9	−0.6802	-0.0^26757	0.5410
1.0	−0.5	0.0	0.0

It must be admitted here that the values of $6\xi^2T_2^{2s}(\xi)$ in Table V of our paper (II) were in error and must be divided by 6.99860 to get correct values.

§3. The results in the last section show that the self-exciting dynamo is possible, at any rate up to the point where spherical harmonics of the first and second degree are included in the argument. As was shown in Fig. 3, however, there are infinite numbers of magnetic fields with $n,\ m>2$ belonging to the group we are considering and it may occur that the self-sustaining dynamo is impossible when the fields of relatively higher harmonics are taken into account. In order to make this point clear, we shall study whether the self-sustaining dynamo is possible or not when spherical harmonics up to the degree four are included in the discussion. In this case, we have twelve equations of the types as in (2.1) among twelve radial functions $S_1^0(\xi)$, $T_2^0(\xi)$, $T_2^{2c}(\xi)$, $T_2^{2s}(\xi)$, $S_3^0(\xi)$, $S_3^{2c}(\xi)$, $S_3^{2s}(\xi)$, $T_4^0(\xi)$, $T_4^{2c}(\xi)$, $T_4^{2s}(\xi)$, $T_4^{4c}(\xi)$ and $T_4^{4s}(\xi)$. When x or α tend to infinity, putting

$$T_2^0(\xi)=x\overline{T}_2^0(\xi),\qquad T_4^0(\xi)=x\overline{T}_4^0(\xi), \tag{3.1}$$

we can transform these equations into

T_2^{2c}, S_3^{2s}, T_4^{2c}, T_4^{4c} and $T_4^{4s}\sim(1/x)=0$,

$$\frac{8}{3}\left(\frac{d^2S_1^0}{d\xi^2}+\frac{4}{\xi}\frac{dS_1^0}{d\xi}\right)-\frac{96\times9}{5}yT_2^{2S}V_2^{2c}\xi^2$$
$$+\frac{96\times12}{7}y\left[\left(\frac{dS_3^{2c}}{d\xi}+4S_3^{2c}\right)V_2^{2c}+S_3^{2c}\left(\xi\frac{dV_2^{2c}}{d\xi}+3V_2^{2c}\right)\right]\xi^2=0\,,$$

$$-\frac{16}{5}S_1^0\frac{dV_1^0}{d\xi}\frac{1}{\xi}+\frac{24}{5}\left(\frac{d^2\overline{T}_2^0}{d\xi^2}+\frac{6}{\xi}\frac{d\overline{T}_2^0}{d\xi}\right)+\frac{48\times6}{35}S_3^0\frac{dV_1^0}{d\xi}\xi=0\,,$$

$$-\frac{288\times6}{35}y\left[\overline{T}_2^0\left(\xi\frac{dV_2^{2c}}{d\xi}+3V_2^{2c}\right)+\frac{d}{d\xi}(\overline{T}_2^0V_2^{2c}\xi^4)\frac{1}{\xi^3}\right]+\frac{96\times6}{5}T_2^{2S}V_1^0$$
$$+\frac{192\times6}{7}S_3^{2c}\frac{dV_1^0}{d\xi}+\frac{32\times6}{7}y\left[\overline{T}_1^0\left(\xi\frac{dV_2^{2c}}{d\xi}+3V_2^{2c}\right)\xi^2+\frac{d}{d\xi}(\overline{T}_4^0V_2^{2c}\xi^6)\frac{1}{\xi^3}\right]=0\,,$$

$$\frac{288\times6}{35}yT_2^{2S}V_2^{2c}+\frac{48}{7}\left(\frac{d^2S_3^0}{d\xi^2}+\frac{8}{\xi}\frac{dS_3^0}{d\xi}\right)+\frac{288\times2}{7}y\left[-3\left(\xi\frac{dS_3^{2c}}{d\xi}+4S_3^{2c}\right)V_2^{2c}\right.$$
$$\left.+2S_3^{2c}\left(\xi\frac{dV_2^{2c}}{d\xi}+3V_2^{2c}\right)\right]-\frac{480\times6}{7}yT_4^{2S}V_2^{2c}\xi^2=0\,,$$

$$\frac{288\times6}{7}y\overline{T}_2^0V_2^{2c}-\frac{480\times12}{7}S_3^{2c}V_1^0-\frac{160\times6}{7}y\overline{T}_4^0V_2^{2c}\xi^2=0\,,$$

$$-\frac{16\times20}{21}S_3^0\frac{dV_1^0}{d\xi}\frac{1}{\xi}+\frac{80}{9}\left(\frac{d^2\overline{T}_4^0}{d\xi^2}+\frac{10}{\xi}\frac{d\overline{T}_4^0}{d\xi}\right)=0\,,$$

$$\frac{960}{7}\left[-4\overline{T}_2^0\left(\xi\frac{dV_2^{2c}}{d\xi}+3V_2^{2c}\right)+3\frac{d}{d\xi}(\overline{T}_2^0V_2^{2c}\xi^4)\frac{1}{\xi^3}\right]-\frac{480\times20}{7}S_3^{2c}\frac{dV_1^0}{d\xi}\xi$$
$$-\frac{480\times6}{77}y\left[10\overline{T}_4^0\left(\xi\frac{dV_2^{2c}}{d\xi}+3V_2^{2c}\right)\xi^2+17\frac{d}{d\xi}(\overline{T}_4^0V_2^{2c}\xi^6)\frac{1}{\xi^3}\right]$$
$$+160\times20T_4^{2S}V_1^0\xi^2=0\,. \tag{3.2}$$

Using the third and fifth differential equations in (3.2), we can express T_2^{2S} and S_3^{2c} in terms of $\overline{T}_2^0(\xi)$ and $\overline{T}_4^0(\xi)$. Inserting the results thus obtained into the first differential equation, we get

$$\frac{d^2S_1^0(\xi)}{d\xi^2}+\frac{4}{\xi}\frac{dS_1^0}{d\xi}=0\,. \tag{3.3}$$

$S_1^0(\xi)$, which satisfies (3.3) and which is finite at $\xi=0$, must be constant. The boundary condition for $S_1^0(\xi)$ is by (2.2)

$$\frac{dS_1^0}{d\xi}+\frac{3}{\xi}S_1^0=0 \tag{3.4}$$

at $\xi=1$. From this, we have

$$S_1^0(\xi)=\text{const}=0\,. \tag{3.5}$$

From (3.2), we get also

$$\frac{d^2S_3^0}{d\xi^2}+\frac{8}{\xi}\frac{dS_3^0}{d\xi}-\frac{28}{11}\xi^2\frac{V_2^{2c}}{V_1^0}y^2\left[3\xi V_2^{2c}\frac{d\overline{T}_4^0}{d\xi}+\left(33V_2^{2c}+8\xi\frac{dV_2^{2c}}{d\xi}\right)\overline{T}_4^0\right]=0\,,$$

$$\frac{d^2\overline{T}_4^0}{d\xi^2}+\frac{10}{\xi}\frac{d\overline{T}_4^0}{d\xi}-\frac{12}{7}\frac{1}{\xi}\frac{dV_1^0}{d\xi}S_3^0=0\,. \tag{3.6}$$

When $V_1^0=1-\xi$ and $V_2^{2c}=(1-\xi)^2$ as in (1.7), the above equations can be reduced to

$$\frac{d^4\bar{T}_4^0}{d\xi^4}+\frac{20}{\xi}\frac{d^3T_4^0}{d\xi^3}+\frac{88}{\xi^2}\frac{d^2T_4^0}{d\xi^2}+\frac{48}{11}y^2\xi(1-\xi)^2\left[3\xi(1-\xi)\frac{d\bar{T}_4^0}{d\xi}+(33-49\xi)\bar{T}_4^0\right]=0\,. \tag{3.7}$$

The corresponding boundary conditions are

$$\bar{T}_4^0=0\,,\qquad \frac{dS_3^0}{d\xi}+\frac{7}{\xi}S_3^0\sim\frac{d^3\bar{T}_4^0}{d\xi^3}+18\frac{d^2\bar{T}_4^0}{d\xi^2}+70\frac{d\bar{T}_4^0}{d\xi}=0 \tag{3.8}$$

at $\xi=1$.

This eigen-value problem was solved numerically to give $y=71=y_4$, say, which is about twice $y_2=42$. If the present problem is to be converging, y must tend to a finite limit on increasing the number of harmonics concerned. From this point of view, the above result is rather unsatisfactory.

When harmonics up to the sixth degree are included in the argument and x or α is made very large, we get

$$S_1^0(\xi)=S_3^0(\xi)=\bar{T}_2^0(\xi)=0 \tag{3.9}$$

in the similar way as in (3.3)-(3.5). We have eight equations of the types as in (3.2) among eight non-vanishing radial functions

$$T_1(\xi)=x\bar{T}_4^0(\xi),\quad T_6^0(\xi)=x\bar{T}_6^0(\xi),\qquad T_2^{2S}(\xi),\ S_3^{2c}(\xi),\ T_4^{2S}(\xi),\ S_5^0(\xi),\ S_5^{2c}(\xi),\ T_6^{2S}(\xi)\,. \tag{3.10}$$

Putting $V_1^0=1-\xi$ and $V_2^{2c}=(1-\xi)^2$ as in (1.7) or in (3.7), we can reduce these equations into

$$\frac{d^4\bar{T}_6^0}{d\xi^4}+\frac{28}{\xi}\frac{d^3\bar{T}_6^0}{d\xi^3}+\frac{180}{\xi^2}\frac{d^2\bar{T}_6^0}{d\xi^2}+\frac{18\times36\times36}{13\times13\times33}y^2\xi(1-\xi)^2\left[3\xi(1-\xi)\frac{d\bar{T}_6^0}{d\xi}+(45-65\xi)\bar{T}_6^0\right]=0\,. \tag{3.11}$$

The corresponding boundary conditions are

$$\bar{T}_6^0=0\,,\qquad \frac{dS_5^0}{d\xi}+\frac{11}{\xi}S_5^0\sim\frac{d^3\bar{T}_6^0}{d\xi^3}+26\frac{d^2\bar{T}_6^0}{d\xi^2}+154\frac{d\bar{T}_6^0}{d\xi}=0 \tag{3.12}$$

at $\xi=1$. This eigen value problem was solved numerically to give $y=117=y_6$ say, which again differs much from y_2 and y_4 obtained before.

Proceeding in this way, we can get the following general results. These results were obtained by TAKEUCHI and BULLARD and reported partly in BULLARD and GELLMAN's paper (see p. 266-267) already cited. In the n-th *approximation*, say, in which harmonics up to the n-th degree are taken into account and x or α is made very large, we get $S_1^0, S_3^0,\cdots S_{n-3}^0$; $S_3^{2c}, S_5^{2c},\cdots, S_{n-5}^{2c}$; $\bar{T}_2^0, T_4^0,\cdots, T_{n-4}^0, T_2^{2S}, T_4^{2S},\cdots, T_{n-6}^{2S}=0$ and we have eight differential equations of the types as in (3.2) among eight non-vanishing radial functions

$$\begin{gathered}T_{n-2}^0(\xi)=x\bar{T}_{n-2}^0(\xi)\,,\qquad T_n^0(\xi)=x\bar{T}_n^0(\xi)\,,\\ T_{n-4}^{2S}(\xi),\ S_{n-3}^{2c}(\xi),\ T_{n-2}^{2S}(\xi),\ S_{n-1}^0(\xi),\ S_{n-1}^{2c}(\xi),\ T_n^{2S}(\xi).\end{gathered} \tag{3.13}$$

Putting $V_1^0=1-\xi$ and $V_2^{2c}=(1-\xi)^2$ as in (1.7) or in (3.7), we can reduce these equations into

$$\frac{d^4\bar{T}_n^0}{d\xi^4}+\frac{4(n+1)}{\xi}\frac{d^3\bar{T}_n^0}{d\xi^3}+\frac{2n(2n+3)}{\xi^2}\frac{d^2\bar{T}_n^0}{d\xi^2}+\frac{162n(n-1)y^2}{(2n-3)(2n-1)^2(2n+1)^2(2n+3)}\xi(1-\xi)^2$$
$$\times\left[A(n)\xi(1-\xi)\frac{d\bar{T}_n^0}{d\xi}+\left\{B(n)-\frac{C(n)}{3}\xi\right\}\bar{T}_n^0\right]=0\,,$$

$$A(n)=4n^4+12n^3-13n^2-33n+18, \quad B(n)=8n^5+36n^4+10n^3-105n^2-63n+54,$$
$$C(n)=32n^6+164n^4+100n^3-485n^2-417n+306. \tag{3.14}$$

The corresponding boundary conditions are

$$\bar{T}_n^0=0, \quad \frac{dS_{n-1}}{d\xi}+(2n-1)S_{n-1}\sim\frac{d^3\bar{T}_n^0}{d\xi^3}+2(2n+1)\frac{d^2\bar{T}_n^0}{d\xi^2}+2(n+1)(2n-1)\frac{d\bar{T}_n^0}{d\xi}=0 \tag{3.15}$$

at $\xi=1$. The eigen value y_n, say, in this general case is shown to be between $O((2n)^{3/2})$ and $O((2n)^{5/2})$ as $n\to\infty$. In the $(n+1)$-th *approximation*, in which harmonics up to the $(n+1)$-th degree are taken into account and $\varkappa$ or α is made very large, $S_{n-1}^0(\xi)$, $S_{n-3}^{2c}(\xi)$, $\bar{T}_{n-2}^0(\xi)$ and $T_{n-4}^{2s}(\xi)$ which did not vanish in the n-th approximation become zero anew. Thus it seems that as n tends to infinity, every radial function vanishes and we have also a strange result that the eigen value $y=4\pi\kappa aV_{2\cdot 2c}$ increases without limit with increasing n.

The most fundamental assumption in carrying out the analysis in the present section is that in dealing with (3.13), for example, we are making the n-th *approximation* for the one and the same system, the first *approximation* of which is the S_1^0-T_2^0-T_2^{2c}-T_2^{2s} dynamo in section 2. From this point of view, y_n obtained by solving (3.14) and (3.15) is the n-th *approximation* for the "true" y and y_n must tend to this finite limit as $n\to\infty$, if the present problem is converging. The result in this section is against this anticipation.

§ 4. Looking from a little different point of view, we can get very hopeful interpretation of the results in the last section. In dealing with (3.13), for example, we considered in the last section that we are making the n-th approximation for the system in section 2. From the present point of view, this interpretation was wrong. Our new interpretation is in dealing with (3.13), we are studying the n-th eigen function (or rather eigen *group of functions*) corresponding to the n-th eigen value y_n, which, from the present point of view, is not the n-th approximation for the first eigen value as was supposed in the last section. There are several reasons in believing that our present point of view is all right. At first, y_n increases without limit as $n\to\infty$. This should be so, if y_n is the n-th eigen value in the present problem. Secondly, only the $(n-4)$, $(n-3)$, $\cdots$, n-th harmonics belong to the group of fields corresponding to y_n. This also should be so, if y_n is the eigen value corresponding to the n-th "over tone". We are, so to say, in the similar position as those who are studying the n-th over tone of vibrating string streched between two fixed points. The differential equation for the vibrating string is

$$\frac{d^2S}{d\xi^2}+yS=0, \tag{4.1}$$

where y is the eigen value to be determined by the following boundary conditions

$$S(\xi)=0 \quad \text{at} \quad \xi=0 \quad \text{and} \quad 1. \tag{4.2}$$

(4.1) is of the similar type as the equations in (2.1), say. If we try to get the n-th over tone of the string in which harmonics up to the n-th degree are included *but not the* $(n+1)$-th harmonic, we shall have

$$y=\left(\frac{n\pi}{l}\right)^2=y_n, \text{ say and } S=\sin\frac{n\pi\xi}{l}=S_n, \text{say.} \tag{4.3}$$

In this case, $y_n=O(n^2)$ as n tends to infinity, to be compared with $y_n=O((2n)^{3/2})\sim O((2n)^{5/2})$ obtained immediately after (3.15). The n-th eigen function in this case is simply $S=\sin(n\pi\xi/l)$, to be compared with the eigen *group of functions* in (3.13). This difference in simplicity is not so serious. By solving the eigen value problem (3.14) with (3.15), we can determine the relative magnitude of each radial function in (3.13). Calculating the field corresponding to each radial function and summing up the results thus obtained, we shall have the expression $H(r, \theta, \phi; y_n)$ or more simply $H(y_n)$, say, for the field corresponding to y_n. This expression $H(y_n)$ is, at least in principle, as simple as S_n in (4.3).

The physical reason why we get the larger eigen value y for the higher over tone is as follows. As is seen from (3.13), fields of the

higher harmonics, which are known to dacay more rapidly are contained in the higher over tone. Thus, as is shown in (2.4), in order to maintain the higher over tone, we must supply it with the more energy, and we have the larger y. From the above consideration, we can get rough idea on what the field $H(y_n)$ will become when it is driven by fluid motion for which $y=4\pi\kappa a V_{2.2c}$ is larger or smaller than y_n. In the former case, given more energy than dissipated, the field $H(y_n)$ will develop, while in the latter case, it will decay. Suppose here that we have in the earth's core y just equal to y_2. Under this condition, the fields corresponding to $H(y_4)$, $H(y_6),\cdots$ will decay soon, even if they existed at a certain time while the field $H(y_2)$ will be sustained. This is very similar to what is occuring in the earth. Thus in our earth, magnetic fields of relatively lower harmonics (the dipole field, for example) remain almost constant through the geological time, while magnetic fields of relatively higher harmonics are changing quite rapidly. From the present point of view, we have no more thing to do for the self-sustaining dynamo model in section 2. It is complete by itself. It is the dynamo corresponding to the first *energy level*, so to say, y_2, not the first approximation for some dynamo, as was supposed in section 2 and 3. The eigen *group of functions* for y_2 is shown in Table 1. It will be interesting to work out the eigen *group of functions* for higher y_n*. A word must be added here on that we have $\overline{T}_2^0(\xi)$, for example, in both $H(y_2)$ and $H(y_4)$. There is no interaction through this (or rather these) $\overline{T}_2^0(\xi)$ between $H(y_2)$ and $H(y_4)$. For example, in the above supposed case, in which we have y just equal to y_2, the $\overline{T}_2^0(\xi)$ field in $H(y_4)$ group will decay according to the decay law of the group, independently of the $\overline{T}_2^0(\xi)$ field in $H(y_2)$, which remains constant through the time.

Although the above results were obtained under the condition that x or α is very large, this condition is not so serious. This is because, except for small α, the eigen value y and the corresponding eigen group of functions vary very slowly with α. In fact, numerical results obtained by BULLARD and GELLMAN (see p. 246 of their paper already cited) show that there is almost no difference between the results obtained when $\alpha=(x/y)$ is 10 and ∞. Thus we may expect the similar results as above when x or α is not so large.

It is now suspected that the earth magnetic field was reversed from time to time through the geological time. At present, we do not know exactly how this reversion took place. From the results obtained above, however, we may construct the following model for the reversion. Suppose that at a certain time in the earth's history, convective fluid motion in the earth's core became weak in strength and the corresponding $y=4\pi\kappa a V_{2.2c}$ became smaller than its stationary value y_2. Suppose further that, after a time of smaller y, the convective motion and the corresponding y came back to what they were before. Through the time of this change, the rotational motion of the fluid was kept stronger than the convective motion, as was assumed in the present paper. This is an event not so unlikely to occur in the earth core. It is not necessary that any motion changes its direction. The convective fluid motion has only to make a certain fluctuation around its stationary value. This kind of thing, more drastic than supposed here, was supposed to occur in the earth mantle in order to explain mountain building cycles (see, for example, D. T. GRIGGS, 1939). Now, let us see what will occur in our model earth. According to what was said before, the field $H(y_2)$ will decay so long as y is smaller than y_2, and will vanish in a time comparable with its free decay time. Given afterward y equal to its stationary value y_2, the field will be restored. Whether the new field, however, is in the same direction as before or not will be determined only by chance. Thus, in some case, we shall have the reversion of the earth magnetic field.

Appendix

Recently, S. KATO and H. TAKEUCHI (Geo-

* see appendix

physical Institute, Faculty of Science, Tokyo University) have made the numerical integration of (3.7) under the boundary conditions (3.8) and obtained the eigen *group of functions* corresponding to $y_4=71$. In a different meaning and in a different way from here, the eigen group of functions has already been obtained by BULLARD and GELLMAN. As was shown in (3.5), S_1^0 in this group must be zero. In BULLARD and GELLMAN's paper (1954), however, this function is not regarded as zero. In fact, in Table 6b in their paper which is concerned with the same problem as ours, we find S_1^0 different from zero. As was pointed out by them (see p 258 of their paper), this illustrates a general difficulty in the numerical solution of complicated sets of differential equations by the finite difference method used by them. Anyway, this error may cause other troubles to make their result useless. From this point of view only, it is desirable to make the numerical integration of (3.7) and get the correct eigen group of functions corresponding to $y_4=71$.

In order to compare our results with theirs, after finishing the numerical integration, we must transform our radial functions into theirs. The correspondence between their notations and ours is shown in Table 1.

Table 1.

BULLARD and GELLMAN's	Ours
r	ξ
$S_n^m(r)$	$-\xi^{n+1}S_n^m(\xi)$
$T_n^m(r)$	$-\xi^{n+1}T_n^m(\xi)$
V	y
ε	$\alpha=x/y$
Q_s	$-\xi^3 V_2^{2c}(\xi)$
Q_T/ε	$-\xi^2 V_1^0(\xi)$

We may disregard the difference of $\pm$sign

Table 2-a.

r	S_3^0	T_2/ε	T_2^{2s}	S_3^{2c}	T_4^{2s}	T_4/ε
0	0.0	0.0	0.0	0.0	0.0	0.0
0.1	-0.0^35000	0.0^21972	0.0^24971	0.0^45224	0.0^42662	0.0^46651
0.2	-0.0^32700	0.01580	0.03210	0.0^37283	0.0^35740	0.0^21123
0.3	−0.01027	0.05341	0.08403	0.0^23113	0.0^21884	0.0^27205
0.4	−0.06163	0.1291	0.1738	0.0^28834	−0.01652	0.01160
0.5	−0.1308	0.2671	0.3421	0.02221	−0.1052	−0.05223
0.6	−0.01842	0.5029	0.4456	0.04839	−0.2136	−0.3047
0.7	0.3619	0.8115	0.0^32100	0.07627	−0.1141	−0.7184
0.8	0.6601	1.0000	−1.0169	0.07425	0.2117	−0.9842
0.9	0.6328	0.7779	−1.4867	0.03269	0.3737	−0.7793
1.0	0.5007	0.0	0.0	0.0	0.0	0.0

Table 2-b.

r	S_3^0	T_2/ε	T_2^{2s}	S_3^{2c}	T_1^{2s}	T_1/ε	S_1^0
0	0.0	0.0	0.0	0.0	0.0	0.0	0.0
0.1	0.000	0.001	0.002	0.000	0.000	0.000	0.000
0.2	0.000	0.005	0.011	0.000	0.000	0.001	0.003
0.3	−0.006	0.019	0.034	0.001	0.000	0.004	0.008
0.4	−0.038	0.056	0.108	0.004	−0.018	0.009	0.020
0.5	−0.089	0.165	0.287	0.013	−0.087	−0.017	0.036
0.6	−0.030	0.431	0.402	0.037	−0.166	−0.157	0.020
0.7	0.231	0.810	−0.038	0.066	−0.100	−0.418	−0.068
0.8	0.435	1.000	−0.930	0.064	0.107	−0.590	−0.152
0.9	0.392	0.729	−1.226	0.027	0.204	−0.458	−0.166
1.0	0.236	0.0	0.0	0.0	0.0	0.0	−0.138

Table 3-a.

r	S_1	T_2/ε	T_2^{2s}
0.0	0.0	0.0	0.0
0.1	0.06599	−0.02287	−0.05648
0.2	0.04219	−0.01506	−0.02829
0.3	0.1742	−0.03324	−0.03227
0.4	0.4156	−0.01179	0.06775
0.5	0.4819	0.1382	0.2579
0.6	−0.03791	0.4625	0.2394
0.7	−0.9820	0.8374	−0.2908
0.8	−1.6279	1.0000	−1.0470
0.9	−1.6883	0.7394	−1.2087
1.0	−1.5322	0.0	0.0

Table 3-b.

r	s_1^0	T_2/ε	T_2^{2s}
0.0	0.0	0.0	0
0.1	0.019	−0.002	−0.006
0.2	0.084	−0.014	−0.021
0.3	0.239	−0.022	0.001
0.4	0.444	0.022	0.121
0.5	0.388	0.199	0.273
0.6	−0.257	0.532	0.169
0.7	−1.211	0.882	−0.394
0.8	−1.764	1.000	−1.085
0.9	−1.741	0.717	−1.177
1.0	−1.568	0.0	0.0

between their radial functions corresponding to the magnetic fields and ours, since in the eigen value problem as ours, we are not interested in the absolute values of the eigen functions.

On the other hand, the difference of sign in the radial function corresponding to the velocity fields cause some difficulties. Anyway in Table 2-a, are shown the values of BULLARD and GELLMAN's radial functions transformed from our calculated results. The corresponding results obtained by BULLARD and GELLMAN are shown in Table 2-b. Comparing these tables, we see no serious difference between them other than in S_1^0. This is a very fortunate result. In order to get the eigen functions corresponding to y_4, we have only to solve a differential equation of the fourth order. Compared with the rather complicated method by BULLARD and GELLMAN to get them, this is a considerable simplification.

By the way, we shall make the similar comparison of the radial functions corresponding to $y_2=42$. In Table 3-a, are shown the values of BULLARD and GELLMAN's radial functions transformed from Table 1 in section 2. The corresponding values by BULLARD and GELLMAN are shown in Table 3-b. Here also, the agreement between the results is good enough.

References

BULLARD, E. C. and GELLMAN, H.:
1954 Homogeneous dynamos and terrestrial magnetism, Phil. Trans. Roy. Soc. London, **247**, 213.

ELSASSER, W. M.:
1946 Induction effects in terrestrial magnetism (Part 1), Phys. Rev., **69**, 106.
1946 (Part 2), Phys. Rev., **70**, 202.
1947 (Part 3), Phys. Rev., **72**, 821.

GRIGGS, D.:
1939 A theory of mountain building, Amer. Journ. Sci., **237**, 611.

TAKEUCHI., H., and Y. SHIMAZU.:
1952 On a self-exciting process in magneto-hydrodynamics, J. Phys. Earth, **1**, 1.
1952 (II), J. Phys. Earth, **1**, 57.
1953 (III), J. Phys. Earth, **2**, 5.
1953 J. Geophys. Res., **58**, 497.

Wave Generations in a Superficial Layer Resting on a Semi-infinite Lower Layer.

By
Hitoshi TAKEUCHI
Geophysical Institute, Faculty of Science, Tokyo University, Tokyo.
and
Naota KOBAYASHI
Department of Precision Mechanics, Faculty of Technology, Chūō University, Tokyo.

Abstract

Wave generations from a line source of SH type in a superficial layer resting on a lower layer are studied. The movement at a point is shown to be composed of pulses, each representing a disturbance arriving at the theoretical time for one of the reflected and refracted waves. When we superpose these component waves, we get, at points far away from the wave origin, the theoretical movement which is very similar to that predicted by the normal mode solution. The reflected and refracted waves are shown to appear at the respective critical distances.

Thus we can make clear how the transition from the aperiodic motion near the origin to the complicated oscillatory motion far away from the origin takes place. The most significant result obtained is that the amplitude of the reflected wave is very large at the respective critical distance given by (3.12).

Examples which have some connections with this result are given in the last section.

§ 1. In connection with the generation of LOVE waves and the propagation of sound waves in the ocean, many theoretical studies have been made on the wave generations from line or point sources in a superficial layer resting on a semi-infinite lower layer (H. JEFFREYS, M. MUSKATS, K. SEZAWA, S. SATO, C.L. PEKERIS, M. EWING, H. HONDA). Formal solutions of these problems are obtained in the forms of complex integrals. The most successful approximate way in evaluating the integrals is to use the steepest descent method or the stationary phase method. When applied to the present problem, it gives the dispersion formula in terms of the group velocity. Using the dispersion formula thus obtained, we can successfully interpret the wave phenomena at points far away from the wave origin. Being essentially the principle of complete wave interference, the steepest descent or stationary phase method is not useful at points near the wave origin, nor immediately after the time of beginning of the movement. At such points and at such a time, another method must be used which is complementary to the steepest descent or stationary phase method.

As such a complementary method, we shall in the analysis to follow use a kind of ray theory. We shall expand the integral in a series of exponentials, each representing a disturbance arriving at the theoretical time for one of the reflected and refracted waves. This method has already been used by some of the authors above refered to. But it seems to the present authors that its importance has never been fully appreciated. To make clear the importance of the ray theory in the problem of wave generations will be one of the objects of the present paper. In the case of explosive wave origin, the movement near the origin is very simple. On the other hand, as is shown by the steepest descent method, the movement far away from the origin is very complicated. Its oscillatory character seems to be due to the multiple reflections in the superficial layer. But it has never been

shown how this transition from the aperiodic motion to the periodic one takes place. In the analysis to follow, by means of the ray theory, this transition will clearly be shown.

§ 2. As the problem of sound wave propagation in a superficial fluid layer is shown to be mathematically quite similar to that of SH wave in superficial elastic layer, we shall confine ourselves to the study of the latter problem. Refering to the rectangular coordinates in Fig. 1, we shall denote the density

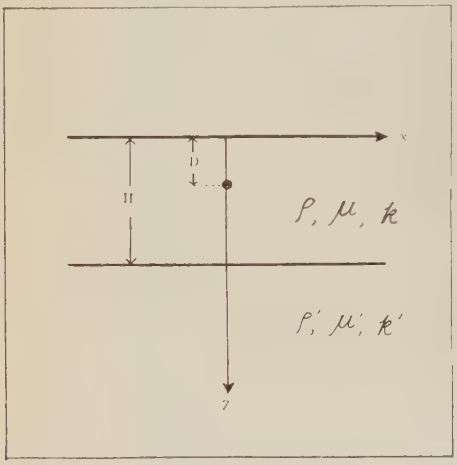

Fig. 1

and rigidity in the superficial and the lower layer by ρ, μ and ρ', μ', respectively. The thickness of the superficial layer is H, and the wave origin is at $(x=y=0, z=D)$. The only non-vanishing displacement component of the *SH* wave is the y component. Denoting this by v and assuming

$$v \propto e^{i(pt+\xi x)} , \tag{2.1}$$

we have the following differential equation for the z part of v, $v(z)$, say, in the superficial layer

$$\left(\frac{d^2}{dz^2} - \beta^2\right) v(z) = 0 , \tag{2.2}$$

where

$$\beta^2 = \xi^2 - k^2 , \qquad k = p\sqrt{\frac{\rho}{\mu}} = \frac{p}{V_s} , \tag{2.3}$$

V_s being the distortional wave velocity in the upper layer. Similarly, in the lower layer, we have

$$\left(\frac{d^2}{dz^2} - \beta'^2\right) v(z) = 0 ,$$

$$\beta'^2 = \xi^2 - k'^2 ,$$

$$k' = p\sqrt{\frac{\rho'}{\mu'}} = \frac{p}{V_s'} , \tag{2.4}$$

V_s' being the distortional wave velocity in the lower layer. The line source at $z=D$ is expressed by

$$v = \frac{\pi}{2i} e^{ipt} H_0^{(2)}(kR) = \frac{e^{ipt}}{2} \int_{-\infty}^{+\infty} \frac{e^{\mp\beta(D-z)+i\xi x}}{\beta} d\xi$$

for $z \lesseqgtr D$, (2.5)

where

$$R^2 = (D-z)^2 + x^2 . \tag{2.6}$$

The z part of v in (2.5) is

$$v = \frac{1}{2\beta} e^{\mp\beta(D-z)} . \tag{2.7}$$

Correspondining to this v, we have some secondary v as the solutions of (2.2) and (2.4). Thus the total v in the upper and lower layer will be

$$v = Ae^{-\beta z} + Be^{\beta z} + \frac{1}{2\beta} e^{\mp\beta(D-z)} \quad \text{for} \quad D \lesseqgtr z \lesseqgtr H ,$$

$$v = Ce^{-\beta' z} \quad \text{for} \quad z \gtreqless H , \tag{2.8}$$

where A, B and C are some constants to be determined by boundary conditions. The boundary conditions to be satisfied are the continuity of stress and displacement at the boundary $z=H$ and the stress vanishiment at $z=0$. These boundary conditions are satisfied by making $v(z)$ and $\mu(dv/dz)$ continuous at $z=H$ and $dv/dz=0$ at $z=0$. Having thus determined A, B and C, we get $v(z=0)$ as follows

$$v(z=0) = e^{ipt} \int_{-\infty}^{+\infty} \frac{e^{-\beta D} + Ke^{\beta(D-2H)}}{\beta(1-Ke^{-2\beta H})} e^{i\xi x} d\xi , \tag{2.9}$$

where

$$K = \frac{\mu\beta - \mu'\beta'}{\mu\beta + \mu'\beta'} . \tag{2.10}$$

Putting $D=0$ for a while, and expanding the integrand in (2.9), we have

$$v(z=0)=\sum_{n=0}^{\infty} v_n ,$$

$$v_n=\varepsilon_n e^{ipt}\int_{-\infty}^{+\infty}\frac{K^n}{\beta}e^{-2nH\beta+i\xi x}\,d\xi , \qquad (2.11)$$

where

$$\varepsilon_0=1 \quad \text{and} \quad \varepsilon_n=2 \quad (n\neq 0) . \qquad (2.12)$$

In order not to make $v(z)$ infinite at $z\to\infty$ and in order to satisfy the radiation condition (Sommerfeld, A.: 1949, p. 189) at $x\to\infty$, we must have

$$\text{the real part of} \quad \beta \text{ and } \beta'>0 . \qquad (2.13)$$

We can satisfy these conditions by interpreting the integral in (2.11) as the limit of the contour integral

$$v_n=\varepsilon_n e^{ipt}\int_L\left[\frac{\mu\sqrt{\zeta^2-k^2}-\mu'\sqrt{\zeta^2-k'^2}}{\mu\sqrt{\zeta^2-k^2}+\mu'\sqrt{\zeta^2-k'^2}}\right]^n \times\frac{\exp(-2nH\sqrt{\zeta^2-k^2}+i\zeta x)}{\sqrt{\zeta^2-k^2}}d\zeta \qquad (2.14)$$

when semi-circles around four points $\pm k$ and $\pm k'$ are made vanishingly small and $\sqrt{\zeta^2-k^2}$ and $\sqrt{\zeta^2-k'^2}$ at the left end of L are assumed to be positive real. The integral in (2.14) is of the similar type as that we had in a previous paper (Takeuchi, H. and Kobayashi, N.: 1955). Thus following the way in that paper, we shall transform (2.14) into

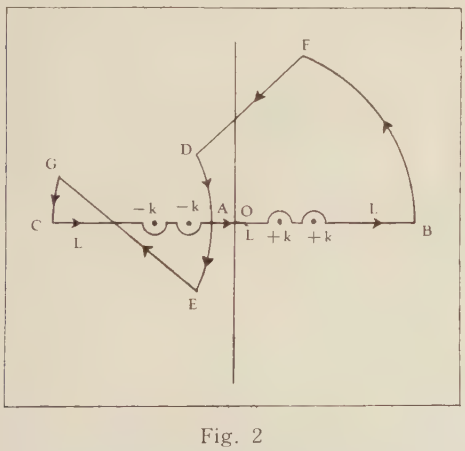

Fig. 2

$$v_n=\varepsilon_n e^{ipt}\int_{E\to A\to D}\left[\frac{\mu\sqrt{\zeta^2-k^2}-\mu'\sqrt{\zeta^2-k'^2}}{\mu\sqrt{\zeta^2-k^2}+\mu'\sqrt{\zeta^2-k'^2}}\right]^n \times\frac{\exp(-2nH\sqrt{\zeta^2-k^2}+i\zeta x)}{\sqrt{\zeta^2-k^2}}d\zeta , \qquad (2.15)$$

where $E\to A\to D$ is the path on which

$$Z=i\zeta x-2nH\sqrt{\zeta^2-k^2} \qquad (2.16)$$

in (2.15) is pure imaginary. The points E and D will be made far away from A in the following analysis.

§ 3. In order to transform (2.15) into a more convenient form for numerical calculations, we shall make some mathematical considerations in the present section.

(a) At first, we shall assume that the wave velocity in the lower layer is larger than that in the superficial layer. This means $k'<k$ as is shown in Fig. 2. Now it can easily be shown that the coordinate ζ at A and Z in (2.16) there are

$$\zeta=-\frac{kx}{r} , \quad Z=-ikr , \quad r=\sqrt{x^2+(2nH)^2} , \qquad (3.1)$$

respectively.

(b) ζ, $\sqrt{\zeta^2-k^2}$ and $\sqrt{\zeta^2-k'^2}$ on AD are of the forms $-(+)+i(+)$, where $(+)$'s are some positive real numbers. ζ on AE is the complex conjugate of that on AD, whereas $\sqrt{\zeta^2-k^2}$ and $\sqrt{\zeta^2-k'^2}$ on AE are $-$(complex conjugates) of those on AD, respectively.

(c) $Z=i\zeta x-2nH\sqrt{\zeta^2-k^2}$ on AD and AE can be put

$$Z=-ikr\cosh\phi , \quad 0\leq\phi\leq+\infty , \qquad (3.2)$$

where

$$\zeta=\frac{k}{r}(-x\cosh\phi\pm i2nH\sinh\phi) ,$$

$$d\zeta=\pm\sqrt{\zeta^2-k^2}\,d\phi , \qquad (3.3)$$

respectively.

(d) By means of (3.3), (2.15) is transformed into

$$v_n=2\varepsilon_n\int_0^{\infty}V(\zeta)\exp\{i(pt-kr\cosh\phi)\}d\phi , \qquad (3.4)$$

where V is the real part of

$$\left[\frac{\mu\sqrt{\zeta^2-k^2}-\mu'\sqrt{\zeta^2-k'^2}}{\mu\sqrt{\zeta^2-k^2}+\mu'\sqrt{\zeta^2-k'^2}}\right]^n$$

on AD.

(e) Putting

$$\zeta=k\zeta'=pb\zeta' , \quad b=\frac{1}{V_s} , \qquad (3.5)$$

and assuming $S(t)$ instead of e^{ipt} in (3.4) for the time variations of the displacement and stress near the origin, we have

$$v_n=2\varepsilon_n\int_0^\infty V(\zeta')S(t-br\cosh\phi)d\phi\ . \quad (3.6)$$

(f) The stress near the origin is given by

$$T_{Rx}=T_{Rz}=0\ ,\quad T_{Ry}=\mu\frac{\partial v}{\partial R}\to-\frac{\mu}{R}S(t)\ . \quad (3.7)$$

In the following numerical calculations, we shall assume

$$S(t)=0 \quad \text{for} \quad t\leqq 0\ ,$$

$$S(t=0)=\infty\ ,\quad \int S(t=0)dt=\text{finite, S, say.} \quad (3.8)$$

(g) For the time variation in (3.8), we have

$$v_n=\frac{2\varepsilon_n S}{br}\left(\frac{V(\zeta')}{\sinh\phi}\right)_{\cosh\phi=t/br=V_s t/r}\ ,$$

$$0\leqq\phi\leqq\infty\ , \quad (3.9)$$

where

$$\zeta'=\frac{1}{r}(-x\cosh\phi+i2nH\sinh\phi)\ ,$$

$$r=\sqrt{x^2+(2nH)^2} \quad (3.10)$$

and $V(\zeta')$ is

the real part of

$$\left[\frac{\mu\sqrt{\zeta'^2-1}-\mu'\sqrt{\zeta'^2-m^2}}{\mu\sqrt{\zeta'^2-1}+\mu'\sqrt{\zeta'^2-m^2}}\right]^n \quad \text{on} \quad AD\ , \quad (3.11)$$

m being $m=b'/b=V_s/V_s'$. It is to be noted here that the real and imaginary part of $\sqrt{\zeta'^2-1}$ or $\sqrt{\zeta'^2-m^2}$ on AD are negative and positive, respectively. (3.9)–(3.11) are the formulas by which we can calculate the displacement on the free surface for the wave origin (3.7) and (3.8).

(h) When

$$\frac{kx}{r}>k' \quad \text{or} \quad x>\frac{2nHk'}{\sqrt{k^2-k'^2}}=\frac{2nHV_s}{\sqrt{V_s'^2-V_s^2}}\ , \quad (3.12)$$

the point A comes to the left-hand side of $\zeta=-k'$ and there occurs the similar difficulty as we had in the paper above refered to. In this case, following the way in the above paper, we have the following additional v_n

v_n (additional)

$$=\frac{2\varepsilon_n SU}{b'x\sqrt{\left(\frac{b}{b'}\right)^2-\xi^2}\left[1-\frac{2nH}{x}\frac{\xi}{\sqrt{(b/b')^2-\xi^2}}\right]}\ ,$$

$$1\leqq\xi\leqq\frac{bx}{b'r}\ ,$$

$$\frac{t}{b'x}=\xi+\frac{2nH}{x}\left[\left(\frac{b}{b'}\right)^2-\xi^2\right]^{1/2}\ , \quad (3.13)$$

whese U is

the imaginary part of

$$\left[\frac{\mu\sqrt{\zeta^2-k^2}-\mu'\sqrt{\zeta^2-k'^2}}{\mu\sqrt{\zeta^2-k^2}+\mu'\sqrt{\zeta^2-k'^2}}\right]^n\ . \quad (3.14)$$

$\sqrt{\zeta^2-k^2}$ and $\sqrt{\zeta^2-k'^2}$ in (3.14) must be interpreted as $i[(b/b')^2-\xi^2]^{1/2}$ and $(\xi^2-1)^{1/2}$, ξ being shown in (3.13).

§ 4. The time of beginning of the elementary wave in (3.9) is given by

$$t=\frac{r}{V_s}=\frac{\sqrt{x^2+(2nH)^2}}{V_s}\ . \quad (4.1)$$

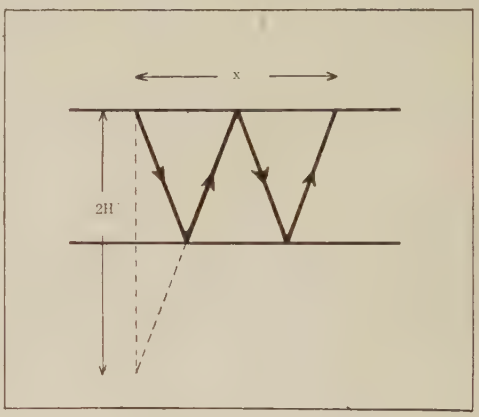

Fig. 3

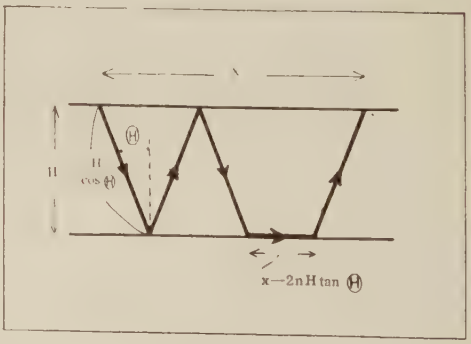

Fig. 4

As is seen from Fig. 3, this is the theoretical time of arriving of the wave reflected n times at the lower boundary. The time of beginning of the elementary wave in (3.13) is given by

$$t=\frac{2nH}{V_s\cos\Theta}+\frac{x-2nH\tan\Theta}{V_s'}\ ,$$

$$\sin\Theta=\frac{V_s}{V_s'}\ . \quad (4.2)$$

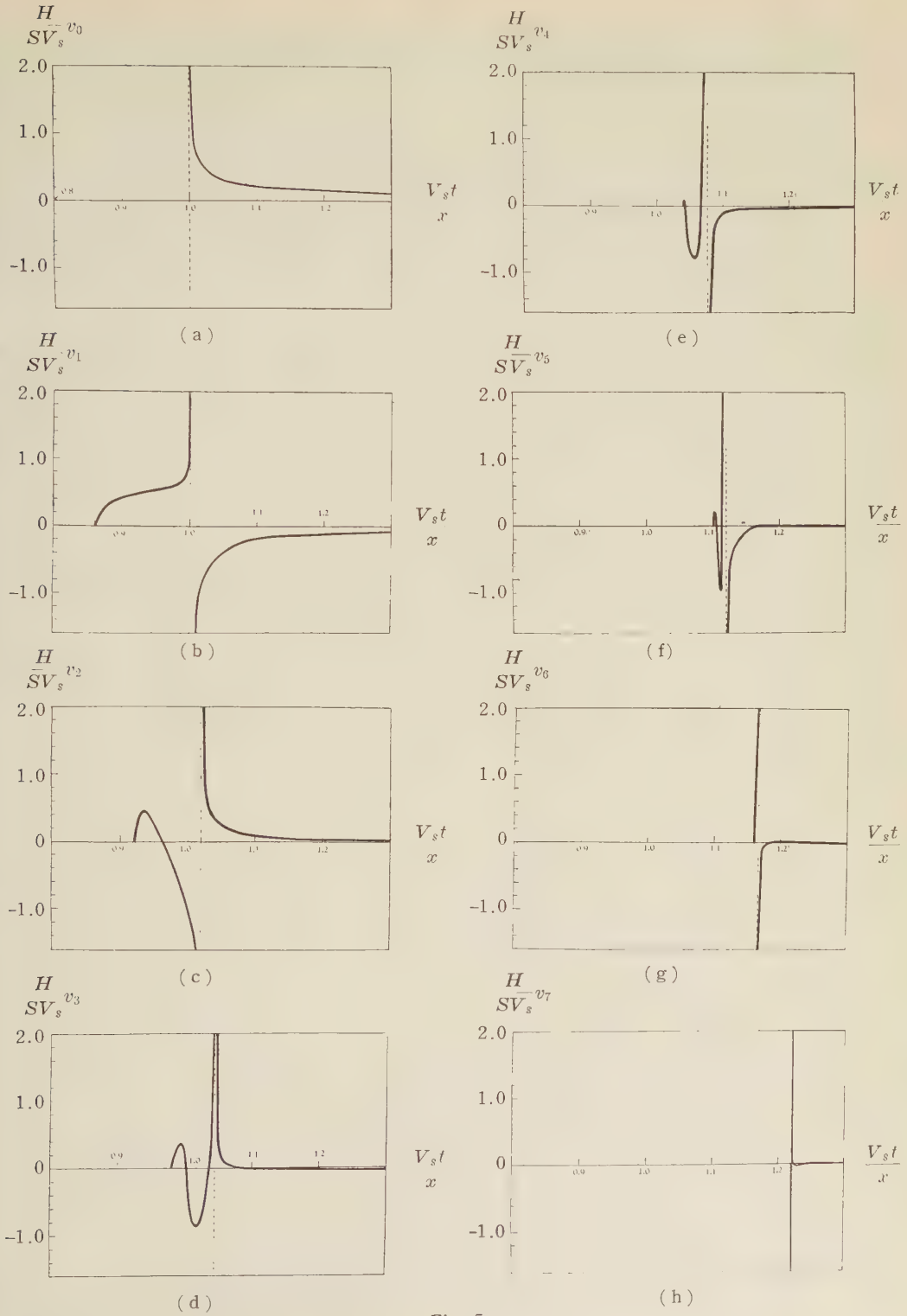
$\frac{H}{SV_s}v_0$
2.0
1.0
0
-1.0
$\frac{V_s t}{x}$
(a)
$\frac{H}{SV_s}v_1$
(b)
$\frac{H}{SV_s}v_2$
(c)
$\frac{H}{SV_s}v_3$
(d)
$\frac{H}{SV_s}v_4$
(e)
$\frac{H}{SV_s}v_5$
(f)
$\frac{H}{SV_s}v_6$
(g)
$\frac{H}{SV_s}v_7$
(h)

Fig. 5

As is shown in Fig. 4, this is the theoretical time of arriving of the wave refracted n times at the lower boundary. From Fig. 4, it can easily be understood that we must have the condition (3.12) for the occurrence of the n-ply refracted wave. Anyway, we see from the above analysis that the movement at a point is composed of the multiply reflected and refracted waves. In order to see the wave forms for the impulsive origin (3.8), putting tentatively

$$\rho=\rho' , \quad V_s=0.8V_s' , \tag{4.3}$$

we calculated the movement at $x=20H$.

The results of the calculation are shown in Fig. 5 and 6. In Fig. 5, the reflected and refracted waves of the n-th order are shown separately, the time t being refered to the arrival time of the direct wave.

In the movement for each n, that before the time of the respective infinte displacment

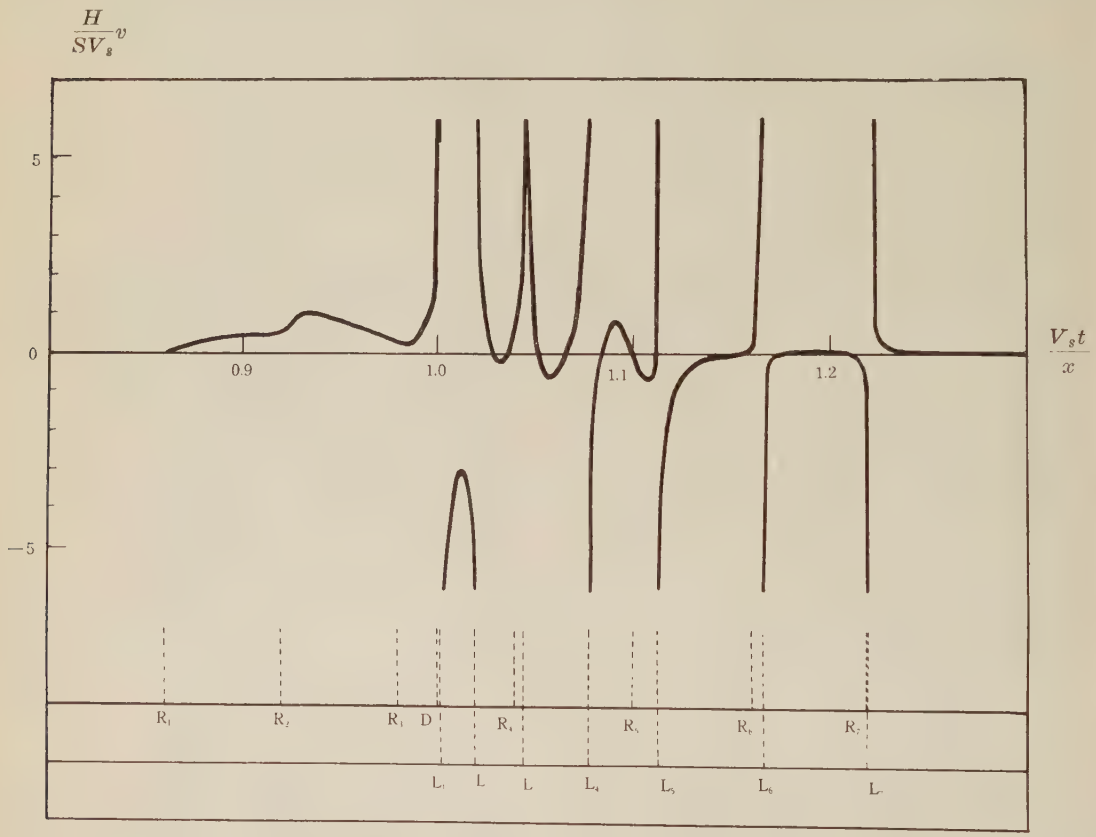

Eig. 6

is due to the refracted wave, whereas that after the time is due to the reflected wave. By the condition (3.12), the number of the refracted wave at $x=20H$ is limited to 7. By this and one more reason to be given later, only the component waves up to the seventh order are shown in Fig. 5, In Fig. 6, is shown the result of superposition of these component waves. The symbols R_1, R_2, $\cdots$, D, L_1, L_2, $\cdots$ in this figure show the arrival times of the refracted waves of the first, second, $\cdots$ order, the direct wave and the reflected waves of the first, second, $\cdots$ order, respectively. From Fig. 5 and 6, we see

(a) The apparent periods of the waves before the arrival time of the direct wave are rather long. They are shorter, the nearer to the direct wave.

(b) The apparent periods of the waves after the arrival time of the direct wave are rather

short. They are shorter, the nearer to the direct wave. The results (a) and (b) are very similar to those obtained by PEKERIS (1948) for the sound wave propagation in the ocean. In this case, the waves before and after the direct wave are called the ground and water waves, respectively, and it was shown by PEKERIS using his group velocity curve that the apparent period becomes very short immediately after the arrival time of the direct water wave.

(c) The refracted waves after the direct wave are masked by the reflected waves, whereas those before the direct wave are clearly seen in Fig. 6. The reflected waves are well separated from one another. In fact, we may easily construct Fig. 6 from the curves for the component reflected waves in Fig. 5. In section 1, we said that the ray theory we are now using is complementary to the steepest descent method and is not suited to the study of wave phenomena far away from the wave origin.

This remark now requires a little correction. From what was obtained above, we see that our present method is fairly suited to the study of wave phenomena away from the wave origin.

We shall now give the reason why we omitted the contributions from the reflected waves of the orders larger than 7 in Fig. 5 and 6. As is seen from (3.9), the amplitude of the reflcted wave v_n becomes infinite for $\phi=0$ or at $t=br$ (the arrival time of the reflected wave in question). This becomes so by the factor $\sinh\phi$ in the denominator of v_n which is zero for $\phi=0$ or at $t=br$. Thus the value of v_n for a very small ϕ, $d\phi$, say, will be

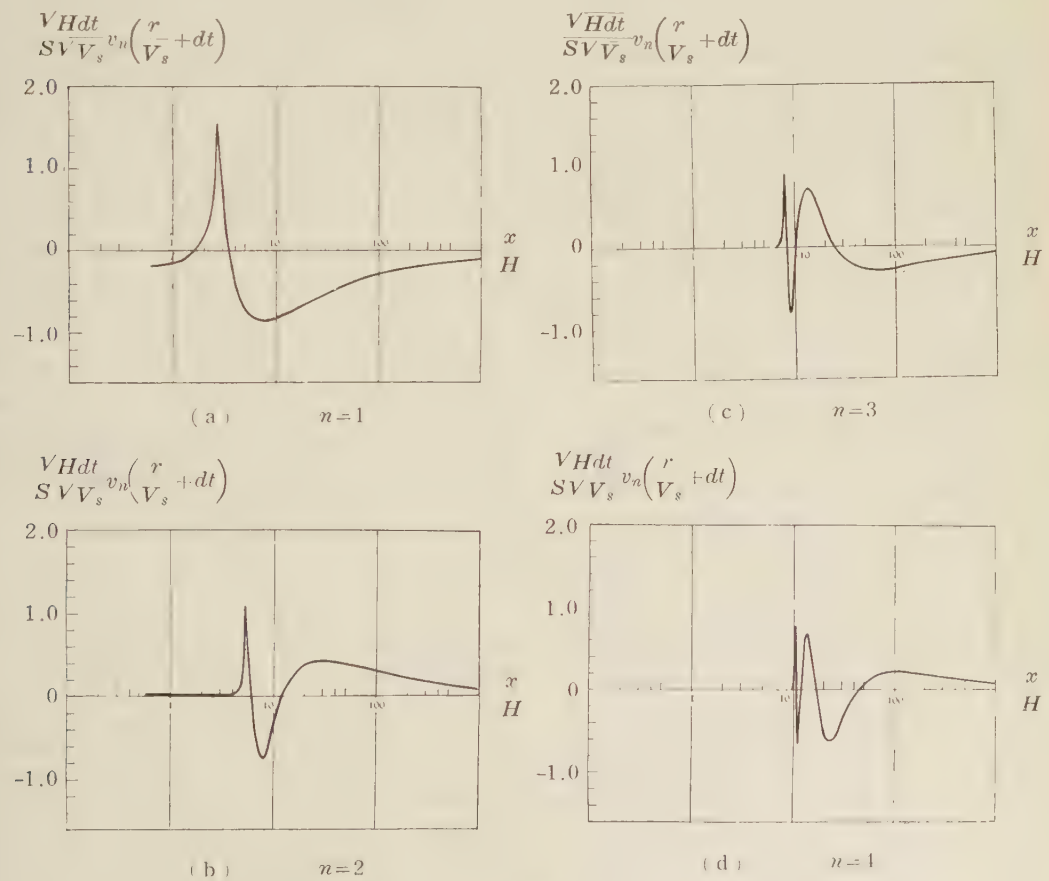

Fig. 7

$$v_n(d\phi)=\frac{2\varepsilon_n S}{br}\frac{V(\zeta')}{\cosh(\phi=0)d\phi}\,. \tag{4.4}$$

ζ' in $V(\zeta')$ in (4.4) may be taken to be equal to that for $\phi=0$, that is, $\zeta'=-(x/r)$ by (3.10). The correspondence between $d\phi$ and dt, which is the time deviation fom $t=br$, is given by

$$t+dt=br\left[\cosh(\phi=0)+\frac{\sinh(\phi=0)}{1!}d\phi+\frac{\cosh(\phi=0)}{2!}(d\phi)^2\right]$$

or

$$\frac{1}{d\phi}=\sqrt{\frac{br}{2dt}}\,. \tag{4.5}$$

Thus we have the value of v_n at $t=br+dt$ as follows

$$v_n(br+dt)=\frac{\sqrt{2}\varepsilon_n S}{\sqrt{bHdt}}\frac{V\{\zeta'=-(x/r)\}}{[(x/H)^2+(2n)^2]^{1/4}},$$
$$r=\sqrt{x^2+(2nH)^2}\,. \tag{4.6}$$

Keeping dt in (4.6) as a small quantity independent of n and r and omitting the common factor $S/\sqrt{bHdt}$, we calculated the relative amplitudes of the reflected waves for several n and x/H. The results of the calculation are shown in Fig. 7. From this figure, we see that the amplitude of the reflected wave of the n-th order is very small up to the critical distance $x=2nHV_s/\sqrt{V_S'^2-V_S^2}$, which is, by (3.12), also the critical distance for the appearence of the refracted wave of of the n-th order. The existence of the common infinite factor will make the above discussion more complicated. But from what was obtained above, we may safely conclude that the number of the reflected waves at a point is the same as that of the refracted waves there. Thus we have seven reflected waves at $x=20H$. This kind of relation between the refracted and reflected waves is familiar in optics. In optics, we have the totally reflected wave when there is no wave to go to the lower layer. In every text book on elementary physics, we can find illustrations of this phenomena for the ray going, for example, from water to air. Almost the same thing is occurrring in our present promblem.

§5. As is shown in (3.8), the movement at the origin is very simple, whereas as was shown by PEKERIS, that far away from the origin is very complicated and oscillatory in character. We can now understand how this transition from the aperiodic motion to the periodic one takes place. It is due to the appearences of new waves by the multiple refraction and reflection. As we go further from the origin, we have more refracted and reflected waves and thus more complicated movement. It is our opinion that this point of view is very useful in understanding the wave phenomena in a layered medium and by using it, we can get from seismograms, for example, more informations on the underground structure.

We shall now give examples which have some connections with the above thoretical results. Hughes (1949) developed a method to meassure the wave velocities through elastic samples. He used the supersonic wave and his samples were in the forms of bars. An impulse was given to the one end of each bar and the resulting movement was recorded at the other end. He obtained the more complicated movements for the longer bars. According to him, the movement is composed of the waves, the arrival times of which are given by

$$t=m\frac{L}{V_D}+nD\frac{(V_D^2-V_R^2)^{1/2}}{V_DV_R},$$
$$n=0,\ 1,\ 2,\cdots,\ m=1,\ 3,\ 5,\cdots, \tag{5.1}$$

where D, L, V_D and V_R are the diameter and length of the bar and the compressional and distortional wave velocities through it, respectively. m and n in (5.1) are subject to the restriction

$$mL\geq nD\tan\theta\,. \tag{5.2}$$

The waves $n=0$; $m=1,\ 3,\ 5,\cdots$ are the direct wave, the waves reflected once, twice, $\cdots$ at each end of the bar, respectively. The waves $m=1$; $n=1,\ 2,\cdots$ are the waves which traverse the bar with the velocity V_R once, twice, $\cdots$ at an angle θ relative to the normal of the boundaries

$$\sin\theta=\frac{V_R}{V_D}\,, \tag{5.3}$$

and then go with the velocity V_D along the boundary to the end where they are recorded. The detailed analysis of this problem will be given in a forth-coming paper. However, it can easily be understood that all the waves in (5.1) other than $n=0$ are a kind of refracted waves, and the condition (5.2) corresponds to our (3.12). Thus the appearence of the successive refracted waves seems to be the essence of this experiment. Observing all the arrival times of these refracted waves, we can determine V_D and V_R more accurately than when we observe only the arrival time of the direct wave.

Using explosives, H. TATEL and others (1953) have tried to determine the crustal structure in the United States. They say that almost all the "phases" in seismograms obtained are spurious ones caused by accidental wave interferences. Rejecting the spurious phases one by one, they arrive at the phase which seems to be the only "true" phase. According to them, this phase corresponds to the totally reflected wave from the MOHOROVICIC discontinuity. This totally reflected wave has very large amplitude at the critical distance similar to that in (3.12) (of course, we must put $n=1$ there) and is observed between 80 to 130 Km. The thickness of the crust obtained by them is about 35 Km. and the wave velocities above and below the discontinuity are 6.1 and 8.1 Km/sec, respectively. By using these values, we can understand the reason why we have no reflected wave up to the skip distance 80 Km. The skip distance is the term in the study of radio wave propagations, where we have the similar phenomena. We may also give the reason why we have no refleted wave beyond 130 Km. Thus, as is shown in Fig. 7, the amplitude of the first reflected wave decreases from the maximum at $x=2HV_s/\sqrt{V_s'^2-V_s^2}$ and becomes zero at about $x=3.5H$. This may correspond to the disappearence of the reflected wave at 130 Km. from the origin. In this connection, it will be interesting to study the existence of the second maximum in the first reflected wave and the appearences of the reflected waves of the higher orders predicted by the present theory. Anyway, by studying the waves totally reflected at the MOHOROVICIC discontinuity, we are sure to know more about the crustal structure. We can also expect to know more about the underground structure by applying the similar method to exploration seismology.

The hydrophone and sono-radio buoy method is reported by M. N. HILL (1952) to be very useful in studying the crustal structure under the ocean. Typical records obtained by him are shown in Fig. 5 in his paper. They are composed of the waves which are separated from one another quite well. He says that the number of pulses for any one distance between shot point and receiver is limited. The number is the more at the more distant point. The path of each wave is shown in his Fig. 10. Each wave is called by him the multiple refraction wave, and some reasons are given why it is not called the multiple reflection wave. But it seems to the present authors to be rather difficult to separate the refracted wave from the reflected wave of the same order, the critical distances for the appearences of these waves being the same. As is shown in Fig. 5, each refracted wave comes earlier than the corresponding reflected wave, but its amplitude is so small that it is liable to be escaped from our notice. In fact, as was said at (c) in section 4 and was shown in Fig. 6, the refracted waves after the direct wave are masked by the reflected waves. From this reason, it seems to the present authors to be better to call the waves in HILL's Fig. 10 the multiple reflection waves. They are the reflected waves from the lower layer of varying velocity and analogous to the reflected radio waves from the ionospheres. A relation between the total reflection and the dispersion formula has been pointed out by several authors (e.g. TOLSTOY, I. and USDIN, E. 1953). The appearence of totally reflected waves of the higher orders at the respective critical distances to form the typical oscillatory movements at the point far away from the origin is probably another aspect of the above relation.

The above analysis has been made for the *SH* wave. The corresponding problems for

the *P*-type origin will be made in a forthcoming paper. However, we are sure that the essence of this kind of problem is exhausted in the present paper.

References

HILL, M. N.:
1952 "Seismic refraction shooting in an area of the eastern Atlantic." Phil. Trans. Roy. Soc. London, **244**, 561.

HONDA, H. and NAKAMURA, K.:
1953 "On the reflection and refraction of the explosive sounds at the ocean bottom." Sci. Rep. Tohoku Univ., Ser. 5, **4**, 125.
1954 —(part 2). —, **6**, 70.

HUGHES, D. S., PONDROM, W. L. and NIMS, R. L.:
1949 "Transmission of elastic pulses in metal rods." Phys. Rev., **75**, 1552.

JEFFREYS, H.:
1925-27 "On compressional waves in two superposed layers. Proc. Camb. Phil. Soc., **23**, 472.

MUSKAT, M.:
1932 "The theory of refraction shooting." Physics, **4**, 14.

PEKERIS, C. L.:
1948 "Theory of propagation of explosive sound in shallow water." Geol. Soc. Amer. Memoir **27**, 1.

PRESS, F. and EWING, M.:
1950 "Propagation of explosive sound in a liquid layer overlying a semi-infinite elastic solid." Geophysics, **15**, 426.

SATO, Y.:
1952 "Study on surface waves (6). Generations of Love and other types of SH waves." Bull. Earthq. Res. Inst., **30**, 101.

SEZAWA, K.:
1935 "Love waves generated from a source of a certain depth." Bull. Earthq. Res. Inst., **13**, 1.

SOMMERFELD, A.:
1949 "Partial differential equations in physics." Academic Press Inc., New York.

TAKEUCHI, H. and KOBAYASHI, N.:
1955 "Wave generations from line sources within the ground." Journ. Phys. Earth, **3**, 7.

TATEL, H. E., ADAMS, L. H. and TUVE, M. A.:
1953 "Studies of the earth's crust using waves from explosions." Proc. Amer. Phil. Soc., **97**, 658.

TOLSTOY, I. ahd USDIN, E.:
1953 "Dispersive properties of stratified elastic and liquid media: A ray theory." Geophysics, **18**, 844.

On Microseisms Produced on the Surface of the Earth due to Passage of Storm over the Deep Sea.

By

Sushil CHANDRA DAS GUPTA

Krishnagar College, Krishnagar, West Bengal, India.

Summary

Several attempts have been made to explain the microseisms, the latest being that of LONGUET-HIGGINS based on the idea that they are produced by stationary waves. In this paper the author has attempted to show that in case of storms, microseisms are also likely to be generated by progressive waves. The character of microseisms has been proved to be of the RAYLEIGH type approximately. The average velocity and wave length of microseisms have been shown to agree approximately with the observational results referred to in this paper. The period-relation observed by BERNARD and DEACON viz. that the period of microseisms is half the period of sea-waves supposed to generate them, is also shown to agree. The ratio of horizontal and vertical maximum amplitudes has been found and has been shown to depend on the geological structure and not on the distance. In conclusion the possible reason for absence of microseisms on the approach of monsoons has been given as noted by GHERZI.

Introduction

Waves produced on the earth due to disturbances at sea have been considered by several authors. GILMORE (1946) and RAMIREZ (1940) particularly made elaborate observations regarding the seismic-waves due to passage of storms over the sea with comparatively high velocity. Others, such as GUTENBERG (1931), BANERJI (1930) and GHERZI (1923; 1928) observed what are called micro-seisms due to various types of disturbances on the sea. BANERJI found microseisms due to the coming of monsoon in the Arabian sea on the Indian coast. GHERZI observed on the China Coast microseisms due to the passage of typhoons but none due to monsoon. Among the many observations RAMIREZ observed the average velocity of microseisms to be 2.66 km per second and the average wave-length as 14.76 kms. Average period of microseisms was observed by him to be 5.2 seconds and the average ratio of vertical to horizontal component of displacement to be 1.21 at St. Louis. GILMORE observed that amplitudes increased from 17 mm to 30 mm when the wind velocity increased from 55 knots to 85 knots per hour. Microseismic activity at Richmond decreased from 32 mm to 20 mm as the strom passed over Florida when the intensity of storm dropped from 85 knots to 40 knots. When the storm reached the land, microseismic activity decreased very much. Observed periods of ordinary sea waves caused by hurricane winds average about 10 seconds with wave-lengths of 500 to 700 feet. Velocity of sea waves seldom exceeds 30 miles per hour.

BERNARD (1946) obtained evidence which led him to believe that microseismic oscillations have periods which are half those of the sea waves which give rise to them. The same ratio was observed by DEACON (1947) between microseisms recorded at Kew and sea-waves recorded at Perranporth on the north-coast of Cornwall.

About the origin of the earth-waves of the type of microseisms, there were three theories in 1937. The first was that of GUTENBERG who considered that these microseisms originated in surf on rock-bound coasts. The second was that held by GHERZI, BANERJI and others that they were generated at the centre of storms at sea. The third opinion was that of BRADFORD, LEE and others that they had

their origin in certain types of frontal disturbances anywhere on land or sea. Discrimination between these possible origins by further statistical correlations was hopeless, because all three often existed simultaneously. Recently Longuet-Higgins (1950) has given a theory of microseisms considering the Miche (1944) term of pressure-relation in a fluid. He has found that the total transmission of energy to the sea-floor is of the right order of magnitude to account for microseisms. He considered that stationary waves give rise to microseisms which have period-relation as observed by Bernard. Darbyshire (1950) considered three storms to show the possibility of stationary waves being generated in an attempt to substantiate the hypothesis of Longuet-Higgins. But there is always a great possibility of progressive waves being generated in the open sea due to storms and there is likelihood of generation of microseisms due to them.

In this paper, the possibility of generation of microseisms due to progressive sea-waves produced by storms has been considered. First, it has been shown that the approximate period of microseismic vibrations is half the period of the sea-waves generating them. Secondly, the character of microseisms is shown to be approximately of Rayleigh type. Thirdly, it is demonstrated that the velocity of propagation is much smaller than that of Rayleigh waves and that the velocity depends mainly on the geological structure. Fourthly, the wave-length has been found to conform to observations. The ratio of the horizontal to the vertical amplitude has been obtained and lastly an explanation of the phenomenon that microseisms are observed in case of typhoons but not in case of monsoons has been given. It has been shown that compressibility of water is a reasonable cause for propagation of surface disturbance to the sea bottom.

1. When the compressibility of sea-water is taken into account the velocity-potential function ϕ at a depth z is given, as shown by Whipple (1935), by the relations

$$\phi=\exp(ipct-ilx)[2\gamma\mu\cosh(\mu z)-(p^2-2\gamma^2)\sinh(\mu z)]e^{-\gamma z} \qquad (1.1)$$

when $p^2<l^2+\gamma^2$

and $\mu^2=l^2+\gamma^2-p^2$,

and $\phi=\exp(ipct-ilx)[2\gamma\nu\cos(\nu z)-(p^2-2\gamma^2)\sin(\nu z)]e^{-\gamma z} \qquad (1.2)$

when $p^2>l^2+\gamma^2$

in which $\nu=i\mu$, $\nu^2=p^2-l^2-\gamma^2$

and $c^2=\frac{g}{2\gamma}$.

We have the frequency equations in case of (1.1) and (1.2) as

$$\frac{\mu}{\gamma}\coth\mu h=\frac{l^2-\gamma^2+\mu^2}{l^2+\gamma^2-\mu^2}, \qquad (1.3)$$

$$\frac{\nu}{\gamma}\cot\nu h=\frac{l^2-\gamma^2-\nu^2}{l^2+\gamma^2+\nu^2}, \qquad (1.4)$$

where h is the depth of the ocean. γh is small, γ being of the order of $2\times10^{-8}\text{cm}^{-1}$ and h of the order of 10^6 cms for the deepest oceans. Equation (1.3) regarded as an equation in μ has one real positive root which approximates to $l-\gamma$ when lh is large. Hence neglecting the square of velocity and remembering that $\eta=\frac{1}{g}\left(\frac{\partial\phi}{\partial t}\right)_{z=0}$ where η is the depression of the sea-surface from the mean-level, the pressure at the bed of the sea can be expressed approximately in the form

$$P=g\rho h+g\rho\eta\left\{\cos\nu h-\frac{p^2-2\gamma^2}{2\gamma\nu}\sin\nu h\right\}$$

or

$$g\rho h+g\rho\eta\left\{\cosh\mu h-\frac{p^2-2\gamma^2}{2\gamma\mu}\sinh\mu h\right\}. \qquad (1.5)$$

We thus see that there is a finite disturbance of pressure at the bottom and is proportional to η.

Let $\eta=Ae^{i(\xi x-pct)}$, (1.6)

where c is the velocity of sound in water and $c^2=\frac{g}{2\gamma}$. Hence the pressure disturbance at the ocean-bed is given by

$$Ag\rho\left\{\cos\nu h-\frac{p^2-2\gamma^2}{2\gamma\nu}\sin\nu h\right\}e^{i(\xi x-pct)}$$

or

$$Ag\rho\left\{\cosh\mu h-\frac{p^2-2\gamma^2}{2\gamma\mu}\sinh\mu h\right\}e^{i(\xi x-pct)}.$$

Writing $pc=p_1$

we have,

$$Ag\rho\left\{\cos \nu h-\frac{p_1^2/c^2-2\gamma^2}{2\gamma\nu}\sin \nu h\right\}e^{i(\xi x-p_1 t)}$$

or

$$Ag\rho\left\{\cosh \mu h-\frac{p_1^2/c^2-2\gamma^2}{2\gamma\mu}\sinh \mu h\right\}e^{i(\xi x-p_1 t)} . \tag{1.7}$$

2. The equations of motion in the elastic earth are given by

$$a^2 \text{ grad div } D-b^2 \text{ rot rot } D=\frac{\partial^2 D}{\partial t^2} , \tag{2.1}$$

where $$a^2=\frac{\lambda+2\mu}{\rho}$$

and $$b^2=\frac{\mu}{\rho} .$$

Taking divergence of (2.1) we get

$$\square_a \text{ div } D=0 , \tag{2.2}$$

where $$\square_a=\triangle-\frac{1}{a^2}\frac{\partial^2}{\partial t^2} .$$

Again taking rotation of (2.1)

$$\square_b \text{ rot } D=0 , \tag{2.3}$$

where $$\square_b=\triangle-\frac{1}{b^2}\frac{\partial^2}{\partial t^2} .$$

Let $$D=\text{grad } \phi+\text{rot } \vec{A} .$$

Therefore,

$$\square_a\triangle\phi=0 ,$$

and $$\square_b(\text{grad div}-\triangle)A=0 .$$

Then $$\phi=\phi_1+\phi_2 ,$$

and $$A=A_1+A_2 ,$$

where $$\triangle\phi_1=0 , \quad \square_a\phi_2=0 \tag{2.4}$$

and $$\text{grad div } A_1-\triangle A_1=0 , \quad \square_b A_2=0 . \tag{2.5}$$

Then $$D=D_1+D_2 ,$$

where $$D_1=\text{grad } \phi_1+\text{rot } A_1 ,$$

$$D_2=\text{grad } \phi_2+\text{rot } A_2 ,$$

$$\text{div } D_1=\triangle\phi_1=0 ,$$

$$\text{rot } D_1=\text{grad div } A_1-\triangle A_1=0 ,$$

so that $$D_1=\text{grad } \phi_1'$$

and $$\triangle\phi_1'=0 .$$

From (2.1) therefore $$\frac{\partial^2 D_1}{\partial t^2}=0 ,$$

so that $$\frac{\partial^2\phi_1'}{\partial t^2}=0 .$$

Hence ϕ_1' is a particular case of ϕ_2 where $\phi_2=\phi_1'$ and $A_2=0$. Therefore,

$$D_2=D_2'+D_2'' ,$$

$$D_2'=\text{grad } \phi_2 , \quad \square_a\phi_2=0 ,$$

$$\square_b D_2''=0 , \quad \text{div } D_2''=0$$

(cf. Hayashi (1942)) .

3. Let us take the x, y plane of the rectangular co-ordinate axis on the undisturbed surface of the semi-infinite homogeneous isotropic elastic medium of the ocean-bed, z-axis being directed inward to the medium. We assume that the disturbance travels with uniform velocity v in a direction which is taken as x-axis. We are interested only in solutions where x and t appear as a combination of $x-vt$. A formal solution of (2.4) is given by

$$e^{-qz+i\alpha x+i\beta y-i\alpha vt} ,$$

where $$q=\sqrt{\left(1-\frac{v^2}{a^2}\right)\alpha^2+\beta^2} , \tag{3.1}$$

and α, β may take any real value. Therefore,

$$\phi=\iint_{-\infty}^{+\infty}\phi(\alpha, \beta)e^{-qz+i\alpha x+i\beta y-i\alpha vt}\,d\alpha d\beta .$$

Similarly the solution of (2.5) is given by

$$A=\iint_{-\infty}^{+\infty}A(\alpha, \beta)e^{-q'z+i\alpha x+i\beta y-i\alpha vt}\,d\alpha d\beta ,$$

where $$q'=\sqrt{\left(1-\frac{v^2}{b^2}\right)\alpha^2+\beta^2} . \tag{3.2}$$

Hence

$$D=\iint_{-\infty}^{+\infty}D_1(\alpha, \beta)e^{-qz+i\alpha x+i\beta y-i\alpha vt}\,d\alpha d\beta$$

$$+\iint_{-\infty}^{+\infty}D_2(\alpha, \beta)e^{-q'z+i\alpha x+i\beta y-i\alpha vt}\,d\alpha d\beta ,$$

where $$D_{1x}=i\alpha\phi , \quad D_{1y}=i\beta\phi , \quad D_{1z}=-q\phi ,$$

($D_{1x}=x$-component of D_1, etc.)

$$D_{2x}=i\beta A_{2z}+q'A_{2y} ,$$

$$D_{2y}=-q'A_{2x}-i\alpha A_{2z} ,$$

$$D_{2z}=i\alpha A_{2y}-i\beta A_{2x} .$$

It is clear that $i\alpha D_{2x}+i\beta D_{2y}-q'D_{2z}=0$. Therefore, we may put

$$D_{2x}=q'\psi_1 , \quad D_{2y}=q'\psi_2$$

and $$D_{2z}=i(\alpha\psi_1+\beta\psi_2) ,$$

$$\text{div } D=\Delta\phi=\frac{1}{a^2}\frac{\partial^2\phi}{\partial t^2}=-\frac{v^2}{a^2}\iint_{-\infty}^{+\infty}\alpha^2\phi(\alpha,\beta)e^{-qz+i\alpha x+i\beta y-i\alpha vt}d\alpha d\beta\,.$$

Let the boundary conditions be $X_z=Y_z=0$ and $Z_z=f(x,y,t)$ at $z=0$. Therefore

$$\frac{X_z}{\mu}=\frac{\partial D_x}{\partial z}+\frac{\partial D_z}{\partial x}=0 \qquad \text{at} \quad z=0$$

or,
$$\iint_{-\infty}^{+\infty}\{-2i\alpha q\phi-(q'^2+\alpha^2)\psi_1-\alpha\beta\psi_2\}e^{i\alpha x+i\beta y-i\alpha vt}d\alpha d\beta=0\,.$$

Hence
$$2i\alpha q\phi+(q'^2+\alpha^2)\psi_1+\alpha\beta\psi_2=0\,. \tag{3.3}$$

Next, we know
$$\frac{Y_z}{\mu}=\frac{\partial D_y}{\partial z}+\frac{\partial D_z}{\partial y}=0 \qquad \text{at} \quad z=0\,.$$

So that
$$\iint_{-\infty}^{+\infty}\{-2i\beta q\phi-\alpha\beta\psi_1-(q^2+\beta^2)\psi_2\}e^{i\alpha x+i\beta y-i\alpha vt}d\alpha d\beta=0\,.$$

Then
$$2i\beta q\phi+\alpha\beta\psi_1+(q'^2+\beta^2)\psi_2=0\,. \tag{3.4}$$

Considering the relation $\frac{Z_z}{\mu}=\frac{\lambda}{\mu}\text{ div } D+2\frac{\partial D_z}{\partial z}$ at $z=0$, we have

$$\iint_{-\infty}^{+\infty}\left[\left\{2q^2-v^2\left(\frac{1}{b^2}-\frac{2}{a^2}\right)\alpha^2\right\}\phi-2i\alpha q'\psi_1-2i\beta q'\psi_2\right]e^{i\alpha x+i\beta y-i\alpha vt}d\alpha d\beta$$
$$=-\frac{1}{4\pi^2\mu}\iint_{-\infty}^{+\infty}g(\alpha,\beta)e^{i\alpha x+i\beta y-i\alpha vt}d\alpha d\beta \tag{3.5}$$

say, so that
$$-\frac{1}{4\pi^2\mu}g(\alpha,\beta)=\left\{2q^2-v^2\left(\frac{1}{b^2}-\frac{2}{a^2}\right)\alpha^2\right\}\phi-2i\alpha q'\psi_1-2i\beta q'\psi^2\,.$$

Hence
$$\left.\begin{aligned}\phi&=-\frac{\left(2-\frac{v^2}{b^2}\right)\alpha^2+2\beta^2}{4\pi^2\mu D(\alpha,\beta)}\,g(\alpha,\beta)\,,\\ \psi_1&=-\frac{2i\alpha q}{4\pi^2\mu D(\alpha,\beta)}\,,\\ \psi_2&=-\frac{2i\beta q}{4\pi^2\mu D(\alpha,\beta)}\,,\end{aligned}\right\} \tag{3.6}$$

where
$$D(\alpha,\beta)=4qq'(\alpha^2+\beta^2)-\left\{\left(2-\frac{v^2}{b^2}\right)\alpha^2+2\beta^2\right\}^2\,.$$

Hence, u, v, w at $z=0$ are given by

$$\left.\begin{aligned}(u)_{z=0}&=\frac{i}{4\pi^2\mu}\iint_{-\infty}^{+\infty}\frac{\alpha\left\{\left(2-\frac{v^2}{b^2}\right)\alpha^2+2\beta^2-2qq'\right\}}{D(\alpha,\beta)}g(\alpha,\beta)e^{i\alpha x+i\beta y-i\alpha vt}d\alpha d\beta\,,\\ (v)_{z=0}&=\frac{i}{4\pi^2\mu}\iint_{-\infty}^{+\infty}\frac{\beta\left\{\left(2-\frac{v^2}{b^2}\right)\alpha^2+2\beta^2-2qq'\right\}}{D(\alpha,\beta)}g(\alpha,\beta)e^{i\alpha x+i\beta y-i\alpha vt}d\alpha d\beta\,,\end{aligned}\right\} \tag{3.7}$$

$$(w)_{z=0}=\frac{v^2}{4\pi^2\mu b^2}\iint_{-\infty}^{+\infty}\frac{\alpha^2 q}{D(\alpha,\beta)}g(\alpha,\beta)e^{i\alpha x+i\beta y-i\alpha vt}d\alpha d\beta\ .$$

Since it is well known that uniform hydrostatic pressure has little influence on the seismic wave motion, we take the boundary conditions as

$$-Z_z=A_1e^{i(\xi x-p_1t)}=f(x,y,t)\ ,$$

where
$$A_1=Ag\rho\left\{\begin{array}{l}\cos\nu h-\dfrac{p_1^2/c^2-2\gamma^2}{2\gamma\nu}\sin\nu h\ ,\\ \cosh\mu h-\dfrac{p_1^2/c^2-2\gamma^2}{2\gamma\mu}\sinh\mu h\end{array}\right\}$$

from (1.7) when
$$vt<x<l_1+vt\ ,\qquad 0<y<l\ ,$$

so that the disturbance is proceeding in the simple form of a rectangle of sides l and l_1. As two sides of the disturbed area are likely to lengthen in the direction of travelling of the disturbance, we take it to be approximately a rectangular one. Z_z is taken to be zero outside this area. Therefore from (3.5) and (3.7)

$$-g(\alpha,\beta)=\mu\iint_{-\infty}^{+\infty}f(x,y,t)e^{-i\alpha(x-vt)-i\beta y}d(x-vt)dy\ .$$

Putting $x-vt=\eta$ and $f(x,y,t)=A_1e^{i(\xi x-p_1t)}$,

$$-g(\alpha,\beta)=\mu\int_0^l\int_0^{l_1}A_1e^{i(\xi\eta-p_1t+\xi vt)}e^{-i\alpha\eta-i\beta y}dyd\eta=A_1\mu e^{i(\xi v-p_1)t}\frac{(1-e^{-i\beta l})(1-e^{-i(\alpha-\xi)l_1})}{\beta(\xi-\alpha)}\ . \tag{3.8}$$

Hence the displacements at $z=0$ are given by

$$(w)_{z=0}=-\frac{A_1v^2}{4\pi^2b^2}e^{i(\xi v-p_1)t}\iint_{-\infty}^{+\infty}$$
$$\times\frac{\alpha^2\sqrt{\left(1-\dfrac{v^2}{a^2}\right)\alpha^2+\beta^2}(1-e^{-i\beta l})(1-e^{-i(\alpha-\xi)l_1})e^{i\alpha(x-vt)+i\beta y}}{\left[4(\alpha^2+\beta^2)\sqrt{\left(1-\dfrac{v^2}{a^2}\right)\alpha^2+\beta^2}\sqrt{\left(1-\dfrac{v^2}{b^2}\right)\alpha^2+\beta^2}-\left\{\left(2-\dfrac{v^2}{b^2}\right)\alpha^2+2\beta^2\right\}^2\right](\xi-\alpha)\beta}d\alpha d\beta\ , \tag{3.9}$$

$$(u)_{z=0}=-\frac{A_1i}{4\pi^2}e^{i(\xi v-p_1)t}\iint_{-\infty}^{+\infty}$$
$$\times\frac{\alpha\left\{\left(2-\dfrac{v^2}{b^2}\right)\alpha^2+2\beta^2-2\sqrt{\left(1-\dfrac{v^2}{a^2}\right)\alpha^2+\beta^2}\sqrt{\left(1-\dfrac{v^2}{b^2}\right)\alpha^2+\beta^2}\right\}(1-e^{-i\beta l})(1-e^{-i(\alpha-\xi)l_1})e^{i\alpha(x-vt)+i\beta y}}{\left[4(\alpha^2+\beta^2)\sqrt{\left(1-\dfrac{v^2}{a^2}\right)\alpha^2+\beta^2}\sqrt{\left(1-\dfrac{v^2}{b^2}\right)\alpha^2+\beta^2}-\left\{\left(2-\dfrac{v^2}{b^2}\right)\alpha^2+2\beta^2\right\}^2\right]\beta(\xi-\alpha)}$$
$$\times d\alpha d\beta\ , \tag{3.10}$$

$$(v)_{z=0}=-\frac{A_1i}{4\pi^2}e^{i(\xi v-p_1)t}\iint_{-\infty}^{+\infty}$$
$$\times\frac{\beta\left\{\left(2-\dfrac{v^2}{b^2}\right)\alpha^2+2\beta^2-2\sqrt{\alpha^2\left(1-\dfrac{v^2}{a^2}\right)+\beta^2}\sqrt{\left(1-\dfrac{v^2}{b^2}\right)\alpha^2+\beta^2}\right\}(1-e^{-i\beta l})(1-e^{-i(\alpha-\xi)l_1})e^{i\alpha(x-vt)+i\beta y}}{\left[4(\alpha^2+\beta^2)\sqrt{\left(1-\dfrac{v^2}{a^2}\right)\alpha^2+\beta^2}\sqrt{\left(1-\dfrac{v^2}{b^2}\right)\alpha^2+\beta^2}-\left\{\left(2-\dfrac{v^2}{b^2}\right)\alpha^2+2\beta^2\right\}^2\right](\xi-\alpha)\beta}$$
$$\times d\alpha d\beta\ . \tag{3.11}$$

4. The expression within the sign of integration will be shown to be a function of the distance of the area of the storm from the position of observation. Hence, the period of disturbance of the waves travelling through the ocean-bed to the position of observation will have the period $\frac{2\pi}{\xi v - p_1}$. But as it has been shown by several observers that the period of such waves is half the period of waves on sea due to storm, we get $\xi v - p_1 = 2p_1$ or, $v = \frac{3p_1}{\xi}$. We therefore expect that the velocity of storms is three times the velocity of waves generated on sea. From theoretical side, Jeffreys (1924; 1925) has shown that the velocity of wind will be at least three times the velocity of sea-waves. According to Gilmore's observations ordinary sea waves caused by hurricane winds average about 10 seconds with wave length 500 to 700 ft. The velocity of such sea waves is ordinarily 30 miles per hour. Hence if we assume the velocity of wind as three times the velocity of generated sea waves we have,

$$\xi v = \frac{\xi}{2\pi} \times 2\pi v = \frac{6 \cdot 28 \times 132}{500} = 1 \cdot 6 \qquad \text{approximately,}$$

$$3p_1 = 3 \cdot \frac{p_1}{2\pi} \cdot 2\pi = \frac{6 \cdot 28 \times 3}{10} = 1 \cdot 8 \qquad \text{approximately.}$$

Thus an approximate agreement with observational result is found. In the absence of larger number of more or less exact data available, agreement could not be shown with greater precision.

5. In order to integrate (3.9) we resolve the expression $(1-e^{-i\beta l})(1-e^{-i(\alpha-\xi)l_1})$ into

$$1 + e^{-i\beta l} e^{-i(\alpha-\xi)l_1} - e^{-i\beta l} - e^{-i(\alpha-\xi)l_1} \tag{5.1}$$

which gives us (3.9) as consisting of four integrals. The first integral of them is

$$\iint_{-\infty}^{+\infty} \frac{\alpha^2 \sqrt{\left(1-\frac{v^2}{a^2}\right)\alpha^2+\beta^2}\, e^{i\alpha(x-r_1)+i\beta y}}{\left[4(\alpha^2+\beta^2)\sqrt{\left(1-\frac{v^2}{a^2}\right)\alpha^2+\beta^2}\sqrt{\left(1-\frac{v^2}{b^2}\right)\alpha^2+\beta^2} - \left\{\left(2-\frac{v^2}{b^2}\right)\alpha^2+2\beta^2\right\}^2\right](\xi-\alpha)\beta} d\alpha d\beta .$$

Substituting $\alpha = s\cos\varphi$, $\beta = s\sin\varphi$, $x - vt = r_1\cos\theta_1$, $y = r_1\sin\theta_1$, the integral becomes,

$$\int_0^{\infty}\int_{-\pi}^{\pi} \frac{\cos^2\varphi\sqrt{1-\tau_1\cos^2\varphi}\, e^{ir_1 s\cos(\varphi-\theta)}}{\{4\sqrt{1-\tau_1\cos^2\varphi}\sqrt{1-\tau_2\cos^2\varphi}-(2-\tau_2\cos^2\varphi)^2\}(\xi-s\cos\varphi)s\sin\varphi} ds d\varphi , \tag{5.2}$$

where $\tau_1 = \frac{v^2}{a^2}$ and $\tau_2 = \frac{v^2}{b^2}$. Now,

$$e^{ir_1 s\cos(\varphi-\theta)} = J_0(r_1 s) + 2\sum_{n=1}^{\infty} i^n J_n(r_1 s)\cos n(\varphi-\theta) . \tag{5.3}$$

Substituting (5.3) in (5.2) and taking the first term of (5.3) as a first approximation, we get the integral of (5.2) as

$$\int_0^{\infty}\int_{-\pi}^{\pi} \frac{\cos^2\varphi\sqrt{1-\tau_1\cos^2\varphi}\, J_0(r_1 s)}{\{4\sqrt{1-\tau_1\cos^2\varphi}\sqrt{1-\tau_2\cos^2\varphi}-(2-\tau_2\cos^2\varphi)^2\}(\xi-s\cos\varphi)s\sin\varphi} ds d\varphi . \tag{5.4}$$

In order to integrate (5.4) with respect to s, we choose a contour as in the following figure

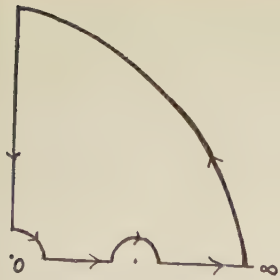

with indentations at the origin and the point given by $-\frac{\xi}{\cos\varphi}$. Hence taking the principal value we get (5.3) as

$$-i\pi\int_{-\pi}^{\pi}\frac{\cos^2\varphi\sqrt{1-\tau_1\cos^2\varphi}\,J_0\left(\frac{\xi r_1}{\cos\varphi}\right)}{\{4\sqrt{1-\tau_1\cos^2\varphi}\sqrt{1-\tau_2\cos^2\varphi}-(2-\tau_2\cos^2\varphi)^2\}\frac{\xi}{\cos\varphi}\cdot\sin\varphi}\,d\varphi, \tag{5.5}$$

the contributions due to the other pole being cancelled by similar expressions from each of the four integrals arising out of resolving $(1-e^{-i\beta l'})(1-e^{-i(\alpha-\xi)l_1})$. In order to integrate (5.5) with respect to φ, we put

$$\cos\varphi=\frac{1}{2}\left(z+\frac{1}{z}\right) \quad \text{and} \quad \sin\varphi=\frac{1}{2i}\left(z-\frac{1}{z}\right) \quad \text{where} \quad z=e^{i\varphi}. \tag{5.6}$$

The contour of integration is the unit circle with necessary adjustments to be done from the following considerations of the poles and branch points of integrand of (5.5) so transformed.

For the ocean bed where the ocean is deep, we take the mean value of the ratio $\frac{\lambda+2\mu}{\mu}$ as 3·5 at high pressure. We take then in (5.5) $\frac{\tau_1}{\tau_2}=\frac{1}{3\cdot5}=\nu$ say. When the substitutions (5.6) are made in (5.5), the expression within the bracket in the denominator assumes the form

$$\zeta=4\sqrt{1-\frac{\nu\tau_2}{4}\left(z+\frac{1}{z}\right)^2}\sqrt{1-\frac{\tau_2}{4}\left(z+\frac{1}{z}\right)^2}-\left\{2-\frac{\tau_2}{4}\left(z+\frac{1}{z}\right)^2\right\}^2. \tag{5.7}$$

Hence

$$\begin{aligned}\zeta\zeta^*&=16\left\{1-\frac{\nu\tau_2}{4}\left(z+\frac{1}{z}\right)^2\right\}\left\{1-\frac{\tau_2}{4}\left(z+\frac{1}{z}\right)^2\right\}-\left\{2-\frac{\tau_2}{4}\left(z+\frac{1}{z}\right)^2\right\}^4\\&=\frac{\tau_2}{4}\left(z+\frac{1}{z}\right)^2\left[16(1-\nu)-(24-16\nu)\frac{\tau_2}{4}\left(z+\frac{1}{z}\right)^2+8\left\{\frac{\tau_2}{4}\left(z+\frac{1}{z}\right)^2\right\}^2-\left\{\frac{\tau_2}{4}\left(z+\frac{1}{z}\right)^2\right\}^3\right].\end{aligned} \tag{5.8}$$

We are to find the zeros of (5.8) which lie within the circle of unit radius. We shall consider only the principal value of the integral (5.5). The expression within the bracket in (5.8) has only two real roots lying within the contour of unit circle viz, $z=\pm\frac{1}{x_1}$ approximately where $x_1=\sqrt{\frac{4\times\cdot95}{\tau_2}}$ corresponding to

$$z+\frac{1}{z}=\pm x_1, \tag{5.9}$$

$\tau_2=\frac{v^2}{b^2}$ being small. Corresponding to $\sin\varphi=\frac{1}{2i}\left(z-\frac{1}{z}\right)$ in the denominator of (5.5) there are two singularities at ±1. The branch points on the real axis are given by

$$\left.\begin{aligned}z&=\pm\frac{1}{h} \quad \text{where} \quad h=\sqrt{\frac{4}{\tau_2}},\\ z&=\pm\frac{1}{k} \quad \text{where} \quad k=\sqrt{\frac{4\times3\cdot5}{\tau_2}}.\end{aligned}\right\} \tag{5.10}$$

The contour is then chosen to be the unit circle with necessary modifications to exclude the singularities and branch points by usual method. It is clear that $k>h>x_1$. Taking then the principal value, the contribution due to the singularity $+\frac{1}{x_1}$ to the integral (5.5) is

$$-\frac{\pi^2 i}{2\xi}\frac{x_1^3\sqrt{1-\frac{\tau_2x_1^2}{4\times3\cdot5}}}{F'\left(\frac{1}{x_1}\right)\left(\frac{1}{x_1}-x_1\right)}J_0\left(\frac{2\xi}{x_1}r_1\right), \tag{5.11}$$

where $F(z)$ is given by the expression (5.6). Similarly the contribution due to the singularity $-\frac{1}{x_1}$ will be the same expression as in (5.11). Hence the total contribution will be

$$-\frac{\pi^2 i}{\xi}\frac{x_1^3\sqrt{1-\frac{\tau_2 x_1^2}{4\times 3\cdot 5}}}{F'\left(\frac{1}{x_1}\right)\left(\frac{1}{x_1}-x_1\right)}J_0\left(\frac{2\xi}{x_1}r_1\right). \qquad (5.12)$$

Taking the next term of the expansion of (5.2) the contributions will be cancelled due to the two singularities $\pm\frac{1}{x_1}$. Hence there will be contributions only from the terms $J_0, J_2, \cdots$ of the expression (5.3).

6. If we take similarly the term $e^{-i\beta l}$ and write $r_2\cos\theta_2=x-vt$, $r_2\sin\theta_2=y-l$, we get on integration of the second integral of (3.9), the same amplitude term as in (5.12). Similar are the other two integrals of (3.8) with

$$r_3\cos\theta_3=x-vt-l_1\,,\quad r_3\sin\theta_3=y\,,$$

$$r_4\cos\theta_4=x-vt-l_1\,,\quad r_4\sin\theta_4=y-l\,,$$

amplitude term being the same as in (5.12) with the factors $e^{i\xi l_1}$ and $J_0\left(\frac{2\xi}{x_1}r_3\right)$, $J_0\left(\frac{2\xi}{x_1}r_4\right)$ respectively. Hence cotribution to w at $z=0$ from these two singularities is

$$\frac{iA_1v^2}{4b^2\xi}\frac{x_1^2\sqrt{1-\frac{\tau_2 x_1^2}{4\times 3\cdot 5}}}{F'\left(\frac{1}{x_1}\right)}\left[J_0\left(\frac{2\xi}{x_1}r_1\right)-J_0\left(\frac{2\xi}{x_1}r_2\right)\right.$$

$$\left.-e^{i\xi l_1}\left\{J_0\left(\frac{2\xi}{x_1}r_3\right)-J_0\left(\frac{2\xi}{x_1}r_4\right)\right\}\right]e^{i(\xi v-p_1)t}$$

approximately as x_1 is large. It is clear that the approximate velocity of propagation of the disturbance is $\frac{\xi v-p_1}{2\xi/x_1}$. As it has been shown that $\xi v-p_1=2p_1$ or $\xi v=3p_1$ we have the velocity as $\frac{2p_1}{2\xi/x_1}=\frac{v}{3}\times\sqrt{\frac{4\times\cdot 95}{v}}\times b=\cdot 65b$ approximately. For the medium where $\frac{\lambda+2\mu}{\mu}=3.5$ we take the value of the velocity of S-waves as 4.4 km, per second. Hence the velocity of microseisms comes out to be 2.86 km. per second. Ramirez observed the average velocity of microseisms as 2.67 km per second. There is thus an approximate agreement.

The additional waves generated which are obtained from the singularities at ± 1 have low velocity and are not likely to be detected by observation. Hence the only waves to be recorded at a distant station are those given by (6.1).

7. The wave-length is given by

$$\frac{2\pi}{2\xi/x_1}=\frac{2\pi}{\xi}\times\frac{x_1}{2}\,. \qquad (7.1)$$

For ordinary sea-waves caused by hurricane winds the wave length as observed by Gilmore is 500 to 700 ft. when the period of sea-waves is 10 seconds. Hence, (7.1) is

$$\frac{2\pi}{\xi}\times\frac{1}{2}\sqrt{\frac{4\times\cdot 95}{v^2/b^2}}=\frac{2\pi}{\xi}\times\frac{1}{2}\times\frac{1\cdot 96}{v}\times b\,.$$

Putting $v=\frac{3p_1}{\xi}$ and $\frac{2\pi}{p_1}=10$ secs., we get the average wave-length to be $3\cdot 3\times b$. If $b=4.4$ km. per second the value of wave-length of the vibration is 14.6 km. approximately, the observed average wave-length being 14.76 km.

8. For maximum amplitude, it is not a worthwhile attempt to find it without very exact data as it depends on the depth, velocity and the period of the waves. At least, it can be seen that the amplitude of the disturbance is of correct order.

The nature of the roots of the equation (5.7) has been discussed in datails by Hayashi (1942). If observations are taken in this light, constitution of the earth below the ocean can be determined at different place.

9. The horizontal component of displacement can be obtained similarly from the expression (3.10) and (3.11) as in article 5. It is clear that, if we follow the method of article 5, the terms containing J_0 will be cancelled due to the two singularities corresponding to $z+\frac{1}{z}=\pm x_1$ given in article 5. Hence the first terms of the integral (3.10) and (3.11) will contain $J_1\left(\frac{2\xi}{x_1}r\right)$ where r is the distance of the point of observation from the approximate extremities of the rectangular

disturbed area on the sea. Then the ratio of the maximum vertical to the maximum horizontal displacement is given by

$$\frac{v^2}{b^2 x_1^2}\sqrt{1-\frac{\nu\tau_2}{4}x_1^2}\,2\left\{-\left(2-\frac{\tau_2}{4}x_1^2\right)+2\sqrt{1-\frac{\nu\tau_2}{4}x_1^2}\sqrt{1-\frac{\tau_2}{4}x_1^2}\right\} \tag{9.1}$$

approximately. As x_1 is the solution of (5.7) in terms of $z+\frac{1}{z}$, we have

$$2\sqrt{1-\frac{\nu\tau_2}{4}x_1^2}\sqrt{1-\frac{\tau_2}{4}x_1^2}=\frac{1}{2}\left(2-\frac{\tau_2}{4}x_1^2\right)^2.$$

Substituting this in (9.1), we get the value of the ratio when $\nu=\frac{1}{3{\cdot}5}$ as 1.6:1. This value is dependent on ν viz. on the geological structure. Average value of the ratio was observed by Ramirez to be 1.21:1 at St. Louis. If the ocean bed is not homogeneous but has a slight variation of elastic properties in the upper part, there may be slight dependence of ratio on the period, wave-length etc. But the mean value will be mainly dependent on geological structure.

10. The expressions for the displacements u, v up to first terms are given approximately, for x_1 large, by

$$u=\frac{iA_1''\cos\theta}{2\xi}e^{i(\xi r-p_1)t}\frac{\left\{2-\frac{\tau_2}{4}x_1^2-2\sqrt{1-\frac{\nu\tau_2}{4}x_1^2}\sqrt{1-\frac{\tau_2}{4}x_1^2}\right\}}{F'\left(\frac{1}{x_1}\right)}\left[J_1\left(\frac{2\xi}{x_1}r_1\right)-J_1\left(\frac{2\xi}{x_1}r_2\right)+e^{i\xi t}{}_1\left\{J_1\left(\frac{2\xi}{x_1}r_3\right)-J_1\left(\frac{2\xi}{x_1}r_4\right)\right\}\right],$$

$$v=\frac{iA_1\sin\theta}{2\xi}e^{i(\xi r-p_1)t}\frac{\left\{2-\frac{\tau_2}{4}x_1^2-2\sqrt{1-\frac{\nu\tau_2}{4}x_1^2}\sqrt{1-\frac{\tau_2}{4}x_1^2}\right\}}{F'\left(\frac{1}{x_1}\right)}\left[J_1\left(\frac{2\xi}{x_1}r_1\right)-J_1\left(\frac{2\xi}{x_1}r_2\right)+e^{i\xi t}{}_1\left\{J_1\left(\frac{2\xi}{x_1}r_3\right)-J_1\left(\frac{2\xi}{x_1}r_4\right)\right\}\right].$$

In evaluating u, v, $e^{i(\varphi-\theta)}$ has been substituted for $\cos(\varphi-\theta)$ and real part of the integral has been taken. Hence the direction of horizontal displacement gives us approximately the direction of the disturbed area. The position of the disturbed area, therefore, can be determined by means of two observing stations and observing the direction of horizontal displacement. The distance between the stations being known the position can be located. Taking more than one observation of the position of disturbed area the direction of motion of the storm can be determined quite accurately.

11. When the end points of the disturbed area are at very great distances viz. $\frac{2\xi}{x_1}r_n$ ($n=1, 2, 3, 4$) is large, contribution to displacement due to $J_0\left(\frac{2\xi}{x_1}r_n\right)$ or $J_1\left(\frac{2\xi}{x_1}r_n\right)$ ($n=1, 2, 3, 4$) becomes too small to be detected at a large distance as

$$J_n(z)\sim\left(\frac{2}{\pi z}\right)^{1/2}\left[\cos\left(z-\frac{1}{2}n\pi-\frac{\pi}{4}\right)\times\left\{1+\sum_{r=1}^{\infty}\frac{(-)^r(4n^2-1^2)(4n^2-3^2)\cdots(4n^2-4r-1^2)}{(2r)!\,2^{6r}z^{2r}}\right\}\right.$$
$$\left.+\sin\left(z-\frac{1}{2}n\pi-\frac{\pi}{4}\right)\sum_{r=1}^{\infty}\frac{(4n^2-1^2)(4n^2-3^2)\cdots(4n^2-4r-3^2)}{(2r-1)!\,2^{6r-3}z^{2r-1}}\right]$$

when $|z|$ is large and $|\arg z|<\pi$ (Cf. Whittaker (1915)). So it is likely that the monsoon which approaches with a very large front is not likely to give appreciable microseisms. In

fact Gherzi observed that on the China-coast microseisms were observed when there was typhoon, but none with the coming of monsoon.

References

Banerji, S. K.:
1930 Phil. Trans. Roy. Soc., A **229**, 287–328.
Bernard, P.:
1941 Ann. Inst. Phys. Globe Met., **19**, 1–77.
Darbyshire, J.:
1950 Proc. Roy. Soc., **202**, 439.
Deacon, G. E. R.:
1947 Nature, **160**, 419–21.
Gherzi, E.:
1923 Notes de Seismologie Obs. de Zi-Ka-Wei, **5**, 1–16.
1928 **8**, 1–12.
Gilmore, M. H.:
1946 Bull. Seis. Soc. Am., **36**, 89–119.
Gutenberg, B.:
1931 Bull. Seis. Soc. Am., **21**, 1–24.
Hayashi, H.:
1942 Physico-Math. Soc. Japan, **24**, 533–48.
Jeffreys, H.:
1924 Proc. Roy. Soc., A **107**, 189.
1925 **110**, 241.
Longuet-Higgins, M. S.:
1950 Phil. Trans. Roy. Soc., A **243**, 1–35.
Miche, M.:
1944 Ann. Ponts et Chauss, 25–78.
Ramirez, J. E.:
1940 Bull. Seis. Soc. Am., **30**, 39–84, 139–178.
Whipple, F. J. W. and Lee, A. W.:
1935 M. N. R. A. S. (Geophys. Sup.), **3**, 287–97.
Whittaker, E. T.:
1915 A Course of Modern Analysis, 362.

Nomographs for the Phase- and Group-Velocity of Love-Waves.

By

Yasuo SATÔ

Earthquake Research Institute, Tokyo University, Tokyo

Summary

Nomographs for the phase- and group-velocity of Love-waves were made. Such nomographs were already made by the same author a few years ago, but the present ones are more convenient for the practical work of seismometry because of the range of parameters and the precision obtainable.

Nomographs convenient for the computation of phase- and group-velocity of Love-waves were made. Similar nomographs were presented by the same author few years ago (SATÔ, 1953). However, they were not appropriate for the practical work, because a wide range of parameters was put into a limited space, and consequently the precision was not high enough for those engaged in observational seismology.

In the present paper, in order to make the precision higher, the domain of parameters was restricted to those as may be found in the practical study of seismometry.

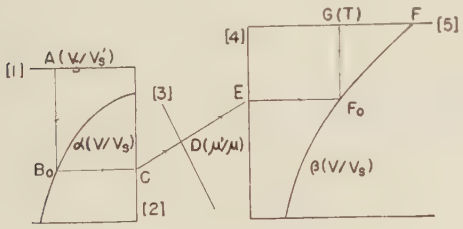

Fig. 1

§ 1. Fundamental formula for the computation of the phase velocity of LOVE-waves of the lowest mode is as follows (SATÔ, 1951, 1953):

$$\omega = \sec\theta \cdot [\operatorname{Arc\,tan}\{\chi \sec\theta \sqrt{\sin^2\theta - \sin^2\theta_0}\}] \quad \cdots\cdots(1.1)$$

where

ω ····frequency of LOVE-waves.

χ $=\mu'/\mu$ (μ' and μ are the rigidity of the lower and upper medium respectively).

$\operatorname{cosec}\theta_0 = V_s'/V_s$ (V_s' and V_s are the velocity of S-waves in the lower and upper medium respectively).

$\operatorname{cosec}\theta = V/V_s$ (V is the phase velocity of Love-waves).

By modifying the above expression the following form is obtained:

$$T\ (=\text{period measured by the unit } H/V_s) = 2\pi \div \left\{ \frac{\frac{V}{V_s}}{\sqrt{\frac{V^2}{V_s^2}-1}} - \operatorname{Arc\,tan}\left\{ \frac{\frac{V}{V_s}}{\sqrt{\frac{V^2}{V_s^2}-1}} \cdot \chi \sqrt{\frac{V_s^2}{V^2} - \frac{V_s^2}{V_s'^2}} \right\} \right\}, \quad \cdots\cdots(1.2)$$

where

H is the thickness of the surface layer.

§ 2. Explanation of the figure and direction for use of the first nomograph.

1° [1] is the axis of V_s/V_s'. When a certain value of V_s/V_s' is given, we take a point A on the axis corresponding to this assigned value.

2° α is the curve of $1/\sqrt{(V_s^2/V^2)-(V_s^2/V_s'^2)}$. At first we choose some value of V/V_s. Following arrow line, we get C on [2] axis, which gives $1/\sqrt{(\sin^2\theta-\sin^2\theta_0)}=1/\sqrt{(V_s^2/V^2)-(V_s^2/V_s'^2)}$.

3° [3] is the axis of μ'/μ. We take a point D on this axis and then obtain the point E on the [4] axis. E gives $1/\chi\sqrt{(\sin^2\theta-\sin^2\theta_0)}$.

4° Finally the curve β, which must have the same parameter V/V_s as the curve α, gives $G(T)$. $(T=2\pi/\omega)$.

Ranges of the parameters are:

V/V_s—0.65~0.97,

V_s/V_s'

V/V_s—1.01~1.10 (every 0.01),
1.10~1.46 (every 0.02),
μ'/μ — 1 ~4 ,
T —0.8~9.0.

§ 3. For the computation of the group velocity by means of the second nomograph, we give V_s/V_s', V/V_s and μ'/μ. The fundamental formula is (according to SATÔ, 1953)

$$\frac{U}{V}=\frac{1+S^2(\chi, Y)}{(V/V_s)^2+S^2(\chi, Y)},$$

where

U, V·····group and phase velocity of Love-waves respectively,
$S^2(\chi, Y)=F(\chi Y)\cdot(1+1/Y^2)$,
$F(Z)=1/\text{Arc tan } Z\cdot(Z+1/Z)$,
$Y=Z/\chi=\sec\theta\cdot\sqrt{(\sin^2\theta-\sin^2\theta_0)}$.

In the following figure (Fig. 2) the process of the calculation is illustrated.

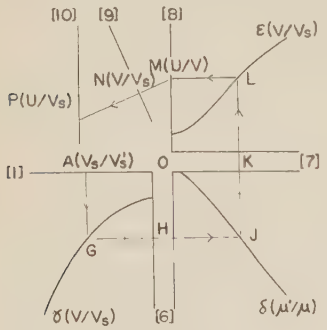

Fig. 2

1° As before we take a point A on [1] axis which gives V_s/V_s'.

2° γ is the curve of

$$1/Y=\cos\theta/\sqrt{(\sin^2\theta-\sin^2\theta_0)}.$$

If we choose a curve γ with a parameter equal to the given value of V/V_s, then the point H on the [6] axis expresses $1/Y$.

3° Next, [7] is the axis of $S(\chi, Y)$. Since the parameter of the curve δ in the second nomograph (right below) is $\chi(=\mu'/\mu)$, we can obtain the value of $S(\chi,Y)=\sqrt{\{F(\chi Y)\cdot(1+1/Y^2)\}}$ by combining $1/Y$ and χ which is naturally determined when the distribution of matter is given.

4° As the third step we obtain U/V. In the third nomograph (right upper), the curve $\varepsilon(V/V_s)$ gives

$$U/V=\{1+S^2(\chi, Y)\}/\{(V/V_s)^2+S^2(\chi, Y)\}.$$

5° If we want to make clear the ratio of the group and the phase velocity of Love-waves, the computation is finished by the above procedure. But if we want to make clear U/V_s, we must multiply the value thus obtained by V/V_s by means of the next nomograph (left upper) and get the final result.

§ 4. The precision of the results obtained will be high enough for the practical work.

References

SATÔ, Y :
1951 Bull. Earthq. Res. Inst., **29**, 1–11.
1953 Bull. Earthq. Res. Inst., **31**, 81–87. 255–260.

PHASE VELOCITY OF LOVE-WAVES

(WITHOUT NODE)

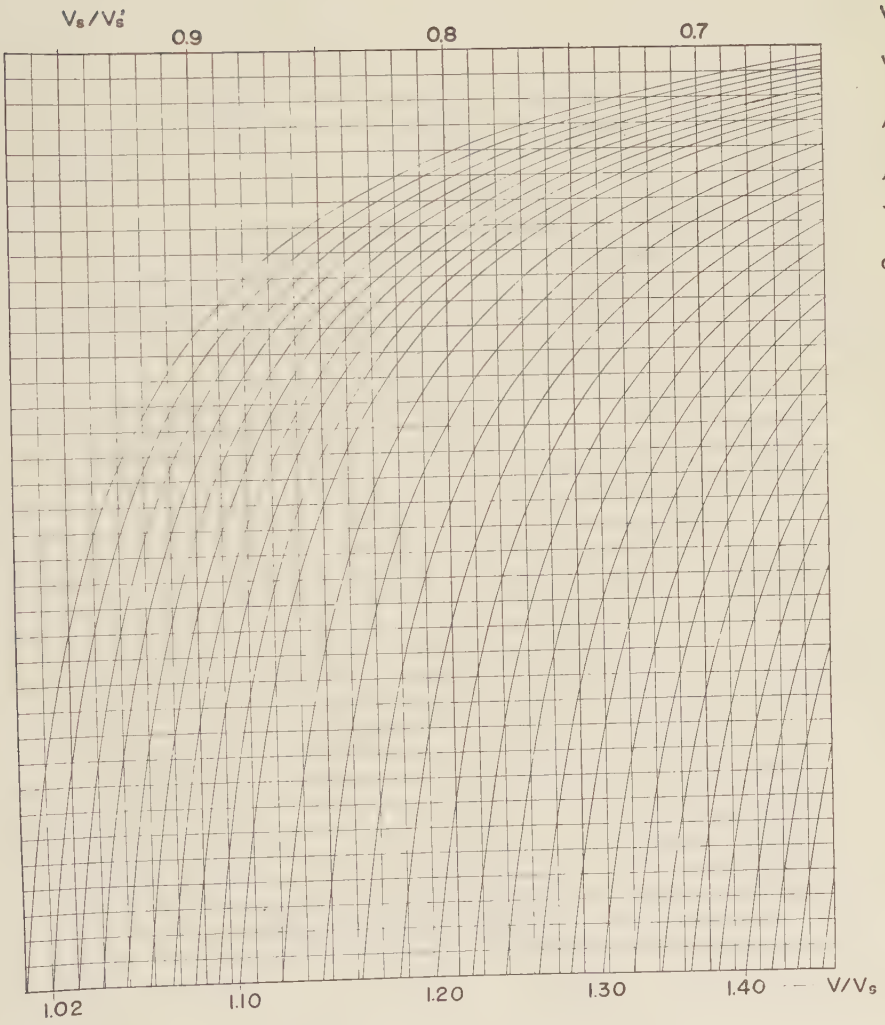

V_s . VELOCITY OF S

V_s' : VELOCITY OF S

V : VELOCITY OF

μ : RIGIDITY IN TH

μ' : RIGIDITY IN TH

T : PERIOD

ω : CIRCULAR FRE

Feb. 1956

Y. SATÔ

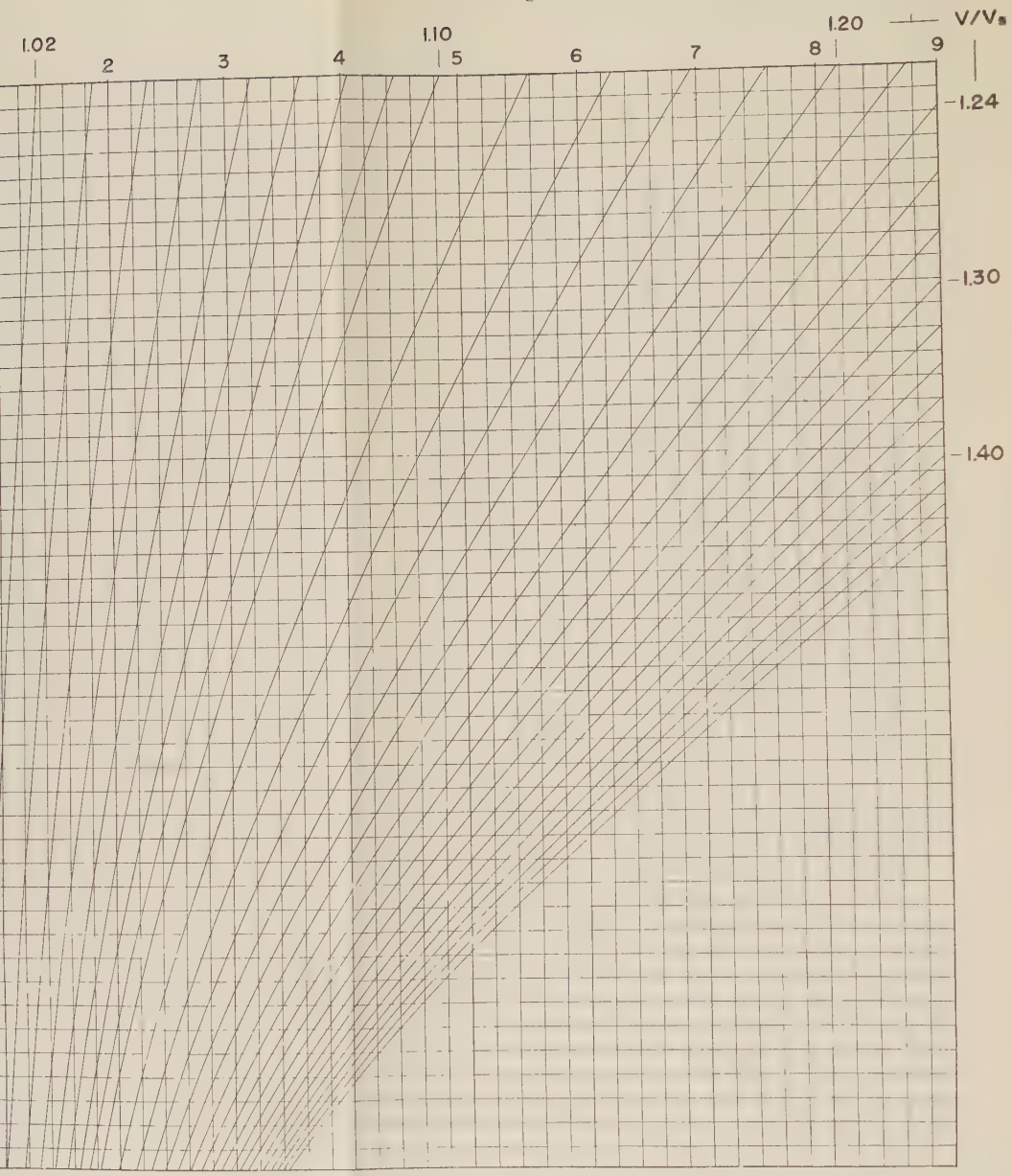
1.02
2
3
4
1.10
5
6
7
8
1.20
9
V/V₀
1.24
1.30
1.40

GROUP VELOCITY OF LOVE-WAVES

U GROUP VELOCITY OF LOVE-WAVES

V PHASE VELOCITY OF LOVE-WAVES

V_s VELOCITY OF S-WAVES IN THE LAYER

V_s' VELOCITY OF S-WAVES IN THE SUBSTRATUM

μ RIGIDITY OF THE LAYER

μ' RIGIDITY OF THE SUBSTRATUM

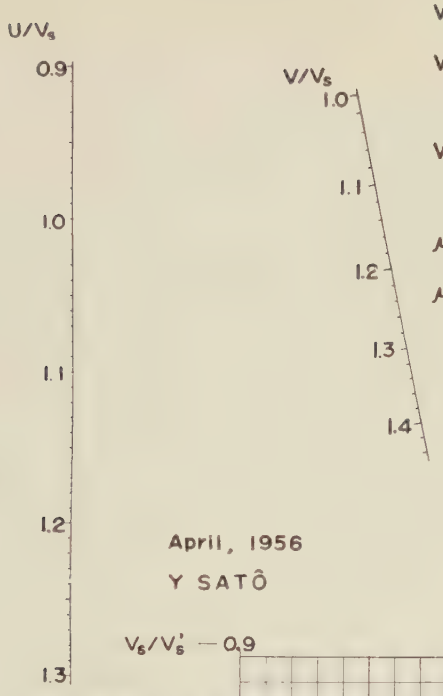

April, 1956

Y SATÔ

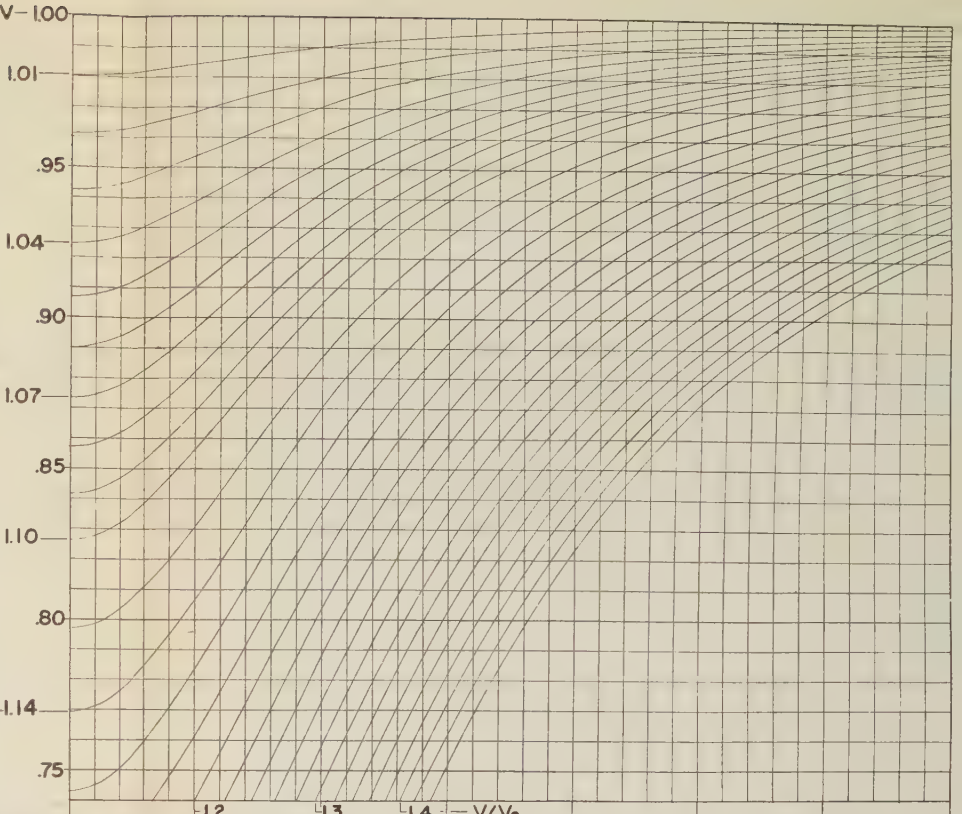

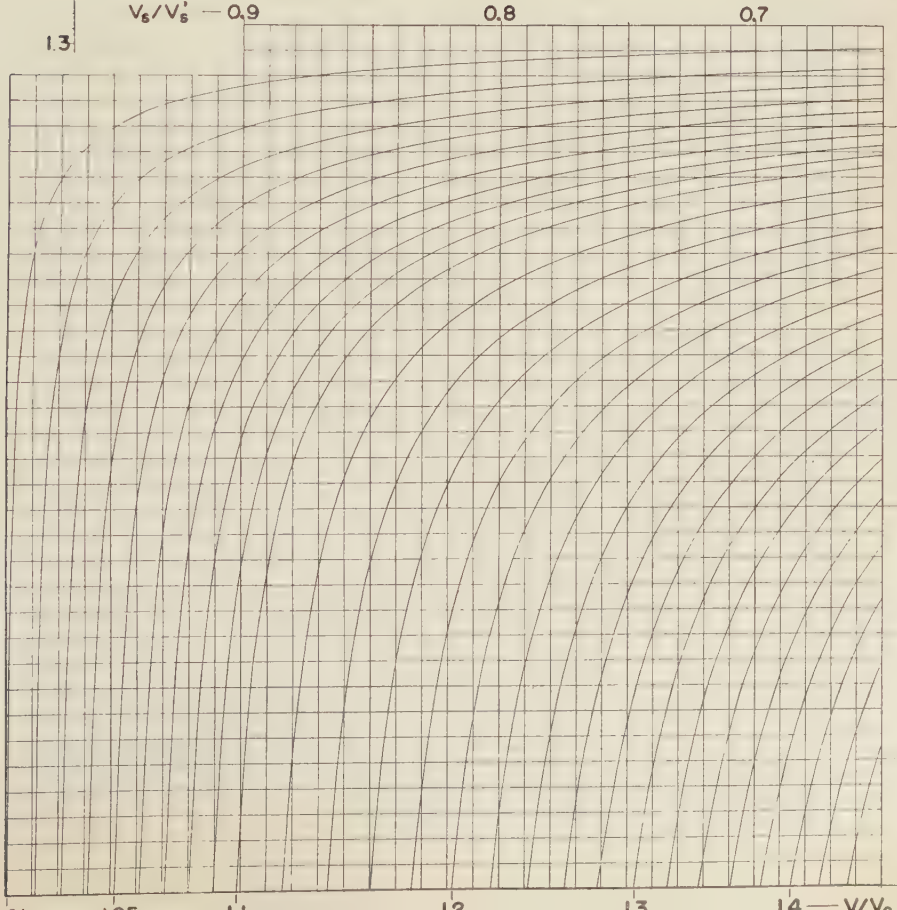

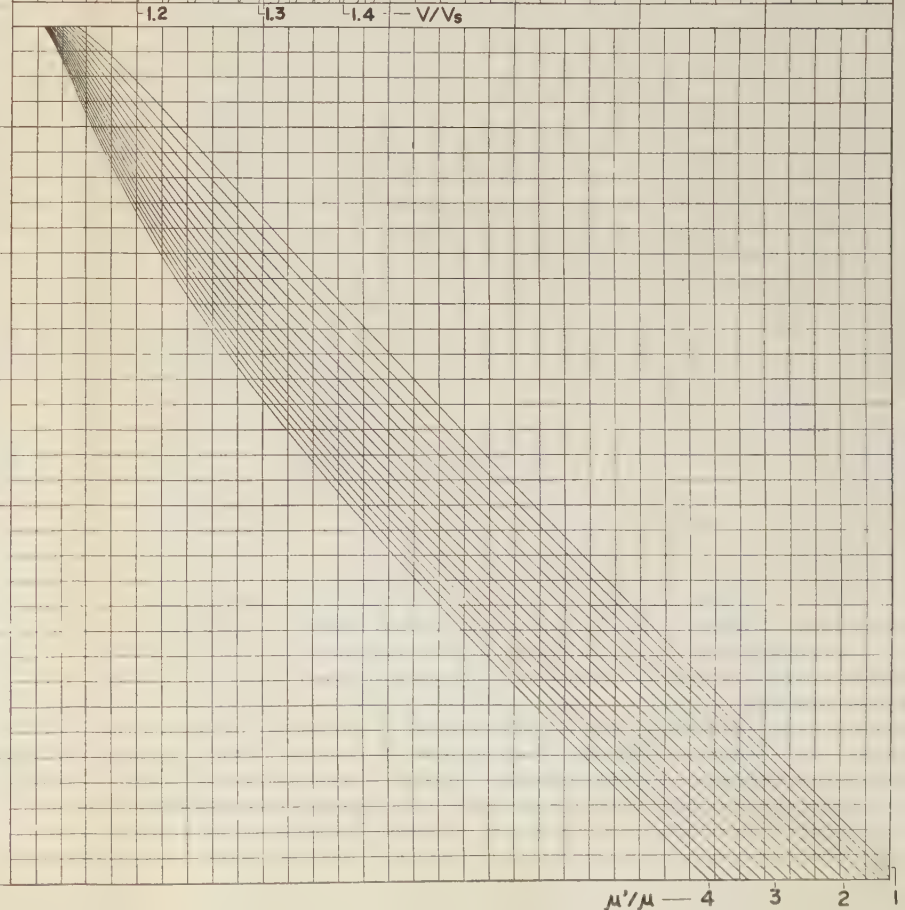

Chemical Equilibrium within Self-Gravitating Planets and Internal Constitution of the Earth

By

Yasuo SHIMAZU

Institute of Earth Sciences, Nagoya University, Nagoya.

Summary

Chemical structure of a simplified model of the planet of which the components are Fe–Si–O is discussed. Chemical equilibrium and hydrostatic equilibrium are assumed and emphasis is placed on gravitational separation due to density differences and chemical interaction among components, which control the equilibrium arrangement of stable phases. It is concluded that the present gravitational field of the earth is too strong for reasonable arrangement of the components.

Models with probable gravitational field are discussed and the following conclusions are obtained; (a) in 2,000°K isothermal model, Fe_2SiO_4 content shows a maximum at a certain depth and SiO_2 and FeO which are at shallower and deeper depths respectively will disappear soon; (b) in 2,000°K (surface)→6,000°K (center) model, the radius of the Fe-core is one-half of the earth's radius. The mantle is composed of Fe_2SiO_4, SiO_2 and isolated O.

1. Introduction

In two previous papers, hereafter referred to as Papers I and II (Y. SHIMAZU [1955, 1956]), we studied chemical equilibrium conditions within the gravitational field and applied the results thus obtained to a detailed study of the chemical structure of the earth. However, Paper I was concerned only with the one-phase and isothermal model of the earth, its constituents being FeO, MgO, SiO_2 and Fe. When Fe and O co-exist within a system, there occur two possibilities. Either Fe–O mixture phase is stable or FeO compound phase is stable. If it is the former, then under what physical (temperature, pressure) condition does it exist? If it is the latter, under what physical condition does this phase exist? In Paper II, we discussed this kind of phase stability and determined the pressure-temperature conditions for the phase stability. This condition is, however, a necessary condition and not a sufficient condition, because the mol ratio of the components should vary with depth, as given in Paper I. Even if the temperature and pressure are sufficient to form FeO phase, gravitational separation effect due to density differences in costituents will drive the heavier Fe downward and the lighter O upward. Then the thicker FeO layer will not be formed because the mol ratio Fe:O is far from unity at both upper and deeper parts of the earth. Isolated O is predominant at the upper part and Fe at the lower. Following is a detailed study of the chemical phase equilibrium within self-gravitating planets based upon the results obtained in Papers I and II.

2. Distribution of elements within self-gravitating planets

Our simplified model of the planet has three independent components Fe–Si–O. Three chemical reactions written below are assumed to occur within the model planet.

$$Fe+O \rightleftarrows FeO\,, \qquad (1)$$

$$Si+2O \rightleftarrows SiO_2\,, \qquad (2)$$

$$2FeO+SiO_2 \rightleftarrows Fe_2SiO_4\,. \qquad (3)$$

The compounds Fe_2O_3 and Fe_3O_4 are omitted from our consideration, because except at the surface layer of the earth they are apparently unstable (T. F. W. BARTH [1948]). $FeSiO_3$ is also omitted since the thermochemical data

for $FeSiO_3$ reaction is not available and, further, the energy and density differences between $FeSiO_3$ and Fe_2SiO_4 are neglected in our rough estimation. Reaction constants for (1)–(3) can be calculated as the functions of pressure and temperature using the results in Paper II.

Chemical equilibrium conditions are written by the results in Paper I as follows:

$$\left(\frac{\partial G_i}{\partial r}\right)_{P,T,n} dr - S_i dT + \left(\frac{\partial G_i}{\partial P}\right)_{r,T,n} dP + \sum_j \left(\frac{\partial G_i}{\partial n_j}\right)_{P,T,r,n_{j-1}} dn_j = 0 , \quad (4)$$

where

G_i: molar GIBBS' free energy of i-th component,
S_i: molar entropy of i-th component,
n_i: molfraction of i-th component; 1=Fe, 2=O, 3=Si, 4=dependent component ($n_1 = 1 - n_1 - n_2 - n_3$),
r: distance from the center,
P: pressure,
T: temperature.

Thermodynamical identities give

$$\left(\frac{\partial G_i}{\partial r}\right)_{P,T,n} = m_i g \quad (5)$$

and

$$\left(\frac{\partial G_i}{\partial P}\right)_{r,T,n} = v_i , \quad (6)$$

where

m_i: molar weight of i-th component,
v_i: molar volume of i-th component.

Hydrostatic equilibrium condition gives

$$\frac{\partial P}{\partial r} = -\rho g . \quad (7)$$

Mean density ρ of the system is a function of molfraction of components and thus it depends upon r even if the incompressible planet is assumed. Nevertheless for simplicity, we put $\rho = 4.0$. Transforming the independent variable r into

$$x = 1 - \frac{r}{a} \quad (a: \text{radius of the planet}),$$

we get from (4)–(7)

$$\frac{d \ln n_1}{dx} = -(\rho v_1 - m_1)\frac{ga}{RT} + \frac{S_1}{R}\frac{dT}{dx} - \frac{\Delta G_1}{RT}\frac{dn_2}{dx} ,$$

$$\frac{d \ln n_2}{dx} = -(\rho v_2 - m_2)\frac{ga}{RT} + \frac{S_2}{R}\frac{dT}{dx} - \frac{\Delta G_1}{RT}\frac{dn_1}{dx} - \frac{1}{2}\frac{\Delta G_2}{RT}\frac{dn_3}{dx} ,$$

$$\frac{d \ln n_3}{dx} = -(\rho v_3 - m_3)\frac{ga}{RT} + \frac{S_3}{R}\frac{dT}{dx} - \frac{1}{2}\frac{\Delta G_2}{RT}\frac{dn_2}{dx} , \quad (8)$$

where ΔG_1 and ΔG_2 are energy changes during the reactions from left to right in (1) and (2) respectively. Second terms of the right-hand sides of (8) vanish in the isothermal planet. We can neglect the second term for even 2,000°K (surface) → 6,000°K (center), since it is only one-tenth of the first and third terms combined. It is noteworthy that dT/dx is the excess of the temperature gradient over the adiabatic gradient for the compressible planet.

As shown in Paper II we have

$$\Delta G = \Delta G^0(T) + P\Delta v , \quad (9)$$

and Δv is given by

$$\Delta v = (v_A - v_B) + \frac{m_C}{\rho_A} , \quad (10)$$

under the reaction $B + C \uparrow \rightleftarrows A$. (See equation (14) of Paper II). Values m_i and v_i of any material are given in Table I. Molar volume of O is calculated from ionic radius (T. F. W. BARTH [1948]).

Table I. Molar weight m_i and molar volume v_i.

	m_i	v_i
Fe	55.85	7.10
Si	28.10	12.06
O	16.00	6.93
FeO	71.85	11.98
SiO_2	60.19	22.64
Fe_2SiO_4	203.8	47.61

We get the unique solution of equations (8) if the molfraction

$$\int_0^a n_1 r^2\, dr : \int_0^a n_2 r^2\, dr : \int_0^a n_3 r^2\, dr \quad (11)$$

for the whole planet is known. It is, how-

ever, obviously prohibitive to solve (8) numerically with boundary condition (11). We will begin integration by giving a suitable surface value. Trial and error method is used to satisfy

$$\sum_{i=1}^{4} n_i \leq 1$$

at any depth.

If we do solve (8), we encounter the following serious difficulty. Assuming the surface temperature to be 2,000°K for the earth, equations (8) become at the surface

$$\frac{d\ln n_1}{dx} = +102.6 + 7.80\frac{dn_2}{dx},$$
$$\frac{d\ln n_2}{dx} = -44.4 + 7.80\frac{dn_1}{dx} + 15.35\frac{dn_3}{dx},$$
$$\frac{d\ln n_3}{dx} = -76.2 + 15.35\frac{dn_2}{dx}. \qquad (12)$$

The first terms of the right-hand sides which give the effect of gravitational differentiation are considerably larger than the second terms which express the effect of chemical interaction. Then we see that Fe and O would separate completely if the structure of the present earth is formed under $g_s \sim 10^3$ (=present value). The present value of gravity is too large! It appears that n_1 (surface) $\ll 1$. The result of a rough calculation shows that n_1 (surface) must be less than $\exp(-16.5)$ for $T < 10^{4}$°K.

3. Variation of gravity during terrestrial evolution

According to H. Brown and C. Patterson's study (1948) on the composition of meteoritic proto-planet, the effect of gravitational differentiation is predominant in the deeper parts of the plant. The molfraction of O varies linearly from only 60 per cent at the top to 49 per cent at the bottom and variation of Fe is from 4 per cent to 15 per cent (see Fig. 2). From Fig. 2, we obtain

$$\frac{d\ln n_1}{dx} \sim +1.1, \qquad \frac{d\ln n_2}{dx} \sim -1.6,$$
$$\frac{d\ln n_3}{dx} \sim -0.16 \qquad (13)$$

at the surface. Putting (13) into (8) we get $g_s a/RT \sim 0.03$ for the meteoritic proto-planet (g_s: surface value of g). Then $g_s a$ must be $0.02\times(g_s a)_{\text{present earth}}$ for $T=3{,}000$°K, which is the temperature given in Brown's paper. Brown deduced also that the chemical reaction in meteorites occurred at a high pressure of the order of 3×10^5 atmospheres. Since the present Mars has 3×10^5 atmospheres at the center, he came to the conclusion that the proto-planet would be of the same size as Mars. However, the present Mars has $g_s a \sim 0.23$ $(g_s a)_{\text{present earth}}$. From our point of view, this seems to be too large.

In a rough calculation, g can be replaced by the mean value g_m. For a homogeneous planet g_m is equal to $\frac{1}{2}\, g_s$. Since $g_s \propto a$ and the total mass M is $M \propto a^3$, we can write

$$g_s a \propto \frac{M}{a}. \qquad (14)$$

On the other hand. G. P. Kuiper (1949) discussed the variation of M/a during terrestrial evolution. According to him, the lighter elements gradually escaped toward outer space after the terrestrial accretion has been completed, and M and a decreased gradually during terrestrial evolution. His study shows also that M/a was equal to $0.4\times(M/a)_{\text{present}}$ at the initial stage, decreased to the minimum value $1/40(M/a)_{\text{present}}$, and then increased to the present value. The escape of comparatively heavy elements such as Fe, Ni, Mg, Si stopped at the minimum M/a-stage and thereafter the variation of M/a was due mainly to the escape of chemically non-active gas such as Xe and Kr. The minimum value $1/40(M/a)_{\text{present}}$ agrees well with 0.02 $(g_s a)_{\text{present}}$ obtained from (13).

Are there other possible ways to avoid the serious difficulty already mentioned? Based upon the assumptions that chemical equilibrium is attained, we can assume

(a) the temperature was much higher than 10^{4}°K, or

(b) hydrostatic equilibrium was not attained at the stage of formation of chemical structure.

To satisfy assumption (a), the temperature

should be higher than $10^{5\circ}$K which seems to be too high. To satisfy assumption (b), we must assume that all chemical reactions occurred at the stage of large $g_s a$ and that afterwards the gravitational separation occurred at smaller $g_s a$, which assumption seems to be rather artificial.

4. Chemical constitution of the simplified earth's model

Solving equations (8) for the special case $g_s a/RT=0.03$, we obtain Fig. 1 (a) and (b), which may be adopted tentatively. The distribution of elements within BROWN's meteoritic proto-planet is shown for comparison in

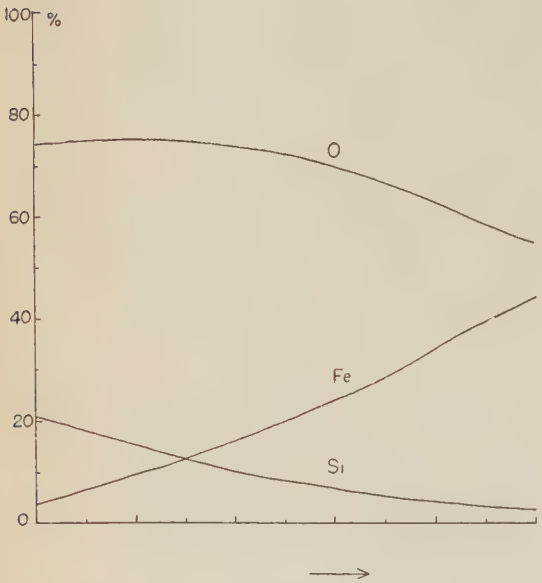

Fig. 1 (a) Distribution of elements within 2,000°K isothermal planet.

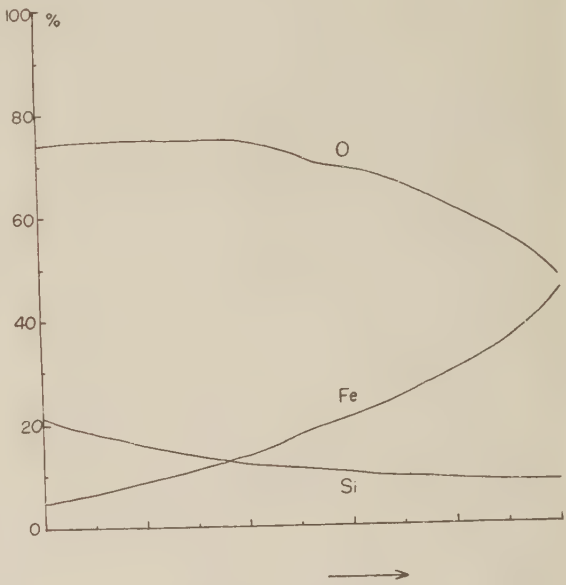

Fig. 1 (b) Distribution of elements within 2,000°K (surface)→ 6,000°K (center) planet.

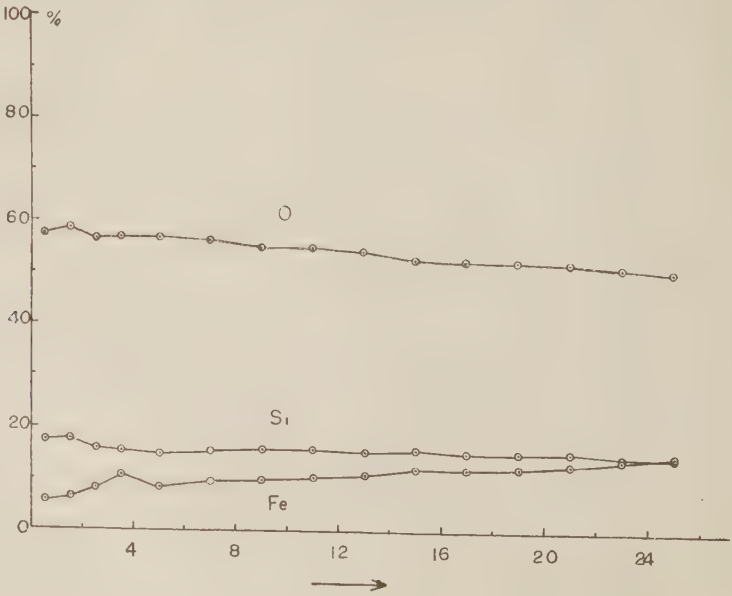

Fig. 2. Distribution of elements within BROWN's meteoritic proto-planet. (after H. BROWN and C. PATTERSON [1948])

Fig. 2. Substituting n_1, n_2, n_3 thus obtained into (1)–(3), we get the complete structure of the model as shown in Fig. 3 (a) and (b).

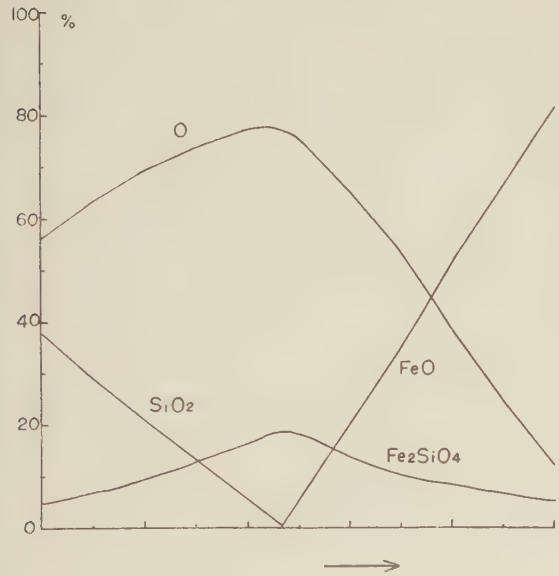

Fig. 3 (a) Chemical structure of 2,000°K isothermal planet.

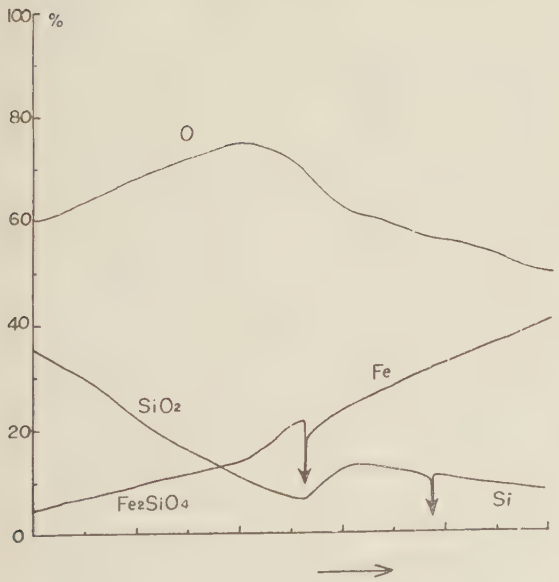

Fig. 3 (b) Chemical structure of 2,000°K (surface) → 6,000°K (center) planet.

Fig. 3 (a) of the 2,000°K isothermal model shows that Fe and Si at any depth are of the oxide forms FeO and SiO_2, and that the remaining O is of isolated form. FeO and SiO_2 tend to combine to form Fe_2SiO_4. Since SiO_2 decreases with depth and FeO increases, Fe_2SiO_4 content shows maximum at about $x=0.5$. When isolated FeO and SiO_2 are at shallower or deeper depth than $x=0.5$ respectively they will disappear. In Fig. 3 (b), i.e., the model with 2,000°K (surface) → 6,000°K (center), FeO and SiO_2 decompose at $x=0.5$ and $x=0.8$ respectively. Then a metal core will be formed of isolated Fe and Si. The mantle is composed of Fe_2SiO_4, remaining SiO_2 and isolated O.

Since O content is too high in our simplified model, it can be found at any depth. In the actual planet, however, isolated O will be of a combined form with elements other than Fe and Si, as for intance Al or Na.

This work was carried out by the writer under receipt of Grant in Aid for Developmental Scientific Research of the Ministry of Education.

References

BARTH, T. F. W.:
1948 The distribution of oxygen in the lithosphere, Jour. Geol., **56**, 41–49.

BROWN, H. & C. PATTERSON:
1948 The composition of meteoritic matter, III. Phase equilibria, genetic relations and planet structure, Jour. Geol., **56**, 85–111.

KUIPER, G. P.:
1951 The atmospheres of the sun and planets. (Rev. Ed.)., Chap. 12, Univ. Chicago Press, Chicago.

SHIMAZU, Y.:
1955 Chemical structure and physical property of the earth's mantle inferred from chemical equilibrium condition, Jour. Earth. Sci., Nagoya Univ., **3**, 85–90.
1956 Chemical phase equilibrium and physical structure within the earth's mantle, Jour. Phys. Earth., **4**, 1–6.

Temperature Distribution within the Mantle.

By

Michiyasu SHIMA

Geophysical Institute, Faculty of Science, Kyoto University, Kyoto.

Summary

Temperature distributions within the mantle have been calculated by the modern theory of solid, on the assumptions that the thermal state is nearly stationary at present and there is only a conductive heat flow within the mantle. The main results obtained are as follows. Under the above assumptions, temperature distributions with γ_G less than 2.25 cannot be obtained in the B-layer (413–1000 km). The temperature gradient there is nearly constant and increases gradually with depth in the D-layer. (1000–2898 km).

Notations. ρ: density, ρ_0: density at $p=0$ and $T=0$, p: pressure, T: temperature, r: distance from the earth's centre, g: acceleration of gravity, K_T: isothermal bulk modulus, K_S: adiabatic bulk modulus, α: coefficient of thermal expansion, γ_G: GRÜNEISEN's parameter, ϕ: K_S/ρ, v_p: velocity of P-wave, v_s: velocity of S-wave, A: mean atomic weight, N: LOSCHMIDT's number, λ, μ, m, n, l: LAME's constants, K: thermal conductivity, P: rate of generation of heat per unit volume, C_v: specific heat at constant volume, C_p: specific heat at constant pressure, δ: constant relating to crystal structure.

There are two points of view concerning the thermal history of the earth. The first assumes that the earth started as a hot gas and has been cooling ever since. The second assumes that the earth started as a cold body and got warmer in the course of time. But if the earth had once entirely molten, its subsequent history would be the same as that of the earth with a hot origin. The point of view that the earth has been cooling through the molten state is considered correct by many geophysicists (B. GUTENBERG, 1951). The epoch immediately after the molten state was characterized by a fast cooling as the results of mixing process and radiation and the cooling velocity became very small after the mantle had solidified. Particularly, the cooling in the mantle and the deeper part is very slow (H. JEFFREYS, 1952). Then the thermal state may be nearly stationary at present and thus it is assumed in the present calculations that there is only a conductive heat flow in the mantle and radioactive matters distributed uniformly there and the rates of heat generation per unit volume are constant respectively in the homogeneous B- and D-layers.

If the condition of hydrostatic equilibrium is satisfied within the mantle, that is, $dp=-g\rho dr$, the variation in density in the homogenous layer is expressed by the following equation (F. BIRCH, 1952)

$$\frac{d\rho}{\partial r}=\left(\frac{\partial\rho}{\partial p}\right)_T\frac{dp}{dr}+\left(\frac{\partial\rho}{\partial T}\right)_p\frac{dT}{dr}$$
$$=-\frac{g\rho^2}{K_T}-\rho\alpha\frac{dT}{dr}\,. \qquad (1)$$

By the thermodynamical relation between isothermal and adiabatic bulk moduli

$$\frac{1}{K_T}=\frac{1+T\alpha\gamma_G}{K_S}\,,$$

the density variation (1) is written as follows

$$\frac{d\rho}{dr}=-\frac{g\rho}{\phi}-\alpha\rho\left(\frac{g\gamma_G T}{\phi}+\frac{dT}{dr}\right)$$
$$=-\frac{g\rho}{\phi}+\rho\eta\,. \qquad (2)$$

We shall divide the mantle into thin shells in the following numerical integrations, the outer and inner radii being r_1 and r_2, and use the suffixes 1 and 2 to distinguish the physical quantities of the materials existing at r_1 and r_2 (H. MIKI, 1952). Then (2) may be approximated by the following equation

$$\eta=\frac{2(1-\rho_2/\rho_1)}{(r_1-r_2)(1+\rho_2/\rho_1)}+\frac{2g}{\phi_1+\phi_2}. \qquad (3)$$

The ratio of densities ρ_2/ρ_1 can be derived from the definition of GRÜNEISEN's parameter,

$$\left(\frac{\rho_2}{\rho_1}\right)^{3\gamma_G-1}=\frac{(v_p^{-3}+2v_s^{-3})_1}{(v_p^{-3}+2v_s^{-3})_2}, \qquad (4)$$

where

$$\gamma_G=-\frac{\partial \log \nu_m}{\partial \log (A/\rho)},$$

$$\nu_m=\left(\frac{9N\rho}{4\pi A}\right)^{1/3}(v_p^{-3}+2v_s^{-3})^{-1/3}=\left(\frac{9N\rho}{4\pi A}\right)^{1/3}c, \qquad (5)$$

$$v_p^2=[\lambda+2\mu+f(16\lambda+20\mu-18l-4m)+f^2(62.5\lambda+65\mu-207l-55m-3n)]/\rho, \qquad (6)$$

$$v_s^2=[\mu+f(3\lambda+9\mu+1.5m+0.5n)+f^2(15\lambda+27.5\mu-27l+1.5m+2.5n)]/\rho. \qquad (7)$$

By (5), (6), (7), we have (Y. SHIMAZU, 1954)

$$\gamma_G=\frac{1}{3}+\frac{(B_1-3)/2+(B_2-B_1/2)f+B_2f^2}{3(1+B_1f+B_2f^2)},$$

where

$$f=\frac{(\rho/\rho_0)^{2/3}-1}{2},$$

$$B_1=12+3(\lambda/\mu-1)+\frac{1.5m+0.5n}{\mu}=12.52+\frac{1.5m+0.5n}{\mu},$$

$$B_2=42.5+15(\lambda/\mu-1)+\frac{7(1.5m+0.5n)}{\mu}=45.19+\frac{7(1.5m+0.5n)}{\mu}\quad\text{(in the mantle)}. \qquad (8)$$

We use the power $m+n=6$ in the following expressions of the potential energy between two atoms $\Phi=\frac{\alpha}{r^m}+\frac{\beta}{r^n}$, in deriving B_1 and B_2 (M. SHIMA, 1955). Then ρ_2/ρ_1 are obtained from (4) and (8), taking γ_G as a parameter.

The stationary and conductive heat flow is expressed as follows

$$\frac{1}{r^2}\frac{d}{dr}\left(r^2K\frac{dT}{dr}\right)=-P. \qquad (9)$$

We obtain by the integration of (9)

$$\frac{dT}{dr}=\left(\frac{dT}{dr}\right)_b\frac{r_b^2K_b}{r^2K}-P\frac{(r^3-r_b^3)}{3r^2K}, \qquad (10)$$

where the suffix b indicates the physical quantities at lower boundaries of each layer. The heat conduction is considered non-metallic in the rocks which constitute the mantle. Thus, the lattice vibrational thermal conductivity K is expressed as follows (S. MIZUSHIMA, 1954)

$$K=\delta\frac{d^{2/3}v_pc^2}{T}, \qquad d=\rho/\rho_a. \qquad (11)$$

We put (11) in (10) and take (2) and (10) into consideration, then

$$-\frac{\eta}{\alpha}-\frac{gT\gamma_G}{\phi}=\frac{r_b^2d_b^{2/3}v_{pb}c_b^2}{r^2d^{2/3}v_pc^2}\left(\frac{dT}{dr}\right)_b\frac{T}{T_b}-\frac{PT(r^3-r_b^3)}{3r^2\delta d^{2/3}v_pc^2}. \qquad (12)$$

On the other hand, from the following equation

$$\frac{1}{c_p}=\frac{1}{c_v(1+T\alpha\gamma_G)}, \qquad \gamma_G=\frac{\phi\alpha A}{c_p},$$

we obtain

$$\frac{1}{\alpha}=\frac{A\phi}{\gamma_Gc_v}-T\gamma_G. \qquad (13)$$

By putting (13) into (2) and (12), we have

$$\frac{dT}{dr}+\left(\frac{g\gamma_G}{\phi}-\eta\gamma_G\right)T=-\frac{\eta\phi}{\gamma_G}\frac{A}{c_v}, \qquad (14)$$

$$-\eta\left(\frac{A}{c_v}\frac{\phi}{\gamma_G}-T\gamma_G\right)-\frac{g\gamma_GT}{\phi}=\frac{r_b^2d_b^{2/3}v_{pb}c_b^2}{r^2d^{2/3}v_pc^2}\left(\frac{dT}{dr}\right)_b\frac{T}{T_b}-\frac{PT(r^3-r_b^3)}{3r^2\delta d^{2/3}v_pc^2}. \qquad (15)$$

(10) and (14) give on integrations

$$T=e^{-\overline{P}(r)}\left(\int_r^{r_b}e^{\overline{P}(r)}\frac{\eta\phi A}{\gamma_Gc_v}dr+T_a\right),$$

$$\overline{P}(r)=\int_r^{r_a}\left(\frac{g\gamma_G}{\phi}-\eta\gamma_G\right)dr. \qquad (16)$$

$$\log T=\log T_a-\left(\frac{dT}{dr}\right)_b\frac{d_b^{2/3}v_{pb}c_b^2}{T_b}\int_r^{r_a}\frac{dr}{r^2d^{2/3}c^2v_p}+\frac{P}{3\delta}\int_r^{r_a}\frac{r^3-r_b^3}{r^2d^{2/3}v_pc^2}dr, \qquad (17)$$

where a indicates the physical quantities at upper boundaries of each layer. ϕ and c can be calculated from the observed values of v_p and v_s and g is nearly constant within the mantle (10^3 cm sec^{-2}). We eliminate P/δ and

A/c_v from (15), (16) and (17) and calculate the temperature distribution, holding them constant in each homogeneous layer. The results are given in Table 1.

Table 1. Absolute temperature within the mantle.

Depth (km)	γ_G=2.25	γ_G=2.5	Depth (km)	γ_G=1.4		γ_G=1.5		γ_G=2.0	
33	*1000	*1000	1000	*2000	*2500	*2000	*2500	*2000	*2500
100	1119	1142	1200	2102	2628	2190	2703	2369	2898
200	1270	1320	1400	2218	2762	2402	2935	2793	3340
300	1380	1491	1600	2343	2897	2646	3216	3230	3778
413	1531	1775	1800	2470	3031	2920	3520	3700	4075
			2000	2596	3170	3201	3842	4259	4650
			2200	2730	3311	3537	4217	4802	5192
			2400	2887	3460	3903	4620	5396	5817
			2600	3068	3616	4314	5098	6000	6408
			2800	3280	3810	4720	5545	6595	7028

* Assumed values.

The values of T are plotted in Fig. 1 against the depth.

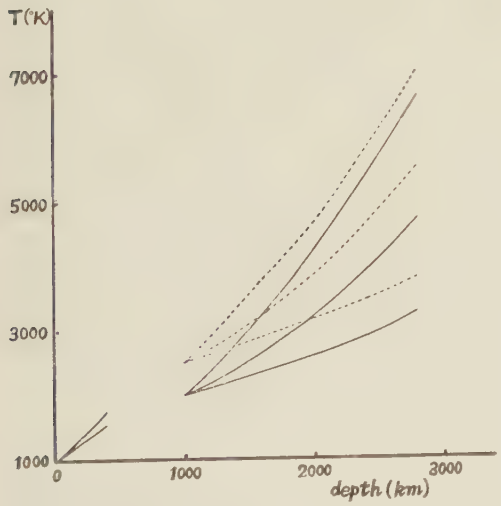

Fig. 1. Absolute temperature versus depth.

The temperature distribution in the C-layer (413–1000 km) was not calculated in the above, since the change of constitution has not been ascertained in it. The temperature distributions in the B-layer with γ_G less than 2.25 are not given in Table 1, because we cannot obtain them keeping P/δ and A/c_v constant in it. The temperature gradients obtained are larger than the adiabatic one, and then the heat may be carried away by conduction. They are nearly constant in the B-layer and gradually increase with depth in the D-layer.

References

Birch, F.:
1952 Jour. Geophys. Res. **57**, 227.
Gutenberg, B.:
1951 Internal Constitution of the Earth, 150.
Jeffreys, H.:
1952 The Earth, 293.
Miki, H.:
1952 Jour. Phys. Earth, **2**, 55.
Mizushima, S.:
1954 Jour. Phys. Soc. Jap. **9**, 546.
Shima, M.:
1955 Zishin, **8**, 38.
Shimazu, Y.:
1954 Jour. Phys. Farth, **2**, 55.

Thermal Process Near the Earth's Crust.

By

Keiiti AKI

Geophysical Institute, Faculty of Science, Tokyo University

Summary

In connection with the earthquake energy problem, the thermal processes which can result in the steady accumulation of necessary energy somewhere close to the bottom of the earth's crust has been investigated. With the aid of experimental and theoretical laws concerning thermal convections, some informations about the physical state at the place have been obtained.

Introduction

It is widely believed that an earthquake is a phenomenon of release of strain energy which has been stored up in the earth's crust. The estimated energy of the largest possible earthquake exceeds 10^{24} erg. It is a very interesting and important problem how and why such a tremendous amount of energy can be accumulated and stored up within the earth's crust. In this paper the writer is going to investigate thermal processes which are possibly taking place near the earth's crust and which he believes are closely connected to the present problem.

As to the fundamental cause of an earthquake, there are at least two important hypotheses. In one of the two, the stress generated within the earth's crust by subcrustal convection currents plays an important role and this view is supported by D. GRIGGS and Vening MEINESZ, while in the other the change in internal pressure accompanying phase changes or general chemical reactions of involved material is essential and this latter view is supported by J. JOLY and R. A. DALY. Recently T. MATUZAWA (1953) has investigated the matter from the latter point of view and made quantitative discussions how a solid-liquid phase transformation can supply strain energy to the crust and make an earthquake occur. According to him if a subcrustal material having a volume of 500 km^3 melts being accompanied by about 10 % increase of its own volume a pressure increment of 300 bars at the place will be generated. Thus the strain energy of 8×10^{24} erg will be stored in the crust. The work done by the elevation of the crust through the gravity field is 4×10^{26} erg. On the other hand the thermal energy consumed as the latent heat is estimated to be 9×10^{27} erg. In his paper Prof. MATUZAWA was chiefly concerned with the mechanical aspect of the problem, and the question how the thermal energy can be supplied to the place concerned still remained open. Before studying quantitatively about the possibility of the supply of heat energy to the *field of earthquake*, it is important to select such processes that will satisfy a certain condition among many processes which may be assumed to take place under the crust. As to this condition, that for stationary increase of heat storage will be reasonably taken.

The conversion of thermal energy into mechanical energy within a system of material usually takes place through the change in volume of the system; for instance, even the thermal convection current in the gravity field is maintained by the work done by volume change. The volume change of a part of material is a result of the accumulation of heat into that part. If there is no such accumulation, the conversion into mechanical energy can never take place however abundant the heat flow through the material may be. In the following discussions we shall confine ourselves to investigate those processes in which heat flows steadily upward from a

high temperature source assumed to exist at greater depths of the earth and the heat is accumulated somewhere close to the crust steadily.

Condition for the steady accumulation of heat

The condition for the steady accumulation of heat into a part of material is satisfied only in the following two cases. Putting the velocity of flow at the part V,

1. $V \neq 0$
2. or in the case of $V=0$, denoting the number of components in the system by β, and the number of phases by α,

$$\alpha=\beta+1 .$$

We can verify the first of these statements easily. The accumulation of heat into a part of material from the outside per unit time is

$$k\int \nabla^2 T dv , \qquad (1)$$

where k is the thermal conductivity. The equation of heat transfer is

$$\frac{\partial T}{\partial t}+(V\cdot \mathrm{grad})T=a\nabla^2 T , \quad a=\frac{k}{\rho c} , \qquad (2)$$

where c is the specific heat and ρ the density. Therefore even in the steady state $\frac{\partial T}{\partial t}=0$, if $V\neq 0$, the heat accumulation can take place. This case corresponds to the process required for convection theory of the earthquake cause.

In the next place, as to the second of the statements the accumulation will appear to be impossible in the case $V=0$, and $\frac{\partial T}{\partial t}=0$. But the equation of heat transfer is correctly written as

$$T\frac{\partial S}{\partial t}=\frac{k}{\rho}\nabla^2 T \qquad (3)$$

where S is the entropy per unit mass. On the other hand there is the following relation,

$$\frac{\partial S}{\partial t}=\left(\frac{\partial S}{\partial T}\right)_{P.M.}\frac{\partial T}{\partial t}+\left(\frac{\partial S}{\partial P}\right)_{T.M.}\frac{\partial P}{\partial t} +\sum\sum\left(\frac{\partial S}{\partial M_n^i}\right)_{P.T.}\frac{\partial M_n^i}{\partial t} \qquad (4)$$

where P is the pressure and M_n^i is the number of mol of the n-th component of the i-th phase of the system. Therefore it may happen that even if temperature and pressure are kept constant, the phase transformation enables the heat accumulation into the system. The composition of a phase can be determined by its concentration c_n^i, and we have

$$c_n^i=M_n^i/\sum M_n^i=M_{ni}/M^i \qquad (5)$$

$$\frac{\partial M_n^i}{\partial t}=M^i\frac{\partial c_n^i}{\partial t}+c_n^i\frac{\partial M^i}{\partial t} . \qquad (6)$$

Assuming the system as a closed one, we get

$$\frac{\partial}{\partial t}\left(\sum_i M_n^i\right)=0 \qquad (n=1, 2, \cdots\cdots \beta) \qquad (7)$$

$$\sum_i\left(M^i\frac{\partial c_n^i}{\partial t}+c_n^i\cdot\frac{\partial M^i}{\partial t}\right)=0 \qquad (8)$$

We shall consider the case of $\alpha\leqq\beta+2$, for the case of $\alpha>\beta+2$ cannot exist by the phase rule. At first, in the case of $\alpha=\beta+2$, the pressure, temperature and concentration should take the thermodynamically determined values for the system. But it seems unnecessary to consider such a strict condition at the interior of the earth.

In the case of $\alpha=\beta+1$, if the value of pressure is once determined, the temperature and concentration are also determined at the same time. Therefore if P is kept constant by some external condition, the temperature and concentration of the system are automatically kept constant as long as the condition $\alpha=\beta+1$ is fulfilled, and we have from the equation (4) and (6) the following equation

$$\begin{aligned}\frac{\partial S}{\partial t}&=\left(\frac{\partial S}{\partial T}\right)_{P.M.}\frac{\partial T}{\partial t}+\left(\frac{\partial S}{\partial P}\right)_{T.M.}\frac{\partial P}{\partial t} +\sum\sum\left(\frac{\partial S}{\partial M_n^i}\right)_{P.T.}M^i\frac{\partial c_n^i}{\partial t} +\sum\left\{\sum\left(\frac{\partial S}{\partial M_n^i}\right)_{P.T.}c_n^i\right\}\frac{\partial M^i}{\partial t}\\ &=\sum_{i=1}^{\alpha}\left\{\sum_{n=1}^{\beta}\left(\frac{\partial S}{\partial M_n^i}\right)_{P.T.}\cdot c_n^i\right\}\frac{\partial M^i}{\partial t} \qquad (9)\end{aligned}$$

On the other hand, we have from the equation (8)

$$\sum_i c_n^i\cdot\frac{\partial M^i}{\partial t}=0 \qquad (n=1, 2, \cdots\cdots \beta) \qquad (10)$$

These equations (9) and (10) together represent a set of linear equations about the variables

$$\frac{\partial M^i}{\partial t} \quad (i=1, 2, \cdots\cdots, \alpha).$$

The number of equations is $\beta+1$, and it is equal to the number of variables in the case of $\alpha=\beta+1$, therefore we can have not vanishing $\frac{\partial M^i}{\partial t}$ and also $\frac{\partial S}{\partial t}=\frac{k}{\rho T}\nabla^2 T$. Then the steady accumulation of heat is possible to occur in the case of $\alpha=\beta+1$.

Finally in the case of $\alpha \leq \beta$, if the stationary condition is established i.e. the pressure, temperature and concentration are kept constant, a set of linear equations can be derived as above. In this case, however, the number of equations $\beta+1$ exceeds the number of variables α. And it can be readily seen that the simultaneous equations are satisfied only when all the M_n^i's and $\frac{\partial S}{\partial t}$ vanish. Thus in this case there should be no steady accumulation of heat into the system, and the verification of the whole statements is completed.

For example, in the case of one single component, the steady accumulation of heat can take place only in the system in which two phases exist at the same time. If the temperature of material at the bottom of the earth's crust is at the melting point, then it should have a constant value determined by the value of the pressure at the place, and consequently the quantity of heat flow through the crust should be determined. Therefore if the heat flow from below into the place exceeds the above determined value, the extra heat will be accumulated at the place and the considerable part of extra heat will be converted into mechanical energy. Hereafter we shall call the substance at the place "working substance."

Heat supply for the phase change

The heat flow to the earth's surface from below is estimated as 1.3×10^{-6} cal. cm^{-2} sec^{-1} by the observation at the surface. On the other hand, if an earthquake of energy of O(10^{25}) erg occurs in a circular area of radius 50 km once in a hundred years, Matuzawa's calculations have shown that heat energy of O(10^{27}) erg should be accumulated into the working substance which is assumed at the bottom of the crust of the area during the period; this is equivalent to the heat flow of O(10^{-4}) cal. cm^{-2} sec^{-1}. This amounts to a hundred times of the quantity of heat flow

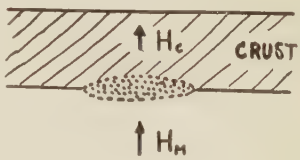

Fig. 1. Heat flow through the working substance.

through the crust. We shall consider in what way such a quantity of heat can be supplied.

A) radioactive energy; At first we shall investigate the possibility that the necessary heat can be generated by radioactive substances contained in the working substance itself. Table 1 shows the radioactive heat generation in some igneous rocks (Birch, F: 1942). The

Table 1. Radioactive heat generation of igneous rocks. (after R.D. Evans and C. Goodman)

Rock Type	Heat Generation
Acidic Igneous Rock	1.7×10^{-13} cal gr.$^{-1}$ sec^{-1}
Basic Igneous Rock	0.6×10^{-13}
Ultrabasic Igneous Rock	0.3×10^{-13}

volume of the working substance is assumed as 500 km^3 in Matuzawa's calculation, so that in a hundred years this may generate the thermal energy of O(10^{22}) erg and this is very little compared to the necessary energy of O(10^{27}) erg. Therefore if there is no extraordinary concentration of radioactive substance, it is impossible to maintain the process by the heat generated inside the working substance. Thus the necessary heat should be transfered from the outside by means of thermal conduction or convection.

B) thermal conduction; At the earth's surface the heat flow from below is observed to have the mean value of 1.3×10^{-6} cal. cm^{-2} sec^{-1}. If we take as the value of thermal conductivity of the crustal substance 0.006

cal sec^{-1} cm^{-1} deg^{-1}, a reasonable value, the temperature gradient throughout the crust may be assumed to be 20°C km^{-1}. There are two possibilities to enable the accumulation of necessary heat only through the thermal conduction into the working substance. If the thermal conductivity beneath the working substance has the same value as that in the crust, the temperature gradient there should be a hundred times of that in the crust. On the other hand, if the temperature gradient beneath the working substance is the same as that throughout the crust, the thermal conductivity there should be a hundred times of that in the crust.

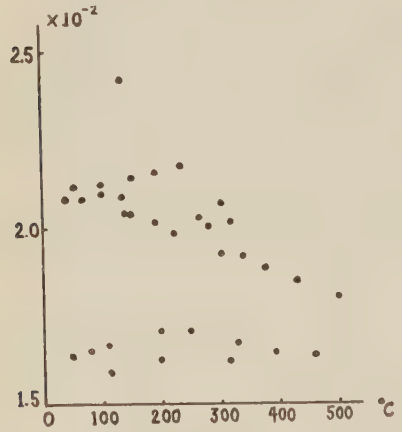

Fig. 2. Thermal conductivity of Basalt (after Poole).

The first possibility is difficult to conceive, for the temperature of a hypothetical heat source should exceeds 10,000°C, if it is taken to be located at the place 5 km apart from the working substance.

Then the second possibility that the thermal conductivity at the place beneath the bottom of the crust can be a hundred times of that throughout the crust should be examined. The temperature dependence of the thermal conductivity of basalt and granite has been studied by Poole (1921), the results being shown in Fig. 2 and 3. The increase in thermal conductivity with the temperature increase is observed only in the case of basalt at lower temperatures. Generally the thermal conductivity of material decreases with the temperature increase except in the case of graphite. hematite, quartz glass and asbest. The effect of pressure is to increase the thermal conductivity. The pressure dependene of the thermal conductivity of basalt has been given by P. W. Bridgman (1949) as

$$K=0.00404+0.000019\ (P/1000)$$

(P in bars. K in cal. sec^{-1}. cm^{-1} deg^{-1})

$$=0.00414+0.0000089\ (P/1000)$$

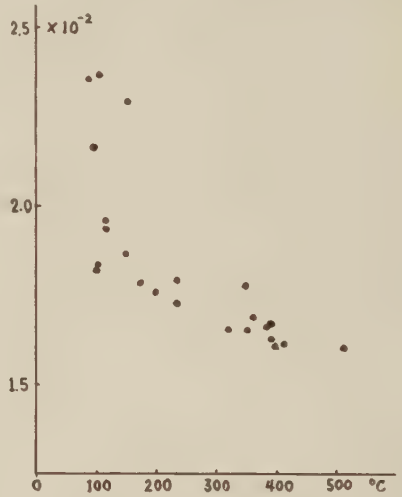

Fig. 3. Thermal conductivity of Granite (after Poole).

The increment is only 2.1~4.7 % by the pressure of 10,000 bars which corresponds to the depth about 35 km below the surface, and at most 50 % by the pressure at the depth of 300 km if the equation holds to such a high pressure. Thus it is not probable that the thermal conductivity of substance under the crust will be notably high owing the effect of high temperature and pressure at the place. The change of material itself with the depth may increase the conductivity at the place, but as shown in Fig. 4 drawn based on the data given in F. Birch's table, the difference of the values among these rocks at lower temperatures gradually diminishes with the increase of temperature. It seems reasonable therefore to conclude that the value of thermal

conductivity under the crust is of the same order as that throughout the crust, and the possibility of the required heat accumulation into the working substance only through the conduction should be rejected.

C) thermal convection: The problem of heat transfer by means of the thermal convection has the long history of theoretical and experimental studies (FISCHENDER, M., and SAUNDERS, O. A.: 1950; ECKART, E.: 1949). The experimental study stands on the basis of dimensional analysis made by W. NUSSELT, and aims to establish the relation among the following nondimensional numbers:

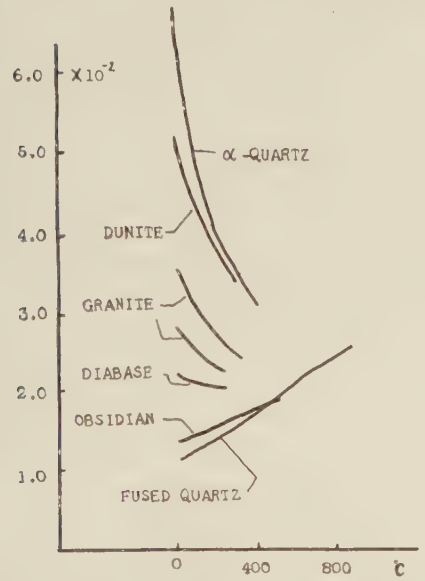

Fig. 4. Thermal conductivity of some rocks and minerals (from BIRCH's table)

i) NUSSELT number: $Nu = \frac{Hl}{k\theta}$

Here l is the length representing the dimension of convection, θ is the temperature difference between the fluid and the boundary, k is the thermal conductivity and H is the heat flow carried by the convection current. Nu represents the ratio of convectional heat flow to conductional heat flow.

ii) REYNOLDS number: $Re = \frac{U\rho l}{\mu}$

iii) PRANDTL number: $Pr = \frac{c\mu}{k}$

in which c is the specific heat and μ is the viscosity. This is the ratio of the viscous diffusion coefficient to the thermal diffusion coefficient.

iv) GRASHOF number: $Gr = \frac{\alpha g \theta \rho^2 l^3}{\mu^2}$

in which α is the thermal expansion coefficient and g is the gravitational acceleration. This number has the same character as that of the REYNOLDS number in the case of fluid motion forced by the buoyancy. We assume that the subcrustal convection current is not of the nature of forced convection which is supported by some external stress field but of one of free convection supported by the buoyancy generated by the thermal expansion of substance. In this case we need not take into account the REYNOLDS number, and a relation can be deduced among Nu, Pr and Gr. It has been derived by theoretical considerations, though

Table 2. The coefficients of equation (12) and (13) for several geometrical shapes.

shape	l	c	c'	authorities
vertical cylinder	height	0.73	0.067	TOULKIAN, HAWKINS, JACOB
vertical plate	height	0.64		BOSCH, MCADAMS
vertical plate or vertical cylinder of large diameter	height	0.56	0.12	SAUNDER
horizontal plate	breadth	0.54	0.14	SAUNDER
horizontal cylinder	diameter	0.53		BOSCH, MCADAMS
horizontal or vertical cylinder	diameter	0.47	0.10	SAUNDER
two horizontal plates	distance/2	0.44	0.19	MULL, REIHER
two vertical plates	distance/2	$0.41\times\left(\frac{L}{H}\right)^{1/9}$	$0.18\times\left(\frac{L}{H}\right)^{1/9}$	MULL, REIHER

there are some objections, that Nu is the function of only $Pr \times Gr$. We have the following formula in the case of laminar flow,

$$Nu = c(Pr \cdot Gr)^{1/4} \tag{11}$$

and in the case of turbulent flow

$$Nu = c'(Pr \cdot Gr)^{1/3} \tag{12}$$

The experimental studies have determined c and c' in many cases of boundary of different geometrical shapes. Table 2 is a summary of some of these experiments, in which the material used are air, water, oil and ethylen glicol.

Although we do not know about the geometry of the heat transfer actually taking place under the crust, it is reasonable to assume that the actual case is included in the range of variation of these examples. If the necessary heat accumulation into the working substance is done only through the convection current, and if the thermal conductivity and the gradient under the crust are assumed to be of the same order as that throughout the crust, the NUSSELT number Nu, i.e. the ratio of convectional heat flow to conductional heat flow, should be taken 100. The value of $Pr \times Gr$ corresponding to NUSSELT number 100 is in the range of $10^{8.5} \sim 10^{9.5}$ as shown in Fig. 5 which is drawn using the data of Table 2 in the case of laminar flow.

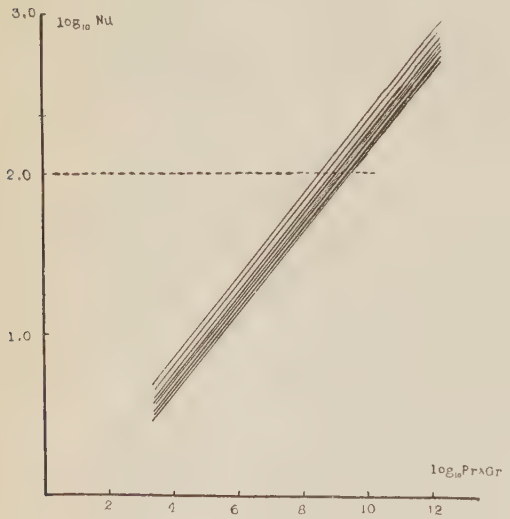

Fig. 5. Relation between the NUSSELT number and the RAYLEIGH number for several geometrical shapes.

Now we shall investigate how much can be said as to the physical state under the crust from the requirement that $Pr \times Gr$ should take the value of $10^{8.5} \sim 10^{9.5}$ there.

$$Pr \times Gr = \frac{c\alpha g\theta}{k\mu}\rho^2 l^3 \tag{13}$$

has the name of "RAYLEIGH number", and determines the condition of generation of BENARD's cell. Among the physical constants at the right hand of the above equation, the specific heat c and the thermal expansion coefficient α have somewhat similar nature; both have zero value at the absolute zero temperature, increase with the temperature,

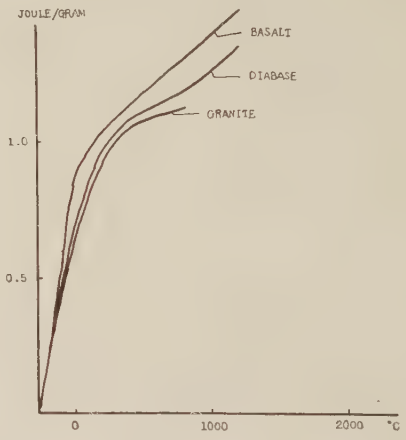

Fig. 6. Temperature dependence of heat capacity of some rocks (from BIRCH's table).

and take extraordinary large value at and near the melting point. On the other hand, the viscosity μ and the thermal conductivity k are both related to the transport phenomena; the former is concerned with the transport of momentum and the latter with that of heat. As the similar quantities are connected by the multiplication in the definition, the RAYLEIGH number is expected to be very sensible to the change of the state.

Among the physical constants involved in the RAYLEIGH number, we can estimate from laboratory experiments the values of specific heat c, thermal expansion coefficient α, density

ρ, and thermal conductivity k of the substance under the crust.

Therefore, if we put the temperature gradient θ/l to be the same as that in the crust, we can obtain a relation between the two unpredictable parameters, i.e. the viscosity μ and the linear dimension of convection current l, from the requirement that the RAYLEIGH number should be within the range of $10^{8.5}\sim10^{9.5}$.

The specific heat has nearly constant value above the DEBYE temperature except in the neighbourhood of melting point. Fig. 6 shows the temperature dependence of the specific heat of basalt, diabase and granite. And the average value of the specific heat of rock at high temperatures, excluding the neighbourhood of the melting point, is estimated as 1.3 joules gr^{-1}. $deg.^{-1}$.

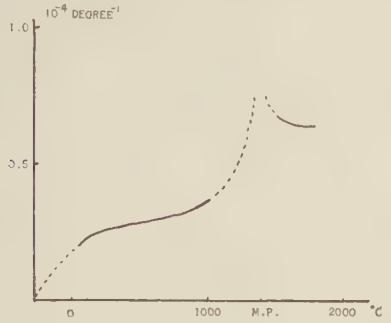

Fig. 7. Temperature dependence of thermal expansion of Diopside. (from BIRCH's table)

Table 3. Thermal expansion of rocks in solid and liquid state.

Rock Type	α (at ordinary temp.)	α (liquid)
Basalt	$1.5\times10^{-5}\,deg^{-1}$	$8.2\times10^{-5}\,deg^{-1}$
Diorite	2.1	14.0

As to the coefficient of thermal expansion, the temperature dependence in the case of diopside is shown in Fig. 7. The value at and near the melting point is extrordinary large as in the case of the specific heat, and the value in the liquid state is somewhat larger than that in the solid state. Table 3 shows the average value of thermal expansion of some rocks at ordinary temperatures and in the liquid state, though the samples used are different between the solid state average and the liquid state average.

The thermal expansion coefficient shows a considerable change by the effect of pressure. The figures in Table 4 is derived from the result of experiments made by P. W. BRIDGMAN in the case of alkali metals, Δv is the change of volume and $\Delta\alpha$ is the change of thermal expansion coefficient by the effect of pressure. The ratio $\Delta\alpha/\alpha_0$ takes almost same value for a fixed value of $\Delta v/v_0$ among the three alkali metals. If it is allowed to extrapolate these figures to the substance in question in the corresponding state, the value at the earth's surface should be reduced by half by the pressure at the depth of 300 km. Under these circumstances it seems reasonable to take as the value of thermal expansion of the substance under the crust 5×10^{-5} $deg.^{-1}$ unless the state is at the melting point.

Table 4. Change of thermal expansion by the change of volume for Alkali metals (estimated from BRIDGMAN's data)

$-\Delta v/v_0$.	$\Delta\alpha/\alpha_0$ (L_i)	$\Delta\alpha/\alpha_0$ (N_a)	$\Delta\alpha/\alpha_0$ (K)
0.05	0.24	0.20	0.17
0.10	0.42	0.37	0.35

The value of the thermal conductivity, of which the temperature and pressure dependences are refered to before, is assumed to be 2×10^{-2} joules $sec.^{-1}$ cm^{-1} $deg.^{-1}$, and also the value of the thermal gradient 20°C km^{-1}, and the density 2.6.

Using the above numerical values, we can obtain the following relation by the requirement that the RAYLEIGH number should be $10^{8.5}\sim10^{9.5}$.

$$l^4\cdot\mu^{-1}=2.4\times(10^{-8.5}\sim10^{-9.5}) \qquad (14)$$

Here the units of l and of μ are km and poise respectively. To enable the accumulation of the necessary quantity of heat into the working substance, the above relation should be satisfied between the dimension of the convection current and the viscosity of

material under the crust. The diagram of $l^4 \cdot \mu^{-1} = 10^{-9}$ is drawn in Fig. 8.

Thus the necessary heat energy for a large earthquake can be accumulated to the working substance, if the relation expressed in the formula (14) holds at the place under the crust between the linear dimension l of convection current and viscosity μ, for instance, $l = 10$ km and $\mu = 10^{13}$ poise, or $l = 100$ km and $\mu = 10^{17}$ poise.

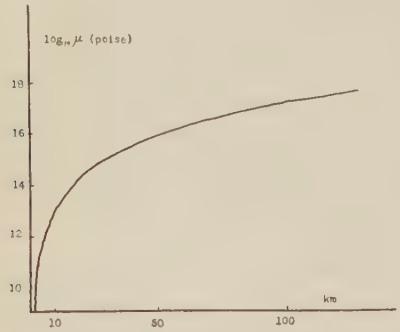

Fig. 8. Relation between the linear dimension of convection current and the viscosity of material for the NUSSELT number 100.

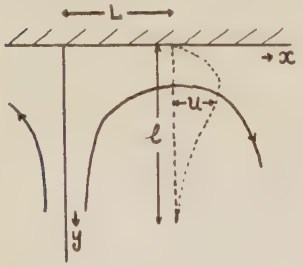

Fig. 9. Assumed velocity profile.

We have not been able to say anything about the velocity of convection current in the foregoing discussions, but if we assume a simple model as to the pattern of current, we can estimate the value of the velocity and furthermore of stress generated at the bottom of the crust by the current from the requirement that the NUSSELT number should be 100.

Estimation of velocity of convection current

Let us consider a simple model of heat transfer from fluid to solid wall through stationary convection current as shown in Fig. 9, in which x-axis is the boundary between the wall and the fluid, and the fluid at high temperature ascends along y-axis from below, and flows turning to the both sides along x-axis. The equation of heat transfer is

$$\frac{DT}{Dt} = a\nabla^2 T , \qquad a = \frac{k}{c\rho} , \tag{15}$$

if we assume near the wall

$$\left| u\frac{\partial T}{\partial x} \right| \gg \left| v\frac{\partial T}{\partial y} \right| , \text{ and } \left| \frac{\partial^2 T}{\partial y^2} \right| \gg \left| \frac{\partial^2 T}{\partial x^2} \right| ,$$

then the equation (15) reduces to

$$u\frac{\partial T}{\partial x} = a\frac{\partial^2 T}{\partial y^2} . \tag{16}$$

Developing u in TAYLOR's series near the wall, and taking only the first term, we have

$$u = \left(\frac{\partial u}{\partial y}\right)_0 y = By ,$$

taking this into account we obtain the following formula from the equation (16)

$$By\frac{\partial T}{\partial x} = a\frac{\partial^2 T}{\partial y^2} . \tag{17}$$

Changing the variables x and y into w according to the relation $w = yx^{-1/3}$, we have the following equation with a single independent variable,

$$\frac{d^2 T}{dw^2} + \frac{B}{3a} w^2 \frac{dT}{dw} = 0 . \tag{18}$$

The solution is given by

$$T = K_1 \int_0^w e^{-\frac{B}{9a}\omega^3} d\omega + K_2 . \tag{19}$$

If the temperature of the wall is t_0, and that of the ascending fluid t_1, the boundary conditions are given by

$$y = 0 , \qquad \omega = 0 , \qquad T = t_0 ,$$

and

$$x = 0 , \qquad \omega = \infty , \qquad T = t_1 .$$

Then we have

$$K_2 = t_0 ,$$

and

$$K_1 = t_1 - t_0 \Big/ \int_0^\infty e^{-\frac{B}{9a}\omega^3} d\omega$$

$$=\frac{3\left(\frac{1}{9}\right)^{1/3}}{\Gamma\left(\frac{1}{3}\right)}(t_1-t_0)\left(\frac{B}{a}\right)^{1/3}.$$

The temperature gradient at the wall is

$$\left(\frac{\partial T}{\partial y}\right)_0=\frac{3\left(\frac{1}{9}\right)^{1/3}}{\Gamma\left(\frac{1}{3}\right)}(t_1-t_0)\left(\frac{B}{a}\right)^{1/3}x^{-1/3}. \quad (20)$$

The heat flow in the direction perpendicular to the wall per length L of the wall is

$$Q=-\int_0^L k\left(\frac{\partial T}{\partial y}\right)_0 dx$$

$$=-\frac{3}{2}\cdot\frac{3\left(\frac{1}{9}\right)^{1/3}}{\Gamma\left(\frac{1}{3}\right)}k(t_1-t_0)\left(\frac{B}{a}\right)^{1/3}L^{2/3}, \quad (21)$$

and the NUSSELT number can be expressed as

$$Nu=\frac{Q\cdot l}{-Lk(t_1-t_0)}=0.8\times\frac{l}{L^{1/3}}\left(\frac{B}{a}\right)^{1/3}, \quad (22)$$

by which we can estimate the value of B, i.e. the velocity gradient at the wall, for a given NUSSELT number, and

$$B=a\cdot\frac{L}{l^3}\left(\frac{Nu}{0.8}\right)^3 \quad (23)$$

The value of a is obtained by the foregoing estimation as 0.6×10^{-2} cm^2 sec.$^{-1}$ Let L be equal to l, and Nu 100, we have

$$B=1.2\times10^{-6}\times l^{-2}\ \text{sec}^{-1} \quad (24)$$

in which the unit of l is km.

The tangential stress at the wall generated by the current is

$$\tau=\mu B=O(10^3)\times l^2\ \text{dyne cm}^{-2}. \quad (25)$$

For the estimation of the absolute value of current velocity by the above simple method we need to know about the type of distribution of velocity, and we assume

$$u=u_1\frac{y}{l}\left(1-\frac{y}{l}\right)^2. \quad (26)$$

This represents the distribution of flow in which the velocity in the direction parallel to the x-axis is zero at the wall and $y=l$, and some authors have used this type of velocity distribution to fit to their results of experiment about free convection current. In this case the maximum velocity U_{max} is equal to $\frac{4}{27}Bl$, so that we can estimate the expected maximum velocity under the crust as

$$U_{max}=5\times10^3\times l^{-1}\ (\text{m year}^{-1}) \quad (27)$$

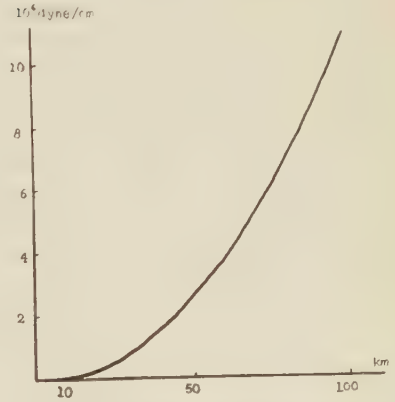

Fig. 10. Relation between the linear dimension of convection current and the stress generated in the case of NUSSELT number 100.

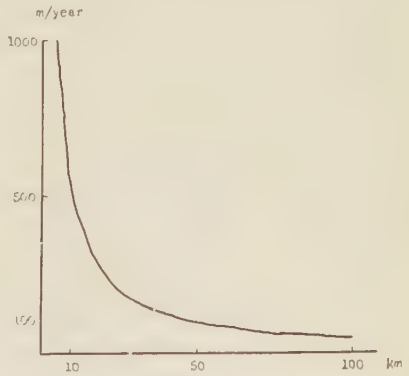

Fig. 11. Relation between the linear dimension of convection current and its maximum velocity in the case of NUSSELT number 100.

in which the units of U_{max} and l are m year^{-1} and km respectively. The relations (27) and (25) tell us that if the thermal convection current transfers and supplies the required energy to an earthquake, the velocity of the current and the tangential stress generated

by it at the bottom of the crust are determined as the function of the linear dimension of the current, as shown in Figs. 10 and 11.

Résumé

The possible thermal processes near the earth's crust are studied with special regard to a process presented by Prof. Matuzawa in his recent paper titled "Feldtheorie der Erdbeben.", in which a solid-liquid transformation plays an important part. Before the discussion of this particular process, the writer gives the necessary condition for the stationary conversion of thermal energy into mechanical energy inside a system of material through which a stationary heat flow exists. It is shown that this condition is satisfied near the crust in two and only two cases, of which in the first a mass flow exists in the system, and in the second the relation $\alpha=\beta+1$ exists between the number α of phases and the number β of components of the system. The first case corresponds to the convection theories of the cause of earthquake and the second corresponds to the phase transformation theories, to which Prof. Matuzawa's theory belongs. The necessary heat supply for a great earthquake was shown quantitatively in his paper. It is empbasized that such an amount of heat energy can only be supplied by the convection current under the crust. And the writer obtains by the aid of experimental and theoretical laws of heat transfer by a free convection the relation between the scale of convection and the viscosity of material under the crust required for the effective accumulation of necessary energy. If such a convection has a linear dimension of 100 km, the viscosity of material must be 10^{17} poise, its maximum current velocity is estimated to be 50 m/year and it exerts a tangential stress of the order of 10^7 dyne/cm^2 along the lower surface of the crust.

Those results that the subcrustal current which is believed to account for the mountain formation may accompany energy accumulation by phase transformation, that the phase transformation which explains well the cause of a great earthquake needs the heat energy supplied by the subcrustal current and that the possible stationary conversion of the thermal energy into mechanical energy must be confined to the above two cases, may lead us to the conclusion that those two processes combined play a very important part in the physical phenomena near the earth's crust.

References

Bridgman, P. W.:
1949 Physics of high pressure, G. Bell and sons, Ltd., London p. 322.

Birch, F.:
1942 Handbook of Physical constants, Geol. Soc. Amer., Special Raper 36.

Eckart, E.:
1949 Wärme und Stoff-austausch, Springer Verlag, Berlin.

Fishenden, M. and O. A. Saunders:
1950 An introduction to Heat transfer, Oxford.

Matuzawa, T.:
1953 Feldtheorie der Erdbeben, Bull. Earthq. Research Inst., **31** 179–202.

Poole, H. H.:
1921 Tables annuelles de Constantes et Donnèes numeriques de Chimie, de Physique et de Technologie, **IV** anées 1913–14–15–16 p. 154, (Publicated by l'Union de Chimie pure et appliquée)

Earthquake Energy, Earthquake Volume, Aftershock Area, and Strength of the Earth's Crust[1].

By

Chuji TSUBOI

Geophysical Institute, Faculty of Science, Tokyo University, Tokyo, Japan, California Institute of Technology, Pasadena, California, U.S.A.

Summary

Various facts appear to suggest that one continuous field of mechanical stress developed in the earth's crust has a certain upper limit for its voluminal extent. The ultimate mechanical stress energy that can be stored up in this whole volume until a break-down takes place in it may be identified with the energy of the largest possible earthquake. The energy deduced on this hypothesis agrees well with those of the actual largest earthquakes. The area A in which aftershocks occur in association with a major earthquake has been found by UTSU and SEKI regularly to increase with the magnitude M of that main shock. This relation, when combined with the magnitude-energy relation due to GUTENBERG and RICHTER, yields a formula

$$E=6\times 10^{2}\times A^{1.5}.$$

The numerical values of the coefficient and of the exponent of A in this formula can be well explained by the hypothesis stated above regarding the spatial distribution of the stress energy within the earth's crust.

The amount of energy which is sent out from the "origin" of a large earthquake in the form of elastic waves is so enormous that it will be difficult to conceive of this much amount having been stored up within a small confined volume of the earth's crust until the outbreak takes place[2]. Since the material of which the earth's crust is made up has the limit of strength which is finite, a huge volume of the earth's crust must be needed for this much energy to be stored up in it in order that at no part within the volume the stress should exceed this limit of strength. Let us call this volume the "earthquake volume". As will be shown later, the stress energy that can be stored up within a unit volume of rock is about 5×10^{3} ergs.

On the other hand, according to our experience throughout the long history of earthquake studies, there is likely a certain upper limit of the energy of one single shock, however large it may be. The largest magnitude of an earthquake listed in GUTENBERG and RICHTER's book "Seismicity of the Earth" is 8.6. Even in Japan which is noted for its high seismic activity and also for its richness in dependable historical records, no description can be found of an earthquake which was so large as to work damages over more than one third or one fourth of the whole area of the country. This may be taken to be another indication that the earthquake energy or the earthquake volume has also a certain upper limit.

In an article published in 1940, the present writer (TSUBOI, 1940) proposed to calculate the energy E of a largest possible earthquake. First of all, he has assumed that the energy E is given by

$$E=\frac{1}{2}\,e\varepsilon^{2}\,V, \qquad (1)$$

where the notations used have the following meanings:

1) Seismological Laboratory, Division of Geological Sciences, California Institute of Technology, Pasadena, Contribution No. 794.

2) Discussions will be confined to shallow shocks only

e: effective elastic constant of the crustal material,
x: ultimate strain of the crustal material,
V: earthquake volume.

The expression (1) amounts to mean that the material within the earthquake volume will be uniformly strained until this uniform strain reaches the value x everywhere at the same time within the volume, when, at the time of earthquake occurrence, the stored energy E is sent out from the whole volume by some kind of mechanism or other. Evidently this uniform strain hypothesis cannot be strictly true, but the essential point of it which the writer would like to emphasize is that x is assumed not to differ notably from one part to another within the volume. To take x everywhere uniform will be understood to be no more than the first approximation in the formulation of the hypothesis. According to the writer's view presented in the article mentioned, vertically the volume cannot exceed the thickness d of the earth's crust, nor horizontally three times the thickness, $3d$. This value of the factor 3 has been derived from the study of local versus regional isostasy. (TSUBOI, 1939). It is related to the ratio

$$\frac{\text{extent of regionality of isostasy}}{\text{thickness of the earth's crust}},$$

where the extent of regionality means, after Vening MEINESZ, the horizontal extent of the largest topography that can be supported by the strength of the earth's crust, that is by a mechanism other than isostasy.

There is also another information in favour of the finite horizontal extent of the earthquake volume of a largest possible shock. In 1949, the writer (TSUBOI, 1949) investigated how the correlation coefficient between the year-to-year numbers of earthquakes ($M \geqq 5.5$) in various compartments of suitable size taken along Japanese islands decreases with the distance a between the two compartments compared. The compartments are bounded by straight lines which are drawn across the islands perpendicularly to their general trend. The correlation coefficients was found to decrease very regularly with the distance until it becomes nearly zero at $a \fallingdotseq 150$ km. The occurrences of these earthquakes may be understood to be the indications of the accumulation of energy in a volume V of the earth's crust, of which the earthquake volume v for each one of the shocks is a small part. That the correlation coefficient becomes zero at $a=150$ km would mean that the volume V cannot extent beyond that length horizontally.

From the above considerations, E may be written as

$$E=\frac{1}{2}ex^2d\cdot 3d\cdot 3d=\frac{9}{2}ex^2d^3. \qquad (2)$$

The value of e may be taken to be $5\times10^{11}\sim10^{12}$ C.G.S.[3] The value of x has been known to be $10^{-4}\sim2\times10^{-4}$ from the studies of deformations of the earth's crust caused by large earthquakes, particularly by those which were associated with seismic faults (TSUBOI, 1933). Thus $1/2\,ex^2$ which is the maximum energy to be stored up within a unit volume of rock will be $1/2\,(5\times10^{11})\times10^{-8}\sim1/2\,(10^{12})\times(4\times10^{-8})$ or $3\times10^3\sim2\times10^4$. The thickness d of the earth's crust may be taken to be $4\times10^6\sim5\times10^6$. Putting these numerical values into the expression (1) for E, the values $1.4\times10^{24}\sim2.3\times10^{25}$ are obtained. If we take $e=5\times10^{11}$, $x=10^{-4}$, $d=5\times10^6$, the value of E will be 3×10^{24}.

From the nature of the problem, no great accuracy can be claimed of these values. They may well be uncertain by a factor of even as much as 5.

Now on the other hand, according to the 1942 formula of B. GUTENBERG and C. RICHER, (1942), the energy of an earthquake is related to its magnitude M as follows:

$$\log E=1.8\,M+12. \qquad (3)$$

If we put $M=8.6$ into this formula, which is the largest magnitude listed in GUTENBERG and RICHTER's book "Seismicity of the Earth,"

$$E=3\times10^{27}$$

is obtained which value is far larger than

3) Hereafter, all the numerical quantities will be expressed in C.G.S. system.

any of the values $1.4\times14^{24}\sim2.3\times10^{25}$ estimated by the present writer. Thus GUTENBERG and RICHTER have naturally stated in their book as follows:

"……This (TSUBOI's estimation)[4] is appreciably less than the largest energies calculated from the revised equation (2) ($\log E=1.8M+12$) for observed earthquakes since 1904, which appear to reach 10^{27} ergs……"

According to the Progress Report, Seismological Laboratory, California Institute of Technology, 1955 (BENIOFF, GUTENBERG, PRESS and RICHTER, 1956), however, the two investigators have recently revised the formula into

$$\log E=1.5\,M+11.8. \qquad (4)$$

If we put $M=8.6$ into this new formula,

$$E=5\times10^{24}$$

is obtained. This value agrees well with the writer's value 3×10^{24}. The agreement may be said to be very good considering the nature of the problem and the uncertainties of the numerical values involved in the calculations.

Although the present writer feels himself much satisfield by this good agreement, he is furthermore going to see if there is any other additional information which will support his hypothesis concerning the spatial extent of the earthquake energy field.

In 1954, T. UTSU and A. SEKI published an interesting article in which they studied the relation between the horizontal area A in which aftershocks of a large earthquake take place and the magnitude M of the main shock. Using as data 30 large earthquakes which had taken place in Japan, they obtained a formula as follows.

$$\log A=M+6. \qquad (5)$$

Let us call A the "aftershock area."

If, for instance, we put $M=8$ in this formula,

$$A=10^{14}=(100\text{ km})^2$$

is obtained. Combining this formula of USTU and SEKI with that of GUTENBERG and RICHTER (4), M can be eliminated with the result

$$\log E-1.5\log A=2.8$$

or

$$E=6\times10^2\times A^{1.5}. \qquad (6)$$

It has already been stated that according to the present writer's view, E is given by

$$E=\frac{9}{2}ex^2d^3. \qquad (2)$$

If the aftershock area A is the earthquake volume projected on the earth's surface, which assumption appears to be a reasonable one, A is equal to $9d^2$,

or

$$d^3=\frac{1}{27}A^{1.5}.$$

Thus we can write

$$E=\frac{1}{6}ex^2A^{1.5}, \qquad (7)$$

and we see that the term $A^{1.5}$ in (6) is but a natural consequence of the hypothesis proposed in this paper. As to the factor $1/6\,ex^2$, if we put $e=5\times10^{11}$, $x=10^{-4}$ into it, we get

$$\frac{1}{6}ex^2=8\times10^2,$$

which is again almost equal to the factor 6×10^2 in the formula (6).

Thus, so far as the above considerations are concerned, a consistent picture has been obtained about the relations among the earthquake volume, aftershock area, and mechanical strength of the crustal material, and above all about the way how the mechanical energy is stored up within the earth's crust until it is released from it in the form of seismic waves.

According to the view presented in this paper, the energy of an earthquake is dependent mainly on the volume within which it has been stored up until the outbreak takes place. This represents a controversial view as compared with another theory that the energy of an earthquake is determined by the crustal strain x rather than by the earthquake volume V, that is a large earthquake corresponds to higher stress and a smaller one to lower stress.

This study was made while the writer was staying at the California Institute of Technology, Pasadena, California. Valuable discussions on this problem which he could have

4) Parentheses by the present writer.

with Drs. H. BENIOFF, C. Hewitt DIX, B. GUTENBERG, F. PRESS and C. RICHTER, all of the Institute, are gratefully acknowledged.

References

BENIOFF, H., GUTENBERG, B., PRESS, F., and RICHTER, C. F.:
1956 "Progress Report, Seismological Laboratory, California Institute of Technology, 1955." Trans. Amer. Geophys. Union, **37**, 232.

GUTENBERG, B., and RICHTER, C. F.:
1942 "Earthquake Magnitude, Intensity, Energy and Acceleration." Bull. Seism. Soc. Am., **32**, 163.

TSUBOI, C.:
1933 "Notes on the Mechanical Strength of the Earth's Crust." Bull. Earthq. Res. Inst., **11**, 275.
1940 "Isotasy and Maximum Earthquake Energy." Proc. Imp. Acad. Japan, **16**, 449.
1949 "On Seismic Activities." Geophys. Notes, **3**, No. 4.

TSUBOI, C., KANEKO, T., MIYAMURA, S. and YABASHI, T.:
1939 "Relation between the Gravity Anomalies and the Corresponding Subterranean Mass Distribution." Bull. Earthq. Res. Inst., **17**, 385.

UTSU, T., and SEKI, A.:
1954 "A Relation between the Area of Aftershock Region and the Energy of Mainshock." Zishin (Earthquake), **7**, 233.

A Simple Method for Calculating the Correlation Coefficients.

By

Yoshibumi TOMODA

Geophysical Institute, Faculty of Science, Tokyo University.

Summary

A simple approximate method for calculating the correlation coefficient $\rho(x, y)$ between two probability variables x and y, say, is given in the present paper. The essential point of this method is to divide the whole range of each variable into two classes and denote the variable x (or y) by $+1$ or -1 according as it is larger or smaller than its mean value. If the correlation coefficient between these new series of x and y is $r(x, y)$, we can prove the relation (3) in section § 1. By using this relation, we can calculate the required coefficient $\rho(x, y)$ with much less numerical labour than otherwise.

§ 1.

The correlation coefficient $\rho(x, y)$ between two probability variables x and y, say, is given by

$$\rho(x, y)=\frac{1}{\sigma_x\sigma_y}\int_{-\infty}^{+\infty}\int_{-\infty}^{+\infty} xy\,P(x, y)\,dx\,dy, \quad (1)$$

where σ_x^2 and σ_y^2 are the variances of x and y respectively, and $P(x, y)\,dx\,dy$ represents the probability that x and y are in the ranges $x\sim(x+dx)$ and $y\sim(y+dy)$. To calculate the correlation coefficient according to this definition, a rather laborious work is needed. Thus, it is usually considered impracticable, if not impossible, to calculate manually long series of correlation coefficients such as those needed for auto-correlation function. Here we are going to propose a simple method to calculate the coefficient. When the sample distribution is normal and the sample size is large enough, the new method enables us to obtain a very good approximation of (1) with very little labour. The essential point of the present method is to divide the whole range of each variable into two classes only. The variable x or y which is larger (or smaller) than its mean value will be denoted by $+1$ (or -1). Thus, we get a new series of variables, all expressed by $+1$ and -1. The correlation coefficient $r(x, y)$, say, for this new series is given by

$$r(x, y)=\frac{N_+-N_-}{N_++N_-}, \quad (2)$$

where N_+ (or N_{-1}) is the number of cases where x and y are the same (or opposite) in sign. The correlation coefficient (2) is very easy to calculate. As will be proved in the next section, $\rho(x, y)$ and $r(x, y)$ are related as follows:

$$\rho(x, y)=\sin\frac{\pi}{2}r(x, y). \quad (3)$$

By using the above relation, we can easily calculate the required true coefficient $\rho(x, y)$.

§ 2.

The proof of the relation (3) is as follows. If the sample distributions of x and y are both normal, by using the normalized variables $X=\frac{x}{\sigma_x}$ and $Y=\frac{y}{\sigma_y}$, the probability $P(X, Y)$ that X and Y are between $X\sim(X+dX)$ and $Y\sim(Y+dY)$ is given by

$$P(X, Y)=\frac{1}{2\pi\sqrt{1-\rho^2}}e^{-\{X^2-2\rho XY+Y^2\}/2(1-\rho^2)}. \quad (4)$$

Then,

$$r(+1, -1)=\frac{N_+-N_-}{N_++N_-}=\iint_{\substack{1\text{st}\\3\text{rd}\\\text{quadrant}}}(X, Y)\,dX\,dY-\iint_{\substack{2\text{nd}\\4\text{th}\\\text{quadrant}}}(X, Y)\,dX\,dY$$

$$=\frac{2}{\pi}\left\{2\tan^{-1}\sqrt{\frac{1+\rho}{1-\rho}}-\frac{\pi}{2}\right\}$$

$$\therefore \quad \rho(x, y)=\sin \frac{\pi}{2} r.$$

§ 3.

In this section, several numerical examples of the application of the present method will be given.

Example 1.

x: Students' mathematics test marks y: Students' language test marks

Sample size: 128

		Mathematics												
	y \ x	35~	40~	45~	50~	55~	60~	65~	70~	75~	80~	85~	90~	95~
Language	65~	1	2	1										
	70~	1	4	2	1	1				1				
	75~			2	7	5	4	6						
	80~				3	4	8	7	5	4	1			
	85~			1			2	2	8	8	4	2	1	1
	90~							1	2	3	6	5	3	4
	95~											1	2	2

ρ (true): 0.84 $r(+1, -1)$: 0.66 $\rho=\sin\frac{\pi}{2}r$: 0.86

Example 2.

x: Students' first test marks
y: Students' second test marks

Sample size: 100

		First test						
	y \ x	65~	70~	75~	80~	85~	90~	95~
Second test	65~	1						
	70~	3	2					
	75~	2	3	5	6	1	1	
	80~	3	3	7	6	4		
	85~	4	4	6	4	9	1	
	90~			1	3	8	1	5
	95~				1	2	3	1

ρ (true): 0.58
$r(+1, -1)$: 0.36
$\rho=\sin\frac{\pi}{2}r$: 0.54

Example 3.

x: Weight of body (in kg)
y: Height of body (in cm)

Sample size: 125

		Weight of body (in kg)							
	y \ x	40~	45~	50~	55~	60~	65~	70~	75~
Height of body (in cm)	150~	2							
	155~	3	2	3	2	1			
	160~		6	12	12	6	1		
	165~		1	10	15	5	3	1	
	170~			3	15	3	4	3	1
	175~				3	1	1	3	2
	180~								1

ρ (true): 0.61
$r(+1, -1)$: 0.31
$\rho=\sin\frac{\pi}{2}r$: 0.47

Example 4.

x: Life-times of fathers y: Life-times of their children

Sample size: 1072

Children \ Fathers	59	60	61	62	63	64	65	66	67	68	69	70	71	72	73	74	75
60					.5	.5	1.										
61					.5				1.								
62		.25	.25		.5	1.	.25	.25	.5	.5							
63		.25	.25	2.25	2.25	2.	4.	5.	2.75	1.25		.25	.25				
64	1.		1.5	3.75	3.	4.25	8.	9.25	3.	1.25	1.5	.75	1.25				
65	2.	1.	1.	2.	3.25	9.5	13.5	10.75	7.5	5.5	3.5	2.5					
66		.5	2.	2.25	5.25	9.5	10.	16.75	17.5	16.	5.25	2.	2.5	1.			
67		1.5	1.5	4.75	3.5	13.75	9.75	26.5	25.75	19.5	12.5	13.75	3.25	5.	1.		
68			1.	2.	7.5	10.	10.25	24.25	31.5	23.5	29.5	13.25	8.5	9.5	2.25		
69					5.25	5.	12.75	18.25	16.	24.	29.	21.5	10.	3.5	2.25		1.
70					1.	2.5	5.7	18.75	11.75	19.5	22.5	19.5	14.5	6.25	3.5	1.5	1.
71						3.25	5.	8.75	10.75	19.	14.75	20.75	10.35	8.	5.	1.	1.
72						2.5	3.	1.25	7.	7.5	10.75	11.25	10.	8.5	2.75	.5	
73					1.		.75	.75	2.5	7.5	6.5	6.	7.5	6.25	3.25	.5	.5
74							1.5	1.5		5.25	2.25	2.5	6.5	3.25	3.25		.2
75										1.	2.		3.5	7.5	1.75	.5	
76										1.25	.25		.5	1.	1.		
77										1.25	.25				1.5		
78														.25	.75		
79														.25	.25		

ρ (true): 0.51 $r(+1, -1)$: 0.36 $\rho = \sin\frac{\pi}{2}r$: 0.54

Example 5.

The autocorrelation correlograms of seismogram shown in Fig. 1 are computed by this new method and are shown in Figs. 2~5.

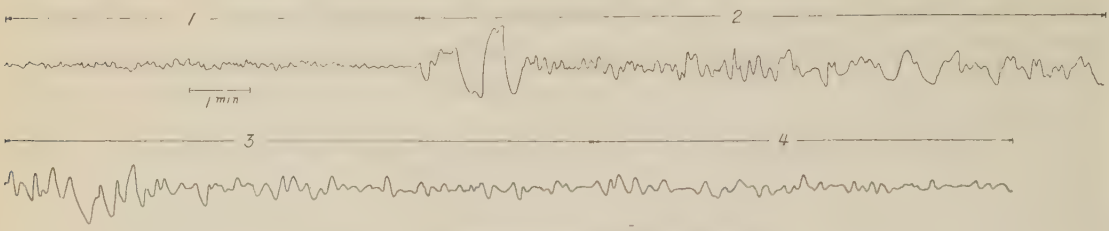

Fig. 1. The seismogram to be analysed.

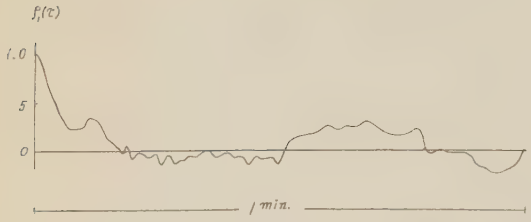

Fig. 2. Auto-correlogram for P wave (Part 1)

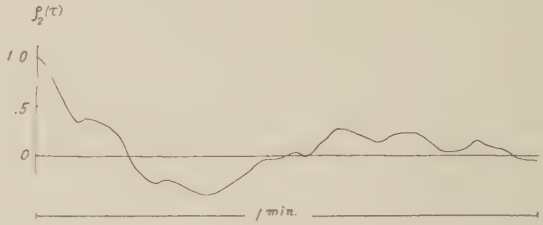

Fig. 3. Auto-correlogram for S wave (Part 2)

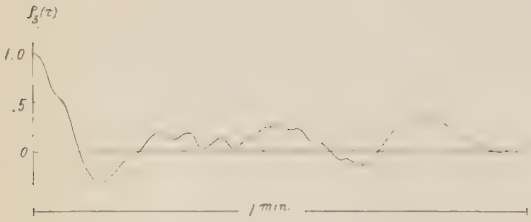

Fig. 4. Auto-correlogram for surface wave (Part 3)

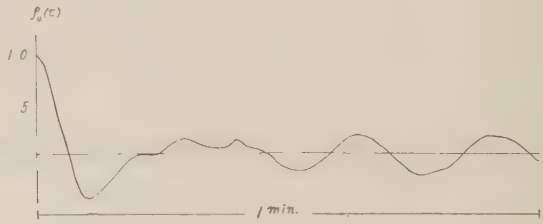

Fig. 4. Auto-correlogram for coda part (Part 4)

Correlogram Analyses of Seismograms by Means of a Simple Automatic Computer.

By

Keiiti AKI

Geophysical Institute, Faculty of Science, Tokyo University.

Summary

An automatic relay computer for calculating autocorrelation coefficients, based on the simplified method of its computation proposed by Y. TOMODA, has been built for the purpose of analysing seismograms. Seismograms of about one hundred near earthquakes recorded at the Central Meteorological Observatory in Tokyo and at the Mizusawa Latitude Observatory were used for the analyses. Each seismogram was divided into several portions, and within each portion, the dependence of the prodominant period of seismic waves upon the magnitude of the earthquakes and upon the crustal structure of the wave path were studied.

§ 1. Introduction

What are the main factors that determine the frequency spectrum of seismic waves? This is a very interesting question from the standpoint of pure and applied seismology. The spectrum may depend both on the crustal structure at the origin of the seismic waves and also that along the passage through which the waves are propagated, as well as on the mechanism of wave generation at the origin. Although many studies have been made about the change in wave period with the epicentral distance, the variation in period with the earthquake magnitude, and so on, there still remain many questions to be investigated.

In the present paper, the writer has made correlogram analyses of actual seismograms. The correlogram of a time series is the FOURIER transform of the periodogram or the spectrum density of the series, and involves the same amount of information about the series as that of the spectrum density. Moreover, in many cases we can infer the spectrum directly from the correlogram without troublesome FOURIER transformations. To make the computation process simpler, an automatic computer is urgently needed. Our computer is that based on the simplified method of computation of correlation coefficient proposed by Y. TOMODA (1956). The computor is very easy to operate and maintain. The cost of its construction is low and the high speed computation is possible.

§ 2. The Automatic Computer and the Method of Analysis

Let $y(t)$ be a given time series, of which the mean value $\overline{y(t)}$ is 0 and the variance $\overline{y^2(t)}$ equals to 1, and let the values of $y(t)$ at $t=\cdots -2\Delta t,\ -\Delta t,\ 0.\ \Delta t,\ 2\Delta t,\cdots$ be $\cdots, y_{-2}, y_{-1}, y_0, y_1, y_2, \cdots$. Then the autocorrelation coefficient is defined by

$$\rho(k\Delta t)=\lim_{n\to\infty}\frac{1}{2n+1}\sum_{r=-n}^{+n} y_r y_{r+k}\ , \qquad (1)$$

A computer to calculate the autocorrelation coefficient according to the formula (1) needs the following parts; input devices such as tapes or cards, arithmetic elements to make additions and multiplications, and output devices such as a printing machine or some other indicators. So far as we stick to this regular method of computation, the computing machine will become a large one, which cannot be very inexpensive.

If we try to deduce the correlation coefficient using the simplified method proposed by Y. TOMODA, however, the computer will become a very simple one. According to this method, the autocorrelation coefficient of $y(t)$ is given as

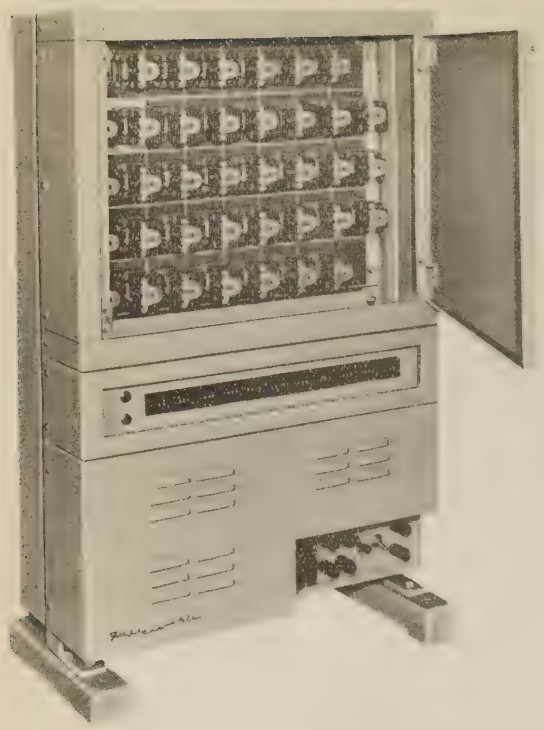

Fig. 1. Autocorrelation computer.

$$\rho(k\Delta t)=\sin\left\{\frac{\pi}{2}r(k\Delta t)\right\} \qquad (2)$$

where $r(k\Delta t)$ means

$$r(k\Delta t)=\lim_{n\to\infty}\frac{1}{2n+1}\sum_{r=-n}^{+n}\mathrm{sign}(y_r)\times\mathrm{sign}(y_{r+k}) \qquad (3)$$

and $\mathrm{sign}(y_r)$ is a function which takes the value $+1$ when the sign of y_r is positive, and takes -1 when the sign of y_r is negative. $r(k\Delta t)$ may be rewritten as

$$r(k\Delta t)=\frac{N_+(k)-N_-(k)}{N_+(k)+N_-(k)} \qquad (4)$$

where $N_+(k)$ is the number of sample pairs for which y_r and y_{r+k} have the same sign, while $N_-(k)$ is the number of sample pairs for which y_r and y_{r+k} have the opposite sign. The number N of the total sample pairs equals to the sum of $N_+(k)$ and $N_-(k)$. On the other hand $N_+(0)$ equals to N by definition, so that if we get $N_+(k)$ for $k=0, 1, 2, \cdots, n$, we have $N_-(k)$ by subtracting $N_+(k)$ from $N_+(0)$ and thus we can deduce the values of $r(kt)$ for $k=0, 1, 2, \cdots, n$, by the use of the formula (4).

Our computer gives automatically $N_+(k)$ for $k=0, 1, 2, \cdots, 10$ from the original record of $y(t)$. What we must know about $y(t)$ are only its sign, so that the input and output systems and the arithmetic elements become very simple.

In tracing the record to be analysed, the sign of $y(t)$ is read from it at regular time intervals, and when $y(t)$ is positive, a contact key is closed manually, while when $y(t)$ is negative, the key is made open. This contact key is connected to an input relay, designated by P, in the computer. Thus we can send input data into the computer directly from the original record without any input devices such as a tape system.

The multiplication in this computer is limited to the following four cases:

$$\begin{aligned}+1\times\ \ 1&=+1\\+1\times-1&=-1\\-1\times+1&=-1\\-1\times-1&=+1\end{aligned}$$

and we can easily construct a circuit of relays for making this arithmetic. The addition in this case is essentially a counting, and can be performed by means of an electromechanical counter. The results of counting of $N_+(k)$'s are given at the indicator of the counter.

To calculate $N_+(k)$'s up to $k=10$ in one cycle of input data, a delay operation is necessary in our computer. Ten sets of two relays are provided for this purpose. The first two relays A_1 and B_1 are made to be in the same state at any moment as that of the input relay P, Δt before the moment. In the similar way, the kth relays A_k and B_k are made to be in the same state as that of P, $k\Delta t$ before the moment.

Now we shall explain the details of our computer. A drum on which a seismogram to be analysed is wound as shown in Fig. 2 is revolved with an appropriate speed. The reading of signs from the record of seismic waves is done through a cross wire, of which the intersection point is adjusted to coincide with the zero line of the recorded curve $y(t)$.

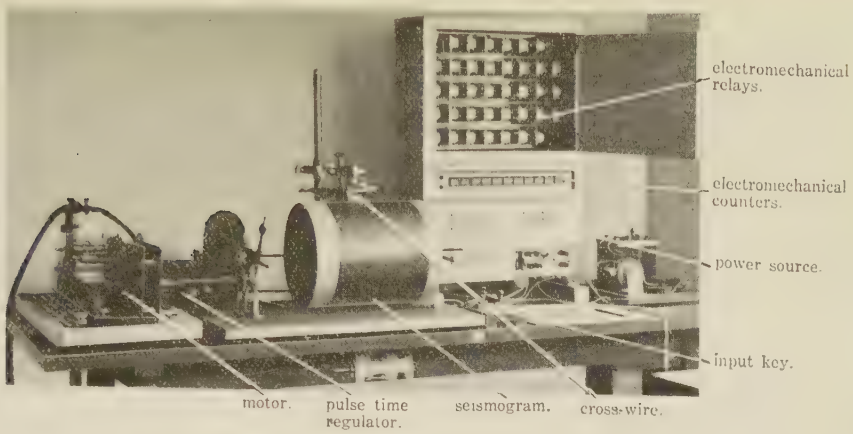

Fig. 2. Computer with appurtenances.

With the revolution of the drum, the recorded curve $y(t)$ moves along the time axis, and when $y(t)$ is positive the contact of the key is closed manually. While $y(t)$ is positive, the contact is kept closed, and at the time when the curve passes through the intersection point of cross wire from the positive side of the zero line to the negative, the contact is made to open and kept opened as long as $y(t)$ is negative. The input relay P in the computer is connected to the contact of the key, and works just in the same way as the manually operated key.

For the control of the operation of addition, multiplication and delay, there is a control unit composed of four relays. The four relays $1, \overline{1}, 2$ and $\overline{2}$ of the unit work according to the time table shown Fig. 3 (left), in which the line represents the duration of closed contact of each relay designated at the top, and the blank represents the duration of open contact. The unit time Δt can be adjusted from outside of the computer. We can obtain by combining the above relays a set of contacts of which the time table of operation is as shown in Fig. 3 (right). In this figure, $\sim\overline{1}$ represents a contact acting reversely to $\overline{1}$, i.e. the contact $\sim\overline{1}$ opens when the coil of the relay is energized, and closes when the coil is deenergized. For instance, the contact $-1-\sim\overline{1}-$ closes only when the contact 1 closes and $\overline{1}$ opens.

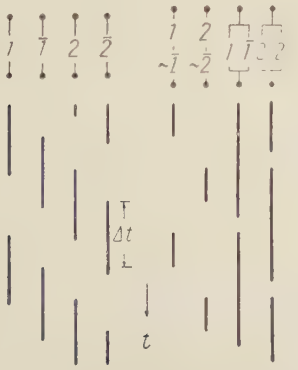

Fig. 3. Time table of operation.

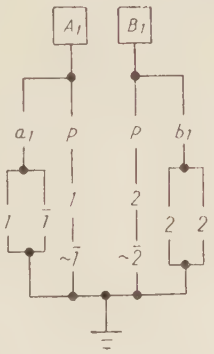

Fig. 4. Delay circuit.

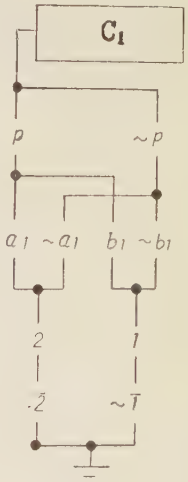

Fig. 5. Multiplication and addition circuit.

A unit of delay circuit is shown in Fig. 4. When the contact of the input relay P is closed (opened) at the time of closure of $-1-\sim\overline{1}-$, the coil of the relay A_1 is energized (deenergized) and the contact a_1 is closed (opened). While $-\left[\begin{smallmatrix}\overline{1}\\1\end{smallmatrix}\right]-$ closes, the contact a_1 is kept closed (opened), thus the signal at the relay P is sent to the relay A_1 and delayed by Δt. On the other hand, at the time of closure of $-2-\sim\overline{2}-$ the signal at the relay P is sent to the relay B_1, and also delayed by Δt. Further the signal at the relay A_1 is sent to the relay B_2 at the time of closure of $-2-\sim\overline{2}-$ and delayed by Δt, thus the signal at B_2 at any moment is the one which was at the relay P, $2\Delta t$ before the moment. In the similar way, the delay of signal up to $10\Delta t$ can be performed by a connection of 10 such units.

Multiplications and additions are done by a circuit of contacts as shown in Fig. 5. At the time of closure of $-2-\sim\overline{2}-$, the signal at P is multiplied by the signal at A_1, and at the time of close of $-1-\sim\overline{1}-$ the signal at P is multiplied by that at B_1. An electromechanical counter C_1 counts the number of cases in which the signal at the relay P is the same as that at the relays A_1 and B_1, thus the indicator of the counter gives $N_+(1)$ in the formula (4). By the use of 9 other similar circuits of contacts and electromechanical counters, we can obtain $N_+(k)$'s for $k=2, 3, 4, \cdots, 10$.

In the present analysis, the unit time Δt has been taken as 0.5 sec, so that from the data of sample size N, $N_+(k)$'s for $k=1, 2, 3, \cdots, 10$ are obtained within $N/2$ seconds.

This computer was constructed by the Fuji Tsushinki Seizo K. K. (Fuji Communication Apparatus Mfg. Co., Ltd.), and was completed in January, 1955.

§ 3. Seismogram

The seismograms used in this study are those recorded at the Central Meteorological Observatory in Tokyo and at the Latitude Observatory at Mizusawa, sixty from the former and fifty from the latter. The epicentres of all these earthquakes and the depths of focus for some of them are determined by the Central Meteorological Observatory. Their magnitudes were independently estimated by C. Tsuboi and H. Kawasumi (1952).

The geographic distribution of the earthquake epicentres recorded at the Central Meteorological Observatory is shown in Fig. 6, and of those recorded at the Latitude Observatory is shown in Fig. 7. As shown in these maps, these earthquakes are grouped according to their epicenters into seven, in order to study the variations of statistical properties of seismograms with respect to epicentral areas from which they come.

Fig. 6. Geographic distribution of epicentres of earthquakes recorded at the Central Meteorological Observatory in Tokyo.

The Mizusawa Latitude Observatory has a history of fifty years of seimological observations and there are abundant available data. Furthermore, this observatory is located just above the line of the very steep increase of gravity anomaly as revealed by C. Tsuboi

and his collaborators (1955). The area to the west of this line (named as the Morioka-Shirakawa line) is characterized by thick Tertiary formations which are developed only poorly in the eastern area. As the statistical properties of seismograms will depend on the crustal structure at the wave origin and also that along the wave path, it is expected that the correlograms of seismograms for the eastern origin earthquakes may differ appreciably from those of the western origin ones.

The seismometer at the Central Meteorological Observatory is of the Wichert type with

Fig. 7. Geographic distribution of epicentres of earthquakes recorded at the Latitude Observatory at Mizusawa.

the static magnification 80 to 100, the free period 3.5 to 5.5 seconds and the damping ratio 2.8 to 5.7. Because of the magnification characteristics of the seismometer and the recording paper speed, the range of reliable period is estimated to be between 0.5–0.7 sec and 5.0–7.0 sec.

The seismometer at the Mizusawa Latitude Observatory is the Omori type with the static magnification 20, the period being 31–38 sec. with no damper.

§ 4. Results

More than one hundred seismograms are loaned from the above two laboratories and put into the relay computer for correlogram analyses. We shall now enumerate some of the notable facts revealed by the analyses.

1) The seismograms of earthquakes coming from the same or nearly the same epicentral area and with the similar magnitude have nearly the same correlograms when recorded at a station.

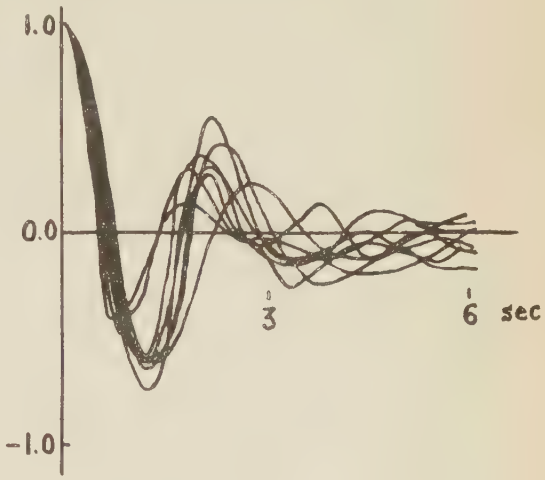

Fig. 8. Correlograms of coda waves of earthquakes occurring in the area *E*.

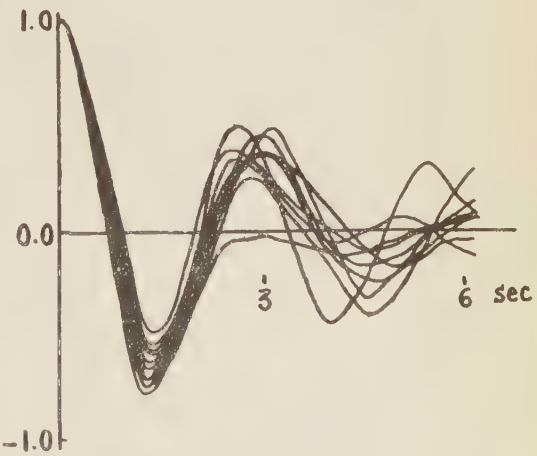

Fig. 9. Correlograms of coda waves of earthquakes occurring in the area *W*.

The correlograms of the coda parts of seismograms of earthquakes originated from the area *E* and *W* are given in Fig. 8 and 9 respectively. All of these earthquakes have the magnitude of 6.0 ± 0.2. It is remarkable that each correlogram is of the similar and

rather simple form. By averaging the correlograms in each figure, we have a mean correlogram for each epicentral area. Both of the mean correlograms are of very simple types as shown in Fig. 10, so that we may assume the spectrum density of the following types.

$$\phi(\omega) = \frac{\beta(\omega_1^2+\beta^2)}{(\omega-\omega_1+i\beta)(\omega-\omega_1-i\beta)(\omega+\omega_1+i\beta)(\omega+\omega_1-i\beta)} \quad (5)$$

Applying this formula to the two mean correlograms, we get 0.83π sec^{-1} and 0.26π sec^{-1}

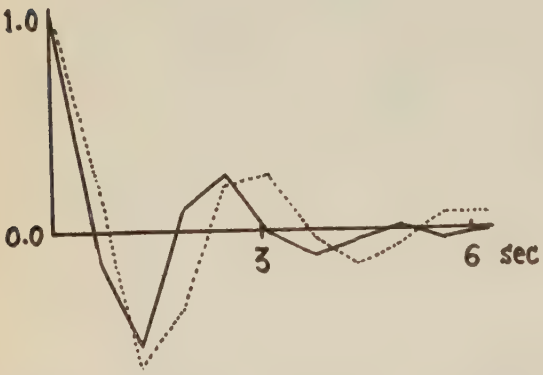

Fig. 10. Averaged correlograms, the thick line for the area E and the dotted line for the area W.

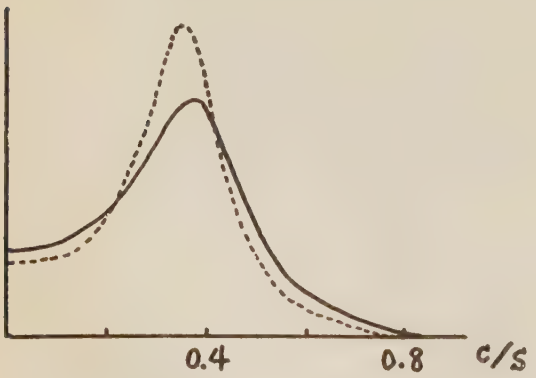

Fig. 11. Spectrum densities corresponding to the averaged correlograms.

respectively as ω_1 and β for the earthquakes originated from the area E, and 0.77π sec^{-1} and 0.19π sec^{-1} for those from the area W respectively. The spectrum density is calculated and is given in Fig. 11.

In general, the correlogram of a part of a seismogram does not always take such a simple form as above, but it is necessary for the reduction of data to assume a spectrum with a single predominant period for each part of a seismogram. We shall hereafter study mainly on the predominant period read from the spectrum or directly from the correlogram.

2) How the predominant period changes with time after the beginning of P wave depends almost on the crustal structure at the epicentre and that along the wave path. In the case of a simple crustal structure, the predominant period is very short in the early part of seismograms and later increases to approach gradually to a steady value in the coda part. On the other hand in the case of

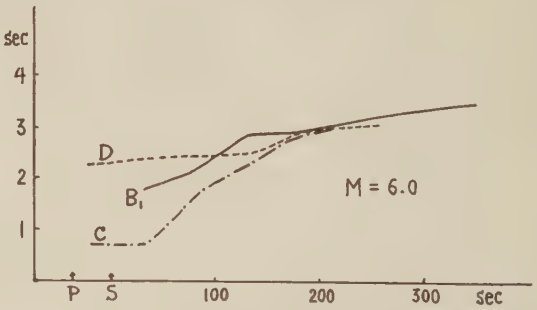

Fig. 12. Change of the mean predominant period with time for earthquakes of the magnitude 6.0.

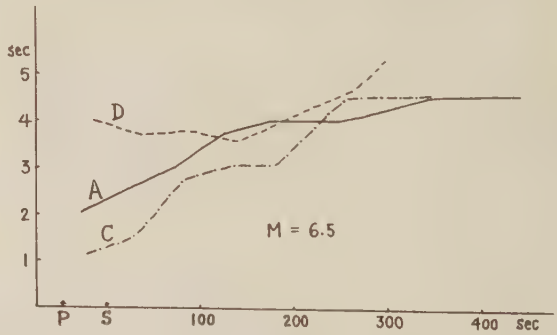

Fig. 13. Change of the mean predominant period with time for earthquakes of the magnitude 6.5.

a complex crustal structure, the predominant period in the early part is nearly the same as that in the latter part.

The change of average predominant period with time for the earthquakes of magnitude

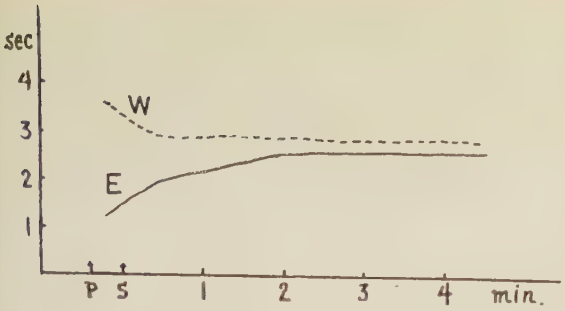

Fig. 14. Change of the mean predominat period with time for earthquakes occured in the areas E and W.

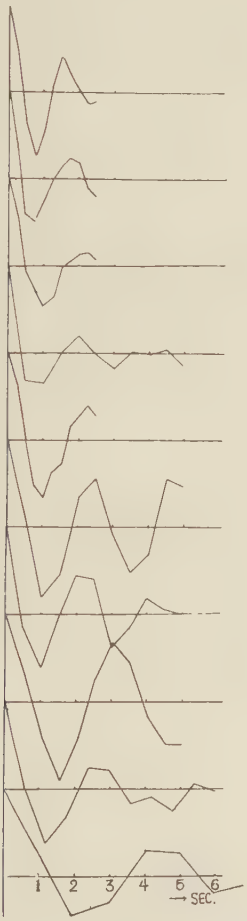

Fig. 15. Correlograms of seismograms arranged in the order of the magnitude.

6.0 and the epicentral areas B_1, C and D, is shown in Fig. 12, and that for the earthquakes of magnitude 6.5 and the epicentral areas A, C and D in Fig. 13. The earthquakes occurring in the area C are deep focus ones and the wave passage from there is regarded as of a simple oceanic type, while on the other hand the wave path from the area D is of a complex inland type, and that from the area A and B_1 is of an intermediate type. Fig. 14 shows the period change in seismograms recorded at Mizusawa for the earthquakes of magnitude 6.0 occurring in the areas E and W. As refered to before, the crust of the western area W of Mizusawa is more complex than that of the eastern area E. The way of period change in the Figs. 12, 13 and 14 agrees with the above statement.

3) As to earthquakes having the same magnitude, the predominant period in the early part of seismogram shows a conspicuous variation with the place of epicentral area and wave passage, but the variation diminishes or dies out in the coda part as seen from the preceding figures. We may say, therefore, that the period of the coda wave is almost determined by the magnitude of earthquake.

4) As to earthquakes coming from the same epicentral area, the predominant period of every part of seismogram increases with the magnitude. But the rate of increase with the magnitude differs among parts of a seismogram, it is rapid in early parts and slow in later parts.

The correlograms of the motions for 50 seconds after the beginning of S wave are arranged in the order of magnitude in Fig. 15. The largest magnitude is 6.8 and the smallest (the top one in the figure) is 5.2. All of these earthquakes occured in the area D. It is evident from the figure that the larger the magnitude, the longer becomes the period.

To see the way of variation of the predominant period with the magnitude, we plotted in Fig. 16 the period read from the correlograms of waves for 50 seconds after the beginning of S wave against the magnitude. The plotted points are scattered widely, but they may be divided into three groups according to their epicentral areas. The first group of earthquakes is of inland origin such as those from

the area D, and shows the longest period. The second guoup is of the deep focus type with the shortest period. The last has the origin in the area A and B, and its period is intermediate.

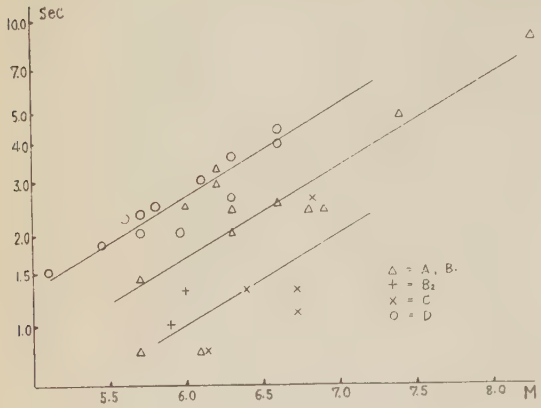

Fig. 16. Variation of predominant period of S wave with the magnitude.

Assuming the following formula for each group

$$\log_{10} T = \text{const.} + \alpha M, \qquad (6)$$

we have α of about 0.3. The lines in Fig. 16 are drawn for $\alpha = 0.3$.

H. Honda and H. Ito (1939) found a relation between the period of P waves and the magnitude of earthquake, and K. Kanai, K. Osada and S. Yoshizawa (1953) extended the study. They got $T^2 = A$ between the period T of P waves and the amplitude A reduced to the place 100 km from the origin. The magnitude M can be written as $M = \log_{10} A +$ const., so that we can convert the above relation to the form as (6) and obtain $\alpha = 0.5$.

After Kanai, the relation between the period of S wave and the reduced amplitude A is the same as that for P wave, but in the case of S wave his diagram seems to suggest the value of α somewhat smaller than 0.5.

According to the study of Hawaiian local earthquakes by A. E. Jones (1938), the upper limits of amplitudes of P and S waves of local shocks are found to vary with the cube of the period. In this case, the value of α becomes 1/3, and approximately agrees with ours.

As stated before, the predominant period of coda waves is mainly determined by the magnitude of earthquake. The periods of coda waves are plotted against the magnitudes of earthquakes in Fig. 17, in which earthquakes of the epicentral area D are omitted.

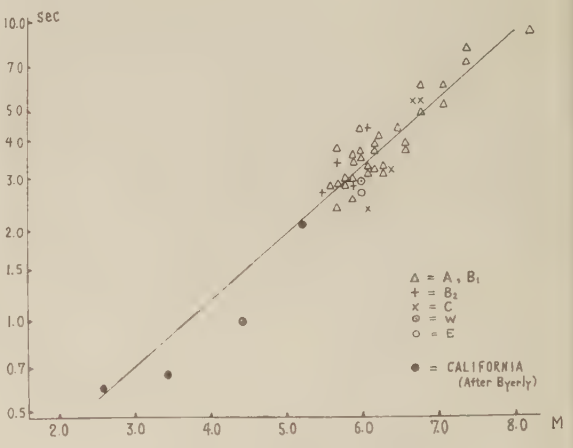

Fig. 17. Variation of predominant period of coda wave with the magnitude.

Fitting the same formula as (6) to this case, we obtain

$$\log_{10} T = -0.82 + 0.22\, M$$

In Fig. 17, the periods of coda waves of local earthquakes in California are plotted against the magnitudes. These values are given in a paper by P. Byerly (1947) who analysed numerous seismograms obtained by a seismometer of the Wood-Anderson type. The points are located on an extrapolated part of our formula.

B. Gutenberg and C. F. Richter (1942) obtained the relation $\log_{10} T = -1.5 + 0.22M$ between the periods T of the wave group of the maximum amplitude and the magnitude M. The value of the factor α is the same as in the case of coda waves, but the value of the constant in the formula is different. Thus the period of the coda wave is 4.8 times of that of the wave group of the maximum amplitude.

§ 5. Acknowledgement

The writer is very much obliged to Dr. W.

Inouye, Mr. Y. Iwai and other officials of the Seismological Section of the Central Meteorological Observatory and to Mr. T. Sugawa and other officials of the Mizusawa Latitude Observatory, who kindly lent him valuable seismograms recorded at the observatories or helped him to copy them.

The writer's thanks are also due to Mr. T. Ikeda and other staff members of the Fuji Tsushinki Seizo K. K. (Fuji Communication Apparatus Mfg. Co. Ltd.) for their helpful advises given him about the design of the computer.

The writer is greatly indepted to Prof. C. Tsuboi for his guidance and encouragement.

This study was made with the help of a Grant from the Department of Education.

References

Akamatu, K.:
1956 in this issue.

Byerly, P.:
1947 The Periods of Local Earthquake Waves in Central California. Bull. Seis. Soc. Amer., **37**, 291.

Gutenberg, B. and Richter, C. F.:
1942 Earthquake Magnitude, Intensity, Energy and Acceleration. Bull. Seis. Soc. Amer., **32**, 163.

Honda, H. and Ito, H.:
1939 On the period of the *P* waves and the magnitude of the earthquake. Geophys. Mag. **13**, 155.

Jones, A. E.:
1938 Empirical Studies of some of the Seismic Phenomena of Hawaii. Bull. Seis. Soc. Amer., **28**, 313.

Kanai, K., Osada, K. and Yoshizawa, S.:
1953 The Relation between the Amplitude and the Period of Earthquake Motion. Bull. Earthq. Res. Inst., **31**, 44.

The Central Meteorological Observatory, Tokyo:
1952 The Seismological Bulletin of C. M. O., Japan for the year 1950, 99.

Tsuboi, C., Jitsukawa, A. and Tazima, H.:
1956 Gravity Survey along the lines of Precise Levels throughout Japan by means of a Worden Gravimeter, Part 7, Tohoku District. Bull. Earthq. Res. Inst., Suppl. Vol. **4**, 311–406.

Tomoda, Y.:
1956 in this issue.

TOMODA's Method for Calculating the Correlation Coefficients as Applied to Microtremor Analysis.

By

Kei AKAMATU

Geophysical Institute, Faculty of Science, Tokyo University, Tokyo.

Summary

TOMODA's method for calculating the correlation coefficients has been applied to microtremor analysis and it is shown that the method can safely be used for the purpose, if the sample size is larger than about 300.

A very simple method for calculating the correlation coefficient between two variables x and y has been proposed by Y. TOMODA (1956). The method consists essentially in comparing the algebraic signs of Δx and the corresponding Δy, where Δx and Δy are the deviations of x and y from their respective mean values. If the number of pairs of x and y for which Δx and Δy are of the same sign is N_+ and that for which they are of the opposite sign is N_-, the correlation coefficient ρ between x and y is given by

$$\rho=\sin\left(\frac{N_+-N_-}{N_++N_-}\frac{\pi}{2}\right).$$

This method is conveniently used especially in those cases in which a large number of correlation coefficients have to be calculated as in the construction of an autocorrelation correlogram.

In the present note, this method of calculation will be applied for microtremor analysis. By microtremor is meant here the so-called ground noise or ground unrest which have periods less than a few seconds. The seismograms used for the analysis are those obtained at Tokyo by two seismometers, one a 1 c/s horizontal and the other a 3 c/s vertical.

Examples of the records used are shown in Fig. 1. On these records, time intervals of 6–8 seconds were chosen, and the mean value within the interval was established. The deflection of the curve $f(t)$ for every 1/50 of a second (τ_0) was read as either $+1$ or -1

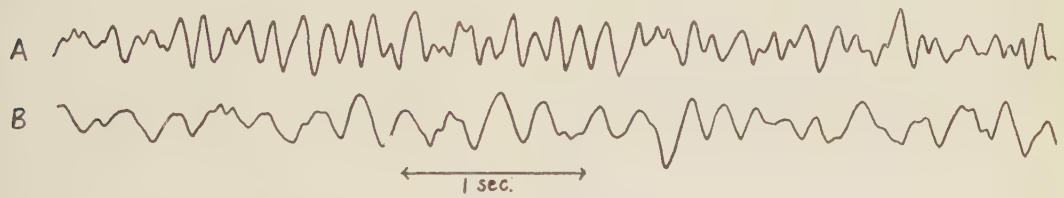

Fig. 1. A 3 c/s vertical seismometer B 1 c/s horizontal seismometer

according as it is above or below the zero line. Thus from 300 to 400 readings of ±1 were obtained. From these readings,

$$\phi(\tau)=\frac{1}{\sqrt{\sigma_1^2}}\frac{1}{\sqrt{\sigma_2^2}}\frac{1}{N}\sum\Delta x\Delta y\,,$$

has been counted, for various values of $\tau=k\tau_0$, k being taken to be 1, 2, 3, $\cdots$, 30 for the 1 c/s seismometer and 1, 2, 3, $\cdots$, 20 for the 3 c/s one. σ_1^2 and σ_2^2 are the variances of Δx and Δy.

The autocorrelation correlograms, which are the curves of $\phi(\tau)$ plotted against τ, are shown by broken lines in Fig. 2. The solid curves shown in the same figure were deduced by the customary method of calculation. The latter calculations would have been extremely

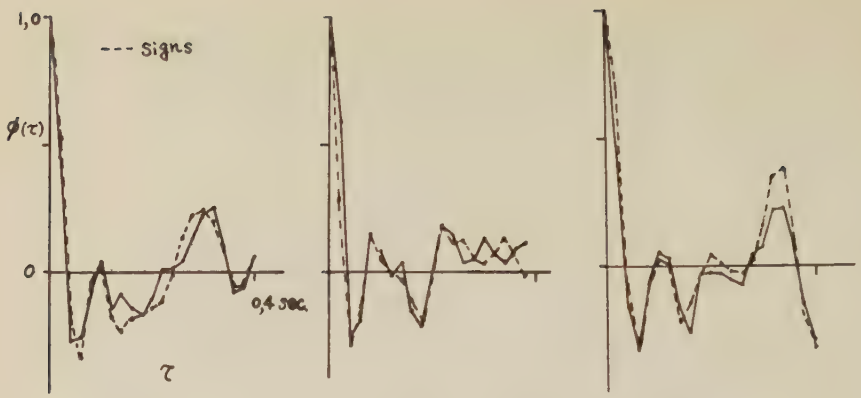

a. b. c.

Fig. 2. Correlograms, 3 c s vertical seismometer

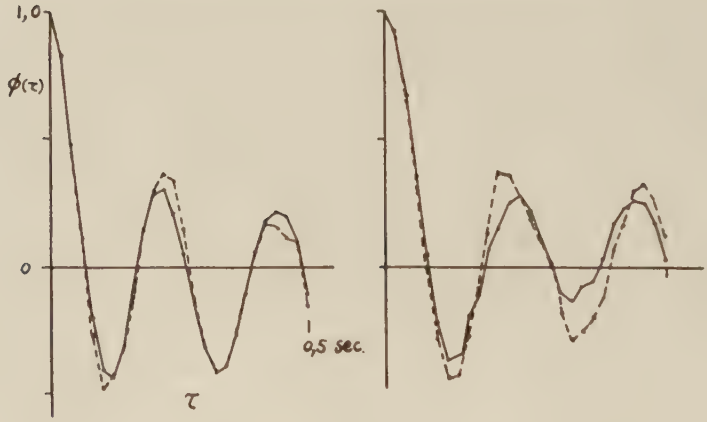

d. e.

Fig. 2. Correlograms, 1 c/s horizontal seismometer

tedious if done manually. Actually, a relay computor FACOM belonging to the Fuji Communication Apparatus Mfg. Co. could be used for the purpose through the courtesy of that company for which the author expresses her thanks. (AKAMATU: 1956).

The curves of solid and broken lines, agree well in general tendancy, although in some cases the correlation coefficients differ notably, even at the first significant figure.

Based on the above results, power spectra of the microtremors were futher constructed. In order to get rid of the effect due to minor fluctuations in $\phi(\tau)$ as seen in Fig. 2. $e^{-\alpha|\tau|}$ was multiplied to the original $\phi(\tau)$, α being tentatively taken to be 6–8. Thus the spectra were actually deduced according to

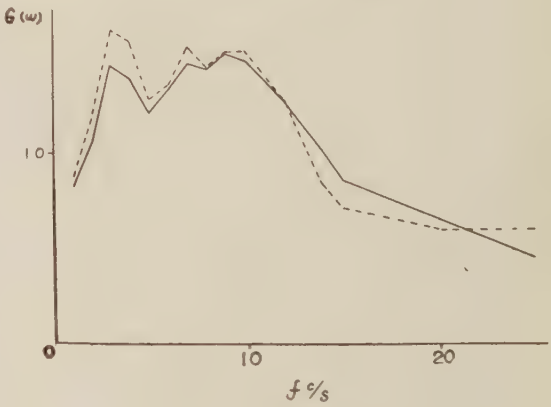

Fig. 3. a. Spectrum from Fig. 2. a.

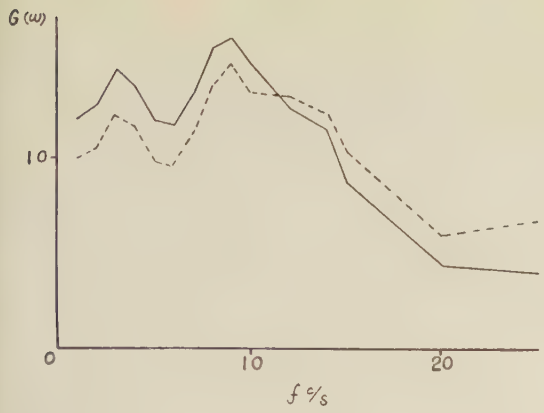

Fig. 3. b. Stpectrum from Fig. 2. b.

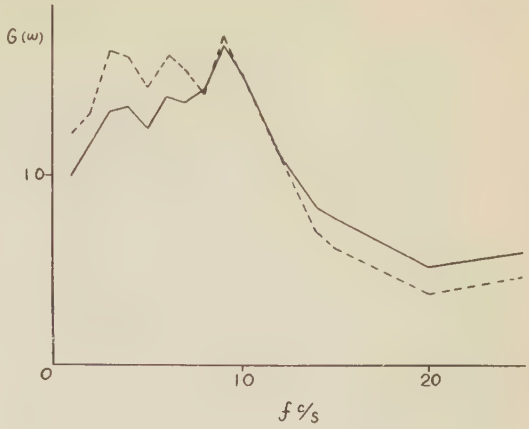

Fig. 3. c. Spectrum from Fig. 2. c.

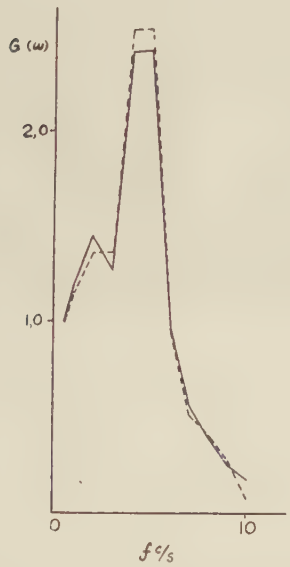

Fig. 3. d. Spectrum from Fig. 2. d.

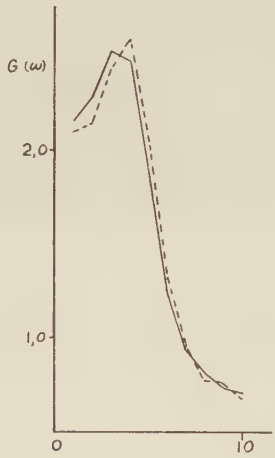

Fig. 3. e. Spectrum from Fig. 2. e.

$$\sum_{k=-n}^{n} \phi(\tau) e^{-\alpha|\tau|} \cos k\omega\tau_0 \ .$$

and they are shown in Fig. 3. The broken line curve which was based on TOMODA's method and the solid line curve based on the customary method agree well.

The conclusion is that TOMODA's method can safely be used in microtremor analysis if the sample size is larger than about 300.

References

TOMODA, Y.:
1956 A Simple Method for Calculating the Correlation Coefficient. Journ. Physics of the Earth, **4**, 67–70.

AKAMATU, K.:
1956 On Microtremors. Zisin (in press)

Fuji Automatic Relay Computer
FACOM-100

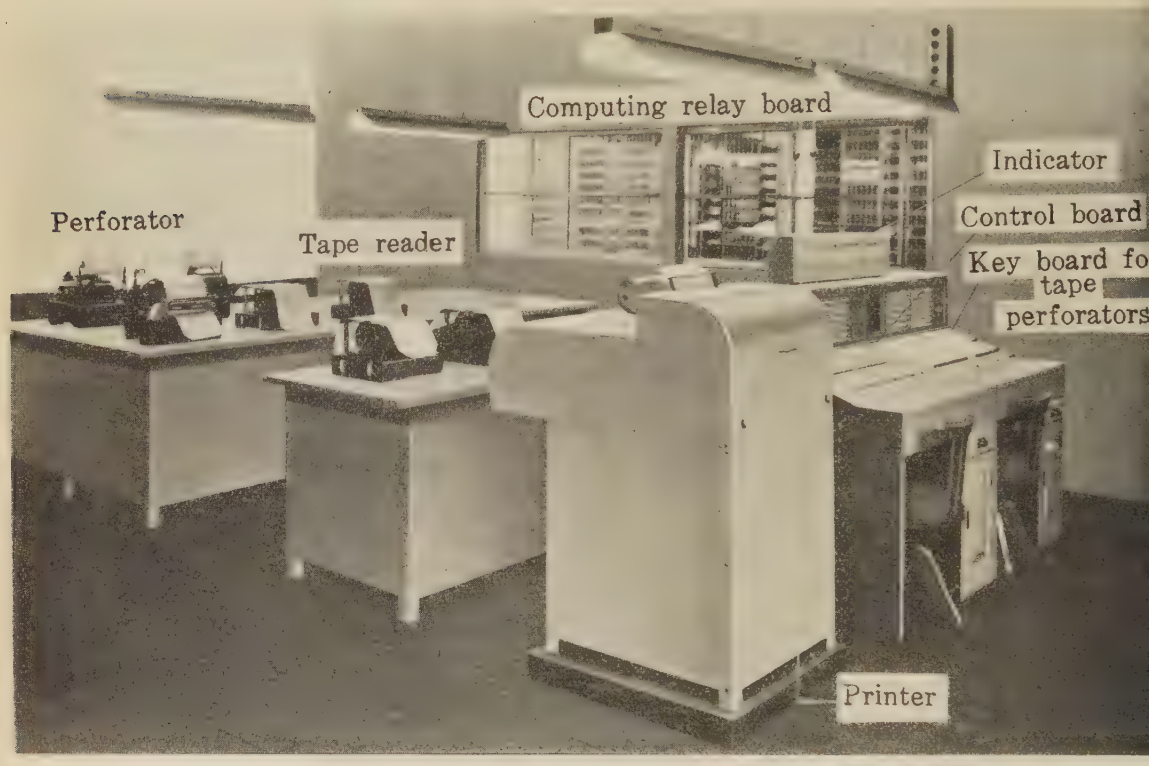

PURPOSE

The equipment can be used for making enormous and complicated calculations very quickly through operation of electromagnetic relays.

COMPONENT

The main components are:

- Manipulating key board for tape perforators
- Control board
- Tape readers
- Relay board for control, computations as well as for storing of given data
- Automatic printing machine

ADVANTAGES

- Easy for programming
- High speed in calculation
- Very accurate in operation
- Durable under severe and continuous use
- Easily accessible for maintenance

APPLICATION

Simultaneous or higher degree algebraic equations; Differential or integral equations; Interpolations; Approximate extension of functions etc. for researching, designing and various investigations in the scientific, technical or economical problems.

FUJI TSUSHINKI SEIZO K.K.

(Fuji Communication Apparutus Mfg. Co., Ltd.)

Mitsubishi No. 21 Bldg., 3-2, Marunouchi Chiyoda-ku, Tokyo

Tel. (28) 6221

JOURNAL OF PHYSICS OF THE EARTH, VOL. 4, No. 3, 1956.

Studies on the Instability of the Layer of Fluid Heated from Below.

By

Yoshinari NAKAGAWA

The Enrico Fermi Institute for Nuclear Studies, The University of Chicago.

Summary

The details of the experimental studies on the instability of a layer of electrically conducting fluid heated from below subject to an external magnetic field are reported. A summarizing discussion on the theoretical studies on the instability of the layer of fluids heated from below under various circumstances is also presented.

Contents

§ 1. Introduction

The thermal instability of the layer of viscous fluid heated from below has become the subject of theoretical investigation since the first attempt of Lord RAYLEIGH (1916) on the experimentally observed cellular convection under such circumstances by H. BÈNARD (1900). RAYLEIGH treated this problem by the method of perturbation, and showed that cellular convection of specified dimension should ensue when a non-dimensional parameter called the RAYLEIGH number exceeds a certain determinate critical value. As RAYLEIGH's theoretical work assumed only boundary conditions of both free plane bounding surfaces of the layer, H. JEFFREYS (1926, 1928, 1930) has extended the theoretical treatment to other bounding surfaces such as two rigid planes, one free and one rigid planes. Thus, JEFFREYS has obtained three different critical values of the RAYLEIGH number under each set of the boundary conditions; 651 for both free surfaces, 1108 for one free and one rigid surfaces, and 1706 for both rigid surfaces.

A. R. Low (1929) discussed this problem from the standpoint of the energy balance in the fluid, and showed that the similarity of the theoretical treatment of this problem to that of the dynamic instability of a viscous flow between concentric rotating cylinders. The latter problem was theoretically investigated by G. I. TAYLOR (1923), and he obtained the criterion of instability in the similar critical value of a non-dimensional number. The critical values of the two criteria closely agreed with each other and JEFFREYS obtained 1706 under both rigid boundary conditions while TAYLOR obtained 1709 for his problem.

A. PELLEW and R. V. SOUTHWELL (1940) have summarized these earlier theoretical studies with discussions on the validity of exchange stability, boundary conditions and the characteristic number a^2. Then, they introduced the method of variation in the evaluation of the critical value of the RAYLEIGH number. Later, this method has been developed by S. CHANDRASEKHAR into a more refined form, and he has studied the instability of the layer of fluid heated from below under various circumstances (1952a, 1952b, 1953b, 1953c, 1954a, 1954b, 1954c). He has also applied the same method of variation to other problems of the instabilities in hydrodynamics and hydromagnetics (1953a, 1953d, 1954d). Thus, the theoretical treatment of this problem practically leads the general theoretical studies of the problem of instability. While CHANDRASEKHAR has been developing such theoretical treatments, independently W.

B. THOMPSON (1951) studied the convection under a magnetic field, and the author (Y. NAKAGAWA and P. FRENZEN 1955) studied the cellular convection of rotating fluids. However, these theoretical studies were completely covered by the works of CHANDRASEKHAR (1952a, 1953b).

The results of earlier theoretical studies, especially JEFFREYS' results, have been examined experimentally by R. J. SCHMIDT and S. W. MILVERTON (1935), R. J. SCHMIDT and O. A. SANDERS (1938) and others. They confirmed that instability really sets in as cellular convection of a specified dimension when the critical value of the RAYLEIGH number is exceeded. However, some disagreements between experiment and theory were noticed in the experiments studied by K. CHANDRA (1938), and O. G. SUTTON (1950) gave a theoretical discussion on this aspect. SUTTON explained that these disagreements were caused by the presence of the other mode of convection which should be able to appear in the layer when the depth of the layer is less than the thickness of the boundary layer of fluids. Then he successfully interpreted the results of CHANDRA's experiments.

The results of the theoretical studies on the rotating fluids were confirmed experimentally by Y. NAKAGAWA and P. FRENZEN (1955) with respect to the theoretical criteria of the exchange stability. The other aspect of the theoretical result, that is, the onset of oscillatory convection, was firstly demonstrated by D. FULTZ, Y. NAKAGAWA and P. FRENZEN (1954) in a trial experiment with a layer of rotating mercury. Later, experiments on this aspect performed by the author (D. FULTZ and Y. NAKAGAWA 1955) obtained a good agreement with the theoretical criteria especially prepared for these experiments by S. CHANDRASEKHAR and D. D. ELBERT (1955).

Experiments on the instability of the layer of electrically conducting fluids under external magnetic fields have been performed by the author (Y. NAKAGAWA 1955)* and K. JIRLOW (1956) and they have provided confirmations for the results of theory. In this paper, the details of the author's experiments are reported with a general discussion covering the whole aspect of the theoretical studies of this problem under various circumstances.

§ 2. The Equation of the Problem

The equations of this problem are discussed by means of conventional vector operations**. By including the influences of rotation and the magnetic field, we have the equation of motion in the following form which is called the equation of magneto-hydrodynamics:

$$\rho\frac{\partial \boldsymbol{V}}{\partial t}+\rho(\boldsymbol{V}\cdot\boldsymbol{\nabla})\boldsymbol{V}+\rho 2(\boldsymbol{\Omega}\times\boldsymbol{V})-\boldsymbol{J}\times\mu\boldsymbol{H}$$
$$=-\boldsymbol{\nabla}P+\rho\frac{\nu}{3}\boldsymbol{\nabla}(\boldsymbol{\nabla}\cdot\boldsymbol{V})+\rho\nu\nabla^2\boldsymbol{V}+\rho\boldsymbol{\nabla}U\,, \qquad (1)$$

where $\boldsymbol{V}$ denotes the velocity, ρ the density, μ the magnetic permeability, P the pressure, ν the kinematic viscosity and U the gravitational potential. The term $2(\boldsymbol{\Omega}\times\boldsymbol{V})$ denotes the CORIOLIS' forces*** and the term $\boldsymbol{J}\times\mu\boldsymbol{H}$ denotes the mechanical force exerted by the magnetic field $\boldsymbol{H}$, to the electrically conducting fluids carrying the current density $\boldsymbol{J}$****. The term due to the space charge is neglected in the equation because the motion of the fluid is naturally much smaller than the velocity of light*****.

The equation of continuity becomes in the form:

$$\frac{\partial\rho}{\partial t}+\boldsymbol{\nabla}\cdot(\rho\boldsymbol{V})=0\,. \qquad (2)$$

The electro-magnetic phenomena of the fluid are described by the MAXWELL's equation of the following forms:

$$\boldsymbol{\nabla}\times\boldsymbol{E}=-\mu\frac{\partial\boldsymbol{H}}{\partial t}\,, \qquad (3)$$

* A brief note was published in Nature.

** See S. LUNDQUIST (1952); some operational relationships are listed.

*** The justification from microscopic view points is given by the author in the foregoing paper.

**** See S. CHAPMAN and T.G. COWLING (1939); the interpretation of this term from microscopic view point can be easily obtained.

***** Discussions are given by G.K. BATCHELOR (1950), S. LUNDQUIST (1952), E. BULLARD (1955) and others.

$$\nabla \times \boldsymbol{H} = 4\pi \boldsymbol{J} , \tag{4}$$

$$\nabla \cdot \boldsymbol{H} = 0 , \tag{5}$$

$$\nabla \cdot \boldsymbol{E} = 0 , \tag{6}$$

$$\boldsymbol{J} = \sigma(\boldsymbol{E} + \boldsymbol{V} \times \mu \boldsymbol{H}) , \tag{7}$$

where $\boldsymbol{E}$ denotes the electric field, σ the electric conductivity, and the last equation is the OHM's law for the moving fluid with velocity $\boldsymbol{V}$. The electro-magnetic cgs. units are used with the approximation of slow motion of fluid compared to the velocity of light. The thermal and kinematic phenomena of the problem are related by the equation of energy*:

$$\frac{\partial T}{\partial t} + (\boldsymbol{V} \cdot \nabla) T + \frac{P}{\rho J C_v} (\nabla \cdot \boldsymbol{V}) = \kappa \nabla^2 T + \frac{\Phi}{\rho J C_v} , \tag{8}$$

where T is the temperature, J the mechanical equivalent of heat, C_v the specific heat for constant volume, κ the thermometric conductivity, and Φ is the "dissipation function". Finally, we have the equation of thermal expansion,

$$\rho = \rho_0 (1 - \alpha \Delta T) , \tag{9}$$

where α denotes the coefficient of volume expansion and ΔT is the difference between the temperature at which the density is ρ and the temperature at which the density is ρ_0.

Before the onset of convection, with the heating from below, a state of thermal equilibrium should be attained in the layer of fluid due to the conductive heat transfer. This leads to the assumption of the initial state of being steady and relatively at rest. Then we obtain the following relations as the initial conditions:

$$\nabla P = \rho \nabla U , \tag{10}$$

$$\nabla^2 T = 0 , \tag{11}$$

$$\boldsymbol{J} = 0 , \tag{12}$$

$$\boldsymbol{E} = 0 , \tag{13}$$

where the equation (10) denotes the hydrostatic relation and the equations (12) and (13) are obtained with an additional assumption of uniform external magnetic field $\boldsymbol{H}$. Integrating the equation (11) with the assumption of uniform temperature in horizontal direction and higher temperature at bottom, we have

$$T = T_0 - \beta z , \quad \left(-\beta = \frac{\partial T}{\partial z} \right) , \tag{14}$$

where T_0 denotes the temperature at the bottom of the layer and β is a constant and denotes the initial vertical adverse temperature gradient.

Now for the investgiation of instability, we assume that the quantities concerned with the unstable motion, i.e. the convective motion to be small enough so that squares and products of such quantities are negligible. Then, taking perturbation of the original equations (1) to (8) we have the following equations:

$$\rho \frac{\partial \boldsymbol{u}}{\partial t} + \rho 2(\boldsymbol{\Omega} \times \boldsymbol{u}) - \boldsymbol{j} \times \mu \boldsymbol{H} = -\nabla p + \rho \frac{\nu}{3} \nabla (\nabla \cdot \boldsymbol{u}) + \rho \nu \nabla^2 \boldsymbol{u} + \rho' \nabla U , \tag{15}$$

$$\frac{\partial \rho'}{\partial t} + (\boldsymbol{u} \cdot \nabla) \rho + (\nabla \cdot \boldsymbol{u}) \rho = 0 , \tag{16}$$

$$\nabla \times \boldsymbol{e} = -\mu \frac{\partial \boldsymbol{h}}{\partial t} , \tag{17}$$

$$\nabla \times \boldsymbol{h} = 4\pi \boldsymbol{j} , \tag{18}$$

$$\nabla \cdot \boldsymbol{h} = 0 , \tag{19}$$

$$\nabla \cdot \boldsymbol{e} = -\mu \boldsymbol{H} \cdot (\nabla \times \boldsymbol{u}) , \tag{20}$$

$$\boldsymbol{j} = \sigma(\boldsymbol{e} + \boldsymbol{u} \times \mu \boldsymbol{H}) , \tag{21}$$

$$\frac{\partial \theta}{\partial t} - (\boldsymbol{u} \cdot \boldsymbol{k}) \beta + \frac{P}{\rho J C_v} (\nabla \cdot \boldsymbol{u}) = \kappa \nabla^2 \theta , \tag{22}$$

where $\boldsymbol{k}$ is a unit vector in the vertical direction and $\boldsymbol{u}$, $\boldsymbol{j}$, p, ρ', $\boldsymbol{e}$, $\boldsymbol{h}$ and θ denote the quantities concerned with the convective motion.

Rewriting the equation of thermal expansion (9) by these quantities, we have

$$\rho' = -\rho \alpha \theta , \tag{23}$$

where ρ' is negative as the density decreases with the increase of the temperature. The equation (23) suggests that due to the factor α the magnitude of the density variation be always smaller than the magnitude of the temperature variation**. Therefore, to the

* See S. GOLDSTEIN (1943) p. 606. For gas C_v can be replaced by C_p with κ replaced by $\kappa\, C_v/C_p$. (see G. K. BATCHELOR 1954).

** This reason also justifies the elimination of terms in the perturbation equations which involved the variation of ρ caused by the initial temperature gradient in the fluid. See the discussion given by A. PELLEW and R. V. SOUTHWELL (1940).

same order of approximation, we can simply write the equation (17) as

$$\nabla\cdot\boldsymbol{u}=0\,. \tag{24}$$

Thus, using the equation (24), the equations (15) and (22) become

$$\rho\frac{\partial\boldsymbol{u}}{\partial t}+\rho 2(\boldsymbol{\Omega}\times\boldsymbol{u})-\boldsymbol{j}\times\mu\boldsymbol{H} =-\nabla p+\rho\nu\nabla^2\boldsymbol{u}-\rho\alpha\theta\nabla U\,, \tag{25}$$

$$\frac{\partial\theta}{\partial t}-(\boldsymbol{u}\cdot\boldsymbol{k})\beta=\kappa\nabla^2\theta\,. \tag{26}*$$

Eliminating $\boldsymbol{e}$ in the equation (17) by equations (18) and (21), we have

$$\frac{\partial\boldsymbol{h}}{\partial t}-(\boldsymbol{H}\cdot\nabla)\boldsymbol{u}=\eta\nabla^2\boldsymbol{h}\,, \tag{27}$$

where $\eta=\dfrac{1}{4\pi\sigma\mu}$. Similar elimination of $\boldsymbol{j}$ in the equation (25) by (18) gives

$$\frac{\partial\boldsymbol{u}}{\partial t}+2(\boldsymbol{\Omega}\times\boldsymbol{u})-\frac{\mu}{4\pi\rho}(\nabla\times\boldsymbol{h})\times\boldsymbol{H}=-\nabla\frac{p}{\rho} +\nu\nabla^2\boldsymbol{u}+\gamma\theta\boldsymbol{k}\,, \tag{28}$$

where $\gamma=g\alpha$. Operating curl $(\nabla\times)$ to the equations (27) and (28), we obtain

$$\frac{\partial\boldsymbol{B}}{\partial t}-(\boldsymbol{H}\cdot\nabla)\boldsymbol{A}=\eta\nabla^2\boldsymbol{B}\,, \tag{29}$$

$$\frac{\partial\boldsymbol{A}}{\partial t}+2(\boldsymbol{\Omega}\cdot\nabla)\boldsymbol{u}-\frac{\mu}{4\pi\rho}(\boldsymbol{H}\cdot\nabla)\boldsymbol{B}=\nu\nabla^2\boldsymbol{A}+\gamma(\nabla\times\boldsymbol{k})\theta\,, \tag{30}$$

where $\boldsymbol{A}=\nabla\times\boldsymbol{u}$ and $\boldsymbol{B}=\nabla\times\boldsymbol{h}$. Another operation of curl to the equation (30) gives

$$\frac{\partial}{\partial t}(\nabla^2\boldsymbol{u})+2(\boldsymbol{\Omega}\cdot\nabla)\boldsymbol{A}-\frac{\mu}{4\pi\rho}(\boldsymbol{H}\cdot\nabla)\nabla^2\boldsymbol{h} =\nu\nabla^4\boldsymbol{u}-\gamma\nabla\times(\nabla\times\boldsymbol{k})\theta\,, \tag{31}$$

where the following relations are used

$$\left.\begin{aligned}\nabla\times\boldsymbol{A}&=-\nabla^2\boldsymbol{u}\\ \text{and}\quad\nabla\times\boldsymbol{B}&=-\nabla^2\boldsymbol{h}\,.\end{aligned}\right\} \tag{32}$$

The equations (26), (27), (29), (30) and (31) give a complete set of equations for further investigation of this problem, but for the simplification and convenience, we will confine the discussion to the vertical components of the various vector quantities, $\boldsymbol{u}$, $\boldsymbol{h}$, $\boldsymbol{A}$ and $\boldsymbol{B}$. Then from the above set of equtions we have

$$\left(\frac{\partial}{\partial t}-\kappa\nabla^2\right)\theta=\beta w\,, \tag{33}$$

$$\left(\frac{\partial}{\partial t}-\eta\nabla^2\right)\chi=Fw\,, \tag{34}$$

$$\left(\frac{\partial}{\partial t}-\eta\nabla^2\right)\phi=F\zeta\,, \tag{35}$$

$$\left(\frac{\partial}{\partial t}-\nu\nabla^2\right)\zeta=Ew+\frac{\mu}{4\pi\rho}F\phi\,, \tag{36}$$

$$\left(\frac{\partial}{\partial t}-\nu\nabla^2\right)w=-E\zeta+\frac{\mu}{4\pi\rho}F\nabla^2\chi+\gamma\nabla_1^2\theta\,, \tag{37}$$

where w, χ, ζ and ϕ denote the vertical components of $\boldsymbol{u}$, $\boldsymbol{h}$, $\boldsymbol{A}$ and $\boldsymbol{B}$ respectively, and E, F and ∇_1^2 are the scalar operators defined as:

$$\left.\begin{aligned}E&=2(\boldsymbol{\Omega}\cdot\nabla)\,,\\ F&=(\boldsymbol{H}\cdot\nabla)\,,\\ \text{and}\quad\nabla_1^2&=\frac{\partial^2}{\partial x^2}+\frac{\partial^2}{\partial y^2}\,.\end{aligned}\right\} \tag{38}$$

Eliminating χ between the equations (34) and (37), we have

$$\left\{\left(\frac{\partial}{\partial t}-\eta\nabla^2\right)\left(\frac{\partial}{\partial t}-\nu\nabla^2\right)-\frac{\mu}{4\pi\rho}F^2\right\}\nabla^2 w +E\left(\frac{\partial}{\partial t}-\eta\nabla^2\right)\zeta=\gamma\left(\frac{\partial}{\partial t}-\eta\nabla^2\right)\nabla_1^2\theta. \tag{39}$$

Similarly, eliminating ϕ between the equations (35) and (36), we obtain

$$\left\{\left(\frac{\partial}{\partial t}-\eta\nabla^2\right)\left(\frac{\partial}{\partial t}-\nu\nabla^2\right)-\frac{\mu}{4\pi\rho}F^2\right\}\zeta =E\left(\frac{\partial}{\partial t}-\eta\nabla^2\right)w\,. \tag{40}$$

Finally, eliminating ζ and θ in the equation (39) by using equations (33) and (40), we have an equation for w alone:

$$\left(\frac{\partial}{\partial t}-\kappa\nabla^2\right)\left\{\left(\frac{\partial}{\partial t}-\eta\nabla^2\right)\left(\frac{\partial}{\partial t}-\nu\nabla^2\right)-\frac{\mu}{4\pi\rho}F^2\right\}^2\nabla^2 w +E^2\left(\frac{\partial}{\partial t}-\kappa\nabla^2\right)\left(\frac{\partial}{\partial t}-\eta\nabla^2\right)^2 w =\beta\gamma\left(\frac{\partial}{\partial t}-\eta\nabla^2\right)\left\{\left(\frac{\partial}{\partial t}-\eta\nabla^2\right)\left(\frac{\partial}{\partial t}-\nu\nabla^2\right)-\frac{\mu}{4\pi\rho}F^2\right\}\nabla_1^2 w\,. \tag{41}$$

The equation (41) is the basic equation for the investigation of the stability and the same

* The similar equation results for compressible fluids: see the studies of H. JEFFREYS (1930) and Y. NAKAGAWA and P. FRENZEN (1955).

equation is also satisfied by θ, χ, ζ and ϕ as it is easily seen from equations (30), (31) and (32).

Under other circumstances, such as when no rotation or no magnetic field is presented in the problem, a simpler form of equation resulted as the basic equations which can be easily derived from the equation (41) by eliminating unnecessary terms.

§ 3. The Functional Form of Solutions and the Boundary Conditions

The experimental observations of cellular convection approved the first step of the separation of variables x and y from z in the solution. Also, the pattern of symmetry of cells suggested a further speculation on the function x and y. A discussion was given by RAYLEIGH on the analogy of the vibration of a horizontal membrane, we can write as $f \propto \nabla_1^2 f$, where f denotes a function of x and y. The customary expression of the above relation in this problem is as follows, with the solution of the form of $f(x, y)g(z)l(t)$,

$$d^2\nabla_1^2 f + a^2 f = 0 , \tag{42}$$

where d is the depth of the layer and a^2 is the "characteristic number". The important meaning of the "characteristic number", a^2, has been discussed by various authors (see Introduction). The practical meaning of a^2 is easily seen in its relation to the size of the cell. For instance, consider a hexagonal cell of the side length L, then f is given by the following function discovered by S. CHRISTOPHESON (1940):

$$f = f_0\left\{\cos\frac{2n\pi}{3L}(\sqrt{3}\,x+y)+\cos\frac{2n\pi}{3L}(\sqrt{3}\,x-y) +\cos\frac{4n\pi}{3L}y\right\}, \tag{43}$$

where f_0 is a constant and n is an integer. Substituting (43) in (42) we have

$$a^2 = \left(\frac{4n\pi}{3L}\right)^2 d^2. \tag{44}$$

Consequently, a^2 represents the horizontal wave numbers of the cellular convection. Similar relations as (44) are easily obtained for other specified shapes of cells such as squares or rectangulars.

The boundary conditions which are immediately apparent to be satisfied by w are

$$w = 0 \tag{45}$$

at the top and bottom surfaces of the layer. Then assuming the constant temperature of boundary surfaces, we have

$$\theta = 0 \tag{46}$$

at the top and bottom of the layer which can be justified under the usual circumstances*.

Further boundary conditions are obtained from the horizontal motion of convection. As no horizontal motion becomes possible at the rigid surface, the following conditions result from the equation of continuity,

$$\frac{\partial w}{\partial z} = 0 \quad \text{and} \quad \zeta = 0 \tag{47}$$

on rigid surfaces. Similarly, from the maximum horizontal motions at free surfaces the following conditions result

$$\frac{\partial^2 w}{\partial z^2} = 0 \quad \text{and} \quad \frac{\partial \zeta}{\partial z} = 0 \tag{48}$$

on free surfaces.

The boundary conditions for electromagnetic quantities are

$$e_x = e_y = 0 \quad \text{and} \quad \chi = 0 \tag{49}$$

on a perfectly conducting surface and

$$e_z = 0 \tag{50}$$

on a free surface adjoining a vacuum. The equations (49) and (50) are derived from the theory of electricity and magnetism and have been introduced by CHANRASEKHAR (1953a, 1954c).

The above conditions are the basic boundary conditions, and in order to define the uniqueness of the solution the same number of conditions as of the order of the basic equation are derived in the following manners. For instance, from equations (33) and (37) we can derive the following conditions by substituting (45) and (46) respectively,

* The cases such as non-conductive boundary $\partial\theta/\partial z = 0$ and others are excluded because they are not essential points of the study. See G. K. BATCHELOR (1954), H. JEFFREYS (1926), A. PELLEW and R. V. SOUTHWELL and others.

$$\left(\frac{\partial}{\partial t}-\kappa\nabla^2\right)\theta=0\,, \tag{51}$$

$$\left(\frac{\partial}{\partial t}-\nu\nabla^2\right)\nabla^2 w+E\zeta-\frac{\mu}{4\pi\rho}F\nabla^2\chi=0\,, \tag{52}$$

where both conditions hold on the top and bottom boundary surfaces. In this manner, the necessary number of boundary conditions are easily obtained even for the cases when the high order of partial differential equation is involved in the study.

§ 4. The Exchange Stability and the Overstability

The time dependant function $l(t)$ in the solutions is customary assumed as an exponential function,

$$l(t)=e^{pt}\,, \tag{53}$$

where p could be a real or complex number.

The principle of the exchange stability assumes the reality of p as discussed by JEFFREYS (1926) and the criterion of the instability is defined by the relation,

$$p=0\,. \tag{54}$$

While the principle of overstability (the name "overstability" is used after A. S. EDDINGTON 1926) assumes the complex value of p so that the criterion of instability is defined as

$$p_r=0 \tag{55}$$

where $p=p_r+ip_i$, and p_r and p_i denote the real and imaginary parts respectively.

In other words, the principle of exchange stability assumes simple monotonous growth or decay of perturbations and the criterion indicates a steady onset of perturbed motion. The principle of overstability assumes the oscillatory motion of perturbations and considers the growth or decay of the amplitude of such oscillations. Then, the criterion indicates a steady oscillation of perturbed motion.

The validity of these two principles of the stability have been discussed by several authors. When the solution of the problem is known, the validity of each stability is discussed from the so-called frequency equation of the stability. Examples of such discussions have been given by CHANDRASEKHAR (1952a, 1953b) and the author (Y. NAKAGAWA and P. FRENZEN 1955). Another type of discussion is also presented by CHANDRASEKHAR (1952a) with the reference to PELLEW and SOUTHWELL.

A summarizing discussion on the validity and the dependence of the RAYLEIGH number upon the important non-dimensional numbers is presented below covering the whole aspect of the problem under various circumstances. Before entering this discussion, we will introduce the conventional notation D which was defined as

$$D=\frac{\partial}{\partial\bar{z}}=d\frac{\partial}{\partial z} \quad \text{and} \quad \bar{z}=\frac{z}{d}. \tag{56}$$

Then, we will write the solutions in the following forms:

$$\left.\begin{aligned} w&=f(x,y)W(\bar{z})e^{pt}\,,\\ \theta&=f(x,y)\Theta(\bar{z})e^{pt}\,,\\ \zeta&=f(x,y)Z(\bar{z})e^{pt}\,,\\ \chi&=f(x,y)X(\bar{z})e^{pt}\,,\\ \phi&=f(x,y)Y(\bar{z})e^{pt}\,, \end{aligned}\right\} \tag{57}$$

where $d^2\nabla_1 f(x,y)+a^2 f(x,y)=0$. Further confining the discussion to the case of $\boldsymbol{\Omega}$ and $\boldsymbol{H}$ both in the vertical direction, we have the following expressions for the scalar operators E and F,

$$E=2\frac{\Omega}{d}D \tag{58}$$

and

$$F=\frac{H}{d}D\,. \tag{59}$$

The substitution of w given by (57) into the equation (41) gives the following equation after a little calculation;

$$\begin{aligned} &\left\{\frac{pd^2}{\kappa}-(D^2-a^2)\right\}\left[\left\{\frac{pd^2}{\eta}-(D^2-a^2)\right\}\right.\\ &\quad\left.\times\left\{\frac{pd^2}{\nu}-(D^2-a^2)\right\}-QD^2\right](D^2-a^2)W\\ &\quad+T\left\{\frac{pd^2}{\kappa}-(D^2-a^2)\right\}\left\{\frac{pd^2}{\eta}-(D^2-a^2)\right\}^2D^2W\\ &=-a^2R\left\{\frac{pd^2}{\eta}-(D^2-a^2)\right\}\left[\left\{\frac{pd^2}{\eta}-(D^2-a^2)\right\}\right.\\ &\qquad\left.\times\left\{\frac{pd^2}{\nu}-(D^2-a^2)\right\}-QD^2\right]W\,, \end{aligned} \tag{60}$$

where

$$Q=\frac{\sigma\mu^2H^2}{\rho\nu}d^2 \tag{61}$$

is the magnetic number*,

$$T=\frac{4\Omega^2}{\nu^2}d^4 \tag{62}$$

the TAYLOR number*, and

$$R=\frac{\alpha\beta g}{\kappa\nu}d^4 \tag{63}$$

is the RAYLEIGH number. If we write

$$q=\frac{pd^2}{\nu}, \quad P=\frac{\nu}{\kappa}, \quad \omega=\frac{\nu}{\eta}, \tag{64}$$

then by combining the expressions, we have

$$Pq=\frac{pd^2}{\kappa}, \quad \omega q=\frac{pd^2}{\eta} \tag{65}$$

where P is the PRANDTL number. Snbstituting these notations in the equation (60) and rearranging the equation, we have

$$R=\frac{\{Pq-(D^2-a^2)\}[\{\omega q-(D^2-a^2)\}\{q-(D^2-a^2)\}-QD^2]^2(D^2-a^2)W+T\{Pq-(D^2-a^2)\}\{q-(D^2-a^2)\}D^2W}{a^2\{\omega q-(D^2-a^2)\}[\{\omega q-(D^2-a^2)\}\{q-(D^2-a^2)\}-QD^2]W} \tag{66}$$

In this equation (66), we can see the complicated dependence of the RAYLEIGH number upon the various non-dimensional numbers of the problem. Under the circumstances considered, the RAYLEIGH number is a function of P, q, ω, Q, T and a^2 as well as the actual functional form of W.

Now, dividing the problem into the following cases, we will discuss the details in each of the specified cases:

(i) $Q=0$, $T=0$, (the case of RAYLEIGH, JEFFREYS and PELLEW and SOUTHWELL),

(ii) $Q=0$, $T\neq 0$, (the case of fluid subjected to rotation),

(iii) $Q\neq 0$, $T=0$, (the case of electrically conducting fluids subjected to an external magnetic field),

(iv) $Q\neq 0$, $T\neq 0$ (the case of electrically conducting fluids subjected to the simultaneous action of magnetic field and rotation)

(i) $Q=0$, $T=0$.

Let Q and T be zero in (66) and eliminating the same operators we have

$$R=-\frac{\{Pq-(D^2-a^2)\}\{q-(D^2-a^2)\}(D^2-a^2)W}{a^2W} \tag{67}$$

In (67) if we apply the principle of overstability, we can write

$$q=ir. \tag{68}$$

The substitution of (68) in (67) indicates an imaginary value of R. As such R must be excluded, we can conclude that under such circumstances the principle of overstability must not be feasible for the criterion of stability. Now, putting $q=0$ in (62), we find that R is the function of a^2 and W

$$R=-\frac{(D^2-a^2)^3W}{a^2W}. \tag{69}$$

Therefore, the criterion based on the exchange stability can be uniquely determined by the specification of a^2 and W. Thus the criterion has been obtained as the minimum value of R with the specifications of a^2 and W in theories and which has been confirmed by the experiments (see Introduction).

Hereafter, in the paper the difference of W for different boundary conditions and the reality of W are understood. Also, the definition of the criterion as the minimum value of R with the specifications of a^2 for the exchange stability, and the minimum value of R with the specification of a^2 and r for the overstability are understood.

(ii) $Q=0$, $T\neq 0$.

In the similar way of obtaining (67) from (66), we have

$$R=-\frac{\{Pq-(D^2-a^2)\}\{q-(D^2-a^2)\}(D^2-a^2)W+T\{Pq-(D^2-a^2)\}D^2W}{a^2\{q-(D^2-a^2)\}W} \tag{70}$$

* More general forms of these numbers are $Q=\frac{\sigma\mu^2H^2\cos^2\vartheta}{\rho\nu}d^2$ and $T=\frac{4\Omega^2\cos^2\vartheta}{\nu^2}d^4$ where ϑ denotes the angle of inclination of H or Ω to the vertical (S. CHANDRASEKHAR 1953b, 1954b). Also Q is sometimes called the HARTMANN's number (R. C. LOCK 1955) after the first work of J. HARTMANN (1937).

In equation (70), we can see the RAYLEIGH number now depends on the parameters P, q, a^2 and T. Also the feasibility of the overstability can be seen in (70) as the odd order of q appears both in the denominator and numerator. Now, by putting $q=0$, that is, the criterion based on the principle of the exchange stability, we find that the PRANDTL number disappears from the equation with q. Therefore, we can conclude that the criterion of the exchange stability is free from the PRANDTL number of fluids and the criterion of the overstability to the contrary.

The criterion of the exchange stability has been obtained as a function of T, and the criterion of the overstability has been obtained as a function T and P. Regardless of the difference due to boundary conditions, the general relations of such criteria become

$$R_c \propto T^{3/2} \qquad (\text{when } T\to\infty) \tag{71}$$

for the exchange stability and

$$R_c^* \propto T^{3/2} \qquad (\text{when } TP\to\infty) \tag{72}$$

for the overstability, where the subscript c is used to denote the critical value of the RAYLEIGH number and superscript $*$ is used to denote the criterion based on the overstability. The experimental confirmations of these criteria and the theoretical condition of the validity of the overstability in terms of the PRANDTL number have been obtained (see Introduction).

(iii) $T=0$, $Q\neq 0$.

After eliminating the term including T in equation (66) we have

$$R=-\frac{\{Pq-(D^2-a^2)\}[\{\omega q-(D^2-a^2)\}\{q-(D^2-a^2)\}-QD^2](D^2-a^2)W}{a^2\{\omega q-(D^2-a^2)\}W}. \tag{73}$$

Again by putting $q=0$ in (73), we conclude that criterion of the exchange stability is free from the PRANDTL number and ω of fluids, while the criterion of overstability is depending upon such numbers. Though the feasibility of overstability can easily be seen in the equation (73), the overstability only becomes valid under astrophysical conditions as shown by CHANDRASEKHAR (1952a). With the assigned external conditions such as P, Q and ω, the general characteristics of the criteria become

$$R_c \propto Q \qquad (\text{when } Q\to\infty) \tag{74}$$

for both principles of stabilities (see the section 7 for the experimental confirmation).

(iv) $Q\neq 0$, $T\neq 0$.

Then the expression (66) remains for the discussion. Putting $q=0$, we have

$$R=-\frac{\{(D^2-a^2)^2-QD^2\}(D^2-a^2)W+T(D^2-a^2)^2W}{a^2\{(D^2-a^2)^2-QD^2\}W}. \tag{75}$$

From (75), we can conclude that the criterion of the exchange stability is still free from the PRANDTL number and ω of fluids. However, the complicated characteristics of the dependence of R on Q and T in (75) have been revealed by CHANDRASEKHAR (1954c). The overstability is feasible as we can see from (66) and the criterion of overstability should include all the parameters. Regardless of the details of both criteria, the general characteristics of R and Q become

$$R_c \propto Q \qquad (\text{when } Q\to\infty) \tag{76}$$

for assigned values of T or T, P and ω.*

§ 5. The Method of Variation

The method of variation has been introduced to this problem by PELLEW and SOUTHWELL and has been developed into more refined manners by CHANDRASEKHAR as mentioned in the Introduction. Except for the case of the boundary conditions of both free planes, this method reduces a great amount of the practical calculation of the criterion of the instability. Fortunately for the case when the boundary surfaces are both free planes, the form

$$W=\cos \pi\bar{z} \tag{77}$$

(where $\bar{z}$ is measured from the center of the layer) becomes the exact solution of W under all circumstances, and we can easily evaluate the criterion by the substitution of (77) in the

* The experimental study is now under preparation by the author.

equations given in the previous section. Also, as the general characteristics of the functional relations between the RAYLEIGH number and the non-dimensional numbers in the criterion mostly remain for all boundary conditions, the solution (77) is an important tool for the investigation (see the discussions, S. CHANDRASEKHAR 1952b, 1953b, 1954c, Y. NAKAGAWA and P. FRENZEN 1955).

The practical criterion of this problem is the minimum value of the RAYLEIGH number. Therefore, if we can evaluate such minimum value of the RAYLEIGH number with the necessary specifications of a^2 or a^2 and r, under certain assigned external conditions such as Q, P, T and ω, we need not have to solve the complicated equations of this problem. In short, the principle of the method of variation is based on such an idea and enables us to determine the criterion without obtaining the exact solutions of the problem.

The detail of this method is illustrated below in relation to the following experiments for the case of $Q \neq 0$ and $T \neq 0$. Under these circumstances, as the overstability is only valid for astronomical conditions we will discuss the criterion of the exchange stability. From (73) by putting $q=0$, we have

$$R=-\frac{\{(D^2-a^2)^2-QD^2\}(D^2-a^2)W}{a^2W}. \tag{78}$$

Rewriting (78) we have the governing equation of W in the following form:

$$(D^2-a^2)G+a^2RW=0\,, \tag{79}$$

where

$$G=\{(D^2-a^2)^2-QD^2\}W\,. \tag{80}$$

The appropriate boundary conditions become

$$W=G=0 \quad \text{on the boundary surfaces} \tag{81}$$

and

$$\left.\begin{aligned} DW&=0 \quad \text{on a rigid surface}\\ D^2W&=0 \quad \text{on a free surface}\,, \end{aligned}\right\} \tag{82}$$

where the second relation of (81) was derived from (52) with the usage of (39), and this derivation can be easily justified.

After multiplying by G and integrating (78) over the whole depth of the layer, we have

$$R=-\frac{\int_{-1/2}^{+1/2}G(D^2-a^2)G\,d\bar{z}}{a^2\int_{-1/2}^{+1/2}GW\,d\bar{z}}\,, \tag{83}$$

where the origin of $\bar{z}$ is taken at the center of the layer. The integral in the numerator and the denominator are easily transformed into the following forms after using partial integrations and the boundary conditions:

the numerator,

$$\int_{-1/2}^{+1/2}G(D^2-a^2)G\,d\bar{z}=-\int_{-1/2}^{+1/2}\{(DG)^2+a^2G\}d\bar{z}\,, \tag{84}$$

the denominator,

$$\int_{-1/2}^{+1/2}GW\,d\bar{z}=\int_{-1/2}^{+1/2}[\{(D^2-a^2)W\}^2+Q(DW)^2]d\bar{z}\,. \tag{85}$$

With these relations (84) and (85), the equation (83) becomes

$$R=\frac{\int_{-1/2}^{+1/2}\{(DG)^2+a^2G)\}d\bar{z}}{a^2\int_{-1/2}^{+1/2}[\{(D^2-a^2)W\}^2+Q(DW)^2]d\bar{z}}\,, \tag{86}$$

which denotes the positive reality of R. Now, consider an arbitrary variation δW in the relation (86), then the effect of such variation on R to the first order of δW can be expressed as

$$\delta R=\frac{1}{a^2I_2}(\delta I_1-a^2R\delta I_2)\,, \tag{87}$$

where

$$I_2=\int_{-1/2}^{+1/2}[\{(D^2-a^2)W\}^2+Q(DW)^2]d\bar{z}\,, \tag{88}$$

$$\delta I_1=2\int_{-1/2}^{+1/2}\{(DG)(D\delta G)+a^2G\delta G\}d\bar{z}\,, \tag{89}$$

$$\delta I_2=2\int_{-1/2}^{+1/2}[\{(D^2-a^2)W\}\{(D^2-a^2)\delta W\}+Q(DW)(D\delta W)d\bar{z}\,, \tag{90}$$

and δG stands for

$$\{(D^2-a^2)^2-QD^2\}\delta W\,. \tag{91}$$

The expressions for δI_1 and δI_2 can be rewritten by partial integration and boundary conditions

$$\left.\begin{aligned} &\delta W=\delta F=0 \qquad \text{at} \quad \bar{z}=\pm\frac{1}{2}\,, \\ &D^2\delta W=0 \qquad \text{on a free surface,} \\ &D\delta W=0 \qquad \text{on a rigid surface.} \end{aligned}\right\} \tag{92}$$

After some calculations, the equation (87) becomes

$$\delta R=-\frac{2}{a^2 I_2}\int_{-1/2}^{+1/2}\delta G\{(D^2-a^2)G+a^2RW\}d\bar{z}\,. \tag{93}$$

In the equation (93) it is easily seen that the condition $\delta R=0$ is only satisfied for arbitrary variations in W provided

$$(D^2-a^2)G+a^2RW=0\,,$$

that is, if W satisfies the original governing equation (79). Therefore, it follows that the exact solution of W would satisfy $\delta R=0$ and if we evaluate R according to (86) with such a solution, we will obtain the critical value of the RAYLEIGH number as the minimum value of R. In practical procedures, the above principle leads us to the followings: assume a function G including one or two parameter and satisfy the boundary condition (81). Then, we can determine a function for W as the solution of the equation (80) satisfying the boundary conditions (81) and (82). Substituting such G and W in (86) and minimizing the value of R with respect to the parameters and a^2 (or a^2 and r if involved), we will have a good approximate critical value of the RAYLEIGH number. As W of a combination of even functions of $\bar{z}$ satisfies both rigid conditions, we can choose the function G in such a form. Also a combination of odd functions of W of (77) satisfies the one rigid and one free conditions, provided the depth of layer, d, be replaced by $d/2$, the function G can be chosen in such a form under these boundary conditions*.

For the present problem the critical values of the RAYLEIGH number have been obtained by CHANDRASEKHAR (1952a) after carrying out the calculation following the above method of variation (see the resultant relation (74)). Under other circumstances, as referred previously, CHANDRASEKHAR has obtained the critical values of the RAYLEIGH number with appropriate choices of the function G convenient to the problems (S. CHANDRASEKHAR 1952a, 1953b, 1954b, S. CHANDRASEKHAR and D. D. ELBERT 1955). The values of R_c thus determined by the successive approximations of adjustments of the parameters in the function like G, and a^2 and sometimes a^2 and r have provided sufficient accurate values because the experimental results mostly have been obtained in the neighbourhood of such values (see Y. NAKAGAWA and P. FRENZEN 1955, D. FULTZ and Y. NAKAGAWA 1955 and the experimental results in this paper).

§ 6. The Method of Experiment

The difference of the amount of heat transfer through the layer between conduction and convection has been used as the base of the experimental determination of the critical values of the RAYLEIGH number. When values of the temperature gradient are plotted against the amount of heat transfer or the amount of heat applied at the bottom of the layer, the onset of convection is easily detected as a change of the relations between these quantities in a diagram.

Such a diagram was firstly made by SCHMIDT and MILVERTON (1935), and they found a sharp break in the relation between the temperature gradient and the amount of heat applied at the bottom of the layer. By defining the critical value of the adverse temperature gradient at the point of break, they obtained the critical value of the RAYLEIGH number in close agreement with the theoretical value. Later, experiments by SCHMIDT and SANDERS (1938) confirmed the onset of the theoretically specified cellular convection at that point of break by optical observations.

Though in most of these experiments, the temperature gradient was evaluated from the temperature measured at the top and the bottom of the bounding surfaces of the layer, the author has developed a method of direct measurement of the adverse temperature gradient. The latter method, especially measuring the

* Studies of the form of solutions of W under various boundary conditions have been made by H. JEFFREYS (1926), A. R. LOW, A. PELLEW and R. V. SOUTHWELL.

adverse temperature gradient inside of the layer has provided various important informations. For example, the existence and the period of oscillation of the overstable convection have been confirmed by this method of measurement (D. Fultz and Y. Nakagawa 1955). In the following sections, the details of such method of experiment are discussed with the results of experiments for the case of a layer of mercury subject to an external magnetic field.

§ 7. The Experiments and Results

The experiments are designed to investigate the functional relation between the critical value of the Rayleigh number and the magnetic number Q, theoretically predicted by Chandrasekhar (1952a). Excluding the overstability under the present experimental conditions the relation of (74) becomes

$$R_c \propto Q\,. \qquad (Q>1{,}000) \qquad (74')$$

The general assembly and the schematic arrangements of the experimental apparatus are illustrated in the Fig. 1 and 2. As a permanent magnet* was used and it only provided a fixed intensity of the field, different depths of layer are used in the experiments. The pole surfaces of the permanent magnet

Fig. 1. The front view of experimental set up.

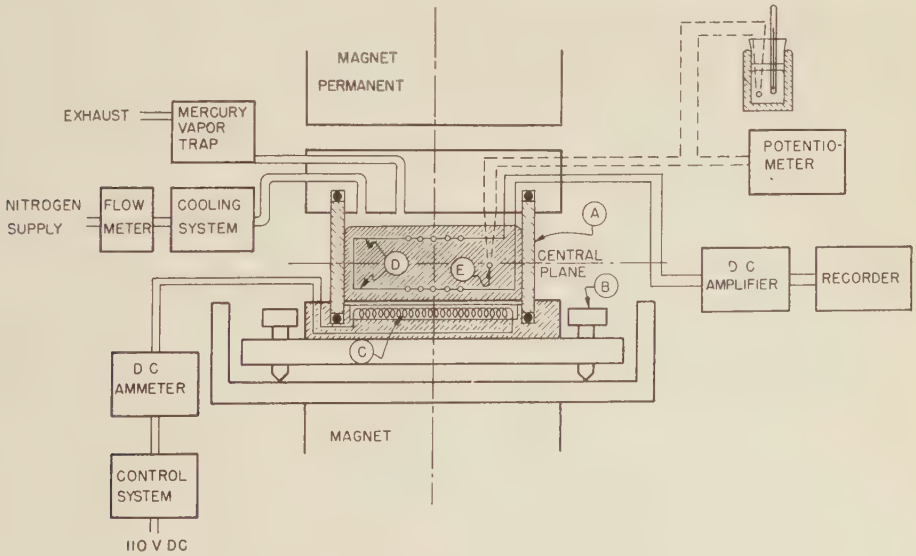

Fig. 2. The schematic diagram of the experimental arrangements.

* The magnet was originally constructed as the deflection magnet for cosmic ray experiment and was very kindly made available for this experiment by Prof. Marcel Schein of the Dept. of Physics, University of Chicago.

were 17.8 cm × 21 cm rectangulars and the gap between the pole surfaces was 21.6 cm. The intensity of the vertical magnetic field varied from the minimum of 1,375 gauss at the center of the gap to maxima of 2,250 gauss at both pole surfaces. Around the center of the gap the surfaces of the same intensity of the field formed coaxial hyperboric surfaces.

A Pyrex-glass cylinder (A) of inside diameter 14 cm and height 8 cm was used for the container of mercury. The leveling screws (B) served to adjust the position of the cylinder in each experimental determination of depth. At the bottom of the cylinder a non-inductively wound resistance heater (C) was placed beneath a plastic coated copper plate. A five-couple copper-constantan thermopile (D) immersed in the mercury was used for the direct measurement of the internal adverse temperature gradient. The junctions of this thermopile were fixed at the levels about 1/2 cm from the top and the bottom surfaces of the layer respectively. Also at each of the levels the junctions were spaced approximately 1 cm apart along a diameter of the cylinder. Thus, the thermal e.m.f. of this thermopile eliminated the effect of the boundary layer of fluid and the variation of the temperature due to the relative positions of junctions and cells.

A single thermocouple was used to obtain the estimate of the temperature of mercury. The measuring junction (E) of this thermocouple was placed at half way of the layer and the reference junction was placed in a constant temperature bath. To remove heat at the top surface, a cooled nitrogen circulation system was used, which also served to keep a constant average temperature of mercury. This system further worked to provide a better experimental approximation to the theory on the establishment of the linear temperature gradient through the layer.

With these arrangements, experiments were performed with four different depths, namely, 3, 4, 5, and 6 cm layers of mercury. At each determination, the positions of the cylinder were adjusted and the levels of the central plane of the layers were kept to coincide with the central plane of the gap of the magnet. Though this procedure reduced the variation of the intensity of the magnetic field to the minimum state, about 10% residual variation of the field was observed around the cylinder. Various rates of heating were applied at the bottom of the layer by the heater (C) with D. C. The current was adjusted by a combination of sliding resistance and measured by a D. C. ammeter. Then the rate of heating was determined by the square of the heating current to a sufficient accuracy. At each fixed rate of heating, a continuous record of the adverse temperature gradient was obtained by a system of d.c. amplifier and milliammeter recorder connected to the thermopile (D). The accuracy of this system was secured to the order of $\pm 1\,\mu$V, and the system reproduced the record within the difference of the thickness of the line for independent trials of same rates of heating. The rates of circulation of cooled nitrogen were also adjusted in each experiment considering the rates of heating applied at the bottom of the layer. Thus, a number of records of the adverse temperature gradient was obtained for each of the four depths of the layer. These records were classified into typical three different types illustrated in Fig. 3.

The records of type (a) were classified as the records of conductive heat transfer because the trend of the adverse temperature gradient were easily interpreted as the gradual establishment of a stationary thermal equilibrium in the layer. This classification was supported from other standpoints. Thus, records of type (a) were only obtained in the lower rates of heating and no convective motion was observed when such records were obtained. The plotting of the final value of adverse temperature gradient (β_f) against the corresponding rates of heating (I_h^2) in a diagram gives the linear relation *dd* shown in the Fig. 4. Considering the general relation of conductive heat transfer;

$$K = k\beta \,, \tag{94}$$

where K denotes the amount of heat transfer, and β and k are the temperature gradient and the thermal conductivity respectively, we can deduce the relations,

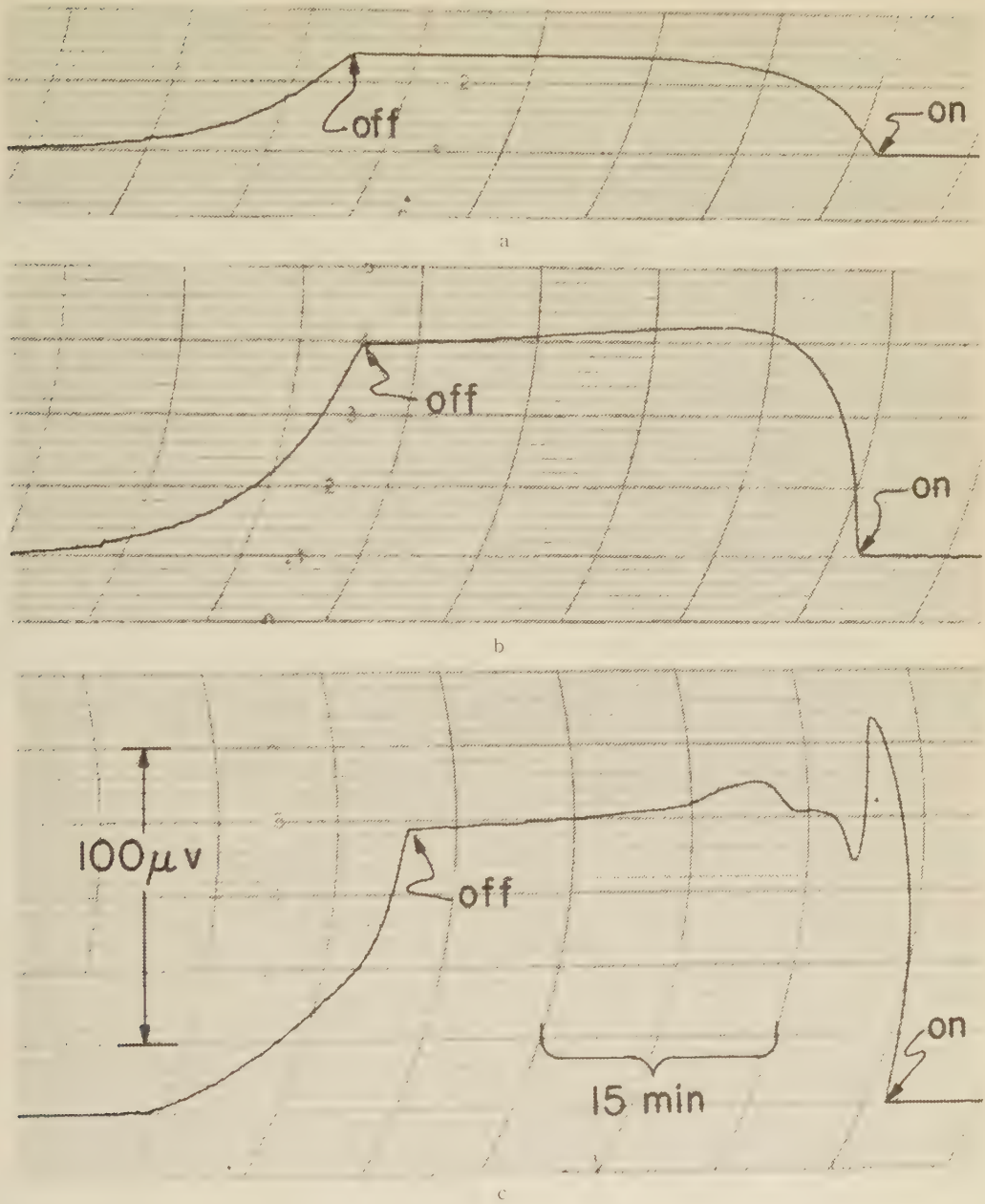

Fig. 3. The records of the adverse temperature gradient obtained in the experiments of $d=6$ cm. The letters "on" and "off" indicate the duration of the heating applied at the bottom. The heating currents were 0.500 amp. for a, 0.800 amp. for b and 1.323 amp. for c, respectively.

$$I_h^2 \propto K \tag{95}$$

and

$$I_h^2 = k' \beta_J \,, \tag{96}$$

where k' is a certain constant.

The records of type (b) and (c) which reached certain maximum values and decreased for the continuous heating indicated the transport of warm fluid to the upper part of the layer and they were classified as the records of convective heat transfer. The plotting of the

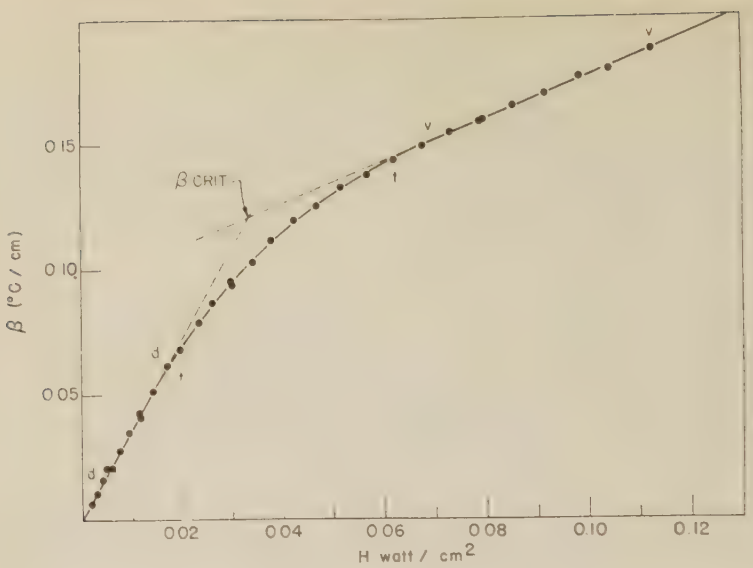

Fig. 4. The relation between the adverse temperature gradient and the rate of heating applied at the bottom. The data are taken from the results of experiments of $d=6$ cm.

maxima (β_p) of the temperature of the records (b) and (c) against the corresponding rates of heating in the similar way as in (a) give the segments like *tt* and *vv* in Fig. 4 respectively. The main difference between the records (b) and (c) was that records of type (c) showed a damped oscillatory trend while type (b) had no such oscillation. This difference of records suggested the difference in the mode of the convective motion, which also are seen in the relations between β_p and I_h^2 in the diagram as the segment *vv* is almost linear while *tt* is a smooth curve.

Considering the method of measurement of the adverse temperature gradient, the difference were interpreted as follows. If the convection started simultaneously over the whole horizontal dimension of the layers, the peak value of the adverse temperature gradient should be recorded as soon as the warm fluid reaches the level of lower set of junctions. Then, a sharp decrease of the adverse temperature gradient should be recorded when this warm fluid reaches the upper set of junctions. Consequently, under such circumstances records of a sharp peak like (c) should be obtained with the onset of convection. While if the convection start at a certain part of the fluid it should be subsided by the surrounding cooler fluid and the resultant slow motion of the convection would produce a round-out peak like the record type (b).

Literally understanding the condition of the criterion (54) and considering the small dimension of the container and the non-uniformity of the magnetic field, the data of the adverse temperature gradient obtained from records type (b) were omitted for the determination of the critical temperature gradient. Thus, the critical adverse temperature gradients which entered the RAYLEIGH numbers are determined by the intersection of the extended linear trends of the segment like *dd* and *vv*, after applying linear least squares approximations for each of the segments respectively.

Another approval of the above procedure could be obtained from the results of theoretical study of this problem under tilted external magnetic field (S. CHANDRASEKHAR 1954b), because under such circumstances smaller critical values of the RAYLEIGH number have been obtained with the cells in the form of roll. Therefore, it is plausible that the segment *tt* is caused by the nonvertical characteristics of the magnetic field.

The final results of the experiments are

Table 1.

Depth cm	Conductive (dd) $\beta_f = k_1 I_h^2 + c_1$			Convective (vv) $\beta_p = k_2 I_h^2 + c_2$			Q $\times 10^4$	R $\times 10^5$
	k_1	c_1	σ_1	k_2	c_2	σ_2		
3	2.878	0.004	0.002	11.945	0.353	0.006	1.22	1.35
4	2.791	0.001	0.001	11.249	0.202	0.003	2.18	2.50
5	2.590	0.000	0.001	8.698	0.120	0.001	3.40	3.81
6	2.784	0.000	0.001	12.047	0.093	0.001	4.90	5.65

σ_l denote the standard deviations from the assumed linear relations. The units are k_l (watt/cm per °C/cm), c_l and σ_l (°C/cm).

summarized in Table 1 in terms of the critical RAYLEIGH number and magnetic number Q with the coefficients of linear relations obtained in the least square fittings. The small standard deviation from the linear relations should be easily noticed in the table, which suggests the reality of linear relation especially in the regime vv as discussed in the next section. The average intensity of the magnetic field is assumed as 1,400 gauss for all cases, considering the results of the mapping of the strength of the field.

The boundary conditions for our experiments were those for the two rigid surfaces, because of the formation of a contaminated film at the top surface preventing any motion at such surface. The results of experiments quantitatively confirmed the theoretical prediction as in Fig. 5. The curves in Fig. 5 are drawn from the theoretical results obtained by CHANDRASEKHAR (1952a) and the solid circles indicate the results of experiments.

§ 8. Heat Transfer by Cellular Convection

The theoretically noticed stationary characteristics in the relation between the critical

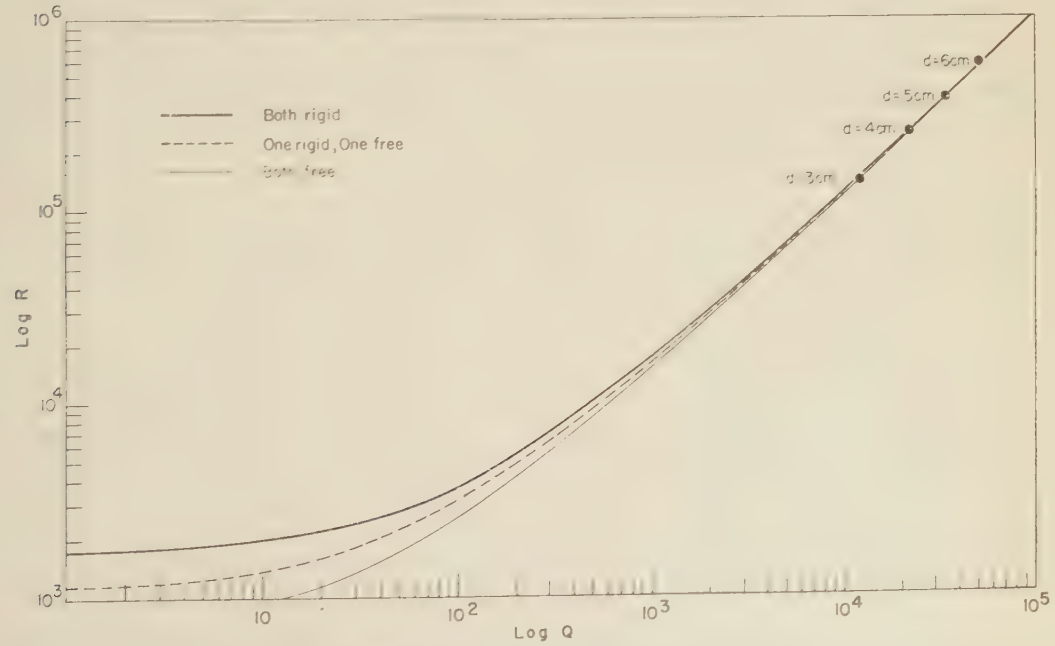

Fig. 5. The dependence of the critical value of the Rayleigh number on the magnetic number Q. The depths of the layer of mercury are indicated.

value of the RAYLEIGH number and a^2 (A. PELLEW and R. V. SOUTHWELL 1940) have been observed in several experiments (R. J. SCHMIDT and O. A. SANDERS 1938, Y. NAKAGAWA and P. FRENZEN 1955 and others). By visible observations, the author has confirmed that the cells appeared at first remain over a certain range of rates of heating beyond the point of intersection, such as β_{CRIT} in Fig. 4. For the range of rates of heating corresponding to the segment vv in Fig. 4 we can safely assume that the convective heat transfer is mainly performed by the similar size cellular convection which appeared first when the critical condition is exceeded.

Then the difference of the peak values of temperature gradient (β_p) of the records (c) are able to be interpreted as the difference in magnitudes of the vertical velocity (w) and the temperature fluctuation (θ) of the convection. Relating the energy of the convection to the external energy supply, we could assume

$$\frac{1}{2}\overline{\rho w^2} \propto I_h^2 , \tag{97}$$

where bar is used to denote the average over the cells. The amount of heat transfer (K) by convection can be expressed as

$$K \propto \int_{-1/2}^{+1/2} \overline{C_p \rho w \theta} d\bar{z} \propto \int_{-1/2}^{+1/2} \overline{C_p \rho w^2} d\bar{z} , \tag{98}$$

where the last relation is obtained from the proportional characteristics between w and θ as shown in the equations of the theoretical studies. Consequently, we can combine (97) and (98) as

$$K \propto I_h^2 . \tag{99}$$

While from the results of experiments we can assume the relation

$$I_h^2 = k'' \beta_p \tag{100}$$

along the segment vv, then using the relation (99) and (100), we can write

$$\beta_p \propto \overline{\theta w} \propto \overline{w^2} . \tag{101}$$

Now, if we assume that the initial well defined oscillation in the record (c) is due to the vertical motion of the warm fluid, we could relate the period (τ) of the oscillation to the vertical velocity in the following manner:

$$\tau = \frac{d}{\sqrt{\overline{w^2}}} , \tag{102}$$

where d is the depth of layer. Then combining (102) and (101) or (102) and (100), we have

$$\tau \sqrt{\overline{\beta_p}} = \text{const.} \quad \text{or} \quad \tau I_h = \text{const.} \tag{103}$$

The relation (103) is satisfied by experiments as illustrated in Fig. 6, where the data was taken from the results of similar experiments (technical reports of the author). In other words, the experimental proof of (103) supports the relation (100) and (101). Then, from (99) we can write

$$K = k''' \beta_p . \tag{104}$$

The relation (104) is the relation which has been especially used in the determination of the critical value of the RAYLEIGH number by some of the experimental investigators.

§ 9. Summary and Remarks

The development of the studies on the instability of the layer of fluid heated from below under various circumstances has provid-

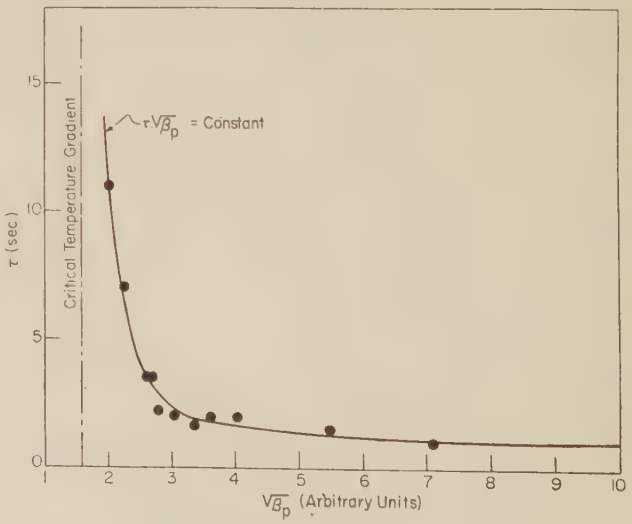

Fig. 6. The empirical relation of τ and $\sqrt{\overline{\beta_p}}$. The data are taken from the results of experiments of rotating layer of water (d=3 cm, Ω=10 rev/min).

ed valuable informations in relation to its applications to the problems of astrophysics and geophysics.

The applications to the meteorological phenomena, especially to the form of clouds have been studied by D. Brunt (1937, 1951) and others. The earlier difficulties on the direction of the convective circulation in meteorological applications, that is, the downwards motion at the center of cell in the air, have been removed by the study of Y. Nakagawa and P. Frenzen (1955). Also, further application of the results of such studies to meteorological problems including the overstable convection has been proposed by the study of the above investigators. An example of the oceanographic application is the formation of stripes on the sea surface which has been observed and explained by A. H. Woodcock and J. Wyman (1947) as the results of cellular convections over the sea.

The experimental studies in cases of the electrically conducting fluids are especially significant because they have provided the justification on the study of the problems of magneto-hydrodynamics, and the only means of study on such subjects have been limited in theory. The applications, such as discussions on the problems of sunspot, magnetic stars and geomagnetism have been presented by S. Chandrasekhar (1953d) and W. M. Elsasser (1955, 1956).

The assumption of the linear temperature gradient in theories before the onset of convection has been justified by experimental investigations as that assumption was found to be satisfactory through the layer of fluids except in the very narrow region of the boundary of the layer (technical report of the author).

A discussion on the possible shapes of the cell was presented by H. Stommel (1947) with the assumption of tessellation of plane by identical poligons. He showed that the shapes of equilateral-triangle, square and hexagon were the shapes which satisfied such assumption. In most of the experiments, the predominance of the identical hexagon has been reported. The particular dimensional proportion of the cell in terms of a^2 has been experimentally confirmed in various circumstances (see the results of R. J. Schmidt and O. A. Sanders 1938, Y. Nakagawa and P. Frenzen 1955).

The effect of the motion of the fluid was studied theoretically by H. Jeffreys (1928) who showed that except the possible deformation of cell in the direction of flow, the criterion would be the same. The effect of a shearing flow in a certain direction or the presence of horizontal temperature gradient has been studied by some authors, and in some experiments cells were deformed to roller patterns in the

Table 2.

	Exchange Stability	Overstability
$Q=0$ $T=0$	R_c is a fixed value. Experiments confirmed.	
$Q=0$ $T\neq 0$	$R_c \propto T^{2/3}$ (when $T\to\infty$) Experiments confirmed.	$R_c^* \propto T^{2/3}$ (when $TP\to\infty$) Experiments confirmed. The validity depended upon P and T.
$Q\neq 0$ $T=0$	$R_c \propto Q$ (when $Q\to\infty$) Experiments confirmed.	$R_c^* \propto Q$ (when $Q\to\infty$) Only feassible for astrophysical conditions, $\gamma < K$.
$Q\neq 0$ $T\neq 0$	$R_c \propto Q$ (when $Q\to\infty$ for fixed T) No experiment. Two different modes become possible depending upon T and Q.	$R_c^* \propto Q$ (when $Q\to\infty$ for fixed T) No experiment. The validity complicatedly depended upon T, P, Q, and w.

Throughout the table the difference due to the boundary conditions are understood. R_c and R_c^* are used to denote the critical values of the Rayleigh number based on the exchange stability and overstability respectively, and other notations denote similar meanings defined in the theoretical studies.

direction of flow (K. CHANDRA 1938) or the direction of temperature gradient (Y. NAKAGAWA and P. FRENZEN 1955). However, with the plausible explanation like the discussion on *tt* in section 7, we can easily interpret the essential feature of the problem.

Finally, the present state of the studies and the results of studies are summarized in Table 2.

Acknowledgement

The author expresses his sincere thanks to Prof. S. SYŌNŌ and Dr. H. TAKEUCHI of Tokyo University for their encouragement and support throughout the preparation of this paper. Also the author owes many thanks to Prof. S. CHANDRASEKHAR, Prof. S. K. ALLISON, Prof. D. FULTZ and Mr. P. FRENZEN of the University of Chicago.

References

BATCHELOR, G. K.:
1950 "On the spontaneous magnetic field in a conducting liquid in turbulent motion", Proc. Roy. Soc. A, **201**, 405.
1954 "Heat transfer by free convection across a closed cavity between vertical boundaries at different temperatures", Quar. Appl. Math. **12**, 209.

BÈNARD, H.:
1900 "Les tourbillons cellularies", Rev. Gen. Sci. Pur. Appl., **12**, 1261, 1309.

BRUNT, D.:
1937 "Natural and artificial clouds", Quar. J. Roy. Met. Soc. **63**, 277.
1951 "Experimental cloud formation", Compendium of meteorology, 1255.

BULLARD, E. C.:
1955 "A discussion in magneto-hydrodynamics", Proc. Roy. Soc. A, **233**, 289.

CHANDRA, K.:
1938 "Instability of fluids heated from below", Proc. Roy. Soc. A, **164**, 231.

CHANDRASEKHAR, S.:
1952a "On the inhibition of convection by a magnetic field", Phil. Mag. (7), **43**, 501.
1952b "The thermal instability of a fluid sphere heated within", Phil. Mag. (7), **43**, 1317.
1953a "The stability of viscous flow between rotating cylinders in the presence of a magnetic field", Proc. Roy. Soc. A, **216**, 293.
1953b "The instability of a layer of fluid heated below and subject to Coriolis forces", Proc. Roy. Soc. A, **217**, 306.
1953c "The onset of convection by thermal instability in spherical shells", Phil. Mag. (7), **44**, 233, 1129.
1953d "Problems of stability in hydrodynamics and hydromagnetics", Mon. Not. Roy. Astron. Soc. **113**, 667.
1954a "The stability of viscous flow between rotating cylinders in the presence of a radial temperature gradient", J. Rat. Mech. Anal. **3**, 181.
1954b "On the inhibition of convection by a magnetic field II", Phil. Mag. (7), **45**, 1177.
1954c "The instability of a layer of fluid heated below and subjected to simultaneous action of a magnetic field and rotation", Proc. Roy. Soc. A, **225**, 173.
1954d "On characteristic value problems in high order differential equations which arise in studies of hydrodynamic and hydromagnetic stability", Amer. Math. Month. **61**, 32.

CHANDRASEKHAR, S. and ELBERT, D. D.:
1955 "The instability of a layer of fluid heated below and subjected to Coriolis forces II", Proc. Roy. Soc. **231**, 198.

CHAPMAN, S. and COWLING, T. G.:
1939 "Kinetic theory of non-uniform gases", Cambridge Univ. Press. chap. 13.

CHRISTOPHESON, D. G.:
1940 "Note on the vibration of membranes", Quar. J. Math. **11**, 63.

EDDINGTON, A. S.:
1926 "Internal constitution of the stars", Cambridge Univ. Press. p. 201.

ELSASSER, W. M.:
1955 "Hydromagnetism I. A review", Amer. J. Phys. **23**, 590.
1956 "Hydromagnetism II. A review", Amer. J. Phys. **24**, 85.

FULTZ, D., NAKAGAWA, Y. and FRENZEN, P.:
1954 "An instance in thermal convection of Eddington's overstability", Phys. Rev. **94**, 1471.

FULTZ, D. and NAKAGAWA, Y.:
1955 "Experiments on over-stable thermal convection in mercury", Proc. Roy. Soc. **231**, 211.

GOLDSTEIN, S.:
1943 "Modern developments in fluid dynamics", Oxford Univ. Press. p. 606.

HARTMANN, J.:
1937 "Theory of the laminar flow of an electri-

cally conductive liquid in a homogeneous magnetic field. Hg-Dynamics I", Math. fys. Medd. **15**, No. 6.

JEFFREYS, H.:

1926 "The stability of a layer of fluid heated below", Phil. Mag. (7), **2**, 833.

1928 "Some cases of instability in fluid motion", Proc. Roy. Soc. A, **118**, 195.

1930 "The instability of a compressible fluid heated below", Proc. Camb. Phil. Soc. **26**, 170.

JIRLOW, K.:

1956 "Experimental investigation of inhibition of convection by a magnetic field", Tellus, **8**, 252.

LOCK, R. C.:

1955 "The stability of the flow of an electrically conducting fluid between parallel planes under a transverse magnetic field", Proc. Roy. Soc. A, **233**, 105.

LOW, A. R.:

1929 "On the criterion for stability of viscous fluid heated from below", Proc. Roy. Soc. A, **125**, 180.

LUNDQUIST, S.:

1952 "Studies in magneto-hydrodynamics", Ark. Fys. **5**, 297.

NAKAGAWA, Y.:

1955 "An experiment on the inhibition of thermal convection by a magnetic field", Nature, **175**, 417.

1956 "Kinetic theory of gases for the rotating system", J. Phys. Earth. **4**, 85.

NAKAGAWA, Y. and FRENZEN, P.:

1955 "A theoretical and experimental study of cellular convection in rotating fluids", Tellus, **7**, 1.

PELLEW, A. and SOUTHWELL, R. V.:

1940 "On maintained convective motion in a fluid heated from below", Proc. Roy. Soc. A, **176**, 312.

RAYLEIGH, LORD:

1916 "On convection current in a horizontal layer of fluid when the high temperature is on the under side", Phil. Mag. (6), **32**, 529.

SCHMIDT, R. J. and MILVERTON, S. W.:

1935 "On the instability of a fluid when heated from below", Proc. Roy. Soc. A, **152**, 586.

SCHMIDT, R. J. and SANDERS, O. A.:

1938 "On the motion of a fluid heated from below", Proc. Roy. Soc. A, **165**, 216.

STOMMEL, H.:

1947 "A summary of the theory of convection cells", Ann. N. Y. Acad. Sci., **48**, 715.

SUTTON, O. G.:

1950 "On the stability of a fluid heated below", Proc. Roy. Soc. A, **204**, 297.

TAYLOR, G. I.:

1923 "Stability of a viscous flow contained between two rotating cylinders", Phil. Trans. Roy. Soc. A, **223**, 289.

THOMPSON, W. B.:

1951 "Thermal convection in a magnetic field", Phil. Mag. (7), **42**, 1417.

WOODCOCK, A. and WYMAN, J.:

1947 "Convective motion in air over the sea", Ann. N. Y. Acad. Sci., **48**, 749.

The Kinetic Theory of Gases for the Rotating System.

By
Yoshinari NAKAGAWA
The Enrico Fermi Institute for Nuclear Studies,
The University of Chicago.

Summary

The kinetic theory of gases for the rotating system is investigated with an appropriate BOLTZMANN's equation for such a system. Thus, the COLIORIS' acceleration is included in BOLTZMANN's equation. The problems of diffusion, hydrodynamics and thermal conduction are studied with the derivations of the coefficients of diffusion, viscosity, and thermal conduction from the microscopic view point.

Introduction

The macroscopic properties of gases and the governing equations of such properties have been interpreted from the microscopic view point. By virtue of the kinetic theory of gases (for examples Sir J. JEANS 1940) and liquids (M. BORN and H. S. GREEN 1949), these macroscopic properties are shown as the "averaged" properties of molecules, also the equations are explained as the "averaged" movements of such properties.

In many fields of astrophysics and geophysics, the rotating coordinate system has become essential for the frame of reference for the study of the motion of such "averaged" molecular properties. Some investigators of the kinetic theory of gases have paid attention to the problems of the rotating gases (see S. CHAPMAN and T. G. COWLING 1939). Their treatments, however, were only referred to the fixed system and their interests were confined to the additional external force potential due to the centrifugal acceleration which came into the velocity distribution function for the equilibrium state.

In this paper, the detailed study of the kinetic theory of gases for the rotating system is undertaken and the appropriate representations of the "averaged" properties and the governing equations of such properties are investigated for such a system.

§ 1. The BOLTZMANN's Equation for the Rotating System

The BOLTZMANN's equation for the rotating system can be derived in the following manner. Consider the number of molecules whose velocity is within the range $\boldsymbol{c}$, $\boldsymbol{c}+d\boldsymbol{c}$ and the position is within the range $\boldsymbol{r}$, $\boldsymbol{r}+d\boldsymbol{r}$ at time t in the velocity-position space and let the number be

$$f(\boldsymbol{c},\ \boldsymbol{r},\ t)d\boldsymbol{c}\,d\boldsymbol{r}\,.$$

After time dt, this number of molecules would form the set

$$f(\boldsymbol{c}+\dot{\boldsymbol{c}}\,dt,\ \boldsymbol{r}+\dot{\boldsymbol{r}}\,dt,\ t+dt)d\boldsymbol{c}\,d\boldsymbol{r}$$

due to the motion of molecules, where the volume occupied by the set would remain the same as $d\boldsymbol{c}\,d\boldsymbol{r}$ by the LIOUVILLE's theorem. However, during dt, some molecules would be deflected out of this set by collision with other molecules, while some other molecules would enter this set as results of collisions. This change should be proportional to $d\boldsymbol{c}\,d\boldsymbol{r}\,dt$. Hence if we denote influences of collision by $\frac{\partial_e f}{\partial t}d\boldsymbol{c}\,d\boldsymbol{r}\,dt$, then, as the result of the net balance of the number of the molecules in the specified set during the time dt, we have the following relation

$$\begin{aligned}\frac{\partial_e f}{\partial t}d\boldsymbol{c}\,d\boldsymbol{r}\,dt &= \{f(\boldsymbol{c}+\dot{\boldsymbol{c}}dt,\ \boldsymbol{r}+\dot{\boldsymbol{r}}dt,\ t+dt)\\ &\quad -f(\boldsymbol{c},\ \boldsymbol{r},\ t)\}d\boldsymbol{c}\,d\boldsymbol{r}\,dt\\ &= \left\{\frac{\partial f}{\partial t}+\dot{\boldsymbol{c}}\cdot\frac{\partial f}{\partial \boldsymbol{r}}+\dot{\boldsymbol{r}}\cdot\frac{\partial f}{\partial \boldsymbol{r}}\right\}d\boldsymbol{c}\,d\boldsymbol{r}\,dt\end{aligned}$$

$$\therefore \quad \frac{\partial_e f}{\partial t}=\frac{\partial f}{\partial t}+\dot{\boldsymbol{c}}\cdot\frac{\partial f}{\partial \boldsymbol{r}}+\dot{\boldsymbol{r}}\cdot\frac{\partial f}{\partial \boldsymbol{r}}, \qquad (1.1)^*$$

where the following relations are used to obtain the final equation,

$$\dot{\boldsymbol{r}}=\boldsymbol{c}, \qquad (1.2)$$

$$\dot{\boldsymbol{c}}=\boldsymbol{F}+2(\boldsymbol{c}\wedge\boldsymbol{\Omega}), \qquad (1.3)$$

and $\boldsymbol{F}$ denotes the force depending on the position, and $\boldsymbol{\Omega}=(\Omega_x, \Omega_y, \Omega_z)$ is the rotation vector.

It is immediately apparent that the term corresponding to the CORIOLIS' force becomes involved in the BOLTZMANN equation. The change in the BOLTZMANN equation can be better understood when we consider the trajectory of molecule, as it is no longer a straight line, but becomes a diverging spiral for the rotating system.

§ 2. The Motion of Molecules and the Dynamics of Collision

Consider a typical rotating system such that the coordinates rotate around z-axis with a constant angular velocity ω**, then the equations of motion of a molecule in such a system are,

$$m\ddot{x}=2m\omega\dot{y}+m\omega^2 x, \qquad (2.1)$$

$$m\ddot{y}=-2m\omega\dot{x}+m\omega^2 y, \qquad (2.2)$$

$$m\ddot{z}=0, \qquad (2.3)$$

where coordinates are taken in the rotating frame and the external force is omitted in order to see the essential features of the results of rotation. The solutions of the equations (2.1), (2.2), and (2.3) are easily obtained and with initial conditions at $t=0$,

$$\left.\begin{aligned} x&=x_0,\ y=y_0,\ z=z_0,\\ \dot{x}&=\dot{x}_0,\ \dot{y}=\dot{y}_0,\ \dot{z}=\dot{z}_0,\end{aligned}\right\} \qquad (2.4)$$

the solutions are

$$x=x_0\cos\omega t+y_0\sin\omega t +\{(\dot{x}_0-\omega y_0)\cos\omega t+(\dot{y}_0-\omega x_0)\sin\omega t\}t, \qquad (2.5)$$

$$y=y_0\cos\omega t-x_0\sin\omega t +\{(y_0-\omega x_0)\cos\omega t-(\dot{x}_0-\omega y_0)\sin\omega t\}t, \qquad (2.6)$$

$$z=z_0+\dot{z}_0 t. \qquad (2.7)$$

Thus, for diverging spiral, with constant velocity $\dot{z}_0$ along the z-axis, these give a planer projection of a diverging spiral on the xy-plane. (see Fig. 1) The solutions (2.5) and (2.6) suggest that the phenomena observed in the rotating coordinates would be somewhat similar to the manner in which ionized gases behave under an external magnetic field.*** In eqations (2.1) and (2.2), if we neglect the last terms in the equations, the solution would give a closed spiral as it is obtained in the ionized gases.

The change in the trajectory brings up the problem of the possible change in the dynamics of the collision. However, in the dynamics of the collision, we can assume that the time duration of collision as infinitesimally small. Then the equations (2.5), (2.6)

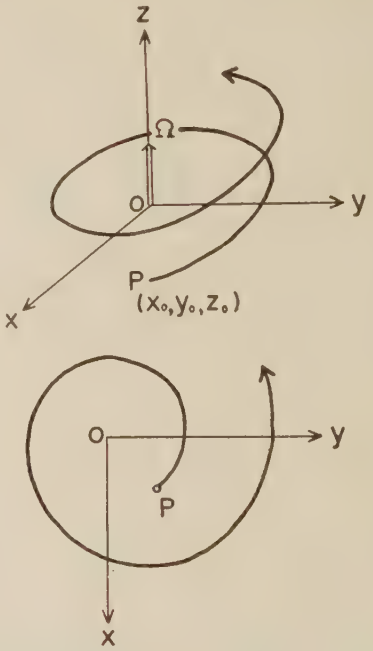

Fig. 1. The trajectory of a typical molecule in rotating coordinates. P denotes the initial position at $t=0$.

* Throughout the paper the notations are used after S. CHAPMAN and T. G. COWLING 1939.

** Through the paper such a coordinate system is mostly used. However, the results obtained can be easily generalized.

*** see ibid. S. CHAPMAN and T.G. COWLING 1939, chapter 13.

and (2.7) would be approximated in the following manner:

$$x=x_0+\dot{x}_0t+O(t^2)\,, \tag{2.8}$$

$$y=y_0+\dot{y}_0t+O(t^2)\,, \tag{2.9}$$

$$z=z_0+\dot{z}_0t\,. \tag{2.10}$$

From these equations, a linear motion of a molecule during the collision would be able to apply for the consideration of the dynamics of the collision. Consequently, the dynamics of the collision be the same as that for the fixed system. Hence, the number of molecules, linear momentum, and the total energy would be conserved during collision. With the conventional notations of the function $\psi^{(i)}$, we could write these collision invariants as below:

the number of molecules;

$$\psi^{(1)}=1\,, \tag{2.11}$$

the linear momentum;

$$\boldsymbol{\psi}^{(2)}=m\boldsymbol{C}\,, \tag{2.12}$$

the total energy;

$$\psi^{(3)}=E=\frac{1}{2}m^2\boldsymbol{C}\,, \tag{2.13}$$

where $\boldsymbol{C}$, $\boldsymbol{C}$ denote the vector and the scalar expressions of the peculiar velocity of the molecule defined by

$$\boldsymbol{C}=\boldsymbol{c}-\boldsymbol{c}_0\,, \tag{2.14}$$

where

$$n\boldsymbol{c}_0=\int f\boldsymbol{c}\,d\boldsymbol{c}\,, \tag{2.15}$$

and $\boldsymbol{c}_0$ denotes the "averaged" peculiar velocity, that is, velocity of the mass motion of gas, and a bar means that the quantity is "averaged" over the whole velocity space.

Rewriting the BOLTZMANN equation (1.1) in terms of the peculiar velocity, we have

$$\frac{Df}{Dt}+\boldsymbol{C}\cdot\frac{\partial f}{\partial \boldsymbol{r}}+\left[\boldsymbol{F}+2(\boldsymbol{c}_0\wedge\boldsymbol{\Omega})-\frac{D\boldsymbol{c}_0}{Dt}\right]\cdot\frac{\partial f}{\partial \boldsymbol{C}}$$
$$+2(\boldsymbol{C}\wedge\boldsymbol{\Omega})\cdot\frac{\partial f}{\partial \boldsymbol{C}}-\frac{\partial f}{\partial \boldsymbol{C}}\boldsymbol{C}:\frac{\partial}{\partial \boldsymbol{r}}\boldsymbol{c}_0=\frac{\partial_e f}{\partial t}\,, \tag{2.16}$$

where

$$\frac{D}{Dt}\equiv\frac{\partial}{\partial t}+\boldsymbol{c}_0\cdot\frac{\partial}{\partial \boldsymbol{r}}$$

is called the "mobile-operator".

A similar equation can be obtained for a function of molecular properties ϕ, after averaging over the whole velocity space,

$$\frac{Dn\overline{\phi}}{Dt}+n\overline{\phi}\frac{\partial}{\partial \boldsymbol{r}}\cdot\boldsymbol{c}_0+\frac{\partial}{\partial \boldsymbol{r}}\cdot n\overline{\phi\boldsymbol{C}}-n\left\{\overline{\frac{D\phi}{Dt}}+\overline{\boldsymbol{C}\cdot\frac{\partial\phi}{\partial \boldsymbol{r}}}\right.$$
$$+\left[\boldsymbol{F}+2(\boldsymbol{c}_0\wedge\boldsymbol{\Omega})-\frac{D\boldsymbol{c}_0}{Dt}\right]\cdot\overline{\frac{\partial\phi}{\partial \boldsymbol{C}}}$$
$$\left.-\frac{\partial\phi}{\partial \boldsymbol{C}}\boldsymbol{C}:\frac{\partial}{\partial \boldsymbol{r}}\boldsymbol{c}_0+2\overline{(\boldsymbol{C}\wedge\boldsymbol{\Omega})\cdot\frac{\partial\phi}{\partial \boldsymbol{C}}}\right\}$$
$$=\int\phi\mathscr{D}f d\boldsymbol{c}\,, \tag{2.17}$$

where

$$\int\phi\mathscr{D}f d\boldsymbol{c}\equiv\int\phi\frac{\partial_e f}{\partial t}d\boldsymbol{c}$$

and the bars denote the averaged values over the world velocity space.

Substitution of the encounter invariants for the function ϕ gives special forms of the equation (2.17), which are the fundamental equations in physical problems.

The substitution

$$\phi=\psi^{(1)}=1$$

results in the equation of continuity,

$$\frac{Dn}{Dt}+n\frac{\partial}{\partial \boldsymbol{r}}\cdot\boldsymbol{c}_0=0 \tag{2.18}$$

or

$$\frac{D\rho}{Dt}+\rho\frac{\partial}{\partial \boldsymbol{r}}\cdot\boldsymbol{c}_0=0\,, \tag{2.19}$$

where

$$\rho=mn$$

denotes the density of the gas.

The substitution

$$\phi=\boldsymbol{\psi}^{(2)}=m\boldsymbol{C}$$

results in the hydrodynamical equation for the rotating system,

$$\frac{D\boldsymbol{c}_0}{Dt}-2(\boldsymbol{c}_0\wedge\boldsymbol{\Omega})=-\frac{1}{\rho}\frac{\partial}{\partial \boldsymbol{r}}\cdot\boldsymbol{P}+\boldsymbol{F}\,, \tag{2.20}$$

where

$$\boldsymbol{P}=\rho\overline{\boldsymbol{CC}}$$

is the pressure tensor. This equation is formally identical with the result obtained by the ordinary transformation of coordinates, but as is shown later, the quantity represented

by the pressure tensor is not immediately identical with the result derived by the coordinate transformation.

The substitution

$$\phi=\psi^{(3)}=E$$

results in the equation of thermal conduction

$$\frac{DT}{Dt}=-\frac{2}{3nk}\left\{\boldsymbol{P}:\frac{\partial}{\partial \boldsymbol{r}}\boldsymbol{c}_0+\frac{\partial}{\partial \boldsymbol{r}}\cdot\boldsymbol{q}\right\}, \tag{2.21}$$

where

$$E=\frac{m}{2}\overline{C^2}=\frac{3}{2}kT$$

and

$$\boldsymbol{q}=n\overline{C\boldsymbol{E}}$$

denotes the energy flux vector. Again the resultant equation bears similarity to the expression derived for the fixed system. However, the pressure tensor $\boldsymbol{P}$ and the energy flux vector $\boldsymbol{q}$ would become different from those for the fixed system as are shown in later sections.

Equation of angular momentum conservation can also be obtained, when we substitute $m\boldsymbol{r}\wedge\boldsymbol{c}$ for ϕ.

§ 3. The Pressure Tensor and the Hydrodynamical Equation

The BOLTZMANN equation (2.16) is solved by the method of successive approximations developed by ENSKOG and others, and the coefficients of thermal conduction, viscosity, and diffusion are obtained in this process of approximation in the similar manner for the ionized gases studied by T. G. COWLING (1932, 1933) to show the effect of rotation.

Suppose the temperature is uniform throughout the gas, the components of the pressure tensor can be obtained in the following forms after a little laborious calculation

$$p_{xx}^{(1)}=-\frac{2\mu}{1+\frac{16}{9}(4\omega^2)\tau^2}\left[\overset{\circ}{\overline{e}}_{xx}+\frac{1}{2}(\overset{\circ}{\overline{e}}_{xx}+\overset{\circ}{\overline{e}}_{yy})\frac{16}{9}(4\omega^2)\tau^2-\overset{\circ}{\overline{e}}_{xy}\frac{4}{3}(2\omega)\tau\right], \tag{3.1}$$

$$p_{yy}^{(1)}=-\frac{2\mu}{1+\frac{16}{9}(4\omega^2)\tau^2}\left[\overset{\circ}{\overline{e}}_{yy}+\frac{1}{2}(\overset{\circ}{\overline{e}}_{xx}+\overset{\circ}{\overline{e}}_{yy})\frac{16}{9}(4\omega^2)\tau^2+\overset{\circ}{\overline{e}}_{xy}\frac{4}{3}(2\omega)\tau\right], \tag{3.2}$$

$$p_{zz}^{(1)}=-2\mu\overset{\circ}{\overline{e}}_{zz}, \tag{3.3}$$

$$p_{xy}^{(1)}=p_{yx}^{(1)}=-\frac{2\mu}{1+\frac{16}{9}(4\omega^2)\tau^2}\left[\overset{\circ}{\overline{e}}_{xy}+\frac{1}{2}(\overset{\circ}{\overline{e}}_{xx}-\overset{\circ}{\overline{e}}_{yy})\frac{4}{3}(2\omega)\tau\right], \tag{3.4}$$

$$p_{xz}^{(1)}=p_{zx}^{(1)}=-\frac{2\mu}{1+\frac{4}{9}(4\omega^2)\tau^2}\left[\overset{\circ}{\overline{e}}_{xz}-\frac{2}{3}(2\omega)\tau\overset{\circ}{\overline{e}}_{yz}\right], \tag{3.5}$$

$$p_{yz}^{(1)}=p_{zy}^{(1)}=-\frac{2\mu}{1+\frac{4}{9}(4\omega^2)\tau^2}\left[\overset{\circ}{\overline{e}}_{yz}+\frac{2}{3}(2\omega)\tau\overset{\circ}{\overline{e}}_{xz}\right], \tag{3.6}$$

where

$$\tau=\frac{3\mu}{2p},$$

and $\overset{\circ}{\overline{e}}_{xx}$, $\overset{\circ}{\overline{e}}_{yy}\cdots$etc. denote the components of tensor $\overset{\circ}{(\partial/\partial\boldsymbol{r})\boldsymbol{c}_0}$, and the rotation vector $\boldsymbol{\Omega}=(0, 0, \omega)$ is taken in z direction. The superscript (1) denotes the order of the approximation, namely in this case the expressions were obtained up to the first approximation of the pressure tensor. μ is the viscosity being defined to the first approximation in ordinary theory.

In the above expressions of the pressure tensor, all the components except $p_{zz}^{(1)}$, indicate the influence of the rotation of the coordinates. However, under the usual circumstances the factor τ is

$$\tau=\frac{3\times10^{-6}}{2\times10^{6}}\sim O(10^{-12}) \tag{3.7}$$

and negligible in these expressions. With this order in mind, the hydrodynamical equations for the rotating coordinates which is rotating around the z-axis with a constant angular velocity ω should be written in the

following form

$$\frac{Du_0}{Dt}-2\omega v_0=-\frac{1}{\rho}\frac{\partial p}{\partial x}+\frac{\nu}{3}\frac{\partial}{\partial x}\Theta+\nu\nabla^2 u_0+\omega^2 x+F_x, \tag{3.8}$$

$$\frac{Dv_0}{Dt}+2\omega u_0=-\frac{1}{\rho}\frac{\partial p}{\partial y}+\frac{\nu}{3}\frac{\partial}{\partial y}\Theta+\nu\nabla^2 v_0+\omega^2 y+F_y, \tag{3.9}$$

$$\frac{Dw_0}{Dt}=-\frac{1}{\rho}\frac{\partial p}{\partial z}+\frac{\nu}{3}\frac{\partial}{\partial z}\Theta+\nu\nabla^2 w_0+F_z, \tag{3.10}$$

where

$$p=nkT$$

is static pressure,

$$\nu=\frac{\mu}{\rho}$$

is the kinematic viscosity, and the notations Θ and ∇^2 are

$$\Theta=\frac{\partial u_0}{\partial x}+\frac{\partial v_0}{\partial y}+\frac{\partial w_0}{\partial z},$$

$$\nabla^2=\frac{\partial^2}{\partial x^2}+\frac{\partial^2}{\partial y^2}+\frac{\partial^2}{\partial z^2}.$$

Hence, the hydrodynamical equations derived by the transformation of coordinates are practically secured for its use in the investigation of the problems under ordinary circumstances by virtue of the foregoing discussions.

§ 4. Thermal Conduction

The thermal conduction for the rotating system is considered in the following manner. Suppose the gas is at rest relative to the rotating frame, that is, the gas is in a state of rigid-body rotation.

If the temperature gradient $\partial T/\partial \boldsymbol{r}$ is the direction of the rotation vector $\boldsymbol{\Omega}$, it can easily be seen in analogy to the ionized gas that the heat conduction parallel to the axis of the rotation is not affected by the rotation of the coordinates.

In the other special case where the temperature gradient is perpendicular to the vector of rotation, we have for the expression of the enegry flux vector $\boldsymbol{q}^{(1)}$

$$\boldsymbol{q}^{(1)}=-\frac{\lambda\left[\frac{\partial T}{\partial \boldsymbol{r}}-2\tau\left(\boldsymbol{\Omega}\wedge\frac{\partial T}{\partial \boldsymbol{r}}\right)\right]}{1+4\omega^2\tau^2} \tag{4.1}$$

where superscript again denotes the expression held to its first approximation and

$$\frac{\partial T}{\partial \boldsymbol{r}}=\left(\frac{\partial T}{\partial x},\ \frac{\partial T}{\partial y},\ 0\right),\quad \boldsymbol{\Omega}=(0,\ 0,\ \omega)$$

and

$$\tau=\frac{3\mu}{2p}.$$

λ is the first approximation to the ordinary thermal conductivity in the fixed system. In this case, the thermal conduction along the gradient of temperature is reduced to $1/(1+4\omega^2\tau^2)$ times, while the other conduction, the "transverse conduction", which is perpendicular to both of the vectors $\partial T/\partial \boldsymbol{r}$ and $\boldsymbol{\Omega}$, becomes in the magnitude $2\omega\tau$ times the former conduction as the results of the rotation of the coordinates.

The order of the quantity τ is, again,

$$\tau=\frac{3\mu}{2p}=\frac{3\lambda}{5c_v p}\sim O(10^{-12}) \tag{4.2}$$

since

$$\lambda=\frac{5}{2}c_v\mu.$$

Consequently by the similar reason as in the previous section, the final form of the equation of thermal conduction under the present assumption would become

$$\frac{DT}{Dt}=\kappa\nabla^2 T \tag{4.3}$$

where

$$\kappa=\frac{2\lambda}{3kn}$$

is the thermometric conductivity.

However, if τ is large, the thermal conduction would mostly be directed along z-axis. Back to the equation (2.21), the term $(\partial/\partial \boldsymbol{r})\cdot\boldsymbol{q}$ are

$$\frac{\partial q_x}{\partial x}=-\frac{\lambda}{1+4\omega^2\tau^2}\frac{\partial^2 T}{\partial x^2}-\frac{2\tau\omega\lambda}{1+4\omega^2\tau^2}\frac{\partial^2 T}{\partial x\partial y}, \tag{4.4}$$

$$\frac{\partial q_y}{\partial y}=-\frac{\lambda}{1+4\omega^2\tau^2}\frac{\partial^2 T}{\partial y^2}+\frac{2\tau\omega\lambda}{1+4\omega^2\tau^2}\frac{\partial^2 T}{\partial x\partial y}, \tag{4.5}$$

$$\frac{\partial q_z}{\partial z}=-\lambda\frac{\partial^2 T}{\partial z^2}. \tag{4.6}$$

By addition of these three equations, the second terms in (4.4) and (4.5) would cancel each other. Therefore, the resultant gives such a conduction that heat would be conduct-

ed mostly along the z-axis, because the horizontal conduction becomes smaller by the factor $1/(1+4\omega^2\tau^2)$, while no transverse conduction appears.

§ 5. Diffusion

Similar results as in the foregoing sections can be obtained in the problem of diffusion by considering a gas-mixture. If we take the case of binary-mixture, we would have the following equations for conservation of molecules, hydrodynamics, and thermal conduction,

$$\frac{Dn}{Dt}+n\frac{\partial}{\partial \boldsymbol{r}}\cdot\boldsymbol{c}_0+\frac{\partial}{\partial \boldsymbol{r}}\cdot(n_1\overline{\boldsymbol{C}}_1+n_2\overline{\boldsymbol{C}}_2)=0\,, \tag{5.1}$$

$$\frac{D\rho}{Dt}+\rho\frac{\partial}{\partial \boldsymbol{r}}\cdot\boldsymbol{c}_0=0 \tag{5.2}$$

(The equation of conservation of mass),

$$\rho\frac{D\boldsymbol{c}_0}{Dt}=\rho_1\boldsymbol{F}_1+\rho_2\boldsymbol{F}_2+2\rho(\boldsymbol{c}_0\wedge\boldsymbol{\Omega})-\frac{\partial}{\partial \boldsymbol{r}}\cdot\boldsymbol{P}\,, \tag{5.3}$$

$$\begin{aligned}\frac{3}{2}kn\frac{DT}{Dt}=&\frac{3}{2}knT\frac{\partial}{\partial \boldsymbol{r}}\cdot(n_1\overline{\boldsymbol{C}}_1+n_2\overline{\boldsymbol{C}}_2)\\&+\rho_1\boldsymbol{F}_1\cdot\overline{\boldsymbol{C}}_1+\rho_2\boldsymbol{F}_2\cdot\overline{\boldsymbol{C}}_2\\&-\boldsymbol{P}:\frac{\partial}{\partial \boldsymbol{r}}\boldsymbol{c}_0-\frac{\partial}{\partial \boldsymbol{r}}\cdot\boldsymbol{q}\,,\end{aligned} \tag{5.4}$$

where notations are used in the usual way and the subscripts 1 and 2 refer to the 1st and 2nd kinds of gases, respectively. From them, and with the assumption of solid rotation and uniform temperature of gases, the velocity of diffusion is obtained as

$$\overline{\boldsymbol{C}}_1-\overline{\boldsymbol{C}}_2=-\frac{p\rho\tau}{\rho_1\rho_2}\frac{\boldsymbol{d}_{12}-2\tau(\boldsymbol{\Omega}\wedge\boldsymbol{d}_{12})}{1+4\omega^2\tau^2}\,. \tag{5.5}$$

This result indicates that the direct diffusion is reduced in the ratio $1/(1+4\omega^2\tau^2)$, while the transverse diffusion is 2τ times the direct diffusion. Therefore, a result similar to that discussed in the last part of section 4 also holds in diffusion provided that $4\omega^2\tau^2$ is large to be comparable with unity. Under the last circumstance diffusion would be mostly directed along z-axis.

§ 6. Summary

The proceeding study has showed that the various dynamical equations in rotating system can be easily derived as the "averaged" properties of molecules of rotating gases, also it confirmed the negligible influence of the rotation in microscopic characteristics of the gases, such as the coefficients of viscosity, thermal conduction and diffusion. The latter indicates, under ordinary circumstances, that the MAXWELLIAN velocity-distribution function should hold in the rotating gas, as well as the equipartition law of energy flow. Consequently, it becomes clear that the cause of the so-called two-dimensionality of the motion in the rotating gas and liquid must be a phenomenological one.

This proof can be easily obtained as follows: If the approximation of the hydrodynamical equation,

$$2(\boldsymbol{c}_0\wedge\boldsymbol{\Omega})=-\frac{1}{\rho}\frac{\partial}{\partial \boldsymbol{r}}p \tag{6.1}$$

holds with the condition of the incompressibility. Then by taking curl of this equation, we can obtain the following relation

$$\left(\boldsymbol{\Omega}\cdot\frac{\partial}{\partial \boldsymbol{r}}\right)\boldsymbol{c}_0=0\,. \tag{6.2}$$

The equation (6.2) denotes that the motion only takes place in planes perpendicular to the axis of rotation, in other words, the motion has the characteristics of the two-dimensionality.

In the large scale circulation of the atmosphere and ocean, these conditions were found in close approximation, also in some experimental studies of the rotating liquids by G. I. TAYLOR (1921, 1923). However, the importance of the study of three-dimensional motion in the rotating system should be easily understood from the results of the present study because the influence of the rotation is negligible in microscopic characteristics.

Acknowledgement

The author expresses his sincere appreciation to Dr. Tomoyasu TANAKA of Kyushu University for his stimulating discussions over this study. Also he owes very much to Prof. S. CHANDRASEKHAR of the Institute for Nuclear Studies and Yerkes Observatory, for his support and encouragement throughout the work, and Prof. T. G. COWLING of the University of Leeds for his criticism and

remarks after reviewing the original manuscript.

References

BORN, M., and GREEN, H. S.,:
1949 "A general kinetic theory of liquids" Cambridge Univ. Press.

CHAPMAN, S., and COWLING, T. G.,:
1939 "The mathematical theory of non-uniform gases" Cambridge Univ. Press.

COWLING, T. G.,:
1932 "Diamagnetism and drift currents in solar atmosphere" Month. Notices Roy, Astron. Soc. **92**, 407.
1933 "The electrical conductivity of an ionized gas in the presence of a magnetic field" Month. Notices Roy, Astron. Soc. **93**, 90.

JEANS, J.,:
1940 "An introduction to the kinetic theory of gases" Cambridge Univ. Press.

TAYLOR, G. I.,:
1921 "Experiments with rotating fluids" Proc. Roy. Soc. **100**, 114.
1923 "Experiments on the motion of solid bodies in rotating fluids" Proc. Roy. Soc. **104**, 213.

Wave Groups Generated by a Very Small Explosion.

By

Kyozi TAZIME

Department of Geophysics, Faculty of Science, Hokkaido University, Sapporo.

Summary

Generation mechanisms of wave groups by a small explosion are studied from a wave theoretical point of view. We see all waves predominant in the seismic records obtained are some kind of surface waves, especially of dispersive RAYLEIGH and SEZAWA waves. These wave groups are shown to satisfy the quarter wave length law which has been established theoretically in the present paper. Owing to shielding effects of a superficial layer, not very many kinds of surface wave groups can grow. This makes our seismograms rather simple.

In seismic prospectings, the surface waves studied in the present paper may be useful, at least, in some cases.

§ 1. Introduction

When geophones are set up on a straight line at equal intervals in field experiments, we observe that all peaks and troughs of every trace in seismic records correspond very well to each other. These peaks and troughs will result in the respective time-distance lines which have one constant slope for one group, but another constant slope for another group. In general there are only a few groups having equally sloped lines.

Within a wave group, we can observe several peaks and troughs at almost equal time intervals. As we have a shock type pulse at the origin, we are apt to attribute the generations of these oscillations in a group to dispersions of seismic waves. In this case, however, we soon meet with the difficulty of explaining the constancy of period in the wave group.

As we have got more or less similar seismic records in our experiments to be described, we shall confine ourselves to the study of records obtained in 1953 at the ground of Geological Survey of Japan.

§ 2. Seismic records

At first a cap was blasted at the depth of 0.75 m. Geophones were set up on the ground at every 0.25 m (or 0.50 m) on a straight line. The epicentral distance spreads from 0.25 m to 25.25 m. E. T. L. (E), S. S. C. (G, O) and SASSA-SANEI's (U) seismic recorders were used.

Seismograms thus obtained are shown in Fig. 1 and Fig. 2. Since various kinds of recorders were used at the same time in this experiment, the forms of these seismograms appear to be different from each other. The wave forms are, however, out of our concern at present.

Fig. 3 shows the time-distance curves for all troughs contained in the above seismograms. Those for the peaks are omitted to avoid a confused figure. This chart is, the author believes, useful for the classification of wave groups. The slopes of the lines connecting each trough indicate the phase velocities of the respective waves. Thus we have four wave groups having different phase velocities as in Table 1.

We have stated about the vertical component of ground motions alone, but the horizontal components were also observed. These are shown in Fig. 4 in which the transversal component is seen very small in all wave groups. On the other hand, the longitudinal component is predominant in the 3rd and the 4th groups, though it is also poor in the 1st

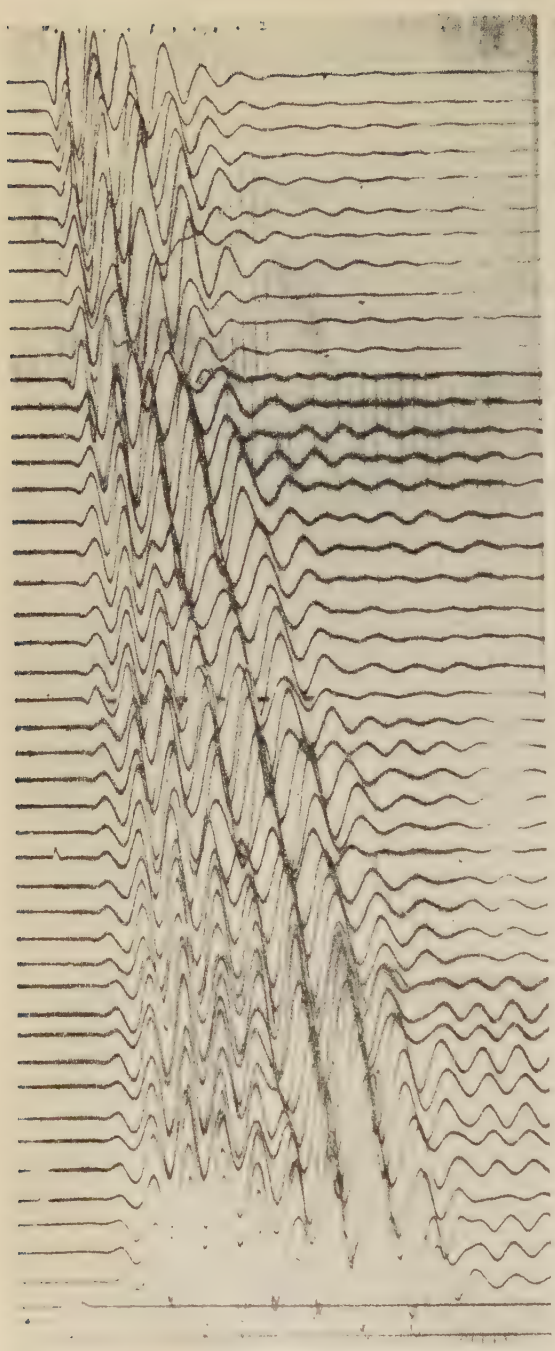

Fig. 1. A cap was blasted at the depth of 0.75 m. The recorders G and O were used. Geophones of vertical components were set up from 0.25 m to 11.50 m.

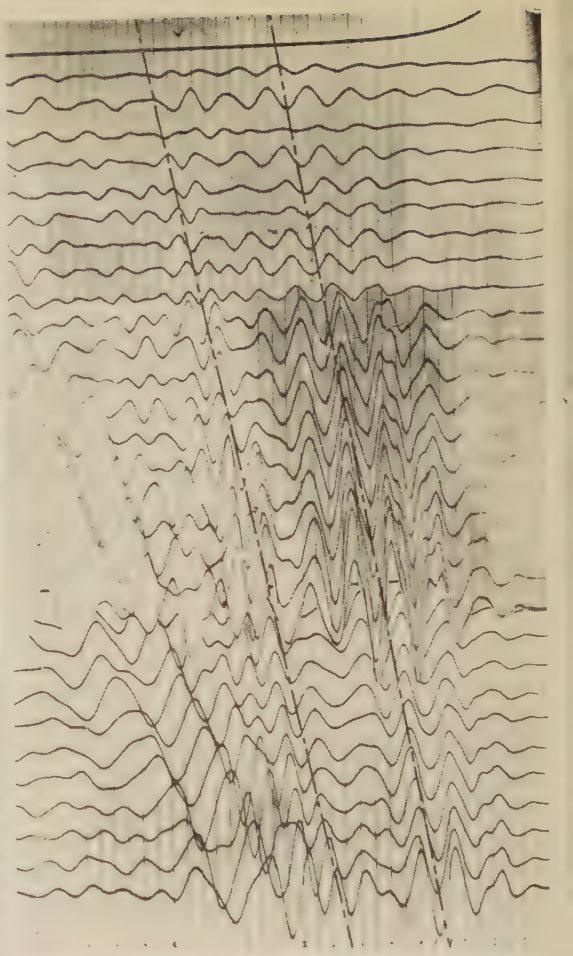

Fig. 2. Vertical U geophones were set up from 11.25 m to 25.25 m.

and the 2nd groups.

The 1st group represents initial motions and contains a few oscillations even at distant observing points. The other groups growing gradually with the epicentral distance, on the other hand, show several oscillations. The wave form of the 1st group is very simple and this initial motion is interpretted to be due to the direct or refracted P wave. From now on, we shall concern with the wave groups except the first one.

The 4th group is conspicuous everywhere including the epicenter and seems, at first sight, to be due to a kind of RAYLEIGH type surface waves, though its oscillatory character

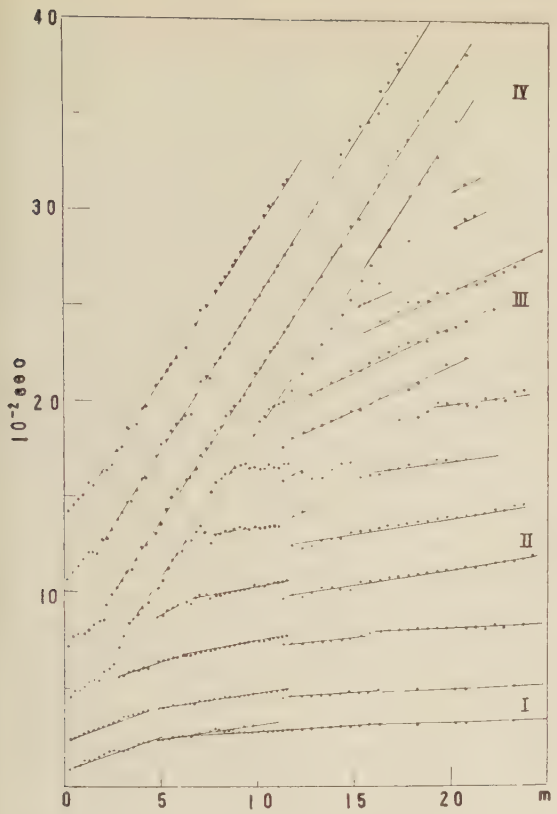

Fig. 3. The time-distance curves of all troughs in Fig. 1 and Fig. 2.

Table 1. Classification of the wave groups.

group	phase velocity	period
I	$1.3\sim18\times10^{2}$ m/s	
II	$5.0\sim6.5$	2.8×10^{-2} sec
III	$2.1\sim2.6$	2.5
IV	$0.6\sim0.7$	3.5

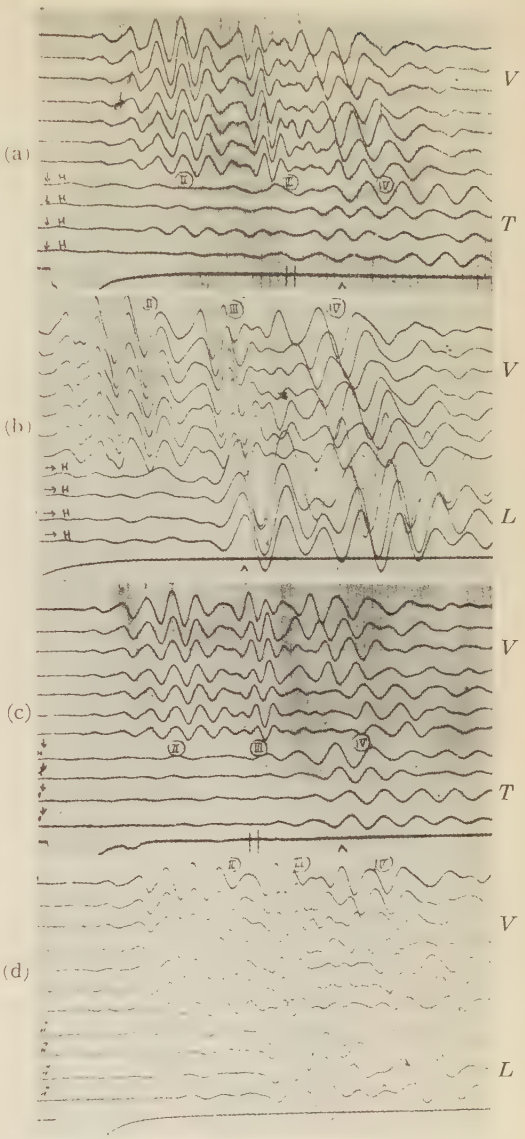

Fig. 4. The upper two; T, L $15.75\sim17.25$ m, and V $15.75\sim18.75$ m.
The lower two; T, L $17.25\sim18.75$ m, and V $17.25\sim20.25$ m.

has not yet been thoroughly understood.

It is more difficult to understand the generation mechanisms of the remaining two wave groups, the 2nd and the 3rd. The phase velocity of 2.5×10^{2} m/s, for instance in Fig. 3, is observed within 6 m from the epicenter as well as beyond 11 m. But it cannot be decided from Fig. 3 alone whether the both tremors belong to the same wave system or not. The same phase velocity in the two parts may be an accidental coincidence.

It must be remarked that the word "wave group" in this paper has no complete physical meaning, but indicates merely the group having the proper phase velocity. The full discussions on this point will be given later.

§ 3. Rise and Fall of the Individual Peak or Trough within One Wave Group with Regard to the Epicentral Distance

SUZUKI and SIMA (1954) found an apparent rule as to the form of each phase recorded on just the same seismogram as in Fig. 2. Modifying the SUZUKI and SIMA's method, we have tried to find the feature of rise and fall of the individual peak or trough within one wave group with regard to the epicentral distance. In order to do this, we read amplitudes of all peaks and troughs in one trace of the seismic record. If fortunately wave groups are separated form one another as in Fig. 2, we take the sum of all amplitudes of peaks and troughs in a group as an amplitude standard of the group. The ratio of each amplitude to the sum is a standardised amplitude of the respective peak or trough within the wave group. Other trace of the seismogram is treated in the same manner and so on. In doing so, the difference in amplification characteristics of recorders may be eliminated at least in the first approximation. Thus we can follow the rise and fall of every phase with respect to the epicentral distance. The other wave groups can be analysed similarly. Fig. 5 illustrates the features of rise and fall for the 2nd, the 3rd and the 4th wave groups. The notation *u* or *d* in the figure corresponds to up or down on the seismograms and the number corresponds to the order of the peak or the trough from the initial motion.

We see in Fig. 5 that one early appearing wave grows gradually at first up to a certain epicentral distance, beyond which it decreases and the next wave comes to be predominant. This feature is seen everywhere from the 2nd group to the 4th group. In order to see this more clearly, we combined the two figures, Fig. 3 and Fig. 5, and obtained Fig. 6 in which the above mentioned distances are

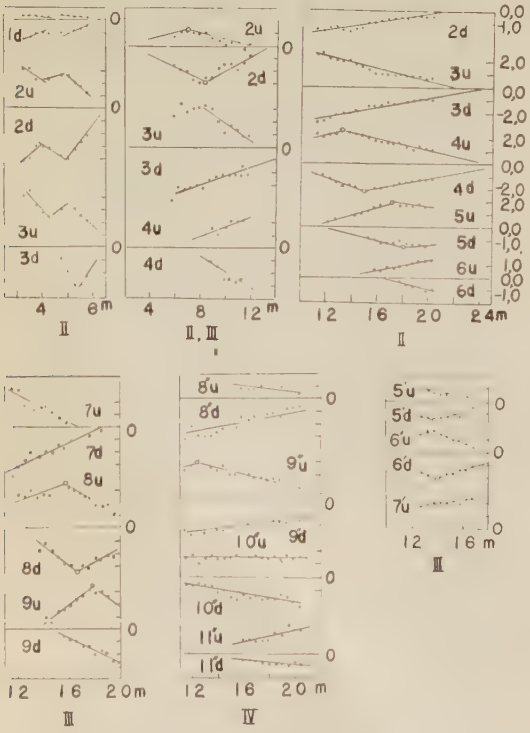

Fig. 5. The amplitudes of peaks and troughs within wave groups.
The abscissa indicates the epicentral distance.

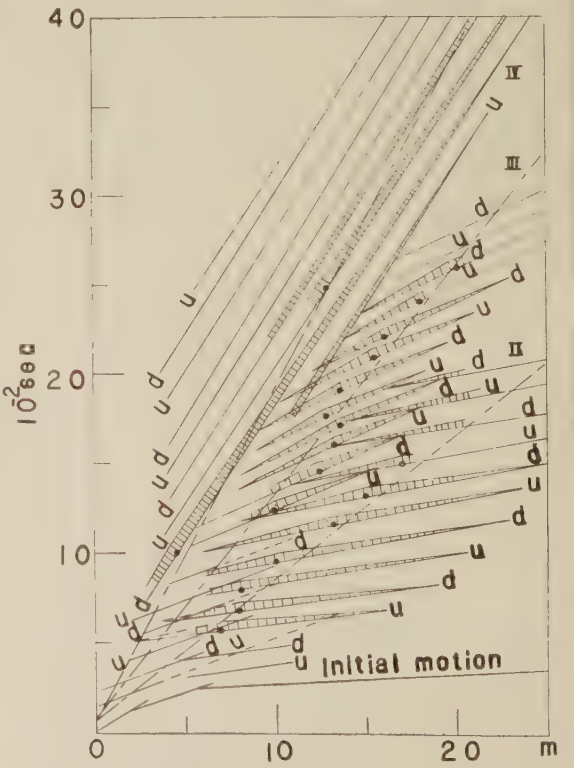

Fig. 6. The two figures, Fig. 3 and Fig. 5, are combined.

marked by small black circles on the time distance lines.

We see that the origin of the wave having 2.5×10^2m/s phase velocity can be traced back to very near the epicenter. The broken lines in Fig. 6 indicate the parts where we cannot trace the wave, because of overlapping of wave groups. The meaning of the chain lines will be explained in the next section.

§4. The Group Velocities Directly Derived from the Seismograms

Looking at the form of a wave group on our seismogram, for instance in Fig. 2, we see it bounded by a spindle-shaped envelope as in Fig. 7.

Fig. 7. Each wave group is enveloped in a spindle-shape.

Tracing the loops of these spindle-shapes, we get the chain lines drawn in Fig. 6, though the starting points of these lines are somewhat obscure. At any rate, it must be noted that the chain lines pass through the black circles already described. This situation is shown schematically in Fig. 8.

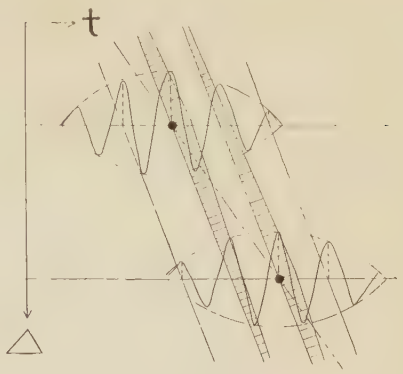

Fig. 8. The amplitude of peak or trough within a wave group changes with respect to time as well as epicentral distance.

Thus we see the maximum amplitude of a wave group is propagated with a certain definite velocity. Thus the slopes of the chain lines show the minimum group velocities of the wave groups. The group velocities U_0, thus decided, are tabulated in Table 2.

For reference the frequency-responses of our recorders are shown in Fig. 9.

Table 2. Observed group velocities.

group	group velocity (U_0)
II	1.3×10^2 m/s
III	0.92
IV	0.52

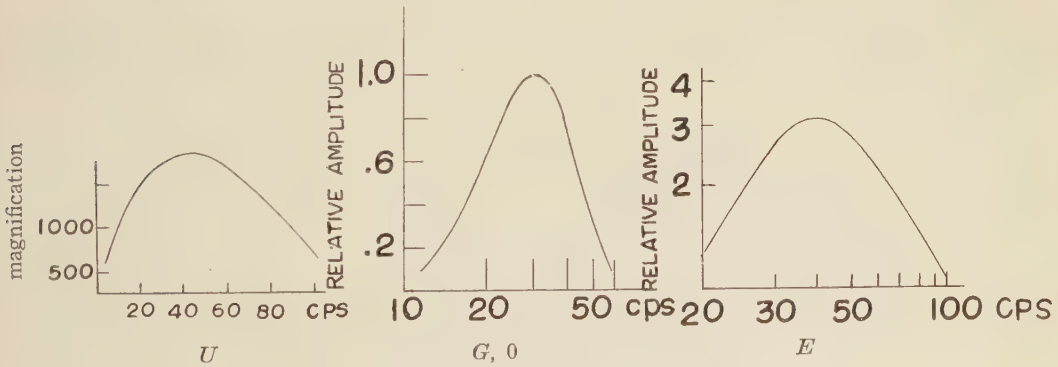

Fig. 9. Frequency-responses of our recorders.

§5. Analysis of the Wave Forms

Notwithstanding hardly noticeable change in periods within the wave groups, dispersion phenomena will be studied here. If we assume that the spindle-shaped wave form as in Fig. 7 is composed of two sinusoidal waves having equal amplitudes, we have

$$y=\cos(2\pi t/\tau)+\cos(2\pi t/\tau')$$
$$=2\cos(2\pi t/\tau)\cos\{\pi t/(\tau\tau'/|\tau-\tau'|)\},$$

where t means time and τ and τ' are periods

which are nearly equal. Therefore the period of an envelope of the waves is

$$T=2\tau\tau'/|\tau-\tau'|\,.$$

Now, for instance, for the 2nd wave group in our seismograms, we have

$$\tau=2.8\times10^{-2}\,\text{sec}$$

and

$$T=22\times10^{-2}\,\text{sec},$$

hence

$$\tau'=\tau T/(T\pm2\tau)=2.5 \text{ or } 3.4\times10^{-2}\,\text{sec}\,.$$

Thus we see the wave group has a very narrow period range outside of which the amplitudes of individual waves will fall off sharply. In practice, it will not be possible to distinguish the change of periods between 2.5×10^{-2} sec and 2.8×10^{-2} sec on an actual seismic record. Thus we must give up to expect dispersion effects as in usual seismograms by natural earthquakes, since we have no changing period within a wave group.

In order to make this point clearer, FOURIER analyses of wave forms were carried out. The result of the analyses for the 2nd wave group is shown in Fig. 10.

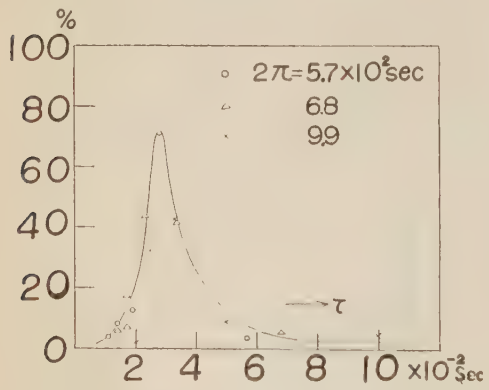

Fig. 10. Result of the FOURIER analysis. ○, △ and × are calculated from the same seismogram, but the time units used are different from one another.

In this figure 2π means the time interval adopted for the analyses. We have moreover tried to find phase velocities of individual FOURIER components. But this attempt is not successful, since enormous errors enter in the culculations of phase velocities outside the above mentioned narrow period range. It seems, however, that the predominant phases in our wave groups have the phase velocities near the inflection points on the dispersion curves. Estimating the group velocities within the narrow range of period from the calculated phase velocities, we obtain respectively almost the same values as those in Table 2 which were directly derived from the seismograms. This discovery makes us believe that the tabulated group velocities are the minimum ones, as are predicted by theoretical studies of this kind of problem.

§ 6. The Subsurface Condition of Our Experimental Ground

By now we have investigated only the wave forms appearing in the seismic records and have not yet discussed generation mechanisms of the wave groups. Now the subsurface condition of our experimental field will be described. We shall start with the discussion of the results obtained by refraction shootings, though there are several boring data as shown in Fig. 11.

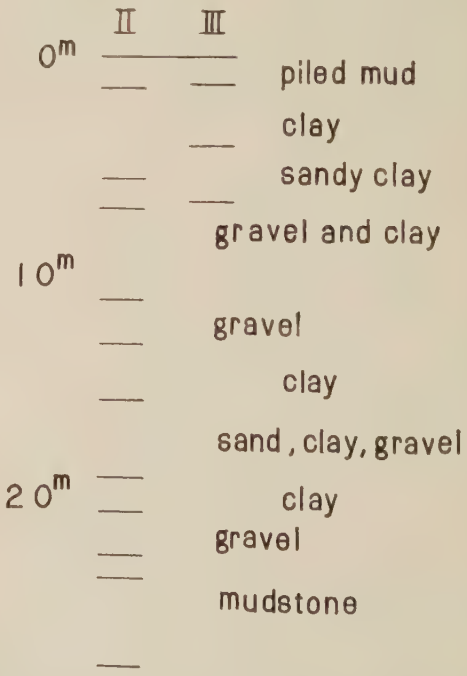

Fig. 11. The boring data at the experimental field.

A reverse shot was done with a cap keeping the other conditions, such as shot depth, positions of geophones and so on, the same as before. The time-distance curves for the reverse shot, shown in Fig. 12, were found quite similar to those by the normal shot in Fig. 3.

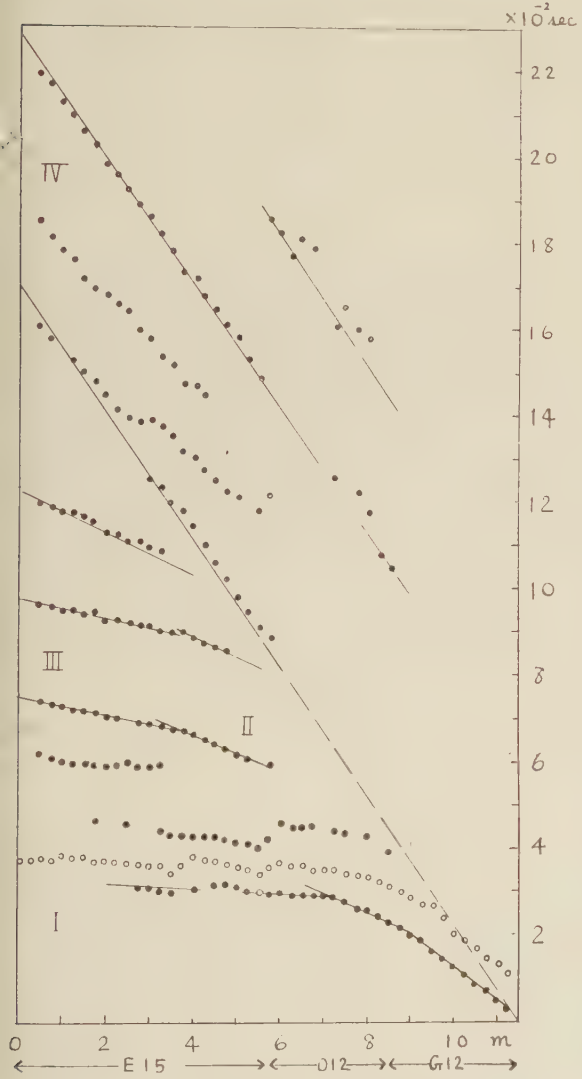

Fig. 12. The time-distance curves for a reverse shot.

Therefore we may regard the subsurface condition to be uniform horizontally. Then the underground structure may easily be deduced from the travel time of the initial motion. The result obtained is given in Fig. 13 (a), where the numerals indicate the velocities of P waves in the respective layers, the unit being 10^2 m/s. Another result may be obtained if we assume a linearly increasing velocity in the superficial layer. This is shown in Fig. 13 (b). The other result (c) was also obtained by Hatakeyama (1954), one of the member of our experimental group, for a deeper shot at the same ground.

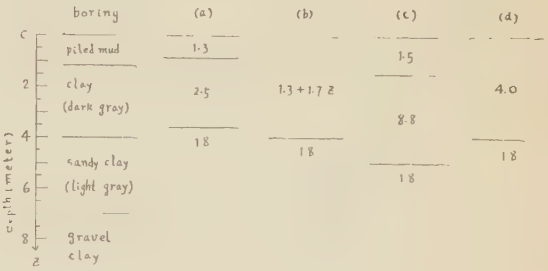

Fig. 13. The subsurface seismic models.

Now we encounter with a difficulty in choosing the model to be adopted. Hatakeyama's model gives the time-distance curve shown by the broken lines in Fig. 14, assuming a surface shot. On the other hand, the full and chain lines correspond respectively to the models (a) and (b) in Fig. 13, small black circles indicating the observed values for initial motions by a near surface shot. In spite of rather large

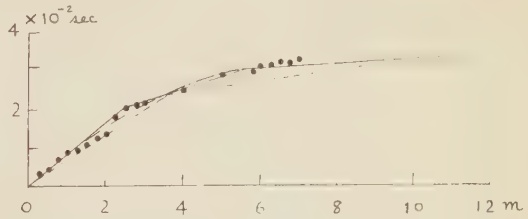

Fig. 14. Time-distance curves calculated for various subsurface models.

differences among the subsurface models, there are little differences among the time-distance curves obtained. As is easily seen, this is unavoidable as long as the initial time-distance curve alone is used for the subsurface analysis. At any rate, we cannot choose one among the three models given in Fig. 13.

As the explosion is very small, *S*-phase appears scarecely in our records. Thus we have no data about *S*-phase. Fortunately, however, MURAUCHI (1955) has observed, by his special technique, the velocity of *S* wave in the superficial mud layer, and got POISSON's ratio (σ) from 0.21 to 0.24. As are seen in Fig. 15, the values of v_p/v_s and v_R/v_s are

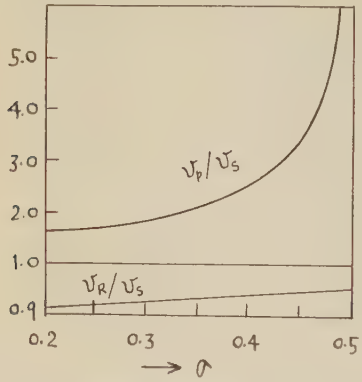

Fig. 15. Relation between v_p, v_s, v_R and POISSON's ratio for a perfectly elastic medium.

nearly constant within the range of POISSON's ratio obtained by MURAUCHI. From now on, we shall assume POISSON's ratio to be 0.25 in our calculations.

Thus the velocities of *S* and RAYLEIGH waves can be estimated by using that of *P* wave given in Fig. 13. The results are tabulated in Table 3.

Table 3. Velocities of *P*, *S* and RAYLEIGH waves for various models.

	(a)			(b)			(c)		
layer	*P*	*S*	*R*	*P*	*S*	*R*	*P*	*S*	*R*
1st	1.3	0.8	0.7	1.3	0.8		1.5	0.9	0.8
2nd	2.5	1.2	1.1	8.0	4.7		8.8	5.2	4.7
3rd	18	11	9.5	18	11	9.5	18	11	9.5

Table 4. Data on later phases.

wave group	component	period	phase velocity	wave length	group velocity
II	vertical	2.8	6.0	17 m	1.3
III	vertical longitudinal	2.5	2.2	5 m	0.9
IV	vertical longitudinal	3.5	0.7	3 m	0.6

time unit 10^{-2} sec; velocity unit 10^2 m/s

Some data on later phases are collected in Table 4. All of the later phases have very small phase and group velocities, exhibiting remarkable dispersions.

§ 7. The Quarter Wave Length Law Applied to the Superficial Layer

We shall now compare records obtained when caps were blasted at various depths. Fig. 16 was obtained by a shot at depth 1.50 m, the other conditions being kept the same as in Fig. 4 (d). We see the 3rd and the 4th groups become very poor while the 2nd group maintains its predominance. These observed facts are summarised in Table 5. Considering

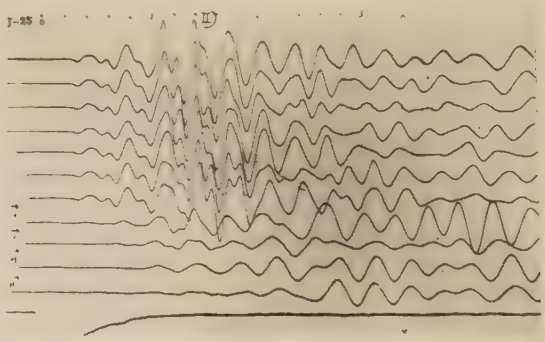

Fig. 16. A cap was blasted at the depth of 1.50 m.

Table 5. Relation between the predominances of the wave groups and the shot depth.

wave group	shot depth (m)		
	0.08	0.8	1.5
II	*F*	*F*	*F*
III	*F*	*F*	*P*
IV	*F*	*F*	*P*

F: fair, *P*: poor

these results in connection with the subsurface models (Fig. 13), we find that some discontinuity plane exists between the depths of 0.75 m and 1.50 m. Thus we must give up the model (b) in Fig. 13. We know also that the 3rd and the 4th wave groups are related almost entirely to the superficial layer, and on the other hand the 2nd group is related to the lower layers. As transversal components are very poor for every wave group, all wave groups we have seen are considered to be dispersive RAYLEIGH or SEZAWA waves,

usually called M-waves.

In the case of a single layer on a semi-infinite medium, fortunately, several dispersion curves of M-waves have already been calculated by SEZAWA (1927), KANAI (1951) and others. As TOLSTOY and EUGENE (1953) explained, there are two groups of waves called M_1 and M_2, and an additional suffix is used to denote the order in the respective groups. For instance, M_{11} or M_{21} means respectively M_1 or M_2-wave of the first order. Now several dispersion curves have been reproduced in Fig. 17 where, unlike usual ones, log-log scales are used and abscissae are converted from wave length to period having a time unit H/v_{s1}. H means the thickness of the superficial layer and v_{s1} means the velocity of S-wave in this stratum. Log-log scales will make the comparison of calculated dispersion curves with those observed easier. The conversion from wave length to period will be useful since we observe on a seismic record the period and not the wave length.

Here we must recall that the predominant

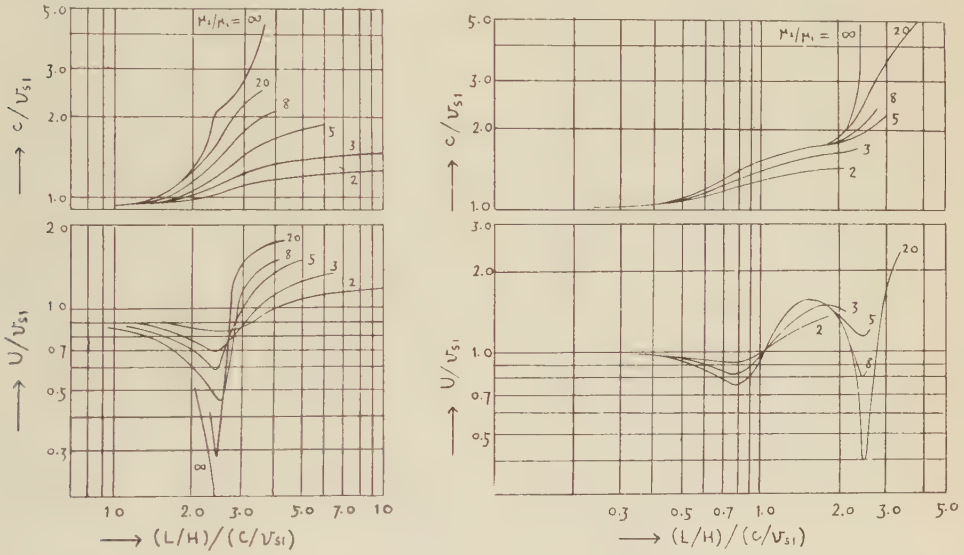

Fig. 17. Theoretical dispersion curves of dispersive RAYLEIGH waves (M_{11}, M_{21}), by SEZAWA and KANAI.

waves in our seismic records seemed to have the minimum group velocities for the respective wave groups. In Fig. 18, are shown the period, phase and group velocities of the AIRY phases as functions of the rigidity ratio μ_2/μ_1. We see that each curve in the uppermost figure has its asymptote as $\mu_2/\mu_1 \to \infty$, that is, the period of each AIRY phase becomes constant. The prefixes of M mean respectively the first and the second minimum group velocities, and L_1 corresponds to the first order LOVE waves.

The asymptotic values of the AIRY phase periods, T_0 say, are

$$T_0/(H/v_{s1}) = (L/H)(c/v_{s1}) = 2.4 \text{ for } M_{11} \text{ and } {}_2M_{21},$$
$$= 0.8 \text{ for } {}_1M_{21},$$
$$= 4.0 \text{ for } L_1,$$

where L means the wave length concerned.

We have previously assumed in Fig. 18 that POISSON's ratio is 0.25, namely

$$v_p = 1.7 v_s .$$

Therefore the above relations may be rewritten as

$$H = (1/4) v_{p1} T_0 \text{ for } M_{11} \text{ and } {}_2M_{21},$$
$$H = (3/4) v_{p1} T_0 \text{ for } {}_1M_{21},$$

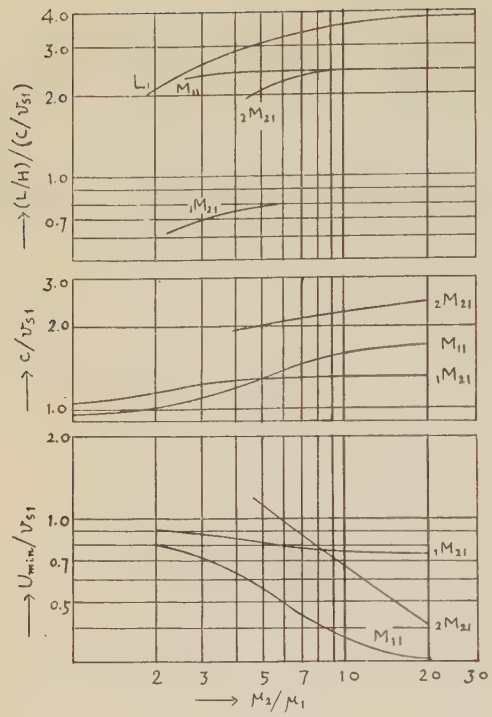

Fig. 18. The period, phase and group velocities of the AIRY phases against the rigidity ratio μ_2/μ_1.

$$H=(1/4)v_{s1}T_0 \text{ for } L_1 .$$

These relations should be understood as quarter wave length laws for doubly stratified layers.

§ 8. Discussions of the Later Phases

Putting the observed values v_{p1} and T_0 in Fig. 13 and Table 4 into the above relations, we have

$$H_1=\begin{cases} 0.8\,\text{m for the 3rd group}, \\ 1.1\,\text{m for the 4th group}. \end{cases}$$

These are well coincident with the thickness of the superficial layer deduced by the refraction method, the latter being 0.9 m to 1.5 m as in Fig. 13 (a) and (c). Comparing further the lower two figures in Fig. 18 with the observed data in Table 4, we see that the observed phase and group velocities for the 3rd and the 4th groups are also well corresponding to the theoretical values in Fig. 18, if we take the rigidity ratio 4 to 5. Thus we see that the 4th group is the AIRY phase of M_{11}-wave and the 3rd group the second minimum of M_{21}-wave in the superficial layer in Fig. 13.

In the above discussion, we have assumed the rigidity ratio of about 4. This rigidity ratio seems adequate, since we get v_{p2}/v_{p1} of about 2 by our assumption on POISSON's ratio, no density jump being assumed. Therefore the subsurface model (a) alone in Fig. 13 will survive from now on.

In the above, we have been able to explain the 3rd and the 4th wave groups by the two layer model, though actually there must be three or more layers. But the observed phases of the 3rd and the 4th groups appear to be scarcely influenced by the existence of lower layers, since the wave lengths of the phases are as short as 4 to 5 meters, being the same order as the depth to the third layer.

The 2nd wave group has the more persistent period and the more regular wave form than the 3rd and the 4th groups. Thus the 2nd group seems again to be the AIRY phase of a dispersive RAYLEIGH or SEZAWA wave. As the wave length of the 2nd wave group are longer than those for other wave groups in Table 4, we may expect the 2nd group will penetrate to the second layer, as shown by the full line in Fig. 19, whereas as the broken line shows, the 3rd group, for instance, will not. We must also keep in mind the fact pointed out in Table 4 that the longitudinal component of the 2nd group is very small in amplitude compared with those of the others. This fact corresponds well to the seismic ray paths considered just now.

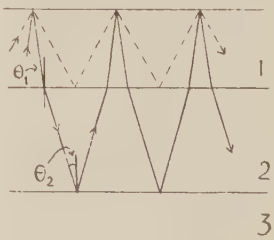

Fig. 19. Seismic ray paths in the strata.

Emergent angles of the ray paths in Fig. 19 can be calculated as follows;

$\theta_{IV}=\sin^{-1}(v_{p1}/c_{0IV})$ imaginary,
$\theta_{III}=\sin^{-1}(v_{p1}/c_{0III})$ 40°,
$\theta_{II_1}=\sin^{-1}(v_{p1}/c_{0II})$ 10°,
$\theta_{II_2}=\sin^{-1}(v_{p2}/c_{0II})$ 25°.

Imaginary value in the above relation seems to be difficult to explain at present and the discussion on it will be left for future.

In the case of triple layers, unfortunately, few dispersion curves have been calculated as to M-waves. Any law as that in the case of doubly stratified layers can not be proved theoretically. Now let us assume the following relation, similar to the previous one,

$$\frac{2n-1}{4}=\frac{1}{T_0}\left(\frac{H_1}{v_{p1}}+\frac{H_2}{v_{p2}}\right)$$

(n means any positive integer).

Putting the following values (see Fig. 13 and Table 4)

$v_{p1}=1.3\times10^2$ m/s, $v_{p2}=2.5\times10^2$ m/s,
$H_1=1.0$ m, $H_2=3.0$ m, $T_0=2.8\times10^{-2}$ sec

into the above equation, we get

$$\frac{2n-1}{4}=\frac{1}{2.8}\left(\frac{1.0}{1.3}+\frac{3.0}{2.5}\right)=\frac{2.9}{4}\ .$$

Since the values above used might be somewhat, though not greatly, uncertain, $(2n-1)/4$ will preferably be taken as 3/4 instead of 2.9/4. Thus we have 3/4 wave length law also in triple layers.

If we consider this result alone, the 2nd wave group seems to be ${}_1M_{21}$ in Fig. 17 (a). But we have a contradiction with respect to its phase velocity, because this is much larger than the phase velocity of ${}_2M_{21}$ which will be found later to spread over upper two layers. The theoretical phase velocity corresponding to the first minimum group velocity must be always smaller than that corresponding to the second one. Thus our 2nd group cannot be ${}_1M_{21}$, although it satisfies the 3/4 wave length law.

We have also examined the Airy phases in the dispersion curves calculated by Tolstoy and Eugene (1953), and have got the relations given in Table 6. Although these are concerned with doubly stratified layers, they may be applied to triple layers by the same reasoning as above. We see M_{12} and ${}_2M_{22}$ also satisfy the 3/4 wave length law like ${}_1M_{21}$.

Table 6. Various wave lengths law predicted by theoretical dispersion curves.

$T_0/(H/v_{p1})$	branch and phase		
1/4	M_{11}	${}_2M_{21}$	
3/4	M_{12}	${}_1M_{21}$	${}_2M_{22}$
5/4			${}_1M_{22}$

Now phase velocities of both M_{12} and ${}_2M_{22}$, the latter in particular, become much larger than that of ${}_1M_{21}$. Thus we can attribute the 2nd wave group to the phase corresponding to the second minimum group velocity of M_{21}-wave in the superficial two layers.

In short, all predominant phases in our seismic records Fig. 1 and Fig. 2 have been explained, although the blast used was restricted to a cap.

§9. Wave Groups Generated by a Larger Explosion

In fact, the seismic records by 30 gm dynamite have more complex features than in the previous cases, the other conditions being kept equal to each other. Some of the records in the later cases are illustrated in Fig. 20, and the time-distance curves of every trough are shown in Fig. 21 where chain and broken lines are respectively group and phase velocities previously observed. In both figures, predominant phases are marked by I′, II′,⋯. Among them III′ wave group has the most complex feature, and this complexity may be, as seen from Fig. 21, due to interferences of the 3rd and the 4th wave groups already mentioned. Variations of periods or wave forms with charge amounts will be discussed in another opportunity. In this section, we shall be concerned only with the classifications of wave groups caused by an explosion.

The time-distance curves of I′ and II′ groups are just the same as those of the 1st (I) and the 2nd (II) groups. The former groups must be identical respectively to the latter ones.

Wave groups which have not been observed

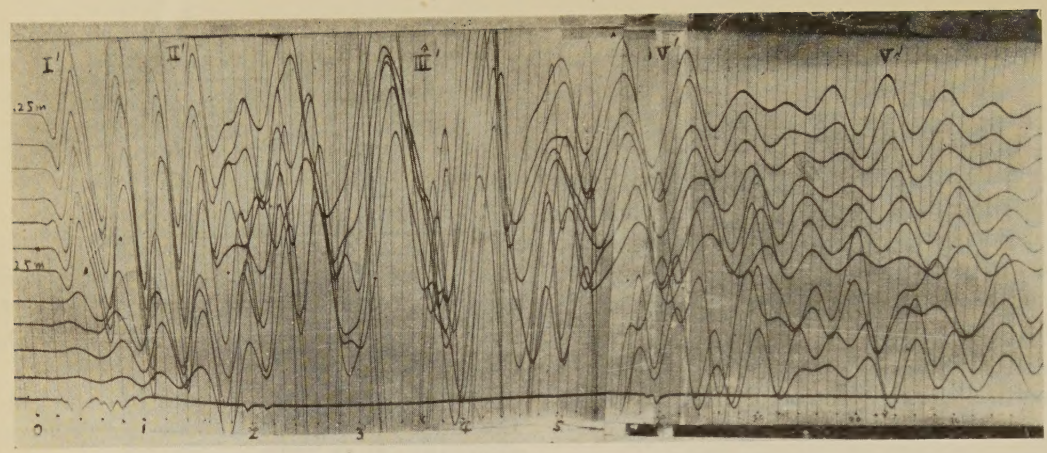

Fig. 20 (a) U, 20.25 m ~ 23.25 m

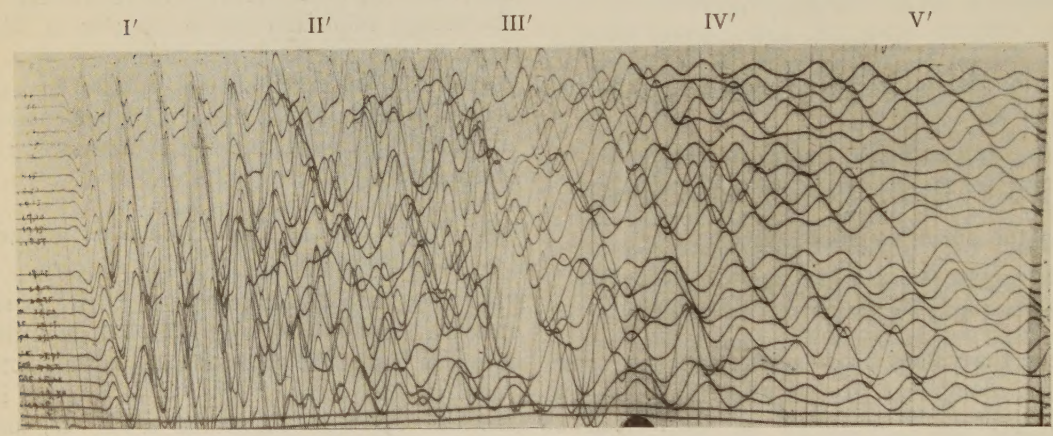

Fig. 20 (b) E, 10.75 m ~ 27.25 m

Fig. 20. An example of the seismic records by 30 gm dynamite.

previously are IV′ and V′ groups marked in Fig. 20 and Fig. 21. Several data on these groups are given in Table 7. Now assuming

Table 7. Collected data on IV′ and V′ groups.

wave group	period	phase velocity	wave length	group velocity
IV′	5~7	0.7~1.0	6 m	0.3~0.35
V′	5~6	0.7~0.9	5 m	0.2~0.25

time unit 10^{-2} sec; velocity unit 10^{2} m/s

again the $(2n-1)/4$ wave length law, we have for the both groups

$$\frac{2n-1}{4}=\frac{1}{6}\left(\frac{1.0}{1.3}+\frac{3.0}{2.5}\right)=\frac{1.3}{4}\,.$$

Admittedly the law is not satisfied perfectly, but their phase and group velocities seem to show that they are the phases near the AIRY phases of ${}_2M_{21}$ and M_{11}-waves in the superficial two layers. Thus we have the results in Table 8.

Table 8. Classifications of wave groups observed.

wave group	I	II=II′	III	IV	III′= III+IV	IV′	V′
type	P	${}_2M_{22}$	${}_2M_{21}$	M_{11}	${}_2M_{21}$, M_{11}	${}_2M_{21}$	M_{11}
layer		1,2	1	1	1	1,2	1,2

Fig. 22 shows particle orbits of all phases observed. The reductions from the recorded

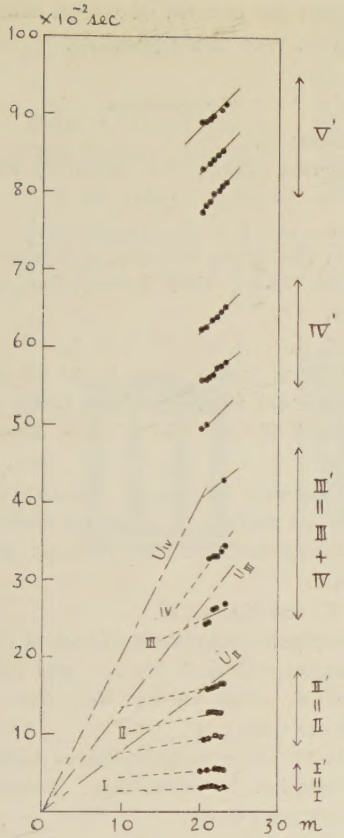

Fig. 21. The time-distance curves in the case of 30 gm dynamite.

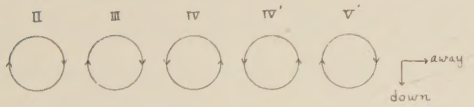

Fig. 22. Particle orbits of all phases observed.

orbits to the true orbits are not made in Fig. 22. Particle orbits of IV′ and V′ groups seem to contradict theoretically expected ones in doubly stratified layers (Sezawa and Kanai (1940)). But the hodograph directly got from the seismic record may have some different feature from the true one. We shall not adhere to the problem at present.

§ 10. Shielding Effects of Upper Layers

Looking at the initial motion in our records once more, we can find very poor waves before the wave of velocity 18×10^2 m/s, which is taken as the initial motion in the present discussion. The velocity of that very feeble initial motion seems to be 25×10^2 m/s, and this may be supposed to be some refracted wave due to a lower stratum than that we have treated by now. But its amplitude is too small to be observed on all records. Looking again at the boring data in Fig. 13, we see that the velocity ratio of the light clay to the following one is only 25/18=1.4, whereas that of the dark clay to the light clay is 18/2.5=7.2. Thus the dark clay layer has shielding effects for seismic waves, not only for refracted waves but also for surface waves. Therefore all wave groups observed by us are concerned only with strata above the light clay layer under which there might be many layers actually. By this reason, we have only a finite number of wave groups at the present experiments.

It will, however, remain questionable why ${}_1M_{21}$, M_{12} and M_{22} in the uppermost layer and ${}_1M_{21}$ and M_{12} in the superficial two layers have not been observed in our seismic records. According to our field experiences, ${}_1M_{21}$ seems to have smaller amplitude than ${}_2M_{21}$ whose group velocity is smaller than that of ${}_1M_{21}$. M_{12} and M_{22} in the uppermost layer must have periods of about 1.0×10^{-2} sec, where the magnification of our recorders is very small. The absence of M_{12} in the upper two layers cannot be explained at present. It will not be explained until we have theoretical knowledges on relative amplitudes of M-waves in these layers.

§ 11. Conclusion

The possibilities of existences of many waves, direct, refracted, reflected and various surface waves, have already been predicted by many theoretical investigations. But it is a different problem to ascertain these waves on actual seismic records. It is most important, in practice, to recognize the characters of the waves predominant on our seismograms. Some of the waves are useful and others may be obstructive for some purposes. Theory and practice in general have not yet stepped up to each other, though a few attempts were made.

The present paper, the author believes, has given the first thorough discussions in this direction.

The present model seismology is confined in a very small scale, but it will be extended to larger scale observations. The refraction method alone cannot decide a unique subsurface model. In such a case, it may be useful to count even the number of the surface waves alone. In order to obtain a good reflection record, the shot depth must be chosen lower than a shielding layer thus determined.

The present discussions on amplitude distributions in the strata concerned and the quarter wave length law are incomplete, but they will be made perfect in another opportunity.

Acknowledgements

The present author expresses his hearty thanks to the members of the Seismic Exploration Group of Japan headed by Prof. Kenzo SASSA for the kind cooperations in the present experiments. Many thanks are also due to the technical experts of Teikoku Oil Company, Transportation Technical Research Institute of Japan and Geological Survey of Japan. The author wishes again to express his thanks to the Government Authority of the Ministry of Education for the grant of the Science Research Fund by the aid of which the present investigation was made possible.

References

HATAKEYAMA, T.
1954 Hansha Jikken. (in Japanese) Rep. Seis. Exp. Group of Japan. No. 1, 3.

KANAI, K.
1951 On the Group Velocity of Dispersive Surface Waves. Bull. Earthq. Res. Inst., **29**, 49.

MURAUCHI, S.
1955 S ha o hassei suru Sochi ni tsuite. (in Japanese) Rep. Seis. Exp. Group of Japan, No. 4, 21.

SEZAWA, K.
1927 Dispersion of Elastic Waves Propagated on the surface of Stratified Bodies and an Curved Surface. Bull. Earthq. Res. Inst., **3**, 1.

SEZAWA, K. and KANAI, K.
1940 Dispersive RAYLEIGH Waves of Positive or Negative Orbital Motion, and Allied Problems. Bull. Earthq. Res. Inst., **18**, 1.

SUZUKI, Z. and SIMA, H.
1954 On Forms of Seismic Waves Generated by Explosion 1. Sci. Rep. Tohoku Univ. Geophys., **6**, 85.

TOLSTOY, I. and EUGENE, U.
1953 Dispersive Properties of Stratified Elastic and Liquid Media. Geophysics, **18**, 844.